

DEVIATING FROM THE PLAN: ASSESSING THE IMPACT OF FOREST  
MANAGEMENT DELAYS ON ECOSYSTEM FUNCTION

by

Kathryn Joyce Murenbeeld



A dissertation

submitted in partial fulfillment

of the requirements for the degree of

Doctor of Philosophy in Geoscience

Boise State University

May 2022

© 2022

Kathryn Joyce Murenbeeld

ALL RIGHTS RESERVED

BOISE STATE UNIVERSITY GRADUATE COLLEGE

**DEFENSE COMMITTEE AND FINAL READING APPROVALS**

of the dissertation submitted by

Kathryn Joyce Murenbeeld

Dissertation Title:    Deviating from the Plan: Assessing the Impact of Forest Management Delays on Ecosystem Function

Date of Final Oral Examination:                    23 February 2022

The following individuals read and discussed the dissertation submitted by student Kathryn Joyce Murenbeeld, and they evaluated the student's presentation and response to questions during the final oral examination. They found that the student passed the final oral examination.

Alejandro Flores, Ph.D.	Chair, Supervisory Committee
Trevor Caughlin, Ph.D.	Member, Supervisory Committee
Vicken Hillis, Ph.D.	Member, Supervisory Committee
Kendra Kaiser, Ph.D.	Member, Supervisory Committee
Jacquelyn Shuman, Ph.D.	Member, Supervisory Committee

The final reading approval of the dissertation was granted by Alejandro Flores, Ph.D., Chair of the Supervisory Committee. The dissertation was approved by the Graduate College.

## DEDICATION

I dedicate this dissertation to all my family, friends, and colleagues who provided support and encouragement through this process. Thank you for finding worth in my work when I could not see it for myself.

## ACKNOWLEDGMENTS

I would like to acknowledge all my committee members, teachers, friends and coworkers in the Department of Geosciences, the Department of Biology, the Department of Human-Environment Systems, the Department of Public Administration, and the Office of Research Computing for their contribution to this dissertation. Additionally, I want to acknowledge the community support from the National Center for Atmospheric Research, including but not limited to, the Land Model Working Group, the FATES user group, and the technical support team for fostering a welcoming and helpful community. Additionally, I want to acknowledge the assistance of Dr. Polly Buotte at Berkeley, Joshua Rady at Virginia Tech, and Dr. Charles Koven at the Lawrence Berkeley National Laboratory. Without their help I would not have been able to complete this work.

## ABSTRACT

Forests are under increasing stress due to changes in disturbance regimes, such as wildfire and pest or disease outbreaks, an increase in more severe and prolonged drought, and changes in land use. These stressors are already having an observable impact on forests in the western United States. Many forests within the western US are managed by the US Forest Service. Forest management is important as a tool for increasing a forest's ability to withstand or recover from these stresses. Additionally, because of the forest's influence on interactions between the land surface and the atmosphere, forest management has implications for future energy, water, and carbon cycles. However, management is driven by socio-economic, political, and ecological needs which can influence the timing of management activities. Forests are dynamic ecosystems, and changes to the timing of management through delays could lead to unanticipated impacts on a forest's structure, productivity, and ecohydrological function. Land surface models (LSMs) are one tool used to investigate land surface processes and land-atmosphere interactions. LSMs represent vegetation dynamics in different and increasingly sophisticated ways. While the fidelity of plant biophysical and biogeochemical process representation has increased in many of these models, the representation of forest management is still very simplistic. Until recently, the temporal aspects of management have rarely been included in studies using LSMs. Here, we addressed this challenge by including the temporal details of representative timber harvest activities from the western USA within LSM simulations. We hypothesized that changes in the timing of

management activities can have long term impacts on the structure and functioning of a forest. To test this hypothesis, we quantified vegetation management activities in the western USA and investigated the role specific project characteristics have on potential project delays. As a proof-of-concept, we used this data to inform the timing of single point scale logging simulations using the Functionally Assembled Terrestrial Ecosystem Simulator of the Community Land Model (CLM-FATES) for a ponderosa pine dominated forest in southern Idaho. A challenge encountered in simulating realistic forests was a bias towards smaller-diameter trees (i.e., <50 cm diameter at breast height), relative to observations. In overcoming this challenge, we expanded on current work within the CLM-FATES and greater LSM community to better parameterize the model for temperate, evergreen forests. We developed methods to generate multiple parameter ensembles and simulated these ensembles under different climate forcing and coexistence conditions. Over the course of this work, we developed significant and important overarching findings about critical facets of simulating managed forest ecosystems. First, we found that environmental regulations (here the type of NEPA analysis required for a project), the length of time to complete that analysis, and the type of management activity had the biggest impact on the probability of project implementation. Second, from logging simulations, we found that the timing of treatments can have long term impacts on the resulting forest size-structure, but timing has less of an impact on the long-term functioning of the forest as indicated by the model. Third, more complex ecosystems – as represented by the addition of an additional plant functional type – can lead to more realistic distributions of tree size classes, although this added ecosystem complexity does not appear to assist in identifying optimal sets of model parameters in CLM-FATES. This

work makes an important contribution to deploying sophisticated, demography based LSMs in western US forests by demonstrating how models can now capture legacies of human interventions and that calibration of model parameters is complex and constrained by the existing structure and makeup of these systems. These results highlight the importance of representing different aspects of human systems in ecosystem models as well as highlighting the tension between a need to improve model calibration without increasing model complexity.

## TABLE OF CONTENTS

DEDICATION .....	iv
ACKNOWLEDGMENTS .....	v
ABSTRACT .....	vi
LIST OF TABLES .....	xiii
LIST OF FIGURES .....	xv
LIST OF ABBREVIATIONS .....	xxi
CHAPTER ONE: INTRODUCTION .....	1
Background.....	2
Forest Management in the United States .....	2
Forests and Surface Process.....	3
Modeling Forests and Management .....	4
Scientific Gap and Research Objectives .....	5
Methods Summary .....	6
Summary of Findings.....	6
CHAPTER TWO: DELAYS TO FOREST MANAGEMENT PROJECTS IN THE WESTERN UNITED STATES .....	8
Introduction .....	8
Methods.....	12
Data Collection.....	12
Project Variables .....	14

Descriptive Statistics.....	19
Survival Analysis.....	19
Results.....	21
Descriptive Statistics.....	21
Survival Analysis Results.....	24
Discussion.....	39
Factors Influencing the Probability of Delay .....	40
Limitations.....	43
The Consequences of Project Delays.....	44
Future Work.....	45
Conclusions.....	47
CHAPTER THREE: THE LONG-TERM IMPACTS OF FOREST MANAGEMENT TIMING ON FOREST STRUCTURE AND FUNCTION.....	48
Introduction.....	48
Methods and Materials .....	51
Model Overview .....	51
The Logging Module .....	53
Model Setup and Experimentation.....	54
Model Analysis.....	61
Results.....	63
Comparison to Target Data .....	64
Structural Responses to the Logging Scenarios.....	65
Functional Responses to the Logging Scenarios .....	78
Discussion.....	85

Necessity of More Temporally Detailed Logging Practices in Land Surface Models.....	88
Limitations .....	89
Future Work.....	91
Conclusion.....	92
CHAPTER FOUR: A METHOD TO IMPROVE PARAMETERIZATION OF TEMPERATE CONIFER FORESTS .....	93
Introduction .....	93
Methods.....	95
FATES Model Description .....	96
Carbon Assimilation and Allocation in FATES.....	97
Plant Allometry in FATES.....	98
Updating FATES PFTs to Represent Conifers in Idaho.....	99
Model Simulation Setup .....	104
Model Analysis .....	106
Results.....	107
Differences Between the Climate Forcings .....	107
Comparison to Observed AGB, LAI, and GPP .....	109
Success at Growing Large Trees: Single-PFT Ensembles.....	114
Success at Growing Large Trees: Multi-PFT Ensembles.....	119
Discussion.....	123
Impacts of Different Climate Forcing Data on Plant Functional Response .....	123
Single-PFT Ensembles and Parameter Distributions .....	124
Species Specific PFTs and Modeled Outputs.....	126

Limitations.....	127
Future Work.....	129
Conclusion .....	130
CHAPTER FIVE: CONCLUSIONS .....	132
Future Directions .....	133
Use of Land Surface Models for Forest Management.....	135
Model Complexity and Model Fidelity .....	137
REFERENCES .....	139
APPENDIX A.....	156
APPENDIX B.....	179
APPENDIX C.....	203

## LIST OF TABLES

Table 2.1	Description of Calculated Variables.....	15
Table 2.2	Description of Project Characteristics .....	18
Table 2.3	Descriptive Statistics of Project Delays (days).....	23
Table 2.4	Kaplan-Meier probabilities of continued delay.....	25
Table 2.5a	Kaplan-Meier Log-Rank Test Results.....	32
Table 2.5b	Kaplan-Meier Log-Rank Test Results – Regions as Dummy Variables ...	32
Table 2.6	Results from the Cox univariate models.....	34
Table 2.7	Results from the larger Cox proportional hazards multivariate model .....	37
Table 2.8	Results from the final Cox proportional hazards multivariate model .....	39
Table 3.1	List of Updated FATES Parameter Values.....	57
Table 3.2	Description of Logging Scenarios.....	58
Table 3.3	Sample Table of Project After Markov Chain Data Processing. ....	60
Table 3.4	Modeled and Observed Values of AGB, LAI, and GPP .....	65
Table 4.1	List of parameters investigated in this study.....	100
Table 4.2	List of 10 Common Conifer Species in Idaho.....	102
Table 4.3	“Successful” ensembles and list of ensembles outside of reasonable AGB values. ....	114
Table 4.4	Results from the KS test for the multi-PFT ensembles. Each parameter value corresponds to the success of growing its corresponding PFT. * p-values < 0.05 .....	119
Table 4.5	Results from the KS test for the multi-PFT ensembles. Each parameter values corresponds to the success of growing its corresponding PFT. ...	122

Table A1	Table of Variables in the Full FS-PALS Dataset.....	157
Table A.2	Correlation matrix of covariates and project delay.....	162

## LIST OF FIGURES

Figure 1.1	A simplified representation of a forest’s role in the biophysical and biochemical process of the land surface. ....	4
Figure 2.1	A conceptual timeline of the planning process. Planning and scoping are followed by the NEPA analysis. The time to complete the NEPA analysis has been studied by Fleischman et al., 2020. The length of the NEPA analysis depends on the type of analysis required (either the project is a categorical exclusion (CE) or requires an environmental assessment (EA) or an environmental impact statement (EIS). Once the NEPA analysis is completed and the project decision signed there is then a period of time from the decision to project implementation (action). In this study we are interested with the action period, specifically if the first activity in the project was completed on the date it was planned to be completed.....	11
Figure 2.2	Map of the continental United States showing National Forests in dark green and USFS administrative regions 1-9. The regions considered in this study (1-6) are highlighted in light green. ....	13
Figure 2.3	Bar plot of the mean and median project delays for all projects considered in the study and grouped by project characteristic. In this study the median is a better measure of central tendency because there are a few projects that are extremely delayed which skew the mean. Mean, median, and standard deviation can be found in Table 3. ....	22
Figure 2.4	Kaplan-Meier survival curve for all projects. In this study survival is equivalent to continued delay. The dashed line shows the median probability of continued delay where a project is just as likely to be initiated as it is to continue to be delayed. The sharp decrease in probability of continued delay at time zero implies that roughly 10% of projects experience no delay in initiation. A similar drop in probability occurs at roughly one year of delay. The curve flattens yet never reaches a probability of zero as some projects in the study are right censored (i.e. were not initiated by the end of the observation period, Dec. 31, 2018)...	26
Figure 2.5	Kaplan-Meier survival curves for projects grouped by NEPA analysis type, where survival indicates continuous delay. EIS and EA have a similar median delays (365 and 312 days respectively) which are twice as long as the median survival for projects that fall under a CE (153 days). Relatively few projects require an EIS leading to wide confidence	

	intervals. Between two and three years the curves begin to converge, and the confidence intervals overlap. ....	28
Figure 2.6	Kaplan-Meier survival curves for projects grouped by litigation (a) and overlap occurrence (b). Litigation against USFS projects is uncommon leading to wide confidence intervals. The curve for litigated projects diverges from the curve for non-litigated projects, while the curves for overlap and no overlap in projects cross after a duration of 6.5 years. Both sets of curves for litigation and overlap show vertical drops in probability at approximately one year indicating a relatively large number of projects are initiated. ....	29
Figure 2.7	Kaplan-Meier survival curves for projects grouped by projects in region 3 and projects in all other regions. The median probability of continued delay occurred at similar delay durations (dashed lines). The region 3 curve shows a very distinct increase in project initiation at an approximately one-year delay duration.....	30
Figure 2.8	Cumulative hazard curves for projects grouped by size. Survival curves can be found in the supplementary materials (A4). The curves for extra-large projects steepened relative to the other sizes after approximately two years of delay showing that extra-large projects are more likely to be initiated relative to the other project sizes with continued delay.....	31
Figure 3.1	Location map for the single point scale at the Boise Basin Experimental Forest (BBEF, red circle). ....	55
Figure 3.2	Sample histogram from the Markov-Chain with peaks highlighted in green for when an activity would likely occur.....	60
Figure 3.3	Moving averages of above ground biomass (AGB) up to 100 years post-logging.....	66
Figure 3.4	Moving averages of leaf area index (LAI) up to 100 years post-logging .	68
Figure 3.5	Moving averages of the area of trees on the grid cell up to 100 years post-logging.....	69
Figure 3.6	Moving averages of basal area (BA) of small trees (0-10 cm DBH) and large trees (30-50 cm DBH) up to 100 years post-logging. ....	72
Figure 3.7	Moving averages of the stem densities of small trees (0-10 cm) and large trees (30-50cm) up to 100 years post-logging. ....	74
Figure 3.8	Seasonal mean GPP with +/- 1 std. from the control scenario at different 5-year increments post-logging. ....	80

Figure 3.9	Seasonal mean ET with +/- 1 std. from the control scenario at different 5-year increments post-logging. ....	82
Figure 3.10	Seasonal mean QIN with +/- 1 std. from the control scenario at different 5-year increments post-logging. Please note the different scale on the y-axes. ....	84
Figure 4.1	Trait matrix of the synthetic trait values for the 10 common conifer species in Idaho. ....	104
Figure 4.2	Location map for the single point scale at the Boise Basin Experimental Forest (BBEF, red circle).....	105
Figure 4.3	Differences between the CRUNCEP and WRF seasonal precipitation. Negative values occur where the WRF data is greater (i.e. wetter) than the CRUNCEP data.....	108
Figure 4.4	Differences between the CRUNCEP and WRF seasonal temperature. Negative values occur where the WRF data is greater (i.e. warmer) than the CRUNCEP data. ....	109
Figure 4.5	Histogram of ensemble mean GPP for the last 50 years of the simulation. Vertical lines are the mean and standard deviation observed GPP from two Metolius Ameriflux tower site. ....	110
Figure 4.6	Histogram of ensemble mean LAI for the last 50 years of the simulation. Vertical lines are the mean and standard deviation from MODIS derived LAI. ....	112
Figure 4.7	Spider plots of annual mean AGB from each ensemble. The solid horizontal line is the mean observed AGB (2560 gC/m <sup>2</sup> ) and the dashed horizontal line is +2 standard deviations of AGB (5900 gC/m <sup>2</sup> ) from Wilson et a. (2013) for the Boise National Forest, where the Boise Basin Experimental Forest is located.....	113
Figure 4.8	Histogram of observed AGB at Boise National Forest from Wilson et a., 2013. ....	114
Figure 4.9	Histogram of “successful” ensemble mean GPP for the last 50 years of the simulation. Vertical lines are the mean and standard deviation observed GPP from two Metolius Ameriflux tower site.....	116
Figure 4.10	Histogram of “successful” ensemble mean LAI for the last 50 years of the simulation. Vertical lines are the mean and standard deviation from MODIS derived LAI.....	117

Figure 4.11	Trait matrix of single-PFT ensembles color coded for successful (orange) and unsuccessful (blue) parameterizations. ....	118
Figure 4.12	Trait matrix of PFT1-pine parameter values for multi-PFT ensembles color coded for parameterization that successfully (orange) and unsuccessfully (blue) grew PFT1-pines >50cm DBH. ....	121
Figure 5.1	The expected relationship between the realism of results from LSMs and increasing model complexity with the actual relationship. Here we show that continually adding realistic aspects (e.g. fire, multiple PFTs) may not improve model results to the extent anticipated. ....	138
Figure 5.2	A conceptual model of changes to model error with increasing model complexity. Figure 1 from Saltelli, 2019. ....	138
Figure B1.1	Ten year moving average of AGB. ....	180
Figure B1.2	Ten year moving average of LAI. ....	181
Figure B1.3	Ten year moving average of the area of trees per grid cell. ....	181
Figure B1.4	Ten year moving average of the BA of small trees (0-10cm diameter at breast height, DBH). ....	182
Figure B1.5	Ten year moving average of the BA of large trees (30-50cm DBH). ....	182
Figure B1.6	Ten year moving average of the number of plants per hectare of small trees (0-10cm DBH). ....	183
Figure B1.7	Ten year moving average of the number of plants per hectare of large trees (30-50cm DBH). ....	183
Figure B2.1	Five (A), 10-(B), and 20-year (C) moving average of AGB compared to the selective logging at a single date scenario (SLS). ....	184
Figure B2.2	Five (A), 10-(B), and 20-year (C) moving average of LAI compared to the selective logging at a single date scenario (SLS). ....	185
Figure B2.3	Five (A), 10-(B), and 20-year (C) moving average of area of trees per grid cell compared to the selective logging at a single date scenario (SLS). ..	186
Figure B2.4	Five (A), 10-(B), and 20-year (C) moving average of BA of small trees compared to the selective logging at a single date scenario (SLS). ....	187
Figure B2.5	Five (A), 10-(B), and 20-year (C) moving average of BA of large trees compared to the selective logging at a single date scenario (SLS). ....	188

Figure B2.6	Five (A), 10-(B), and 20-year (C) moving average of number of plants of small trees compared to the selective logging at a single date scenario (SLS).....	189
Figure B2.7	Five (A), 10-(B), and 20-year (C) moving average of number of plants of large trees compared to the selective logging at a single date scenario (SLS).....	190
Figure B3.1	Annual mean GPP with +/- one standard deviation of the control scenario. ....	191
Figure B3.2	Annual mean NPP with +/- one standard deviation of the control scenario. ....	192
Figure B3.3	Annual mean ET with +/- one standard deviation of the control scenario. ....	193
Figure B3.4	Annual mean QR with +/- one standard deviation of the control scenario. ....	194
Figure B3.5	Annual mean QIN with +/- one standard deviation of the control scenario. ....	195
Figure B4.1	Seasonal mean NPP with +/- one standard deviation from the control scenario at different 5-year increments post-logging. ....	196
Figure B4.2	Seasonal mean surface runoff (QR) with +/- one standard deviation from the control scenario at different 5-year increments post-logging. Please note the different scale on the y-axes. ....	197
Figure B4.3	Seasonal average GPP with +/- one standard deviation of scenario SLS at different 5-year increments post-logging. Please note the different y-axes on the top row of figures.....	198
Figure B4.4	Seasonal average NPP with +/- one standard deviation of scenario SLS at different 5-year increments post-logging. Please note the different y-axes on the top row of figures.....	199
Figure B4.5	Seasonal average ET with +/- one standard deviation of scenario SLS at different 5-year increments post-logging. Please note the different y-axes on the bottom row of figures.....	200
Figure B4.6	Seasonal average surface runoff (QR) with +/- one standard deviation of scenario SLS at different 5-year increments post-logging. Please note the different y-axes in the middle row of figures.....	201

Figure B4.7	Seasonal average Infiltration (QIN) with +/- one standard deviation of scenario SLS at different 5-year increments post-logging. Please note the different y-axes on all the rows of figures.....	202
Figure C.1	Trait matrix of PFT1-pines parameter values for multi-PFT ensembles color coded for parameterization that successfully (orange) and unsuccessfully (blue) grew PFT1-pines >50cm DBH. ....	204
Figure C.2	Trait matrix of PFT2-fir parameter values for multi-PFT ensembles color coded for parameterization that successfully (orange) and unsuccessfully (blue) grew PFT2-pines >50cm DBH.....	205

## LIST OF ABBREVIATIONS

AGB	Above Ground Biomass
BA	Basal Area
BBEF	Boise Basin Experimental Forest
BNF	Boise National Forest
CC	Clearcut (a logging scenario in Chapter 3)
CE	Categorical Exclusion
CLM	Community Land Model
CRUNCEP	Climate Research Unit and National Centers for Environmental Prediction
DBH	Diameter at Breast Height
EA	Environmental Assessment
EIS	Environmental Impact Statement
ET	Evapotranspiration
FATES	Functionally Assembled Terrestrial Ecosystem Simulator
FIA	Forest Inventory Analysis
FS-ACT	Aggregated dataset of United States Forest Service management activities
GPP	Gross Primary Productivity
LAI	Leaf Area Index
LSM	Land Surface Model

NCAR	National Center for Atmospheric Research
NEPA	National Environmental Policy Act
NPP	Net Primary Productivity
PAL	The planning, appeals, and litigation dataset from the United States Forest Service
PALS-ACT	A dataset combining the University of Minnesota’s United States Forest Service planning, appeals, and litigation dataset on NEPA compliance with the aggregated dataset of United States Forest Service management activities
PFT	Plant Functional Type
SL	Selective Logging
SLD-EA	Selective Logging Delayed based on Environmental Assessment (a logging scenario in Chapter 3)
SLM	Selective Logging at Multiple Dates (a logging scenario in Chapter 3)
SLR	Selective Logging that is Repeated (a logging scenario in Chapter 3)
SLD-R4	Selective Logging Delayed based on Forest Service Region 04 (a logging scenario in Chapter 3)
SLS	Selective Logging at a Single Date (a logging scenario in Chapter 3)
UMN-PALS	The University of Minnesota’s USFS planning, appeals, and litigation dataset on NEPA compliance

USFS      United States Forest Service  
WRF      Weather Research and Forecasting



## CHAPTER ONE: INTRODUCTION

Forests cover nearly one-third of the earth's land surface, and they play an important role in maintaining ecosystem function and socioeconomic well-being (Bonan and Doney, 2018; FAO, 2018). Forest structure and composition influence local and regional climate as well as water quality and quantity (Bonan, 2008; Bonan, 2016; National Research Council, 2008). Humans, by directly removing, planting or otherwise changing forest cover and composition, also play an important role in the ecosystem function of forests and the ecosystem services they provide (Costanza et al., 2017; Daily et al., 1997; Krieger, 2001). Within the United States, approximately one-fifth of forested land (145 million acres) are managed by the U.S. Forest Service (Oswalt et al., 2019). Recently, as managers grapple with protecting forests from the stresses of climate change and changing patterns of disturbance, national forests are increasingly managed with the objective to increase a forest's resistance to disturbances and increase the forest's ability to recover to previous ecosystem function after a disturbance (North et al., 2022). However, forest managers exist within their own dynamic system of social considerations and political objectives, in addition to the natural ecosystem in which forests exist and must be managed. This socio-political environment can impact the timing of important management activities with potentially long-term consequences for the structure and function of forests. One challenge is anticipating how forest management and the timing of forest management will impact forest ecosystem functioning. A way to address this challenge is by integrating realistic management practices into physics-based models of

the land surface and forests. However, representing forest management within land surface models is in development and have rarely considered the temporal aspects of forest management.

## **Background**

### Forest Management in the United States

National forests were originally created as forest reserves to preserve them during the period of Western expansion and homesteading in the United States (Wilkinson, 1992; Wilson, 2014). For much of their history, the national forests were managed under a philosophy of “wise” and sustainable use for timber harvest (Wilson, 2014). From the late 1960s through the mid-1990s, new laws and policies were enacted that emphasized a shift to multiple-use and ecosystem services management philosophies (Grumbine, 1994; Wilson, 2014). One of these laws, the National Environmental Policy Act (NEPA) requires that any activity that could potentially impact the land surface must complete a, sometimes lengthy, analysis which needs to consider public input and provide management alternatives (42 U.S.C. Section 4321; Fleischmann et al., 2020).

Forest managers must balance the competing interests of multiple environmental laws, federal objectives, and a diverse citizenry that desire different uses for national forests (Anderson et al., 2013; Stern et al., 2010). Litigation due to NEPA regulations and requirements receives a lot of attention but is quite rare (Ruple and Race, 2020). However, the time it takes to complete a NEPA analysis, litigation, and a variety of other factors, such as access to resources or environmental conditions, can impact when forest management projects are implemented. Due to the dynamic nature of forests and their

impact on biophysical and biochemical surface processes, inaction through project delays can potentially have as much ecosystem impact as management action.

### Forests and Surface Process

Forests interact with their surroundings in numerous ways. Moving from left to right in Figure 1.1, we provide a simplified explanation for how forests can influence the energy, carbon, and hydrological fluxes of the earth's surface (Bonan, 2016). Their cover and color control the albedo of the land surface impacting the amount of incoming shortwave radiation reflected or absorbed, and forests emit longwave radiation. Forest size and structure add roughness to the land surface impacting the flux of sensible heat while the process of evapotranspiration can cool the immediately surrounding air. Forests can act as a carbon sink through a relatively higher rate of carbon sequestration in woody stems and roots or as a carbon source through a relatively higher rate of respiration and decomposition (Pan et al., 2011). Forests also influence the water cycle by intercepting precipitation and channeling precipitation down stems. Tree litter, forest duff, and tree roots impact the quantity and rate of water infiltration to the soil with implications for surface runoff as well as the amount of water that can reach a stream (Neary et al., 2009). Representing these interacting biophysical and biochemical processes is challenging, but great strides have been made since the creation of the earliest global climate models.

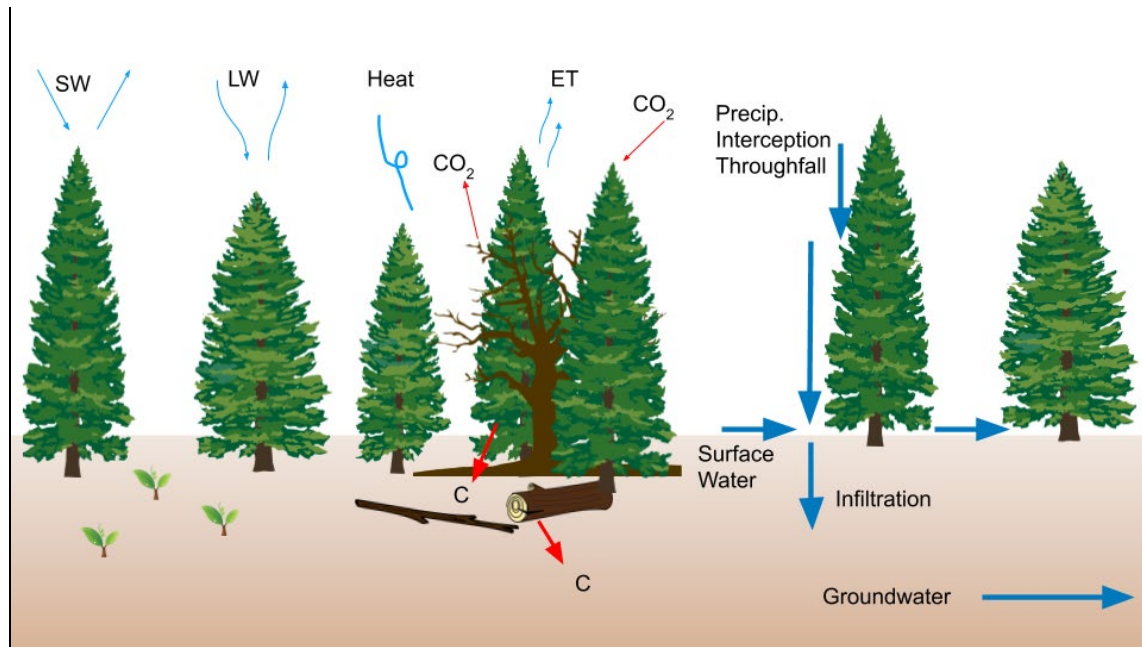


**Figure 1.1** A simplified representation of a forest's role in the biophysical and biochemical process of the land surface.

### Modeling Forests and Management

The importance of terrestrial ecosystem dynamics in studies of past and future climate has been well established for decades, yet land surface and vegetation model components were not developed for climate models until the late 1960s and early 1970s (Deardorff, 1978; Fisher and Koven, 2020; Manabe, 1969; Pielke et al., 1998; Pitman, 2003). A single vegetation layer was first added into land surface model schemes in 1978, which greatly improved global climate models and laid the foundation for the future representation of vegetation in land surface models (Deardorff, 1978). Various modeling schemes now exist that integrate vegetation dynamics into land surface models (Fisher et al., 2015; Fisher et al., 2018; Medvigy et al., 2009; Sato et al., 2007; Smith et al., 2001). One such model, the Functionally Assembled Terrestrial Ecosystem Simulator module of the Community Land Model (FATES-CLM), uses a cohort approach to represent

vegetation and capture plant competition and succession in a computationally efficient manner (Fisher et al., 2018; Moorcroft et al., 2001).

Within FATES-CLM, Huang et al. (2020) have developed a selective logging module to represent landscape level logging practices. Within the selective logging module, the timing and spatial extent of a logging event can be set. The selective logging model improved the representation of forest management in LSMs by incorporating indirect plant mortality from logging practices as well as removing surface carbon pools after harvest. However, the model does not allow for the realistic timing of logging, nor does it allow for the rates of logging and removal to be PFT specific. Rady et al. (2022) have developed a novel vegetation management driver which includes other forest management activities such as thinning and planting, and, most importantly for our purposes, the new vegetation management driver provides the ability to specify multiple and irregular dates for the occurrence of management activities.

### **Scientific Gap and Research Objectives**

While great strides have been made to the representation of vegetation dynamics and forest management in land surface models, there is still a lack of research and experimentation incorporating the temporal aspects of forest management. To address this gap, we were guided by three research objectives and questions:

1. Quantifying the temporal aspects of forest management in the western United States. Do specific project characteristics influence delays to project implementation and for how long?

2. Incorporating forest management data into a land surface model. Does the time difference from planned to actual completion date (delay in implementation) impact forest structure and function?
3. Parameterizing land surface models within a management context. How can we better parameterize FATES-CLM to represent forest structure in a way that forest managers may find useful?

### **Methods Summary**

To meet these objectives and answer our research questions we first used data from the US Forest Service to investigate and quantify forest management projects in the western United States. Here we focused on those activities that directly impact the land surface through the removal or addition of plants. We performed a survival analysis to determine which project characteristics impact the probability of project implementation and the probability of continued project delay. We then used these findings to inform a series of logging scenarios simulated using FATES-CLM at a single point in a semiarid forest of the western US. Finally, as we prepared to scale up these simulations, we parameterized FATES-CLM for the western US with the coexistence of two PFTs with different plant strategies and in a way that potentially better represents forest structure.

### **Summary of Findings**

Through this research we found that the average harvest project duration in the western United States is 543 days and has a median delay of 197 days. The type of NEPA analysis required for a forest management project, the length of time to complete the NEPA analysis, the location of the project can all impact the median project delay. The type of NEPA analysis required and the type of activities performed in a project

corresponded with different probabilities of project implementation and risk of continued delay. When these quantities were considered in logging scenarios within FATES-CLM, we found that small changes to the implementation date of a timber harvest project led to long-term changes in the size structure of the modeled forest. However, these small changes to the timing did not impact the long-term functioning of the modeled forest. And finally, we found that in order to parameterize FATES-CLM for forests in the western US one may need to include competing PFTs and consider a range of possible parameter values based on the observed plant traits of a smaller number of local species.

## CHAPTER TWO: DELAYS TO FOREST MANAGEMENT PROJECTS IN THE WESTERN UNITED STATES

### **Introduction**

Extreme disturbances leading to large scale tree mortality or state transition of forests are predicted to increase with climate change (Cobb et al., 2017; Field et al., 2020; Westerling et al., 2006). To meet the challenge extreme disturbances pose, new forms of anticipatory management are being proposed to maintain ecosystem function by inhibiting tree mortality, stopping, or easing state transitions, and preventing ecosystem collapse (Bradford et al., 2018; Cobb et al., 2107; Field et al., 2020; Millar and Stephenson, 2015). While scientists propose different management approaches to address growing concerns over the impact of extreme climate phenomena on forests, they do not often consider the bureaucratic processes or administrative laws associated with those recommendations (Bradford et al., 2018 citing Craig et al. 2017 is one exception). These processes and policies can constrain management actions and can potentially impede adaptive and anticipatory management.

Within the United States, millions of acres of forested land have been managed by the Federal government via the United States Forest Service (USFS), for over one hundred years. To meet the need for sustainable forest management, the United States has enacted a series of laws to guide and regulate forest management beginning in 1891 with the General Revision Act, which gave the President the power to set aside a forest reserve and continuing today through various acts and the annual Farm Bills (Wilson, 2014).

Personnel within the USFS must balance the tensions inherent within these laws and a diverse citizenry that advocates for multiple, and sometimes contradictory, uses of natural areas (Anderson et al., 2013; Nie and Metcalf, 2016; Stern et al., 2010). Within the agency, personnel must also balance their own values and biases all while planning and implementing projects within the context of these laws and their requirements (Predmore et al., 2011; Stern et al., 2010).

There is a, perhaps common, perception that environmental regulations, usually through the National Environmental Policy Act (NEPA), and litigation citing NEPA and other environmental laws can unnecessarily delay implementing forest management activities. Under NEPA, any federal activity with the potential for environmental impact must complete an analysis to determine if the impact will be significant, and if so, to provide alternative methods or activities for consideration (42 U.S.C. Section 4321). Depending on the amount of potential environmental impact, a project will require either an environmental assessment (EA) or an environmental impact statement (EIS). Certain activities or projects may also be considered a categorical exclusion (CE) if the project meets specific requirements. NEPA and other regulations require periods of public comment and collaboration is encouraged for forest projects. In addition to the perception of environmental regulation and litigation as impeding forest management activities, there is another perception that these environmental laws and the use of the courts are essential. Some stakeholders are distrustful of the Forest Service and the collaborative process (Nie and Metcalf, 2016). These parties rely on litigation to actively participate in the planning process and ensure regulatory enforcement and oversight (Nie, 2008; Nie and Metcalf, 2016).

The USFS completes NEPA analyses more quickly compared to other federal agencies (Fleischmann et al., 2020; Ruple and Tanana, 2020). The USFS is also one of the most litigated federal agencies, with NEPA being one of the most cited laws (Broussard and Whitaker, 2009; Keele et al., 2006; Malmshiemer et al., 2004). However, litigation against NEPA is rare (0.22% of NEPA actions are litigated), and NEPA accounts for only 0.43% of all civil environmental litigation with the federal government as the defendant (Ruple and Race, 2020). The rate of litigation, although increasing until the early part of the century (Miner et al., 2010; Miner et al., 2014) is declining, along with the number of NEPA analyses completed overall (Fleischmann et al., 2020; Ruple and Race, 2020).

It is important to consider perceptions of regulatory or legal delays to seemingly urgent forest management projects. These perceptions can drive the conversation and attention in the legislature, potentially leading to new laws and policies. Since some forest management projects appear urgent and scientists call for more adaptive and anticipatory management, understanding all the temporal aspects of the project planning procedure is important. While there have been studies on the USFS on the length of time to complete a NEPA analysis (Fleischmann et al., 2020) and the time spent in court (Keele and Malmshiemer, 2018), there is a lack of quantitative research into the time from the completion of the planning process to actual project implementation (Figure 2.1). Regardless of the perception, unforeseen delays to forest management projects do occur, and they occur within a dynamic socio-ecological-system. If a project or activity is put on hold, the ecological dynamics of the system, for example natural forest regeneration or the encroachment of invasive species, continues.

Figure 1. Conceptual Timelines of Forest Management Processes

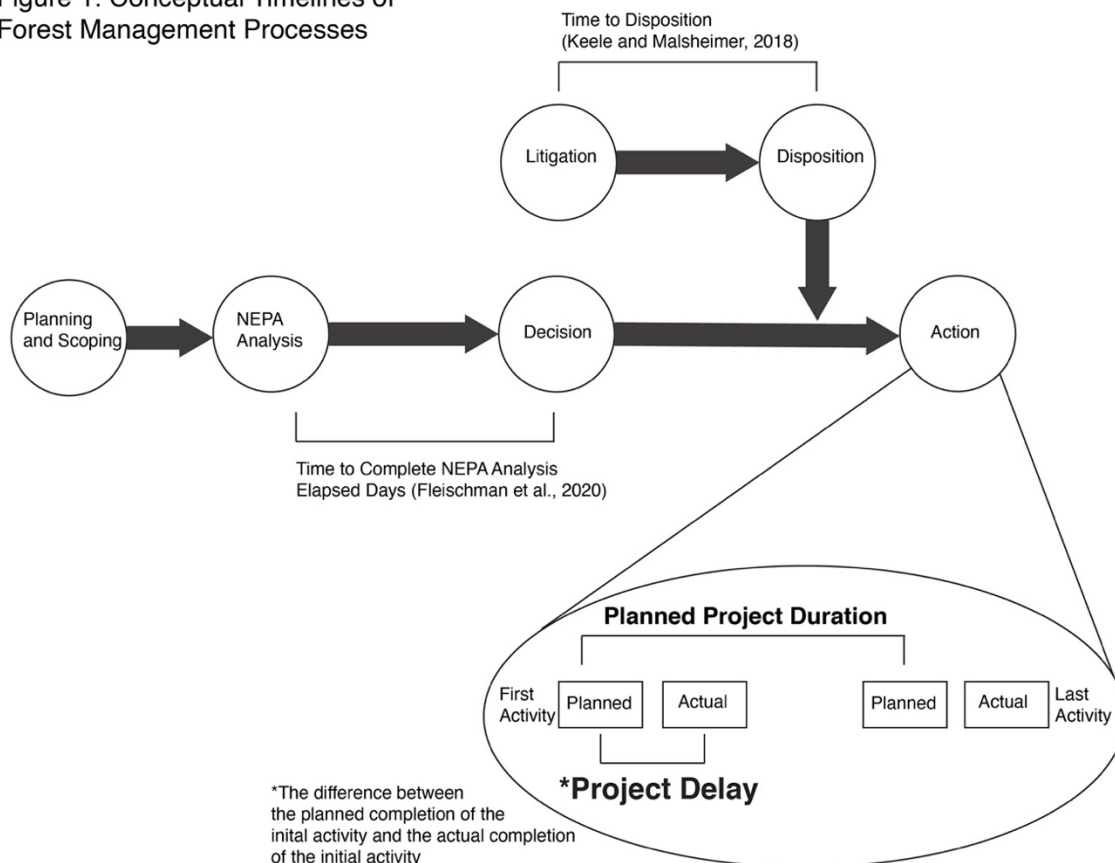


**Figure 2.1** A conceptual timeline of the planning process. Planning and scoping are followed by the NEPA analysis. The time to complete the NEPA analysis has been studied by Fleischman et al., 2020. The length of the NEPA analysis depends on the type of analysis required (either the project is a categorical exclusion (CE) or requires an environmental assessment (EA) or an environmental impact statement (EIS)). Once the NEPA analysis is completed and the project decision signed there is then a period of time from the decision to project implementation (action). In this study we are interested with the action period, specifically if the first activity in the project was completed on the date it was planned to be completed.

Our objectives in this study were to fill the gap in research on delays to forest management implementation by answering the following questions: (a) What are the mean and median delay in project implementation?, (b) What effect does the length of a project's delay in implementation have on the probability that the project will continue to be delayed?, and (c) what is the effect of various project characteristics (i.e. NEPA analysis type required, administrative region, type of activities, etc.) on the expectation of

a project being initiated? To answer these questions, we used a survival analysis approach to investigate USFS projects planned for the Western US from 2005 to 2018 focusing on activities related to logging, reforestation, timber stand improvements, and hazardous fuels treatments. Our goal was to provide quantitative analyses; therefore, we will not offer policy or management recommendations. However, these data and analyses are offered as an aid to forest managers as they plan projects and adapt to changing environmental, economic, and social conditions.

### **Methods**

To answer these questions, we combined several datasets from USFS databases of management projects and activities for the western administrative regions, and the USFS NEPA analysis dataset compiled by Fleischman et al. (2020). For the first question, we determined the mean, median, and standard deviation of managerial project delays in the western National Forests. To answer the second question, we completed a survival analysis using the Kaplan-Meier approach to predict the probability of a project's continued delay given the project's delay duration. To answer the final question, we used a Cox proportional hazards model to determine the effect of various project characteristics on the probability of project initiation.

#### Data Collection

We combined an aggregation of select USFS activity datasets, hereafter referred to as FS-ACT, with the University of Minnesota's USFS planning, appeals, and litigation dataset on NEPA compliance, hereafter referred to as UMN-PALS (Fleischman et al., 2020). We chose to focus on the western administration regions which include Regions 1 through 6 for two reasons (Figure 2.2). First, the majority of national forest acreage is

located within these western regions. Second, due to the frequency of wildfires within these regions, regulatory and management reform for forests is often promoted using forests in the western US as evidence.

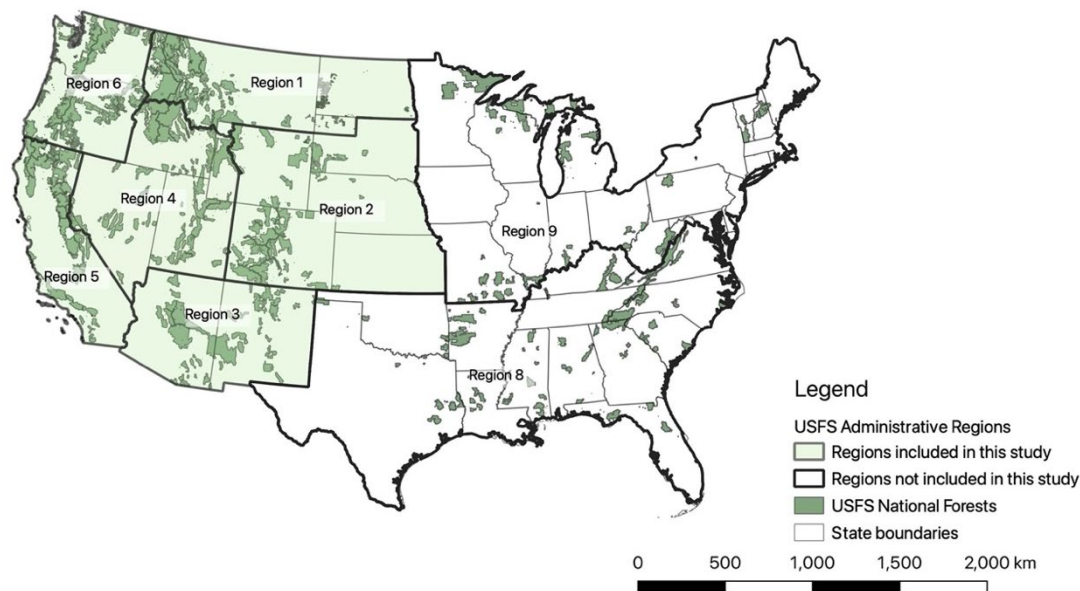


**Figure 2.2 Map of the continental United States showing National Forests in dark green and USFS administrative regions 1-9. The regions considered in this study (1-6) are highlighted in light green.**

To create the FS-ACT dataset we combined the timber harvest, timber stand improvement, reforestation, and hazardous fuels activity datasets by project for all available years. The FS-ACT dataset contains information for each individual activity that occurs within each project (A1). The UMN-PALS dataset was compiled by Fleischmann et al. (2020) and combined USFS NEPA project characteristics from the USFS' planning, appeals and litigation (PALS) database with appeals and litigation data from 2005 to 2018. Data entered into the PALS database prior to 2005 were considered unreliable and excluded from the dataset (Fleischman et al., 2020). We selected variables from the UMN-PALS dataset which cover the project's name, location, and temporal

aspects of the NEPA process (A1). The UMN-PALS and FS-ACT datasets were combined for the years 2005 through 2018 and grouped by NEPA project number to create the PALS-ACT dataset. This resulted in a combined dataset with 3557 unique NEPA projects. A more detailed explanation of the larger dataset and its creation is included in A3 and a GitHub repository.

### Project Variables

Within the FS-ACT dataset, activities have two dates, the date when an activity was planned to be completed (plan date) and the date when an activity was actually, physically, completed (complete date). When the PALS-ACT dataset was created, we kept the minimum plan and complete dates and the maximum plan and complete dates for each project. From these dates we determined the most important variables in this study, the project initiation and project delay. A project is considered initiated if it has a minimum complete date, meaning that the earliest activity in the project has been completed. The project delay is the difference in days between the minimum plan date and the minimum complete date. Other temporal variables were calculated from the minimum and maximum plan and complete dates including the planned project duration and overlap (Figure 2.1, Table 2.1).

**Table 2.1 Description of Calculated Variables**

<b>Temporal variable</b>	<b>Description</b>
Initiated?	If there is a minimum date completed, then the earliest activity in a project has been completed, and the project is considered initiated. A binary variable. 0 = project has no minimum complete date (project is not initiated) and 1= project has a minimum complete date (project is initiated).
Project delay	<p>The delay in project initiation. Here defined as the difference in days between when the first (initial) activity was planned to be completed and when the first (initial) activity was physically completed.</p> <p>Project delay (days) = minimum complete date – minimum plan date</p>
Planned project duration	<p>The planned length of the project. Here calculated as the difference in days between the minimum date planned and the maximum date planned.</p> <p>Planned project duration (days) = maximum plan date – minimum plan date</p>
Elapsed days	From Fleishmann et al. (2020). The time in days it takes to complete the NEPA analysis process. The time from the beginning of the NEPA analysis to when the appropriate record of decision is made.
Overlap	<p>The time in days that occurs from when the record of decision is made to when the first (initial) activity was planned to be completed.</p> <p>Overlap = ROD (date) – minimum plan date</p> <p>Overlap <math>\geq</math> 0 means that the completion of the NEPA analysis did not “overlap” with the date when the first activity in a project was planned to be completed.</p> <p>Overlap <math>&lt;</math> 0 means that the ROD “overlapped” with the date when the first activity in a project was planned to be completed.</p>
Minimum date planned/completed	The date that the first activity in a project was planned to be completed (planned) and the date that the first activity was, physically completed. May not be the same activity as planned.

<b>Temporal variable</b>	<b>Description</b>
Maximum date planned/completed	The date that the last activity in a project was planned to be completed (planned) and the date that the last activity was, physically completed. (n.b. may not be the same activity as planned).

There are several project characteristics that may impact a project's delay (Table 2.2). The type of NEPA analysis required for a project and any subsequent litigation are often assumed to cause delays to project implementation. Here we tested this assumption by including the NEPA analysis (as categorical data and binary data for CEs), the time to complete the NEPA analysis (elapsed days, Fleischmann et al., 2020) and litigation occurrence as covariates in our statistical analyses. The time to complete a NEPA analysis, the number of different analyses completed, and the number of litigated cases vary by administrative region, therefore we include a project's location at the regional level as another covariate (Fleischmann et al., 2020; Malmshheimer et al., 2004; Miner et al., 2010; Keele et al., 2006). The region covariate is included as a categorical variable as well as a series of binary variables (e.g. the project is in region 1 or not in region 1). In this study, we included other characteristics that are perceived to increase the risk of litigation and considered in defensive planning, such as the size of a project, the number of activities in a project, the planned duration of the project, and the types of activities in a project (Bixler et al., 2016; Mortimer et al., 2011; Stern et al., 2013). We used the cumulative area to account for the fact that multiple activities can occur in the same area throughout the course of the project. For example, through the duration of a project the same 100-acre unit can undergo a thin, followed by a second thin, and then a final clearcut, resulting in a cumulative area treated of 300 acres. We included size as both

categorical and continuous data. We also wanted to determine the effect of other temporal aspects of projects on a project's delay, so we included the project duration as planned and overlap. Here overlap refers to the number of days in which the date a NEPA decision was made may overlap with the earliest planned date of completion for an activity within a project (Table 2.1). Overlap is included as a numerical and a binary variable. We did not include project appeals. In 2012, the appeals process for USFS projects changed from a post-decisional appeal to a pre-decisional appeal meaning that for roughly half of the study period the appeals process would be captured in the time to complete a NEPA analysis (Consolidated Appropriations Act, 2012). We found no strong correlations between the project covariates included in this analysis (Table A.2).

**Table 2.2 Description of Project Characteristics**

<b>Variable Name</b>	<b>Description</b>
Project delay	The length of the delay in days before the first activity in a project was completed. This is the duration time, t.
Initiated?	Has the project been initiated? In this case, has at least one activity in the project been completed? This is the event of interest in the survival analysis. This is a binary variable
Region*	Forest Service administrative region.
NEPA type*	NEPA analysis type required for the project. Categorical Exclusion (CE), Environmental Assessment (EA), Environmental Impact Statement (EIS)
Elapsed days	The time in days to complete the NEPA analysis. From UMN-PALS dataset.
Planned project duration	The planned duration of a project in days.
Overlap*	Time in days from the NEPA decision to the earliest planned completion date for an activity in a project. Values $\geq 0$ overlap did not occur. Values $< 0$ overlap did occur.
Litigated?	Was the project litigated?
Size**	Cumulative size in acres
Number of activities in a project	The total number of planned activities within a project.
Percentage of activity type	The proportion of activity types that occurred within each project. Can be timber harvest (th), reforestation (rf), timber stand improvement (tsi), or hazardous fuels (hf).
* Indicates the variables also occurs as a “dummy” or binary variable.	
** Indicates the variable also occurs as a categorical variable.	

### Descriptive Statistics

We analyzed the PALS-ACT dataset for descriptive statistics of mean, median, and standard deviation for the project delay. This analysis was completed with the PALS-ACT data grouped by binary and categorical project characteristics: whether a project was litigated, overlap occurred, the NEPA analysis type, region, and relative size. For the relative size categories, we used the quartile ranges for the planned cumulative area treated for each project.

### Survival Analysis

Our application of survival analysis techniques is meant to make predictions on the probability of a project's continued delay using the Kaplan-Meier method, and determine the effect size of the project characteristics on a project's expectation of initiation using the Cox proportional hazards model. Survival analysis is a statistical technique that determines the probability of an event occurring within a duration of time and the effect size of different variables on the expectation, or likelihood, of that event occurring (Box-Steffensmeier and Jones, 1997; Miller, R. G., 2011). In this study, the event of interest was whether a project is initiated. The duration was the project delay in days. We kept right-censored projects (i.e. the event did not occur within the observation period) and calculated their project delay based on the end of the period of observation.

#### Kaplan-Meier Estimation

We determined a project's probability of continued delay, meaning the event of interest (initiation) has not occurred, as a function of a project's delay using the non-parametric Kaplan-Meier (KM) estimation (Kaplan and Meier, 1958). Initially, we estimated the probability functions, or curves, for the entire dataset. Then, we estimated

the probability curves for each of the binary or categorical project characteristics: litigation, overlap occurrence, NEPA analysis type, region, and relative size. The KM estimator is predictive, and the survival curves can be used to predict the probability of continued delay while the cumulative hazard curves can be used to predict the probability of initiation. The KM approach does not handle continuous variables well, which is why we created categorical relative size instead of the planned cumulative size. We used the log-rank approach to determine the difference between probability curves for different project groupings. The log-rank approach compares the KM life tables of different probability curves and assumes a null hypothesis in which there is no difference in the probability functions for each project characteristic (Miller, R. G., 2011). The log-rank approach uses a chi square measurement and p-value to reject the null hypothesis.

#### Cox Proportional Hazards Model

The Cox proportional hazards model is a semiparametric regression model that determines the effect a covariate has on the expectation of project initiation at any point in time (Cox, 1972). We used this method to determine the effect of project characteristics on project survival. The Cox model enables multiple types of covariates, including categorical and continuous data (Bewick et al., 2004). An assumption of Cox regression is that hazards for different groups of data are proportional. The hazard rates can change through time, but the ratios are assumed to remain proportional. The Cox model also assumes covariates do not change through time, as is the case for all of the covariates we considered. None of the covariates considered here are time dependent, the project's characteristics will not change. To determine which covariates to include in the Cox model we first ran a series of univariate regression models with each covariate. From

the univariate analysis we chose the covariates with likelihood ratio test p-values  $< 0.05$  to include in a multivariate regression model. The final model only includes those covariates that satisfy the Cox assumptions. Those potential covariates included whether the project required a CE NEPA analysis type, overlap occurrence, the number of days taken to complete the NEPA analysis (elapsed days), and the percentage of timber harvest and reforestation activities within the project. From the final Cox model, we report the beta coefficient, the hazard ratio, and the p-value covariate and level.

All analyses were completed in R (R Core Team, 2020) using the survival package (Therneau and Lumley, 2015), and plots were created using ggplot (Wickham, 2009). More detailed descriptions of the survival analyses can be found in the appendix (A3). Code for data downloading, processing, and the analyses are included in a GitHub repository.

## **Results**

### Descriptive Statistics

Results from the descriptive analysis can be found in Table 2.3 and Figure 2.3. For all projects the mean project delay was 397 days, and the median project delay was 197 days. For projects that experience an overlap between the record of decision and the minimum planned date, the median delay was 352 days while projects that did not experience the overlap had a median delay of 141 days. Litigated projects accounted for only 3.15% (112) of the total projects in the study, but they had a much longer median delay (323 days) than non-litigated projects (193 days). Projects requiring a CE had the shortest median delay (149 days), while projects requiring an EA or an EIS had longer median delays at 291 and 342 days, respectively. By region, the median delay ranged

from 120 to 227 days. Region 2 had the longest median (233 days), and region 4 had the shortest median delay (120 days). The median project delay for small projects was 136 days increasing to 259 days for extra-large projects. For an in-depth statistical analysis of the NEPA analysis type, litigation, and appeals (the UMN-PALS dataset) across all administrative regions, including temporal trends, see Fleischmann et al. (2020).

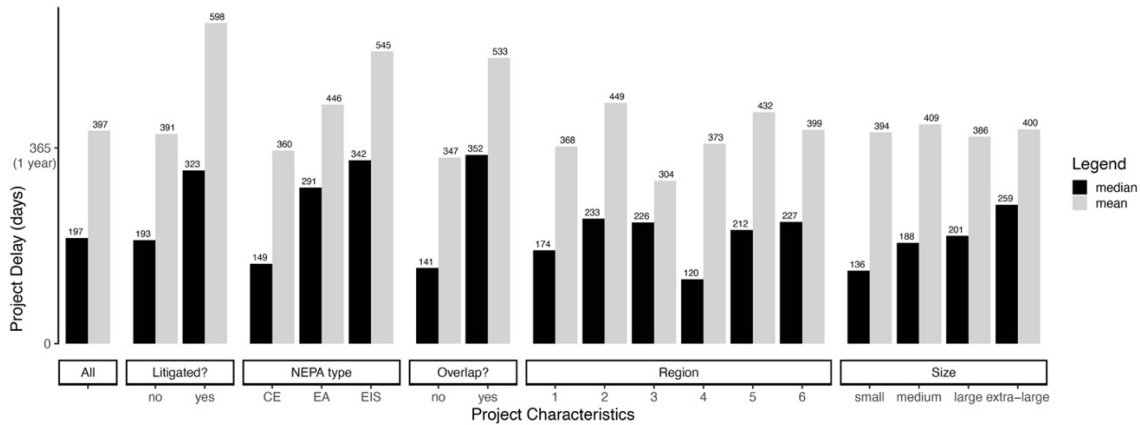


**Figure 2.3** Bar plot of the mean and median project delays for all projects considered in the study and grouped by project characteristic. In this study the median is a better measure of central tendency because there are a few projects that are extremely delayed which skew the mean. Mean, median, and standard deviation can be found in Table 3.

**Table 2.3 Descriptive Statistics of Project Delays (days)**

	<b>Mean</b>	<b>Median</b>	<b>Standard Deviation</b>	<b>Count</b>
All Data	397	197	447	3557
Overlap? No	347	141	604	2597
Overlap? Yes	533	352	635	960
Litigated? No	391	193	609	3445
Litigated? Yes	598	323	821	112
NEPA Type: CE	360	149	629	2266
NEPA Type: EA	446	291	557	1073
NEPA Type: EIS	545	342	744	218
Region: 1	368	174	569	538
Region: 2	449	233	745	455
Region: 3	304	226	456	301
Region: 4	373	120	661	540
Region: 5	432	212	654	928
Region: 6	399	227	541	795
Relative Size: Small	394	136	697	888
Relative Size: Medium	409	188	664	890
Relative Size: Large	386	201	582	888
Relative Size: Extra-Large	400	259	514	891

## Survival Analysis Results

### Kaplan-Meier Curves

The survival curves created using the KM estimation show the probability that a project will continue to be delayed at a given delay duration. The median probability of continued delay represents the point where a project has a 0.5 probability of initiation occurring (dashed lines in Figures 2.4 – 2.7). Table 4 shows the median probability of continued delay along with other probabilities. When the data was pooled for all projects, the median probability of continued delay occurred at 213 days (Table 2.4 and Figure 2.4). There were 325 projects that were not delayed, which was reflected in a vertical drop from a probability of 1.0 to 0.91 at time 0. After a one-year (365 day) delay, there was a slight vertical drop showing an increase in project initiation events (Figure 2.4). At an approximately three-year (1098 days) delay, a project that had yet to be initiated still had a probability of 0.10 (10%) of continued delay (Table 2.4).

**Table 2.4 Kaplan-Meier probabilities of continued delay**

<b>Time in Days for Various Probabilities of Continued Delay</b>						
<b>Probability</b>	<b>0.10</b>	<b>0.25</b>	<b>0.5 (Median)</b>	<b>0.75</b>	<b>0.90</b>	<b>Count</b>
All Data	1098	487	213	45	1	3557
Overlap? No	1004	413	149	30	0	2597
Overlap? Yes	1358	689	361	137	38	960
Litigated? No	1087	481	207	45	1	3445
Litigated? Yes	3354	669	374	83	14	112
NEPA Type: CE	1017	396	153	31	0	2266
NEPA Type: EA	1182	638	312	83	12	1073
NEPA Type: EIS	1422	719	365	130	21	218
NEPA = CE? No	1188	648	324	91	14	1291
NEPA = CE? Yes	1017	396	153	31	0	2110
Region: 1	1026	485	179	47	5	538
Region: 2	1233	539	245	41	0	455
Region: 3	608	363	245	53	2	301
Region: 4	1097	402	126	29	0	540
Region: 5	1254	520	228	51	8	928
Region: 6	1046	576	245	55	1	795
Relative Size: Small	1262	440	139	32	0	888

Time in Days for Various Probabilities of Continued Delay						
Probability	0.10	0.25	0.5 (Median)	0.75	0.90	Count
Relative Size: Medium	1133	528	204	41	1	890
Relative Size: Large	1123	472	224	46	2	888
Relative Size: Extra-Large	1004	525	272	77	10	891

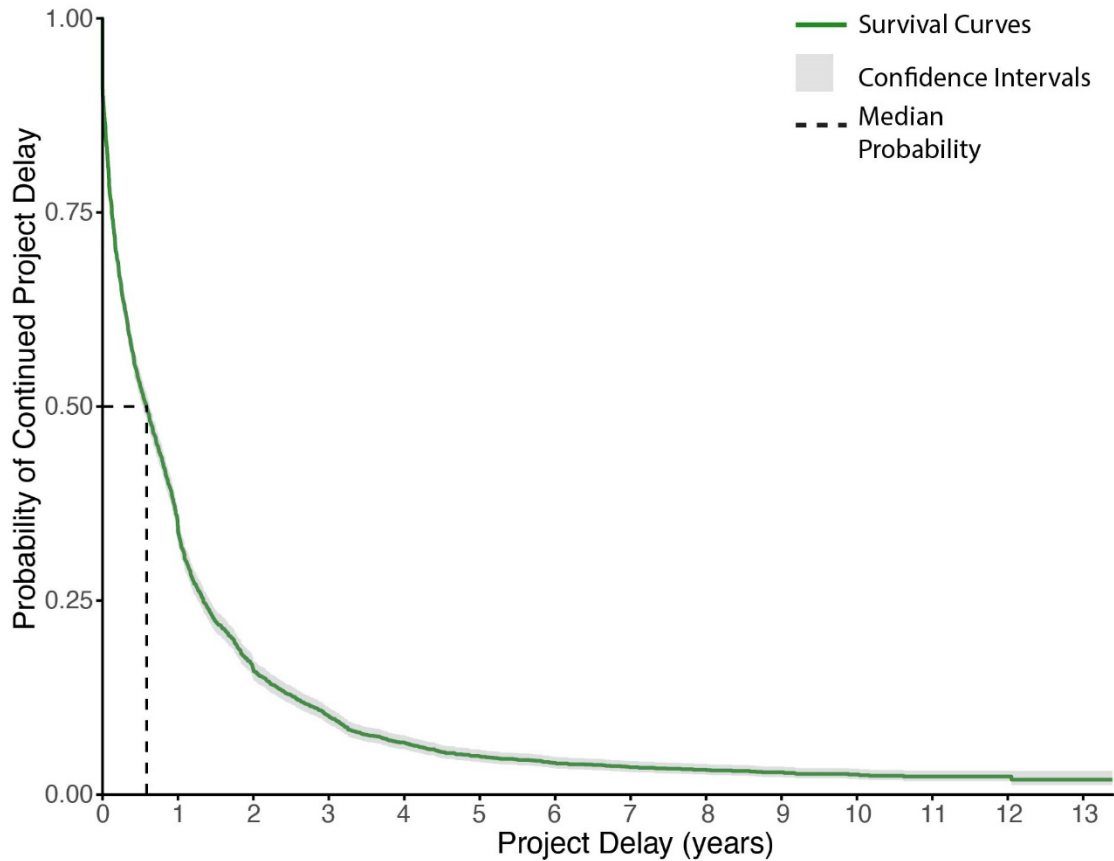


**Figure 2.4** Kaplan-Meier survival curve for all projects. In this study survival is equivalent to continued delay. The dashed line shows the median probability of continued delay where a project is just as likely to be initiated as it is to continue to be delayed. The sharp decrease in probability of continued delay at time zero implies that roughly 10% of projects experience no delay in initiation. A similar drop in probability occurs at roughly one year of delay. The curve flattens yet never reaches a probability of zero as some projects in the study are right censored (i.e. were not initiated by the end of the observation period, Dec. 31, 2018).

When the projects were grouped by NEPA analysis type, there was a distinction between the projects that required a CE and those that required an EA or EIS (Figure 2.5). The median probability of delay for a CE occurred at 153 days while for projects that required an EA or EIS the median probability of continued delay occurred at more than twice that of a CE (312 days and 365 days respectively). The curves for an EA and EIS were similar, and their confidence intervals overlapped. After a duration of approximately one year, the curves and confidence intervals for projects requiring an EA and EIS began to overlap with the curve and confidence interval for projects requiring a CE. When the NEPA analysis type CE was treated as a binary variable, the median probability for projects requiring a CE stayed at 153 days and increased to 324 days for projects that required an EA or EIS (Table 2.4).

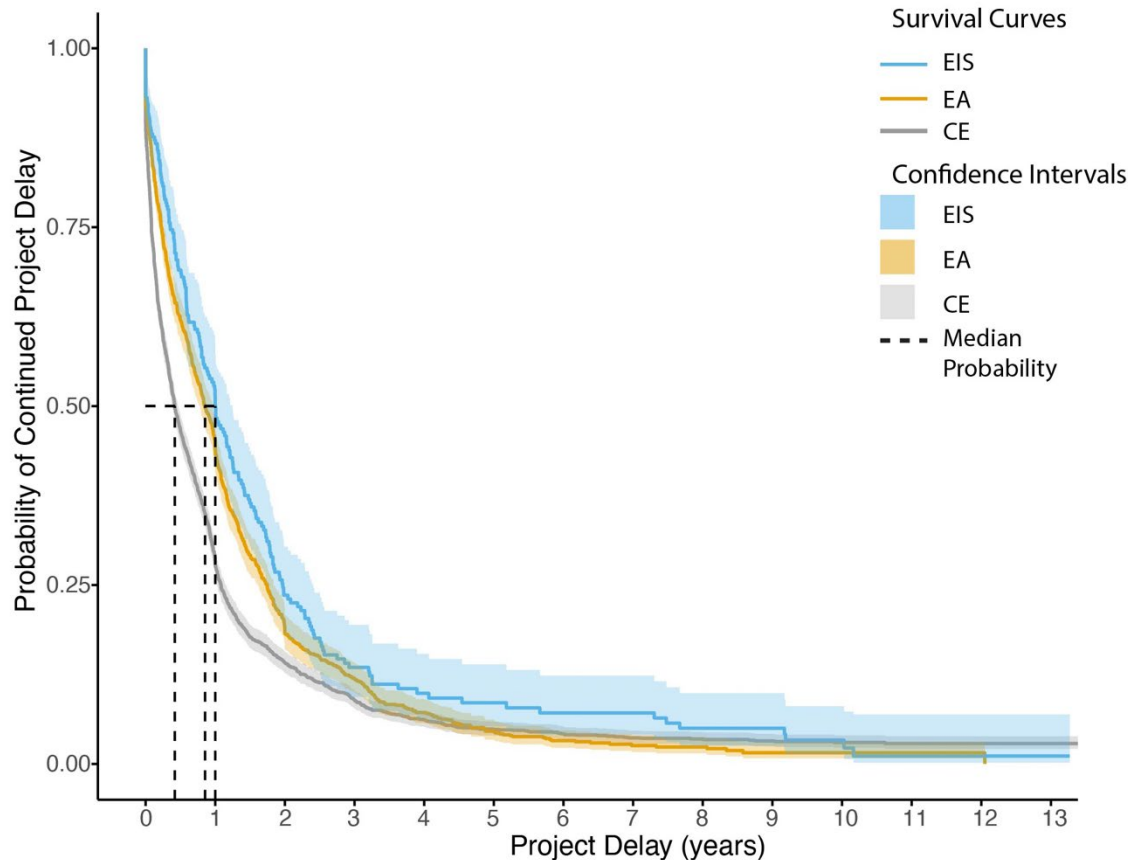


**Figure 2.5** Kaplan-Meier survival curves for projects grouped by NEPA analysis type, where survival indicates continuous delay. EIS and EA have a similar median delays (365 and 312 days respectively) which are twice as long as the median survival for projects that fall under a CE (153 days). Relatively few projects require an EIS leading to wide confidence intervals. Between two and three years the curves begin to converge, and the confidence intervals overlap.

Projects in which overlap occurred had longer median probability times than projects in which no overlap occurred (Table 2.4, Figure 2.6a). For projects with overlap the median probability of continued delay occurred at 361 days. Projects that did not experience overlap had a median probability of continued delay at 149 days. The probability curves crossed each other at approximately a six-year delay (2190 days) (Figure 2.6a). Projects that had undergone litigation had longer median probability times than those that had not faced such actions (Table 2.4). For litigated projects the median probability of continued delay occurred at 374 days, while for non-litigated projects the

median probability occurred at 207 days (Table 2.4, Figure 2.6b). The curves for litigated and non-litigated projects were visually different, yet after approximately a two-year (730 days) delay duration, the gap between the two curves decreased and then increased again (Figure 2.6b). Although the confidence intervals for the litigated project curve is quite wide, the confidence intervals for the two curves never overlap.

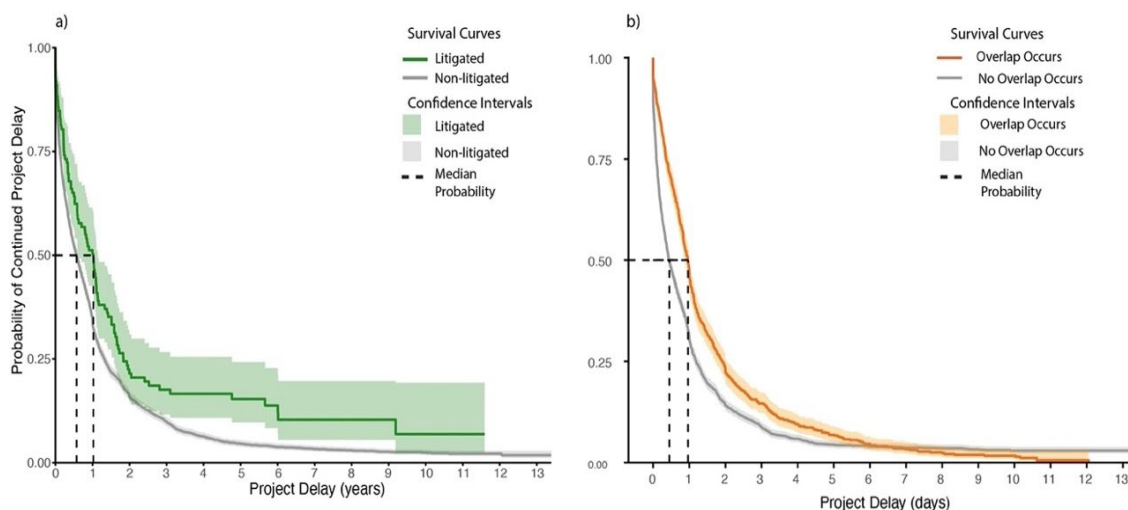


**Figure 2.6 Kaplan-Meier survival curves for projects grouped by litigation (a) and overlap occurrence (b). Litigation against USFS projects is uncommon leading to wide confidence intervals. The curve for litigated projects diverges from the curve for non-litigated projects, while the curves for overlap and no overlap in projects cross after a duration of 6.5 years. Both sets of curves for litigation and overlap show vertical drops in probability at approximately one year indicating a relatively large number of projects are initiated.**

For the projects grouped by region, the median probability ranged from 126 days (region 4) to 245 days for regions 2, 3, and 6 (Table 2.4). Once a project had been delayed approximately two years (730 days) there was little difference in the relationship between the duration of a project's delay and the probability of a project starting among the six regions except for region 3. When comparing probability curves with all the regions as binary variables, the most distinct curve occurred for region 3 (Figure 2.7). For projects occurring in region 3, there was a sharp decline in the probability curve at one

year (365 days), and the lower probabilities of delay (0.25 and 0.10) occurred earlier than the other regional variables (Table 2.4, A4).

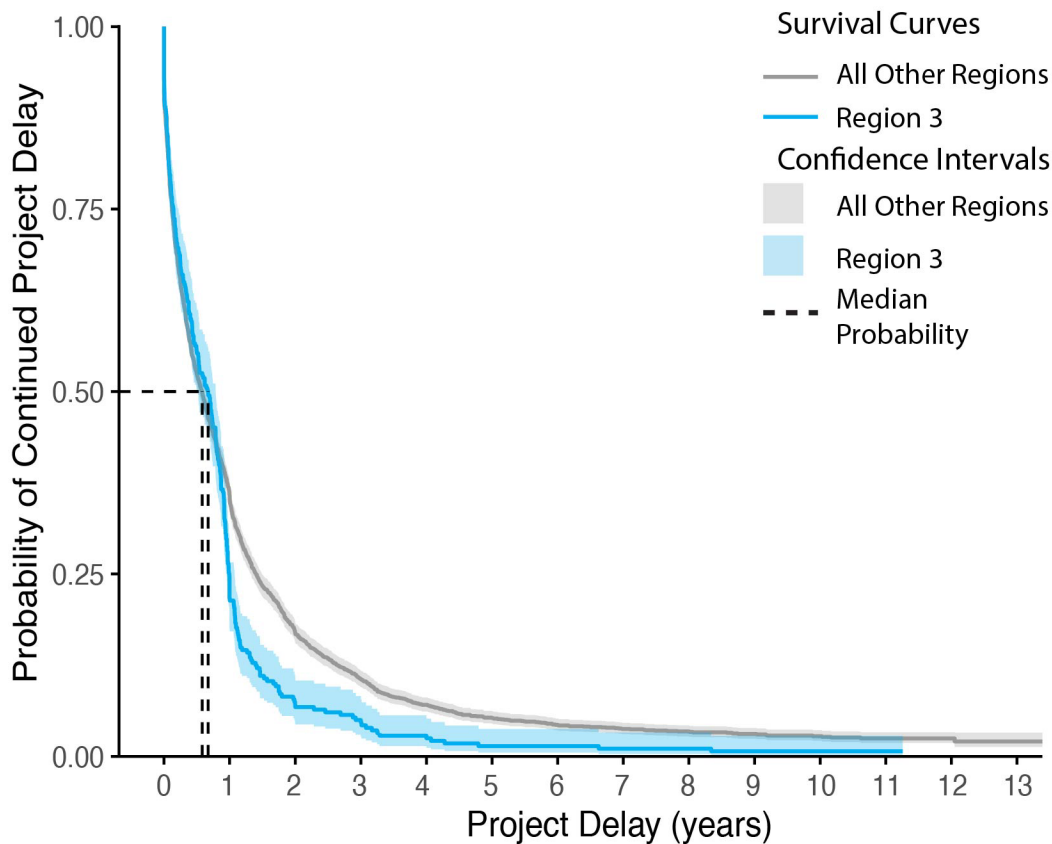


**Figure 2.7** Kaplan-Meier survival curves for projects grouped by projects in region 3 and projects in all other regions. The median probability of continued delay occurred at similar delay durations (dashed lines). The region 3 curve shows a very distinct increase in project initiation at an approximately one-year delay duration.

The median project probability of continued delay by size ranged from 139 days for small projects and 272 days for extra-large projects (Table 2.4). Once a project had been delayed approximately two years (730 days) there was little difference between the four size curves. To better capture the differences between the project size classes in the probability of continued delay we considered the inverse, the probability or expectation of project initiation, using the cumulative hazard plot (Figure 2.8). The cumulative hazard

plot showed that after three years, the extra-large project's expectation of project initiation increased relative to the other size classes (Figure 2.8).

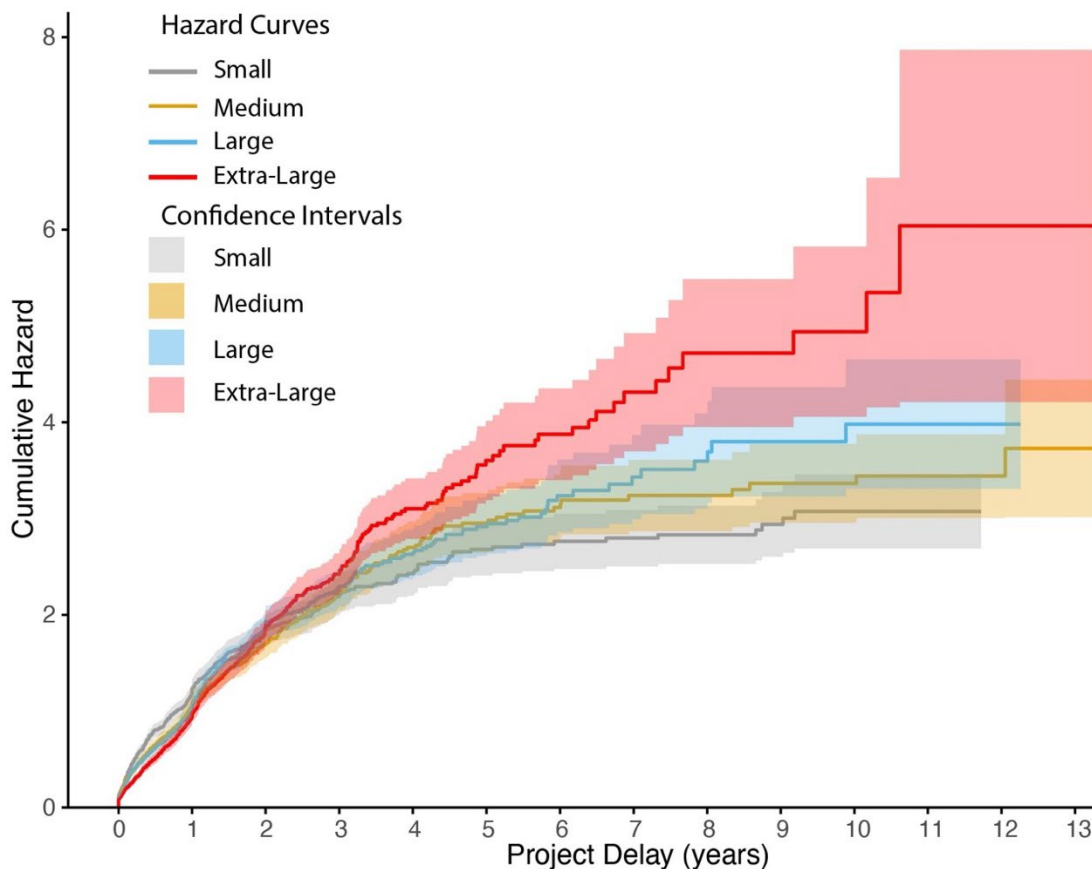


**Figure 2.8** Cumulative hazard curves for projects grouped by size. Survival curves can be found in the supplementary materials (A4). The curves for extra-large projects steepened relative to the other sizes after approximately two years of delay showing that extra-large projects are more likely to be initiated relative to the other project sizes with continued delay.

#### Kaplan-Meier Rank Tests

The results from the log-rank tests performed for each covariate group can be found in Tables 2.5a and 2.5b. From the log-rank tests, relative cumulative size was the only group of survival curves that did not reject the null hypothesis ( $p$ -value = 0.6). For all other curves, there was a significant difference ( $p < 0.05$ ) between the grouped survival curves (Table 2.5a). However, when the regional binary variables were used, region 3

was significantly different from the null hypothesis (p-value = 4e-04) while regions 4 and 5 showed a slight statistical significance (p-values = 0.01 and 0.02 respectively) (Table 2.5b). Regions 1, 2, and 6 did not reject the null hypothesis.

**Table 2.5a Kaplan-Meier Log-Rank Test Results**

	Overlap?	Litigated?	NEPA Type	Regions	Relative Size	NEPA = CE?
Chi squared	81.7	12.4	60.3	27.1	1	57.1
p-value	<2E-16	4E-04	8E-14	6E-05	0.6	8E-14
Degree of Freedom	1	1	2	5	3	1

**Table 2.5b Kaplan-Meier Log-Rank Test Results – Regions as Dummy Variables**

	Region 01	Region 02	Region 03	Region 04	Region 05	Region 06
Chi squared	1.7	3.4	12.6	6.4	5.5	1.9
p-value	0.2	0.06	4E-04	0.01	0.02	0.2
Degree of Freedom	1	1	1	1	1	1

#### Cox Proportional Hazards Model

We present the beta values, Wald test p-values, and likelihood ratio test p-values from the Cox univariate analyses in Table 2.6. Positive beta values indicate that as the covariate value increases the “risk” (here expectation) of initiation increases, while negative beta values indicate that as the covariate values increases the expectation of

initiation decreases. Covariates with positive beta values included: the NEPA type CE, the number of acres planned to be treated in a project, regions 1, 3, and 4, and the percentage of reforestation, hazardous fuels, and timber stand improvement activities within a project. Beta values were negative for all other covariates: a NEPA type of EA or EIS, litigation, the number of days to complete the NEPA analysis, the number of activities planned in a project, the planned duration of the project, the overlap in days and overlap occurrence, regions 2, 5, and 6, and the percentage of timber harvest activities within a project (Table 2.6). Using the Wald test and likelihood ratio test p-values, we found that litigation, the NEPA type CE, regions 3 thru 5, all percentage of activity types, the overlap in days and overlap occurrence, the elapsed days, the planned project duration, and the number of activities in a project all had p-values of  $<0.05$ . These covariates were all included in a multivariate Cox proportional hazards model (Table 2.7).

**Table 2.6 Results from the Cox univariate models**

	<b>beta</b>	<b>hazard ratio (95% CI)</b>	<b>Wald test</b>	<b>p-value (Wald)</b>	<b>p-value (LRT)</b>
Litigated? Yes	-0.37	0.81 (0.57-0.85)	12	0.00045	2.0E-04*
NEPA Type (dummy): CE	0.28	1.3 (1.2-1.4)	57	4.2E-14	2.1E-14*
NEPA Type (dummy): EA	-0.21	0.81 (0.75-0.88)	30	4.8E-08	3.2E-08**
NEPA Type (dummy): EIS	-0.32	0.69 (0.63-0.84)	18	2.3E-05	9.0E-08**
Region (dummy): 1	0.063	1.1 (0.97-1.2)	1.7	0.2	0.2
Region (dummy): 2	-0.096	0.91 (0.82-1)	3.2	0.072	0.068
Region (dummy): 3	0.22	1.2 (1.1-1.4)	12	0.00045	0.00064*
Region (dummy): 4	0.12	01.1 (1-1.2)	6.4	0.011	0.012*
Region (dummy): 5	-0.094	0.91 (0.84-0.98)	5.6	0.018	0.017*
Region (dummy): 6	-0.057	0.94 (0.87-1)	1.9	0.17	0.17
Activity type (%): th	-0.98	0.37	170	2.3E-38	2.6E-43*

	<b>beta</b>	<b>hazard ratio (95% CI)</b>	<b>Wald test</b>	<b>p-value (Wald)</b>	<b>p-value (LRT)</b>
		(0.32-0.43)			
Activity type (%): rf	0.99	2.7 (2.3-3.1)	170	1.0E-39	1.7E-32*
Activity type (%): hf	0.16	1.2 (1-1.3)	7.9	0.0051	0.0049*
Activity type (%): tsi	0.21	1.2 (1-1.5)	6.2	0.013	0.015*
Overlap (days)	- 0.00016	1	49	2.7E-12	7.3E-12*
Overlap (dummy)	-0.35	0.7 (0.65-0.76)	82	1.5E-19	1.9E-20*
Elapsed days	- 0.00032	1	47	8.4E-12	9.7E-13*
Planned project duration	-2.9E-05	1	4.4	0.036	0.035*
Planned size	-0.35	1	0.02	0.89	0.89
Number of activities	-0.35	1	6.4	0.012	0.0079*

Within the larger multivariate model, several of the covariates failed to uphold the Cox assumptions (A5). Therefore, the final model included only those covariates that upheld the Cox assumptions: the NEPA CE binary variable, overlap occurrence, the elapsed days, and the percentage of timber harvest and reforestation activities within the

project. A summary of the beta, hazard ratios (with confidence intervals), and p-values for the final Cox model are found in Table 2.8. From the c-log-log test we determined that the categorical covariates from the final model conform to the proportionality assumption (A5). However, at the end of the observation period the hazard ratios no longer maintain proportionality due to the small number of projects yet to be initiated.

**Table 2.7 Results from the larger Cox proportional hazards multivariate model**

<b>Covariate</b>	<b>beta</b>	<b>hazard ratio (95% CI)</b>	<b>p-value (LRT)</b>
Litigated? Yes	-1.3	0.88 (0.72-1.1)	0.24
NEPA Analysis Type (dummy): CE	0.1	1.1 (1.0-1.2)	0.028*
Region (dummy): 3	0.078	1.1 (0.95-1.2)	0.23
Region (dummy): 4	0.043	1.0 (0.94-1.2)	0.41
Region (dummy): 5	-0.065	0.94 (0.86-1.0)	0.13
Activity type (%): th	-0.96	0.38 (0.31-0.47)	<2E-16***
Activity type (%): rf	0.89	2.4 (2.0-3.0)	<2E-16***
Activity type (%): hf	-0.026	0.97 (0.82-1.2)	0.77
Activity type (%): tsi	NA	NA	NA
Overlap (days)	-0.43	1	0.54
Overlap (dummy)	-1.8E-05	0.65 (0.59-0.71)	<2E-16***
Elapsed days	-0.00012	1.0	0.02*

<b>Covariate</b>	<b>beta</b>	<b>hazard ratio (95% CI)</b>	<b>p-value (LRT)</b>
Planned project duration	-2.5E-06	1	0.88
Number of activities	0.00018	1	0.13

From the final hazard ratios of the final model, the occurrence of overlap and the percentage of the project that consisted of timber harvest activities (% th) had negative beta values and very low p-values. The percentage of a project that consisted of reforestation activities (% rf) had a positive beta value and a very low p-value. A project requiring a CE had a positive beta value and a p-value of 0.045, while the amount of time required to complete the NEPA analysis (elapsed days) had a negative beta value and a p-value of 0.014 (Table 2.8).

**Table 2.8 Results from the final Cox proportional hazards multivariate model**

<b>Variable</b>	<b>beta</b>	<b>hazard ratio (95% CI)</b>	<b>Wald test</b>	<b>p-value</b>
NEPA Type (dummy): CE	0.086	1.1 (1.0-1.2)	2.0	0.045
Activity type (%): th	-0.98	0.38 (0.33-0.45)	-12.4	<2E-16
Activity type (%): rf	0.99	2.5 (2.2-2.9)	12.2	<2E-16
Overlap (dummy)	-0.44	0.64 (0.60-0.69)	-11.2	<2E-16
Elapsed days	-0.00013	1.0	-2.5	0.014

### **Discussion**

Our study aimed to: (a) quantify the mean and median delay length from planned to actual implementation of USFS projects in the western United States; (b) determine the impact of a project's delay duration on the probability of continued delay; and (c) determine the impact of various project characteristics on the expectation of a project's initiation. Our research showed that the median project delay was longer for projects that faced legal challenges, required more detailed NEPA analyses, experienced overlap, and had a larger cumulative size. Through this study we determined that the median probability of continued delay occurred at a later delay duration for projects in which overlap occurred, that required more detailed NEPA analyses (EAs and EISs), were litigated, or occurred in either regions 3, 4, or 5. Finally, we found that whether a project

was a CE, encountered overlap, had a longer time to complete the NEPA analysis, and the percentage of timber harvest or reforestation activities within the project had a significant impact on the expectation of project initiation.

### Factors Influencing the Probability of Delay

We address two findings from the Kaplan-Meier survival curves that may be of interest to managers and for future study. First, we noted a significant drop in continued delay probability at the start ( $t = 0$  days) and at one year ( $t = 365$  days). The vertical drop at  $t = 0$  days occurred because 9.1% ( $n=325$ ) of projects experienced no delay, and this implies that many projects are initiated on time and with no delay (Figure 2.3). The less pronounced vertical drop at  $t = 365$  days may reflect an administrative or budgetary process that encourages project initiation after one year of delay. This vertical drop at one year is very pronounced in region 3 (Figure 2.7). Region 3 (Arizona and New Mexico) was unique compared to the other regions in the study in that it completed the fewest NEPA analyses, the fewest EIS, and took the longest time to complete those analyses (Fleischmann et al., 2020). In the early 2000s this region also had the least number of appeals, although the number of legal challenges was similar to other regions (Keele and Malsheimer, 2018; Laband et al., 2006; Malsheimer et al., 2004). One hypothesis that might explain this finding is that the longer time spent preparing NEPA analyses leads to projects that are more easily implemented as planned and are less likely to be litigated (Ruple and Race, 2020; Ruple and Tanana, 2020). However, this does not explain the increase in project initiations at a delay duration of one year. This increase may be the result of an administrative process more commonly used in region 3 and is worthy of further research.

Second, the KM curves mostly flattened and converged after two to three years of delay duration (Figures 2.4-2.7). The probability of continued delay was low after the two-to-three-year delay duration, however, flattening and convergence implied that the probability of continued delay does not change regardless of the project's characteristics. These projects with prolonged delays may be truly exceptional projects which were held up for years due to litigation, or these projects may be delayed due to extenuating circumstances such as a larger disturbance. Another possibility is that these projects may have some flexibility written into the plan. For example, purchase contracts for timber harvest may have up to five years to implement a harvest. Additionally, as priorities are anticipated to shift, work on some forests can have a buffer of several years to implement projects. For those projects with exceptional delays, understanding that after a certain point the probability of continued delay does not decrease may encourage some managers to redesign a project even though the planning process can take several years.

From the hazard ratios of the final multivariate Cox model, the occurrence of overlap and the percentage of the project that consisted of timber harvest activities (% th) most significantly increased the time to initiation for a project. The percentage of a project that consisted of reforestation activities (% rf) most significantly decreased the time to project initiation. To a lesser extent, a project requiring a CE decreased the time to project initiation, while the amount of time required to complete the NEPA analysis increased the time to initiation of the project (Table 2.8).

Environmental regulations and litigation are commonly perceived to negatively impact forest management through delays. Alternatively, others view these regulations as vital to environmental protection and view delays through litigation as a valuable "time-

out” for contentious projects (Nie, 2008). When considered by itself, litigation did have a significant impact on the expectation of initiation within the Cox univariate model (Table 2.6) and was significant for the probability of continued delay (Table 2.5). However, here we found that litigation did not have a significant impact on the expectation of initiation compared to other project characteristics when considered in a multivariate model ( $p$ -value  $> 0.05$ , Table 2.7). Litigation is very rare (Fleischman et al., 2020; Ruple and Race, 2020), and while it may significantly impact the likelihood of initiation for a small percentage of projects, here we found that litigation was not as significant as the type of NEPA analysis required or the types of activities in a project.

The time to complete a NEPA analysis (elapsed days) and length of an overlap had a significant effect on the probability of continued delay and the expectation of project initiation. For all the projects, 22% of them experienced overlap. For projects requiring an EIS, 31% experience overlap. This was not surprising, Fleischmann et al. (2020) found that EIS analyses take longer to complete than the analyses for EAs and CEs. For litigated projects, 34% experienced overlap, and two thirds of these projects required either an EA or EIS. Again, given that more EIS and EA were litigated than CEs, this overlap was not surprising (Fleischman et al., 2020). A longer time to complete the NEPA analysis or litigation can lead to overlap, and overlap itself was a measure of delay, however, no collinearity was found between these variables (A2). Even though overlap may have occurred, the difference between the planned date of completion and the actual date of completion for the earliest project may not have been large. However, overlap may have led to a ripple effect in the implementation process as resources or

priorities may have shifted in the forest during the planning process accounting for the negative impact on the expectation of initiation.

### Limitations

Survival analysis is a useful methodology when the variable of interest, in this case a project's delay, is a duration. One strength, but also a limitation, of using the KM approach is that it is most useful for grouped or categorical data. Because of this limitation, continuous data in our study was grouped in a way that may be limiting, such as categorizing the cumulative size. Additionally, this study included quite different management activities lumped into broad categories which may not have allowed for the best comparisons. For example, site prep for natural regeneration, which is a reforestation activity, may require much less time and resources compared to a commercial thin, which is a timber harvest activity, or a prescribed burn, which is a hazardous fuels activity. Even within the broad activity types there can be a difference in the amount of time and tools required to complete the activity. Many national forests share resources, meaning that the large, regional scale and activity categories used in this study may not capture important aspects of project implementation in the KM approach, such as limitations to equipment or operating timber mills for timber sales.

While this study was able to quantify median delays, examine the impact of project characteristics on the probability of continued delay and the expectation of initiation, we only investigated specific project activities related to timber harvests in the western US (administrative regions 1-6). USFS projects can consist of many other activities not included in this study, such as road maintenance or facilities construction. The project delays shown here may not represent an entire project but were deemed the

most important as these activities directly impact the vegetation of the land surface by the removal or addition of trees. This study may not be representative of all national forests, but most of the national forests are within the western US, and the implementation of forest management treatments are vital to forest health in the face of the increasing drought and forest fires these regions are experiencing (Bottero et al., 2017; Graham, R.T., 1999; Sohn et al., 2016).

### The Consequences of Project Delays

Much hand wringing concerning environmental regulations and litigation can occur at the state and Federal policy levels (Congressional Western Caucus) and even at the agency level as seen in the defensive planning used to make EAs or EISs difficult to challenge in court or completing EISs in lieu of EAs and EAs in lieu of CEs (Bixler et al., 2016; Mortimer et al., 2011). However, defensive planning is working by keeping litigation rare. These environmental laws and regulations serve an important purpose and were created in such a way to allow for public participation through collaboration or through the courts (Nie and Metcalf, 2016). Case studies can show both the negative economic impact of litigation against USFS projects (Morgan and Bladridge, 2015 citing a timber harvest project in Montana) or the positive impact of environmental regulations on Federal lands to local economies (Ruple and Tanana, 2020, citing examples from oil and gas on Bureau of Land Management land).

Regardless of the potential economic outcome of regulations, the environmental cost of inaction through delays remains uncertain. Some activities can only happen during certain seasons (e.g. restoration activities), after work by other agencies is complete (e.g. after wildlife surveys), or within a certain time frame post-disturbance

(e.g. salvage logging). For the USFS, these constraints lead to logistical challenges and may necessitate the need for flexible, multi-year time frames for implementation to occur. A quantitative understanding of project delays, their length, and their probability of continuing could help to guide management maneuvers. Additionally, this quantitative understanding can inform future work to determine the potential impact of management delays on metrics of forest structure and function, such as stem density or net primary productivity.

### Future Work

The potential impact of delays on forest health, especially in the face of global change, is uncertain. Land surface models (LSMs) can be used to address this uncertainty as they are important tools for simulating and predicting the water, energy, and carbon budgets of the terrestrial earth's surface and incorporate increasingly complex representations of human activities like forest management (Bonan et al., 2016; Fisher and Koven, 2020). Improving the current representation of forest management activities within these models will aid in understanding the ecological impact of project delays within forested ecosystems (Huang et al., 2020; Littleton et al., 2020). This work provides evidence that the temporal aspects of forest management can be quantified from extant datasets in ways that would allow their parameterization in these models. The results can inform future modeling scenarios to test the timing of forest management activities on the carbon, energy, and water budgets at various scales and concomitant implications for regional impacts on climate, hydrology, and carbon stocks.

This study could provide a useful starting point for more generalizable national scale studies or studies that include more management objectives and activities, such as

those related to recreation or grazing. Reducing the spatial scale from the regional level to the national forest or even the forest district level and including other spatial covariates such as the number, size, and proximity of forests to forest fires could show how sharing or diverting resources for wildfire suppression could impact delays. Including information about the number of public comments received, the number of visitors to a forest, or even the proximity of urban areas could highlight the impact of public involvement or interest on project delays. Additionally, previous researchers found a correlation between project litigation and the time to complete a NEPA analysis with Federal executive administrative cycles (Fleischmann et al., 2020; Keele and Malmshemer, 2018). Including administrative cycles in future work could reveal their potential influence on USFS project delays as well as contribute to a better understanding of the temporal trends in USFS project planning and implementation.

Given the many layers of human decision making that goes into forest management, there are numerous reasons why a project could be delayed. A mixed methods approach to qualitatively explore other causes of delays (outside of those discussed here) and the use of delays as a tool by various forest stakeholders would provide valuable insight into potential mechanisms to decrease unintentional delays. Delays can be viewed as unavoidable or even a necessary part of adaptive management. For example, in the case of a disturbance such as a wildfire, a salvage project may have to take priority over another project in the same or neighboring National Forest. Forest managers must also consider other environmental aspects of the planned activities within a project. Some activities can only be performed during certain seasons or after wildlife surveys are completed (Bradford et al., 2018; Field et al., 2020). Unplanned seasonal

delays, such as weather impacts on the supply chain for timber could also play a role in a project's delay (Rönnqvist et al., 2015). Legal challenges can be used by special interest groups to delay projects or activities those groups may deem as unnecessary or not following the law or legal requirements (Keele and Malmshemer, 2018; Malmshemer et al., 2004; Nie, 2008; Stern et al., 2013; Teich et al., 2004). Identifying how these interacting processes impact forest management may provide insights to the types of interventions or policy changes needed for forest management.

### **Conclusions**

The main motivations of this study were to address uncertainty in the temporal aspects of forest management by quantifying project delays in a way that may be useful both for forest managers and for land surface modelers. This study quantified the relative impact of various project characteristics on the probability of continued delay and the probability of initiation. We found that the type of activities planned for a project had a statistically significant effect on the expectation of project initiation, much more so than litigation. There are many potential causes for delays to project initiation, and our results here imply that a focus of environmental regulation and litigation may be overemphasized.

## CHAPTER THREE: THE LONG-TERM IMPACTS OF FOREST MANAGEMENT TIMING ON FOREST STRUCTURE AND FUNCTION

### **Introduction**

Forests provide numerous benefits to life on earth, but changes to disturbances from shifting fire regimes and an increase in the length and severity of drought all stress forest health and vitality (Field et al., 2020; Westerling et al., 2006). The impact of these stressors is already being observed within the forests of the western United States. Tree mortality and forest die-off events due to an increase in severe fires, prolonged droughts, and mountain pine beetle outbreaks have occurred from Colorado to California.

Nearly 20% of forests in the United States are managed by the US Forest Service (USFS) (Oswalt et al., 2019). The objectives of this management have transformed through time from managing forests for increased timber growth and yield to managing forests for multiple uses (Wilson, 2014). With this increase in stress from changes to disturbance regimes, management has again shifted to managing for increased forest resistance and resilience forests (North et al., 2022). However, human management also acts as a disturbance with potentially far-reaching impacts on regional and global water, energy, and carbon cycles through the role of forests in land-atmosphere interactions (Bonan, 2008; Bonan and Doney, 2018; Swann et al., 2018). Land surface models (LSMs) offer an opportunity to examine the impact of disturbances, both natural and human driven, on land surface processes. However, incorporating land changes caused by

human intervention, specifically forest management, is a continuing challenge in land surface models.

Various modeling schemes now exist that aim to integrate vegetation dynamics into land surface models (Fisher et al., 2015; Fisher et al., 2018; Medvigy et al., 2009; Sato et al., 2007; Smith et al., 2001). The Functionally Assembled Terrestrial Ecosystem Simulator module of the Community Land Model (FATES-CLM) uses the cohort approach to represent vegetation and capture the plant competition in computationally efficient way (Fisher et al., 2018; Moorcroft et al., 2010). Within FATES-CLM, Huang et al. (2020) have developed a selective logging module to represent a variety of logging practices at a landscape level. In the selective logging module, the timing and spatial extent of a logging event can be set. Additionally, the selective logging module calculates the fraction of trees damaged during the logging process, assigns a calculated survivorship to the remaining trees within the disturbed area, and removes harvested material from the area by updating coarse woody debris and litter pools (Huang et al., 2020). To date, the selective logging module has been parameterized and tested only within tropical Amazon forests, but it shows promising results for simulating changes to the energy, water, and carbon budgets and forest structure and composition after logging events (Huang et al., 2020). A new vegetation management scheme is in development which captures the same carbon removal as the selective logging module but allows for users to specify multiple management activity types at multiple timesteps in the model (Rady and FATES, 2022; Rady et al., 2022).

Even with the improvements in representing plant dynamics and incorporating more detailed plant management into LSMs, few studies using these models account for

the temporal aspects of forest management activities. For example, in Huang et al. (2020), the logging activities (i.e. timber harvest) occurred at one timestep. In reality, forest management projects are temporally complex due to internal project complexity and external project complexity. Within projects, logging activities are a part of larger projects that can take several years to complete. Outside of projects, there is temporal complexity due to delays in project implementation. The length of time between activities within a project and a delay to project implementation may have important implications for the long-term impact of forest management on forest health, structure, as well as surface energy, water, and nutrient fluxes.

For this study our objectives were twofold. First, we wanted to investigate the impact that the timing of timber harvests can have on forested ecosystem structure and function. More specifically, would the delay of a timber harvest project impact the structure, productivity, and hydrological fluxes of the forest and for how long post-harvest? Second, we sought to determine the need for including more detailed and realistic management practices within vegetation demography models. By addressing these objectives, we aim to test the functionality of including more detailed forest management timing into land surface models. To better understand these implications, we employed a novel and temporally detailed representation of forest management practices within the FATES-CLM vegetation management module based on USFS timber harvest project data from Idaho (Rady and FATES, 2022). We found that including the temporal details of management in simulated logging scenarios led to long term changes in forest structure, while the timing of management had little long-term impact on changes to forest productivity.

## Methods and Materials

We used the vegetation management driver (Rady and FATES, 2022) within the FATES to simulate six logging scenarios within a hypothetical ponderosa pine forest in southern Idaho. In addition to a control simulation with no logging we simulated the following scenarios: (a) a clearcut logging treatment occurring at a single date (CC), (b) selective logging occurring at a single date (SLS), (c) selective logging occurring at multiple dates (SLM), (d) the multi-date logging scenario delayed by 291 days (SLD-EA, median delay for projects requiring an environmental assessment) , and (e) the multi-date logging scenario delayed by 120 days (SLD-R4, median delay for projects occurring in USFS Region 4 which contains southern Idaho, Nevada, and Utah), and (f) the multiple date logging scenario repeated every 15 years (SLR). We compared modeled outputs of structural variables, size class distributions (number of individuals per hectare), basal area (BA) ( $\text{m}^2/\text{ha}$ ), the area of trees per grid cell (fraction), leaf area index (LAI,  $\text{m}^2/\text{m}^2$ ) and aboveground biomass (AGB,  $\text{kgC}/\text{m}^2$ ) from the selective logging and clearcut scenarios to the control scenario and from the multi-date selective logging scenarios (SLM, SLD-EA, SLD-R4, and SLR) to the single date selective logging scenarios (SLS). We made the same comparisons of modeled outputs of the following functional variable rates: gross and net primary production (GPP and NPP,  $\text{gC}/\text{m}^2\text{s}$ ), evapotranspiration (ET,  $\text{mm}/\text{s}$ ), surface runoff (QR,  $\text{mm}/\text{s}$ ), and infiltration (QIN,  $\text{mm}/\text{s}$ ).

### Model Overview

FATES is a size and age structured vegetation model developed after the individual plant and forest disturbance ecosystem demography (ED) model of Moorcroft et al. (2001) with the individual trees scaled to the forest level canopy using the perfect

plasticity approximation of Purves et al. (2008). Spatially, FATES is constructed of patches which can contain multiple cohorts, the number of which can change through time. Following the ED approach, the growth and mortality of plants are tracked through cohorts of similar size and disturbance history. New cohorts are formed through recruitment and cohorts are reduced through natural mortality and disturbance events such as fire and logging. If individual trees in the cohort become too dissimilar then the cohort is split, and if cohorts become more similar, then they are fused. This splitting and fusing of cohorts and the dynamic nature of patches leads to spatial ambiguity within FATES. Meaning, a patch in FATES only refers to a fraction of the potentially vegetated area consisting of all parts of the ecosystem with similar disturbance history. Following the PPA approach, cohorts can either be classified within discrete levels of the understory or within the canopy. Through growth and mortality, a cohort's canopy location is also flexible and dynamic.

Cohort growth rates are determined by their carbon use. At the leaf level, carbon assimilation through photosynthesis is based on the amount of solar radiation which is determined by the canopy level of a tree and by climate and water availability. The assimilated carbon is then allocated to different plant organs for growth. FATES mortality is controlled by an adjustable background mortality rate, but mortality can occur through physiological causes such as carbon starvation or hydraulic failure as well as disturbance events such as fires and logging. Physiological processes (e.g., photosynthesis, respiration, and transpiration) are computed on half-hourly time-steps and are referred to as “fast processes”, while growth, mortality, recruitment, and disturbance are computed on daily time-steps and are referred to as “slow processes”.

These vegetation processes are coupled with the land and atmosphere within a “host” land model. In this study we used FATES coupled with the Community Land Model version 5 (CLM, Lawrence et al., 2019). For a more detailed description of the FATES model please see Fisher et al. (2015), Koven et al. (2020), and the FATES technical documentation online at [10.5281/zenodo.3517271](https://zenodo.org/record/3517271). For CLM, see Lawrence et al. (2019) and the CLM technical documentation online at [https://escomp.github.io/ctsm-docs/versions/release-clm5.0/html/tech\\_note/index.html](https://escomp.github.io/ctsm-docs/versions/release-clm5.0/html/tech_note/index.html).

### The Logging Module

The selective logging module within FATES simulates the effects of logging on the biogeophysical and biogeochemical processes within a forested ecosystem (Huang et al., 2020). Within the selective logging module, the user sets the timing and spatial extent of a logging event. The module calculates the fraction of trees damaged during the logging process, assigns a calculated survivorship to the remaining trees within the disturbed area, and removes harvested material from the area by updating coarse woody debris and litter pools (Huang et al., 2020).

Within the selective logging module, the user controls the timing of logging activities through the same parameter file used for specifying plant traits. This creates a technical difficulty in running logging scenarios with multiple events, especially if those events occur within relatively quick succession (e.g., within the same year or month). Here we used a new vegetation management driver developed by Rady and FATES (2022) which solves these technical difficulties to run our logging scenarios. The new driver provides more efficient logging simulations by allowing the user to set multiple logging dates. The driver also contains options for other vegetation management practices

such as thinning, clearcutting, and planting trees and allows for these practices to occur at different rates for different plant types. However, unlike the selective logging module, the vegetation driver does not include the indirect damage and mortality caused by the logging process. These parameters and values associated with indirect damage are not well defined for many locations. (For more information about the Vegetation Management Module please see the active documentation at [https://joshuarady.github.io/VegetationManagement/.](https://joshuarady.github.io/VegetationManagement/))

### Model Setup and Experimentation

#### Location Description

We simulated a ponderosa pine (*Pinus ponderosa*) dominant forest for a single grid cell in southern Idaho at the Boise Basin Experimental Forest (BBEF, Figure 3.1). We chose this site because of the availability of diameter and height data for parameterizing allometric relationships. This grid cell was approximately 15.5 km<sup>2</sup> and at approximately 1300 m elevation. The climate in the area could be considered semi-arid or Mediterranean with warm, dry summers and cool, wet winters. Temperatures here range from -4 °C in the winter to 19 °C in the summer and has average annual precipitation of 635 mm which mostly falls from October through June (Graham and Jain, 2004), with a large fraction falling as snow in the winter. Soils in the area are granitic and have a pH ranging from 5.5 to 7.0 (Graham and Jain, 2004).

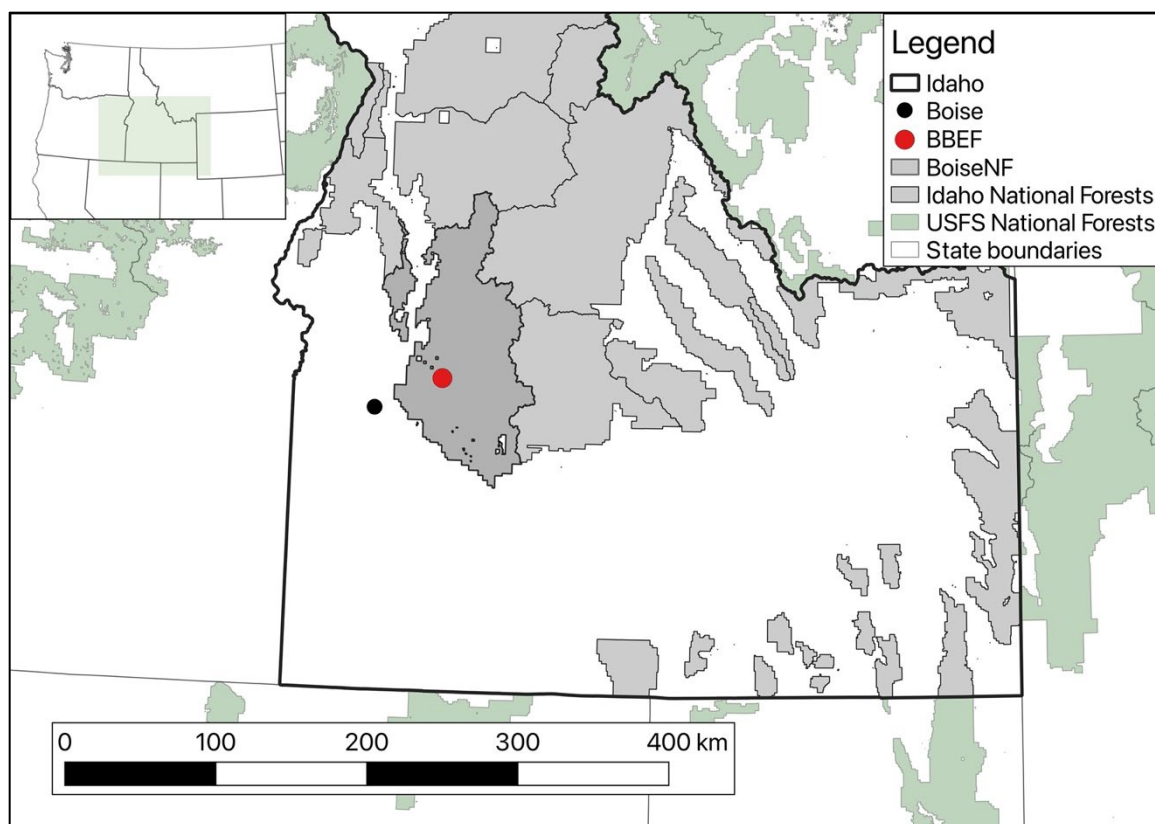


**Figure 3.1** Location map for the single point scale at the Boise Basin Experimental Forest (BBEF, red circle).

#### Model Setup and Plant Parameterization

For these simulations we used the multivariate adaptive constructed analogs downscaled dataset from the Climate Research Unit and National Centers for Environmental Prediction (CRUNCEP, Mitchell and Jones, 2005) climate data from Buotte et al. (2019) hereafter referred to as the MACA climate data. This dataset was downscaled to a 4 km-by-4 km, 3-hourly resolution from the daily climate data generated by Abatzoglou, 2013 (Buotte et al., 2019, SI Appendix 2). We recycled 35 years of the MACA data from 1979-2014 throughout the simulations to obtain total simulation times of 310 years.

We modified the default FATES evergreen needleleaf tree plant functional type (PFT) parameter values to better represent the ponderosa pine physiology of the western

US. The model was calibrated by running multiple parameter iterations as separate simulations. We compared modeled results of leaf area index (LAI) and gross primary productivity (GPP) to MODIS derived LAI and GPP and modeled aboveground biomass (AGB) to AGB maps derived from Forest Inventory and Analysis (FIA) data (Wilson et al., 2013). Trees must grow to at least 15 cm diameter at breast height (DBH), as this is generally the minimum size harvested in Idaho (Simmons et al., 2014). Our final parameter file consisted of updated values for: wood density, maximum tree height, initial seedling density parameter, the nitrogen stoichiometry values for the C:N leaf ratio, and the DBH to height allometry parameters optimized using the allometry equation from O'Brien et al. (1995) (Table 3.1). We used height and diameter data of ponderosa pines from the biomass and allometry database (BAAD, Falster et al., 2015) as well as Boise Basin Experimental Forest (BBEF) specific DBH and height data and the “curve\_fit” function in Python (Virtanen et al., 2020) to optimize the two parameter values in the height to DBH allometric equation.

**Table 3.1 List of Updated FATES Parameter Values**

<b>Parameter name</b>	<b>Description</b>	<b>Value</b>
fates_wood_density	Mean density of woody tissue in plant	0.367 g/cm <sup>3</sup>
fates_allom_DBH_maxheight	The diameter (if any) corresponding to maximum height, diameters may increase beyond this	250 cm
fates_recruit_initd	Initial seedling density for a cold-start near-bear-ground simulation	0.08 stems/m <sup>2</sup>
fates_prt_nitr_stoich_p1 fates_prt_nitr_stoich_p2	Nitrogen stoichiometry, parameters 1 and 2 for leaf tissue	0.019 gN/gC
fates_allom_d2h1 fates_allom_d2h2	Parameters 1 and 2 for the O'Brien et al. 1995 diameter to height allometry (intercept, or c)	0.61, 0.38

### Logging Scenarios

We referenced United States Forest Service (USFS) timber harvest activity data for the western United States to inform our logging scenarios. We created six different logging scenarios to evaluate the impact of logging intensity and delays (Table 3.2). The first scenario (CC) was a high intensity clearcut that occurred at a single time step in which 100% of the trees are removed, in this case all vegetation. The following scenarios were all lower intensity harvests in which only a fraction of trees was selected for harvest (i.e., selective logging). The second scenario (SLS) selectively harvested 80% of all trees between 10 and 40 cm DBH on a given date. The single date selective logging scenario (SLS) acts similarly to the control scenario as a point of reference or comparison for the other logging scenarios since the activity only occurred on at a single day. In the third

scenario (SLM), 50% of trees between 10 and 40 cm were removed sequentially through time to represent the multiple harvests that can occur within a timber harvest project. The time between logging events was determined using a Markov Chain (MC) explained below.

**Table 3.2 Description of Logging Scenarios**

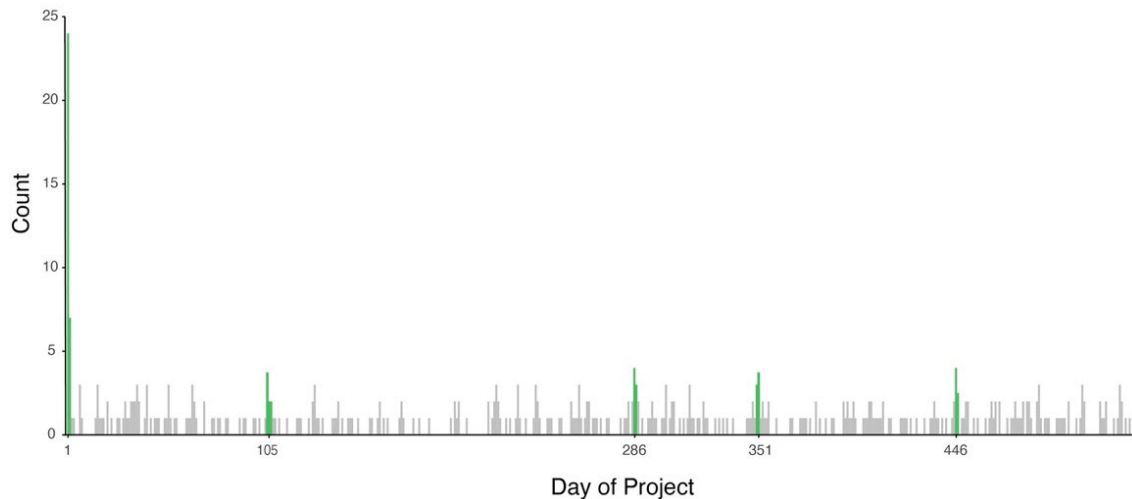
<b>Name (abbreviation)</b>	<b>Description</b>
Control	No logging scenario occurred. Represents an intact forest.
Clearcut (CC)	Clearcut scenario. All vegetation removed at a single time step.
Single Day Selective Logging (SLS)	A single date selective logging scenario, 80% of trees size 10-40 cm DBH were removed at a single time step.
Multiple Day Selective Logging (SLM)	A multi-date selective logging scenario, 50% of trees (10-40cm DBH) were removed at five different time steps within 543 days.
Multiple Day Delayed Selective Logging EA (SLD-EA)	A multi-date logging scenario with the same sequence and intensity as S3, but the activities were all delayed 291 days.
Multiple Day Delayed Selective Logging R4 (SLD-R4)	A multi-date logging scenario with the same sequence and intensity as S3, but the activities were all delayed 120 days.
Multiple Day and Repeated Selective Logging (SLR)	A multi-date logging scenario with the same sequence and intensity as S3, but the activities were all repeated at 15-year intervals.

To create a synthetic logging scenario, we compiled USFS project data for forests in southern Idaho from 2000 to 2020 from the USFS Timber Harvests database (available at <https://data.fs.usda.gov/geodata/edw/datasets.php>). Projects within the USFS are

composed of a set a of activities which are planned to be completed on specific days. From the projects compiled from the Timber Harvest database we first grouped the activities and their completion date by project (when the activity was physically completed) and then filled in the dates between those dates. We created a binary variable of “Action” or “No Action” representing whether an activity occurred on that day. We also created a variable called sequence days which is a count of the days within a project. Table 3.3 shows an example of what a project would look like after the data processing. From this data we created a MC of logging activities using the markovchain package in R (R Core Team, 2020; Spedicato, G. 2017). The binary “Action” variable informed the transition matrix used to calculate the MC, and the states used to inform the MC were either Action or No Action. We then simulated 1000 random chains based on the MC of logging activities, with the initial state equal to 1 (Action), for 543 days, which is the mean project length for our subset of timber harvest data. Each chain can be thought of as one synthetic timber harvest project comprising a series of activities. From these 1000 synthetic projects, we generated a histogram showing the frequency of an Action state for each day of the synthetic project chain (Figure 3.2). We arbitrarily chose the top four peaks in the histogram after the initial activity to determine the final synthetic timber harvest project used as the multi-date selective logging scenario (SLM).

**Table 3.3 Sample Table of Project After Markov Chain Data Processing.**

Activity	Date	Action	Sequence Days
Shelterwood preparatory cut	01-Sept-2018	1	0
No activity	02-Sept-2018	0	1
No activity	03-Sept-2018	0	2
No activity	04-Sept-2018	0	3
...	...	...	...
Shelterwood cut	15-Oct-2019	1	410

**Figure 3.2 Sample histogram from the Markov-Chain with peaks highlighted in green for when an activity would likely occur.**

The fourth and fifth logging scenarios (SLD-EA, SLD-R4), consisted of the same logging sequence as SLM, but with delayed initial start dates. The initial activity in SLD-EA was delayed by 291 days, the median project delay for timber harvest activities within the western US that required an environmental assessment (see Chapter 2). In SLD-R4, the initial action date was delayed by 120 days which is the median project delay for projects that occur in the USFS administrative region 4 (see Chapter 2). The last scenario (SLR) contained the same logging sequencing as the multi-date selective logging scenario (SLM), but the synthetic project was repeated every 15 years which is a common time to repeat selective or group logging within the USFS. This scenario will show how repeated actions in an area may impact the resulting forest structure, productivity, and hydrology of the area.

We ran all model simulations, including the control, for 310 years to capture at least 150 years post-disturbance for each scenario. We completed an initial spinup of 150 years from bare ground to reach a state where trees could grow large enough for harvesting. The multi-date selective logging simulations each lasted approximately 1.5 years which was roughly the average project length for timber harvest projects in southern Idaho.

### Model Analysis

We considered several modeled outputs for analysis, and we classified these variables as either structural or functional. Structural variables represent the physical structure of the forest and are given as an amount per area. Structural variables include: the area of trees per grid cell (i.e., the area occupied by woody plants, fraction), the number of trees per size class (number of individual trees/m<sup>2</sup>), the basal area per size

class (BA,  $\text{m}^2/\text{ha}$ ), the leaf area index (LAI,  $\text{m}^2/\text{m}^2$ ), and the aboveground biomass (AGB,  $\text{gC}/\text{m}^2$ ). Although we only considered one grid cell for these simulations, there can be multiple patches which may or may not be vegetated leading to area trees having values of  $<1.0$ . The BA is the cross-sectional area of trees at breast height for an area and is one way to describe forest density. For the LAI, we considered the total projected leaf area. The LAI describes the plant canopy structure. Aboveground biomass refers to the total carbon in the aboveground portion of live trees.

The functional variables all describe important processes within a forested landscape and are rates or fluxes. Functional variables include gross primary productivity (GPP  $\text{gC}/\text{m}^2\text{s}$ ), net primary productivity (NPP  $\text{gC}/\text{m}^2\text{s}$ ), evapotranspiration (ET  $\text{mm}/\text{s}$ ), total liquid surface runoff (QR  $\text{mm}/\text{s}$ ), and infiltration (Qin  $\text{mm}/\text{s}$ ). GPP and NPP will inform the assimilation and retention of carbon for the simulated forest under the different logging scenarios. The ET, QR, and Qin will all inform changes to the water fluxes within the simulated forest under the different logging scenarios.

We plotted the structural variables as moving averages using five-, 10-, and 20-year windows up to 100 years post-logging activity. We varied the window size in order to smooth annual fluctuations and larger fluctuations caused by the climate forcing recycling. We plotted the results from all logging scenarios compared to the control scenario and one standard deviation of the control values. We also plotted the results from the multi-date selective logging scenarios (SLM, SLD-EA, SLD-R4, and SLR) compared to the single date selective logging scenario (SLS) and included one standard deviation of SLS.

We plotted the functional variables as time series of the annual mean values up to 100 years post-logging. We plotted the results from all logging scenarios compared to the control scenario and included one standard deviation of the control values. We also plotted the results from the multi-date selective logging scenarios (SLM, SLD-EA, SLD-R4, and SLR) compared to the single date selective logging scenario (SLS) and included one standard deviation of SLS. Additionally, we compared the seasonal trends of the functional variables at various five-year increments after the logging treatments and included one standard deviation of the control or SLS values for the five-year increments post-logging. We looked at the increments from 0-5, 10-15, 20-25, 50-55, 70-75-, and 95-100-years post-logging. For all comparisons, we considered the difference in modeled outputs of the logging scenarios from control or SLS through time to be important or significant if the modeled values from the logging scenarios exceeded one standard deviation. All simulations were completed on the National Center for Atmospheric Research (NCAR) Cheyenne high performance computer system (CISL, 2019). All analyses were completed on the NCAR Casper data analysis and visualization cluster (CISL, 2019).

## **Results**

We first present the results comparing modeled outputs of the control scenario to observational data. Then we present the resulting structural variables, followed by the results of the functional variables. For all the results we first compared the results of all the logging scenarios to the control scenario. Then we compared the results of the multi-date logging scenarios (SLM, SLD-EA, SLD-R4, and SLR) to the single date logging scenario (SLS). In the results, the time “post-logging” refers to the time after the first

logging treatment of the scenario. For all scenarios, including the repeated selective logging scenario (SLR) but excluding SLD-EA, the initial harvest activity occurs at simulation year 150. In SLD-EA the initial logging treatment occurs in simulation year 151 because of the length of the delay applied in that scenario.

### Comparison to Target Data

To determine how well our model parameterizations represented the forest at BBEF we compared the modeled AGB, LAI, GPP, and stem density of large trees (50-60cm DBH) to observations. AGB observations were from the AGB derived from FIA data for the Boise National Forest (BBEF is located within the Boise National Forest) (Wilson et al., 2013). LAI and GPP observations were obtained from MODIS derived data from a small area containing BBEF (Myneni et al., 2015; Running et al., 2015). The observed stem density values were obtained from the FIA 1991 inventory of ponderosa pines for southern Idaho (USFS, 2021). Modeled average annual AGB from the control scenario was  $2120.0 \text{ gC/m}^2 (\pm 368.0)$ . For all the Boise National Forest, where BBEF is located, mean AGB was  $2649.8 \text{ gC/m}^2 (\pm 1624.4)$  (Table 3.4). Modeled mean annual LAI was  $2.4 \text{ m}^2/\text{m}^2 (\pm 0.3)$ . The average LAI from MODIS for BBEF was  $1.9 \text{ m}^2/\text{m}^2 (\pm 0.6)$  (Table 3.4). Modeled average annual GPP from the control scenario was  $1076.9 \text{ gC/m}^2\text{yr} (\pm 246.9)$ . The GPP from MODIS was  $1894.1 \text{ gC/m}^2\text{yr} (\pm 513.7)$ . The GPP from the ponderosa pine dominant Metolius Fluxtower sites in Oregon were  $784.9 \text{ gC/m}^2\text{yr} (\pm 71.4)$  for the young forest site and to  $1551.0 \text{ gC/m}^2\text{yr} (\pm 175.1)$  for the mature forest site (Table 3.4). Size class distributions are skewed towards small trees, and our simulated forest has fewer large trees relative to FIA data on ponderosa pine for southern Idaho (Table 3.4).

**Table 3.4 Modeled and Observed Values of AGB, LAI, and GPP**

	Modeled (Control Scenario)		Observations	
	Mean	Standard Deviation	Mean	Standard Deviation
AGB (gC/m <sup>2</sup> )	2120.0	368.0	2649.8 <sup>1</sup>	1624.4
LAI (m <sup>2</sup> /m <sup>2</sup> )	2.4	0.3	1.9 <sup>2</sup>	0.6
GPP (gC/m <sup>2</sup> yr)	1076.9	246.9	1894.1 <sup>3</sup>	513.7
			784.9 <sup>4,y</sup>	71.4
			1551.0 <sup>4,o</sup>	175.1
Stem Density (individual trees/ha)	0.4	0.4	9.1 <sup>5</sup>	5.3

<sup>1</sup>From Wilson et al., 2013

<sup>2</sup>From MODIS

<sup>3</sup>From MODIS

<sup>4</sup>From Ameriflux, young site (y) and old site (o)

<sup>5</sup>From US Forest Service Forest Inventory Analysis (FIA) 1991 inventory

#### Structural Responses to the Logging Scenarios

##### Moving Averages Relative to the Control Scenario

The 5-year moving average of modeled AGB showed that relative to the control scenario all the logging scenarios, except for the repeated selective logging scenario (SLR), returned to within one standard deviation of the control after approximately 25 years (Figure 3.3a). The clearcut scenario (CC), returned to within one standard deviation of the control earlier than the other selective logging scenarios (SLS, SLM, SLD-EA, and SLD-R4). SLR had significantly lower AGB relative to the control scenario until approximately 60 years post-logging when it recovered to within one standard deviation of the control AGB. The same pattern was seen for the 10- and 20-year moving averages

(Figures 3.3b and B1.1, the 10-year moving averages for all results can be found appendix B1). For all scenarios, once the resulting AGB returned to within one standard deviation of the control the values did not deviate beyond the standard deviation envelope.

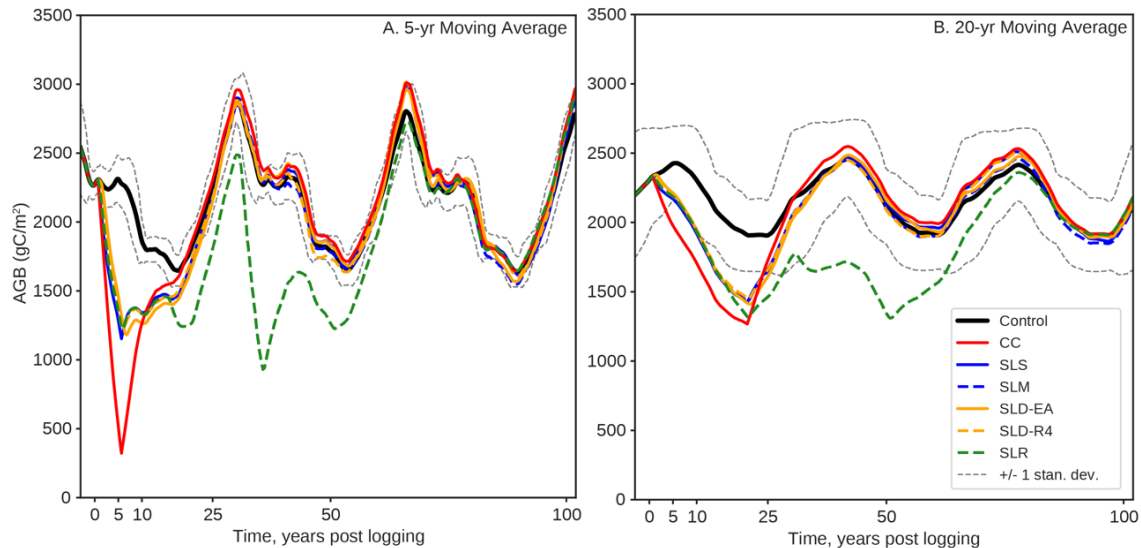


**Figure 3.3** Moving averages of above ground biomass (AGB) up to 100 years post-logging

The 5-year moving average of modeled LAI showed that initially all the scenarios resulted in LAI lower than one standard deviation relative to the control scenario and recovered to within one standard deviation after approximately 10 years (Figure 3.4a). Then, the LAI from the clearcut scenario (CC) exceeded the one standard deviation threshold for several years before returning within the standard deviation envelope. The repeated selective logging scenario (SLR) dropped below the standard deviation envelope approximately 30 years post-logging (the second iteration of the logging project) but recovered within 5 years. At 50 years post-logging several of the scenarios, SLM, SLD-EA, and SLD-R4 exceeded the control's standard deviation, and at approximately 90

years post-logging SLM, SLD-R4, and SLR exceeded the control's standard deviation. When using a 10-year moving average window, which begins to smooth some of the cyclical pattern caused by the climate forcing repetition, only CC was initially below the control's standard deviation before recovering approximately 15 years post-logging (B1.2). Modeled LAI from CC decreased below the control's standard deviation approximately 40 years post-logging. Again, at approximately 50 years post-logging, the modeled LAI from SLM, SLD-EA, and SLD-R4 exceeded the control's standard deviation, and at approximately 90 years post-logging the modeled LAI from SLM, SLD-R4, and CC exceeded the control's standard deviation. Using a 5- and 10-year moving averages, the modeled LAI from the logging scenarios exceeded the one standard deviation within the first 10 years and along the rising limbs and peaks in LAI that occurred between 50- and 100-years post-logging (Figure 3.4a and B1.2). When using a 20-year moving average window, only CC produced an initial LAI below the control's standard deviation (Figure 3.4b). The modeled LAI from CC then recovered within 25 years post-logging. No other scenario produced an LAI that exceeded beyond the control's standard deviation with a 20-year moving average window.

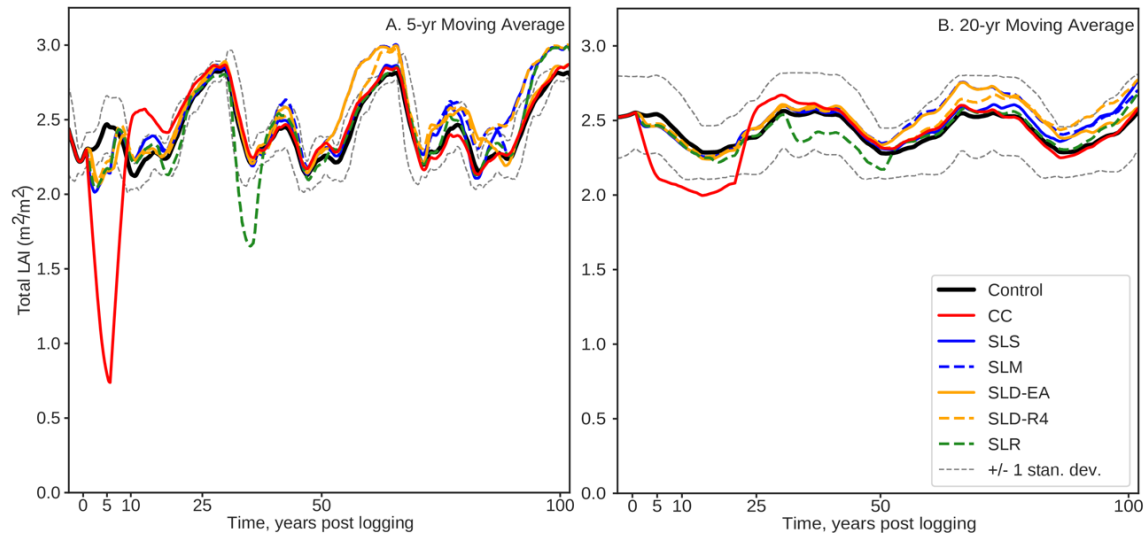


**Figure 3.4 Moving averages of leaf area index (LAI) up to 100 years post-logging**

The 5-year moving average of the total area of trees on the grid cell showed an initial decrease of modeled area trees for CC beyond one standard deviation of the control which then recovered after approximately 10 years post-logging (Figure 3.5a). Several scenarios produced an area of trees which were larger than the control's standard deviation. The modeled area of trees from CC and SLR were larger than the control's area of trees from approximately 10 to 15 years post-logging. At 45 to 50 years post-logging, SLS produced an area of trees larger than the control's standard deviation. From approximately 50 to 100 years post-logging, several of the scenarios reached and then maintained 100% area of trees on the simulated grid cell which was beyond the control's standard deviation. Using a 10-year moving average window, SLR is the only scenario that produced an initial decrease in area trees that moves outside of the control's standard deviation (B1.3). At 50 years post-logging, SLS and SLM produced an area of trees larger than the control's standard deviation. SLM maintained an elevated area trees value, greater than the standard deviation, up to 100 years post-logging. SLS recovered to within one standard deviation of the control at approximately 80 years post-logging,

where SLD-EA resulted in area trees values that exceeded the control's standard deviation. By the 100 years post-logging SLS, SLM, SLD-R4, and SLR were all at 100% area of trees per grid cell which was greater than one standard deviation from the control scenario's area of trees. Using a 10- and 20-year moving average window, CC was the only scenario that produced an initial decrease in area trees that moved outside of the control's standard deviation (Figure 3.5b and B1.3). At 50 years post-logging SLM and SLD-EA produced an area of trees values that were slightly beyond the control's standard deviation until approximately 90 years post-logging. From 90 years post-logging to 100 years post-logging SLS and SLD-R4 maintained area of trees on the simulated grid cell that were greater than the control's standard deviation.

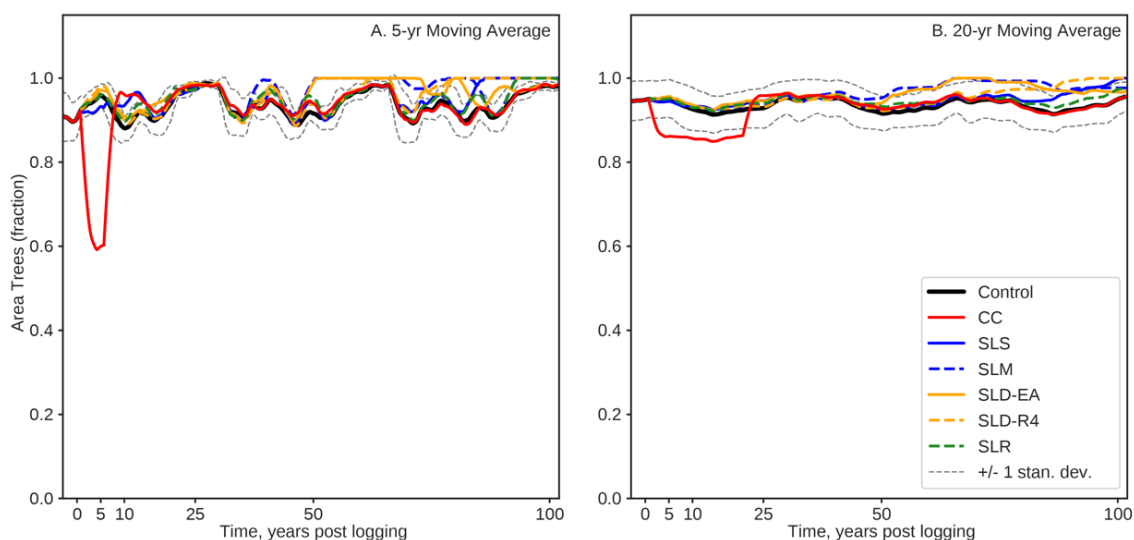


**Figure 3.5** Moving averages of the area of trees on the grid cell up to 100 years post-logging

We considered the moving averages of stem density and basal area (BA) for small trees (0-10cm DBH) and large trees (30-50cm DBH) (Figures 3.6a-d, 3.7a-d). In the 5-year moving average of modeled BA for small trees, only CC was initially below the one standard deviation envelope of the control scenario (Figure 3.6a). The modeled BA of

small trees from CC then recovered and exceeded the one standard deviation at approximately 10 years post-logging. The CC scenario also resulted in a BA of small trees below one standard deviation from 20-30 years post-logging. The selective logging scenarios (SLS, SLM, SLD-EA, SLD-R4) resulted in a BA of small trees values which exceeded one standard deviation from approximately 5 to 20 years post-logging. Modeled BA of small trees from the repeated selective logging scenario (SLR) exceeded one standard deviation from approximately 5 to 30 years post-logging and from 30 to 55 years post-logging. The modeled BA of small trees from SLS, SLM, and SLD-EA exceeded one standard deviation near the peak at approximately 55 years post-logging, and the modeled BA of small trees from SLS, SLM, SLD-EA, and SLD-R4 exceeded one standard deviation near the peak at 90 years post-logging. The modeled BA of small trees from SLS also exceeded the control standard deviation at the peak near 90 years post-logging. CC, SLM, and SLD-EA all resulted in a BA of small trees that exceeded the lower one standard deviation at the trough approximately 70-75 years post-logging. The 10-year moving average of modeled BA of small trees resulted in a similar pattern to the five-year moving average, but no scenarios exceeded the lower one standard deviation at the troughs in BA of small trees (B1.4). Using a 20-year moving average window, the modeled BA for small trees all the scenarios resulted in values that exceeded one standard deviation of control from 10-25 years post-logging (Figure 3.6b). However, the BA of small trees from SLR still exceeded standard deviation of control from 50-60 years. Otherwise, with a 20-year moving average window, all values were within one standard deviation.

The five-year moving average of the BA of large trees showed that the selective logging scenarios all resulted in a BA of large trees, classified here as 30-50cm, much lower than the control's standard deviation envelope from approximately five to 40 years post-logging (Figure 3.6c). The BA of large trees from CC then exceeded the control's standard deviation envelope from approximately 40 to 55 years post-logging. However, the resulting BA of large trees from CC then tracked near the control value (i.e., stays within the one standard deviation envelope) up to 100 years post-logging. The BA of large trees from SLR continued to be near zero and well below the control's standard deviation envelope from five to approximately 75 years post-logging. The selective logging scenarios (SLS, SLM, SLD-EA, SLD-R4) all showed a distinct dip in the BA of large trees that exceeded the control's standard deviation envelope at approximately 65 to 90 years post-logging (Figure 3.6c). The patterns of modeled BA of large trees from the logging scenarios remained when using a 10- and 20-year moving average window (Figure 3.6d, B1.5).

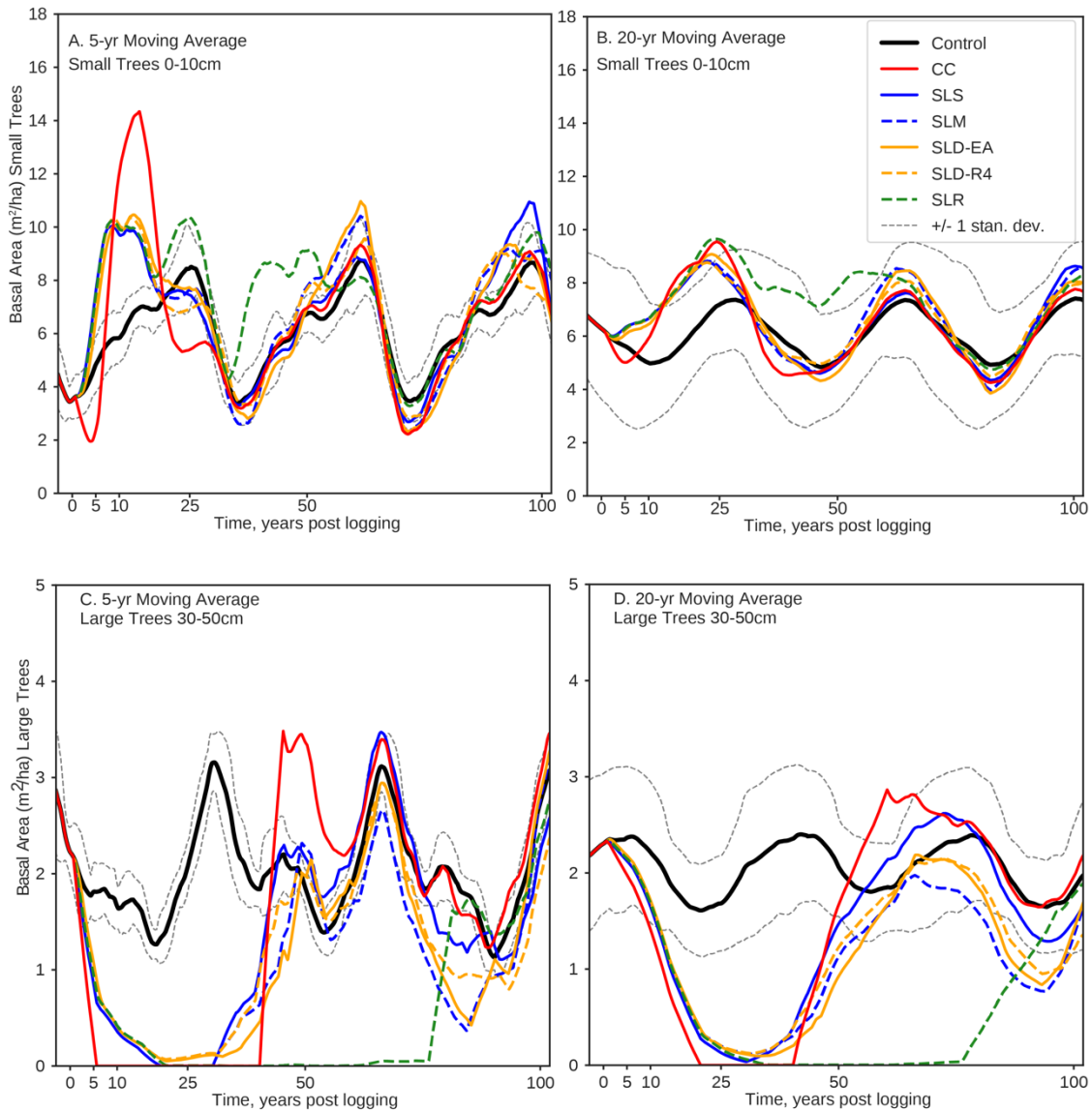


**Figure 3.6** Moving averages of basal area (BA) of small trees (0-10 cm DBH) and large trees (30-50 cm DBH) up to 100 years post-logging.

The modeled stem density of small trees was relatively noisy when we used a 5-year moving average window (Figure 3.7a). With the 5-year moving average, only CC resulted in an initial decrease in small trees outside of one standard deviation from the control scenario. In general, where the control scenario resulted in peaks of stem density, the logging scenarios resulted in peak stem densities greater than one standard deviation of the control (Figure 3.7a). Eventually the modeled stem densities from CC and SLR

recovered to within one standard deviation of control. However, SLS, SLM, SLD-EA, and SLD-R4 had stem densities larger than control by more than one standard deviation for the final peak from approximately 75 to 90 years post-logging. When we used a 10-year moving average window, the initial decrease in stem density from SLR was only briefly low enough to occur outside of one standard deviation (B1.6). The other selective logging scenarios modeled stem densities of small trees peaked beyond one standard deviation where the control values also peak. At the final peak (approximately 75-90 years post-logging) SLS, SLM, SLD-EA, and SLD-R4 stem densities were greater than the control values by more than one standard deviation. With a 20-year moving average window there was no initial decrease in trees beyond one standard deviation of control (Figure 3.7b). Only SLS, SLM, and SLD-R4 resulted in stem density values greater than the control scenario by one standard deviation at the second peak (approximately 50 years post-logging). At the peak occurring approximately 100 years post-logging, the stem density values from SLS, SLM, SLD-EA, and SLD-R4 were greater than the control by more than one standard deviation.

The modeled stem densities of larger trees (30-50cm DBH) were orders of magnitude smaller than the small tree stem densities. With a 5-year moving average, the initial stem densities of larger trees decreased relative to the control for all the logging scenarios, S1-S6 (Figure 3.7c). Then, the stem densities from CC, SLS, SLM, SLD-EA, and SLD-R4 all recovered to within one standard deviation of control within 50 years post-logging. The stem densities from SLR remained well below the control value until recovering to within one standard deviation at approximately 80 years post-logging. The resulting stem densities from CC recovered and then exceeded the control values by more

than one standard deviation. At approximately 80 years post-logging the stem densities from SLS, SLM, SLD-EA, and SLD-R4 were all lower than the control by more than one standard deviation, but the values recovered to within one standard deviation within 100 years post-logging. The same pattern observed with a 5-year moving average window size was also observed for 10- and 20-year moving window sizes (Figures 3.7c-d, B1.7).

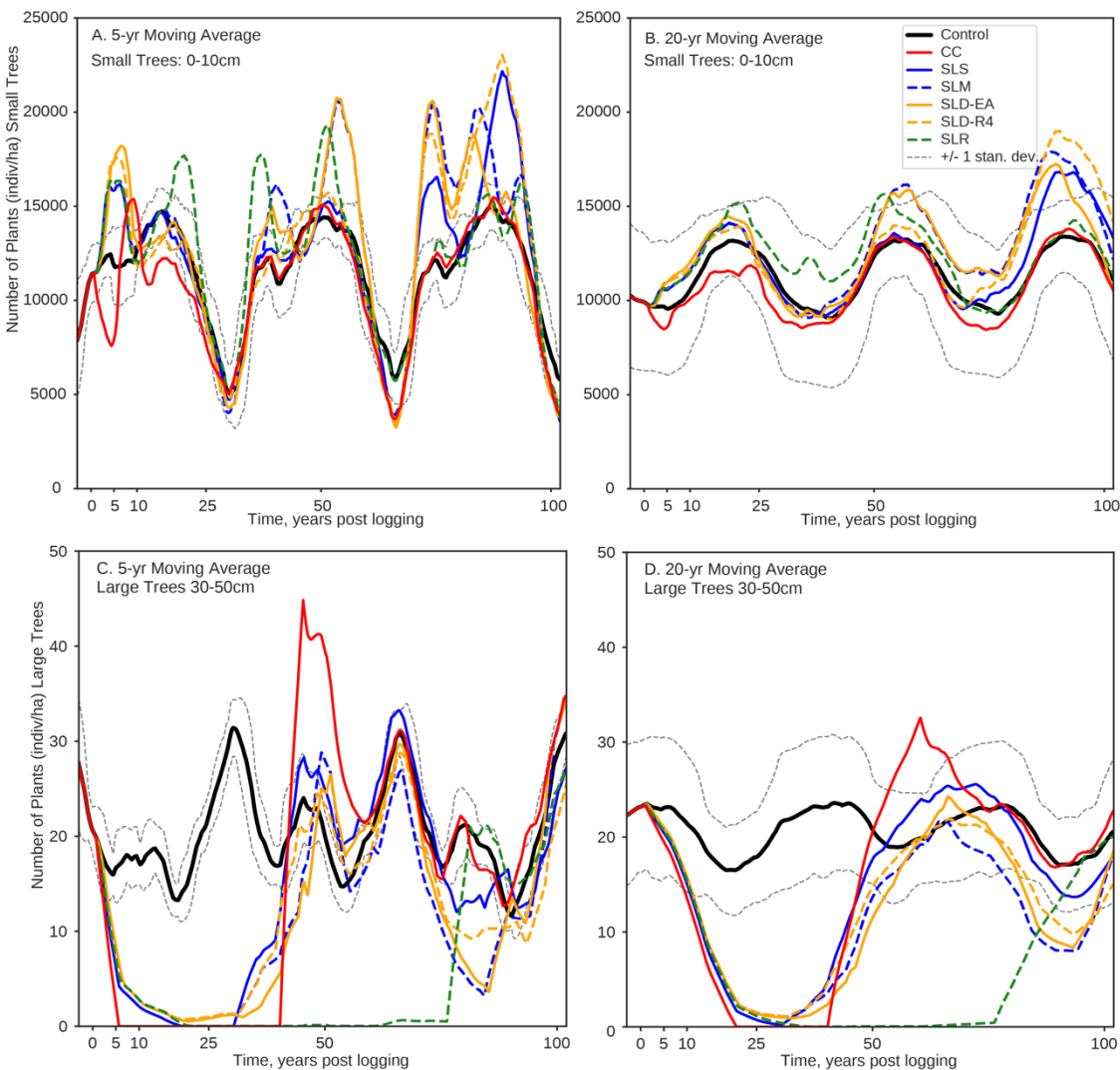


**Figure 3.7** Moving averages of the stem densities of small trees (0-10 cm) and large trees (30-50cm) up to 100 years post-logging.

### Moving Averages Relative to the Single Date Logging Scenario (SLS)

Relative to the single date selective logging scenario (SLS), the modeled AGB from the multi-date selective logging scenarios (SLM, SLD-EA, SLD-R4, and SLR) were within one standard deviation of SLS (B2.1). SLR remained outside the one standard deviation envelope of SLS from 30 to 60 years post-logging. The same pattern is seen for the 10- and 20-year moving average windows (B2.1).

Relative to SLS, modeled LAI from the selective logging scenarios tracked closely to SLS except for SLR (B2.2). SLR was below one standard deviation of SLS at 30 years post-logging. SLM, SLD-EA, and SLD-R4 all exceeded one standard deviation at approximately 60 years post-logging. SLD-EA was below the one standard deviation envelope from approximately 90 to 100 years post-logging. SLM and SLR were both briefly below the one standard deviation envelope at 90 years post-logging. Using a 10-year moving average, the same patterns occurred but were slightly smoothed (B2.2). Using a 20-year moving average, all scenarios were within the one standard deviation envelope of SLS (B2.2).

Relative to SLS, the modeled area of trees per grid cell only exceeded the standard deviation of SLS briefly within 50 years post-logging (B2.3). After 50 years post-logging, the modeled area of trees was 100% for SLM and SLD-EA which exceeded the standard deviation envelope. At 100 years post-logging, all scenarios except for SLD-EA were at 100% area of trees indicating full coverage of the grid cell by trees. Only SLD-EA was below the standard deviation of SLS. With a 10-year moving average window, the scenarios were within the SLS standard deviation envelope up until 50 years post-logging when SLM and SLD-EA reached 100 % area trees. Once SLS reached

100% area of trees, only SLR and SLD-EA were below the standard deviation envelope. The modeled area of trees from the repeated selective logging scenario (SLR) eventually reached 100% at approximately 95 years post-logging (B2.3). With a 20-year moving average, the scenarios tracked closely to SLS until 50 years post-logging where SLM and SLD-EA clearly deviated although still within the standard deviation envelope (B2.3). All scenarios were within the standard deviation up until approximately 100 years post-logging when SLM, SLD-EA, and SLD-R4 were below the standard deviation envelope.

Relative to SLS, only the modeled BA of small trees from SLR exceeded the one standard deviation envelope within the first 50 years post-logging (B2.4). SLM exceeded the peak at approximately 60 years post-logging, and SLD-EA was lower than the standard deviation envelope at approximately 90 years post-logging where a peak in the BA of small trees occurred. Using a 10-year moving average, only SLR exceeded the standard deviation envelope from 20-50 years post-logging. The rest of the scenarios were within the standard deviation envelope (B2.4). Using a 20-year moving average window, SLR exceeded the standard deviation from 40-60 years post-logging (B2.4). All other scenarios were within the standard deviation envelope.

Relative to SLS, SLR resulted in a BA of large trees that exceeded the lower standard deviation envelope from 30-75 years post-logging (B2.5). From approximately 20 to 30 years post-logging the BA of large trees from SLS was 0 and SLM, SLD-EA, and SLD-R4 were all above the standard deviation. After the BA of large trees from SLS recovered to above 0 around 30 years post-logging, the results from SLM, SLD-EA, and SLD-R4 were all lower than the BA of large trees from SLS. The BA of large trees from SLM, SLD-EA, and SLD-R4 occasionally dipped below the standard deviation envelope

from 30 to 80 years post-logging. At approximately 80 years post-logging there was a clear dip in the BA of large trees from SLM and SLD-EA below the standard deviation envelope of SLS. However, SLR exceeded the standard deviation envelope at 80 years post-logging. SLM and SLD-EA both exceeded the standard deviation from approximately 90 to 100 years post-logging. Using a 10-year moving average showed a similar, albeit smoother, deviation pattern (B2.5). Using a 20-year moving average SLM, SLD-EA, and SLD-R4 were within the standard deviation envelope of SLS, except where the BA of large trees from SLM was below the envelope at approximately 90 years post-logging (B2.5). SLR was below the standard deviation envelope from approximately 45 to 80 years post-logging.

Relative to SLS, the stem density of small trees was variable for the other selective logging scenarios (B2.6). In general, there are three peaks and three troughs in the modeled stem density. At the first peak, from 0 to 25 years post-logging, only SLR exceeded the standard deviation envelope. At the two later peaks, all scenarios exceeded the standard deviation envelope at some time. Only SLR produced a stem density of small trees that occurred below the standard deviation envelope, and this occurred at the third peak between 75- and 90-years post-logging. Using a 10-year moving average, a similar pattern in the modeled stem densities was observed, but only SLM and SLD-EA exceeded the standard deviation envelope at the third peak approximately 75 to 90 years post-logging (B2.6). Using a 20-year moving average, the peaks were nearly completely smoothed, and only SLM, SLD-EA, and SLR exceeded the standard deviation at the second peak approximately 50 years post-logging (B2.6).

Relative to SLS, the stem density of larger trees from SLR occurred below the lower standard deviation envelope from 30-75 years post-logging (B2.7). Similar to the BA of large trees, the stem densities of large trees from SLM, SLD-EA, and SLD-R4 were all lower than SLS values and occasionally exceeded the lower standard deviation envelope at various times from approximately 30 to 80 years post-logging. At 80 years post-logging, there was a clear dip in the stem density of large trees from SLM and SLD-EA below the standard deviation envelope of SLS. However, SLR exceeded the standard deviation envelope at 80 years post-logging. SLM and SLD-EA both exceeded the standard deviation from approximately 90 to 100 years post-logging. Using a 10-year moving average showed the same, although smoother, pattern (B2.7). Using a 20-year moving average, the stem densities of large trees from SLM, SLD-EA, and SLD-R4 were within the standard deviation envelope of SLS. However, SLM was below the standard deviation envelope at approximately 90 years post-logging, and SLR was below the standard deviation envelope from approximately 45 to 80 years post-logging (B2.7).

### Functional Responses to the Logging Scenarios

#### Time Series of the Annual Mean

We found that the annual mean GPP from the clearcut scenario (CC) was the only instance that occurred outside of the control standard deviation envelope (B3.1). The GPP values were below the control standard deviation for two years post-logging before returning close to the time series for the control and other logging scenarios. We found that NPP and ET from the clearcut scenario (CC) also approached the lower control standard deviation values two years post-logging but did not move outside of the envelope (B3.2-3). Runoff (QR) and infiltration (QIN) values did not move beyond the

control standard deviation envelope for any of the logging scenarios. None of the modeled functional variables from the selective logging scenarios (SLS, SLM, SLD-EA, SLD-R4, and SLR) occurred outside of the standard deviation envelope for the single selective logging event scenario. All the time series for the functional variables can be found in appendix B3.

#### Changes in the Seasonal Trends Compared to Control

We found that the modeled GPP from the clearcut scenario (CC) was significantly reduced relative to the control scenario 0-5 years post-logging from spring to early-fall and in December (Figure 3.8). The other logging scenarios did not result in greatly reduced seasonal GPP 0-5 years post-logging. The peak GPP from CC also occurred a month earlier compared to the control and the other logging scenarios at 0-5- and 5-10-years post-logging. By 20-25 years post-logging the modeled GPP for all scenarios was very similar to the control scenario. From 50-55 years post-logging, the modeled GPP from SLM and SLD-EA exceeded one standard deviation in April. From 70-75- and 90-95-years post-logging the modeled GPP from the selective logging scenarios all occurred within the one standard deviation envelope of the control scenario.

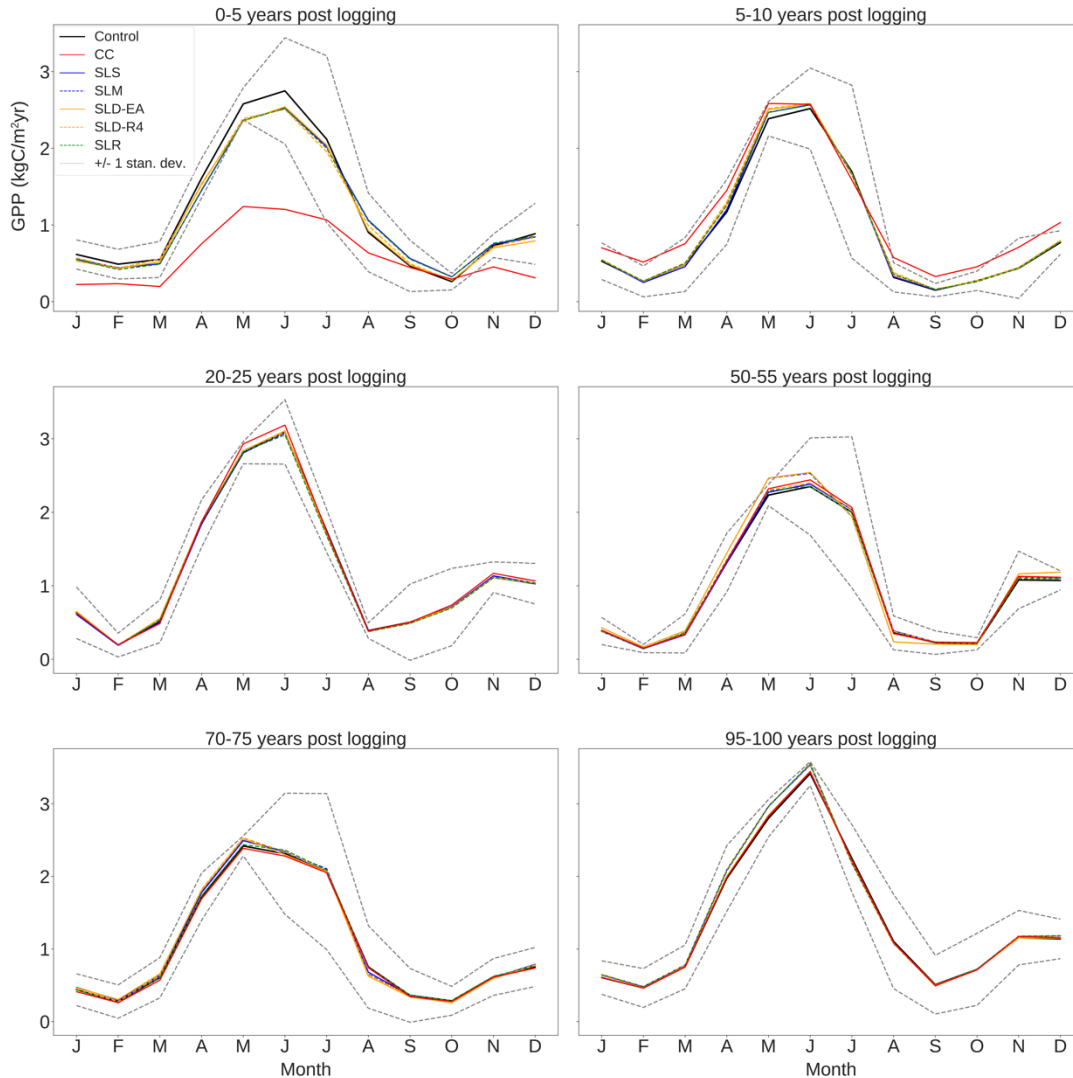


**Figure 3.8** Seasonal mean GPP with  $\pm 1$  std. from the control scenario at different 5-year increments post-logging.

The modeled seasonal NPP from the clearcut scenario (CC) was lower than the control scenario from April to July and in December relative to the control scenario 0-5 years post-logging (B4.1). At 5-10 years post-logging NPP from CC was slightly elevated relative to the control scenario and exceeded the one standard deviation envelope in February, August, September, October, and December. As with the GPP, the NPP from the control scenario peaked a month earlier than the control and other logging scenarios at 5-10 years post-logging. From 50-55 years post-logging only SLD-EA exceeded the

one standard deviation envelope from control in March. For all other time intervals, the modeled seasonal NPP from the selective logging scenarios was within one standard deviation of the control scenario.

The modeled ET for the clearcut scenario (CC) was lower than the control scenario in the winter and spring, from December to June for 0-5 years post-logging (Figure 3.9). From 5-10 years post-logging, CC exceeded the one standard deviation in September. For all other time intervals, all the logging scenarios produced a seasonal ET that was within one standard deviation of the control scenario. There was no change in when peak ET occurred when comparing the logging scenarios to the control scenario.

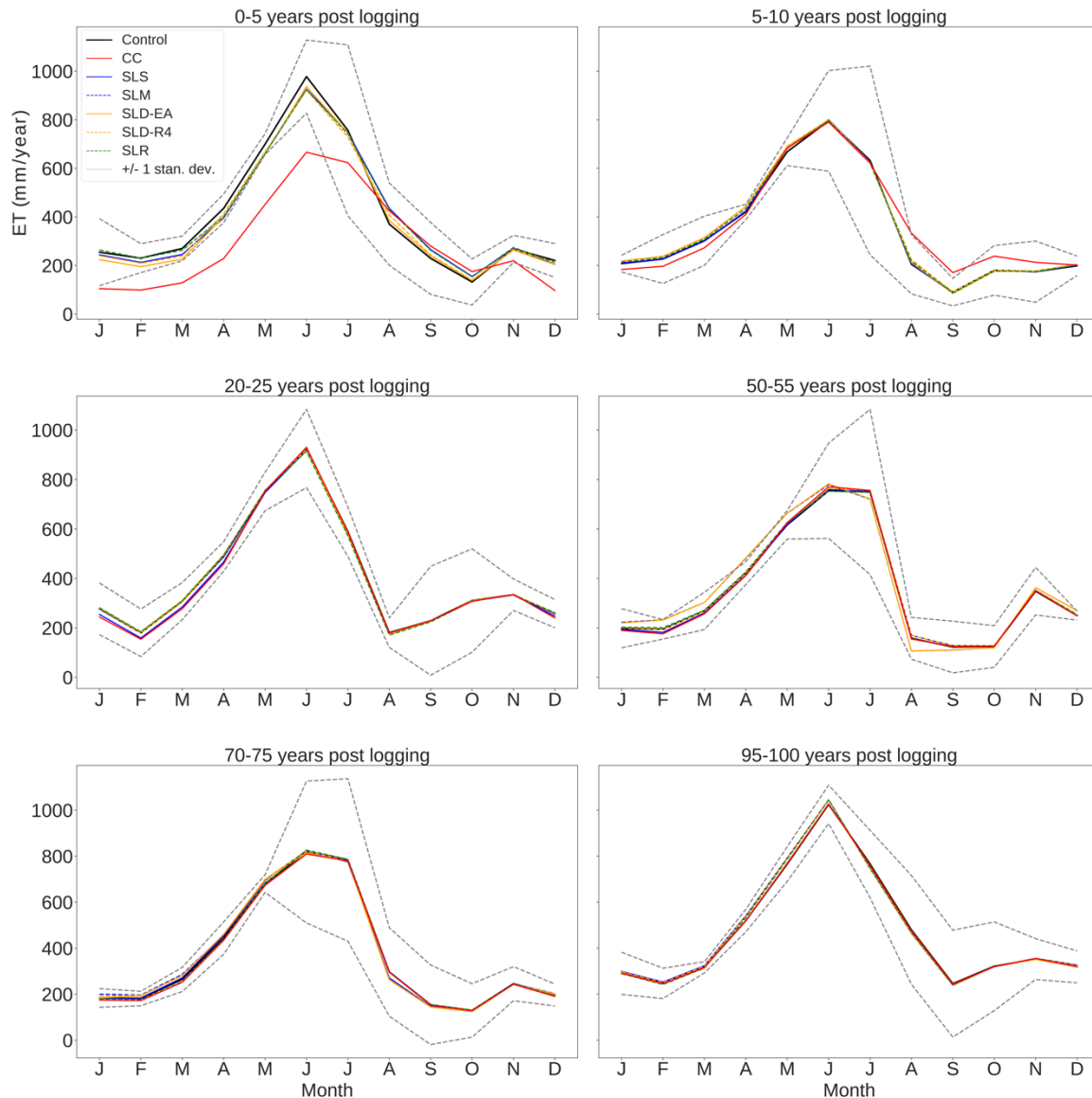


**Figure 3.9 Seasonal mean ET with +/- 1 std. from the control scenario at different 5-year increments post-logging.**

The modeled seasonal runoff (QR) from the clearcut scenario (CC) peaked higher than the control scenario 0-5 years post-logging but only exceeded one standard deviation from the control in May (B4.2). At 0-5 years post-logging, SLD-EA and SLD-R4 (the delayed selective logging scenarios) peaked a month earlier in March relative to the control and the other logging scenarios. At 5-10 years post-logging, modeled QR from CC was within one standard deviation of the control but peaked one month later than the

other scenarios in May. From 50-55 years post-logging, QR for SLM and SLD-EA was within one standard deviation of the control and peaked one month earlier in March. At all the time intervals, except from 0-5 years post-logging, none of the scenarios produced QR that was outside of one standard deviation from the control scenario.

The modeled seasonal infiltration (QIN) from the clearcut scenario (CC) peaked significantly higher than the control scenario 0-5 years post-logging and peaked one month later in May relative to the control (Figure 3.10). The lowest QIN occurred in August for the clearcut scenario 0-5 years post-logging while the lowest QIN occurred in October for the control and all other scenarios. For all other time intervals, only SLD-R4 occurred outside of the control's standard deviation at 70-75 years post-logging. At 70-75 years post-logging, SLD-R4 was near zero in November and December which was outside of the control's standard deviation.

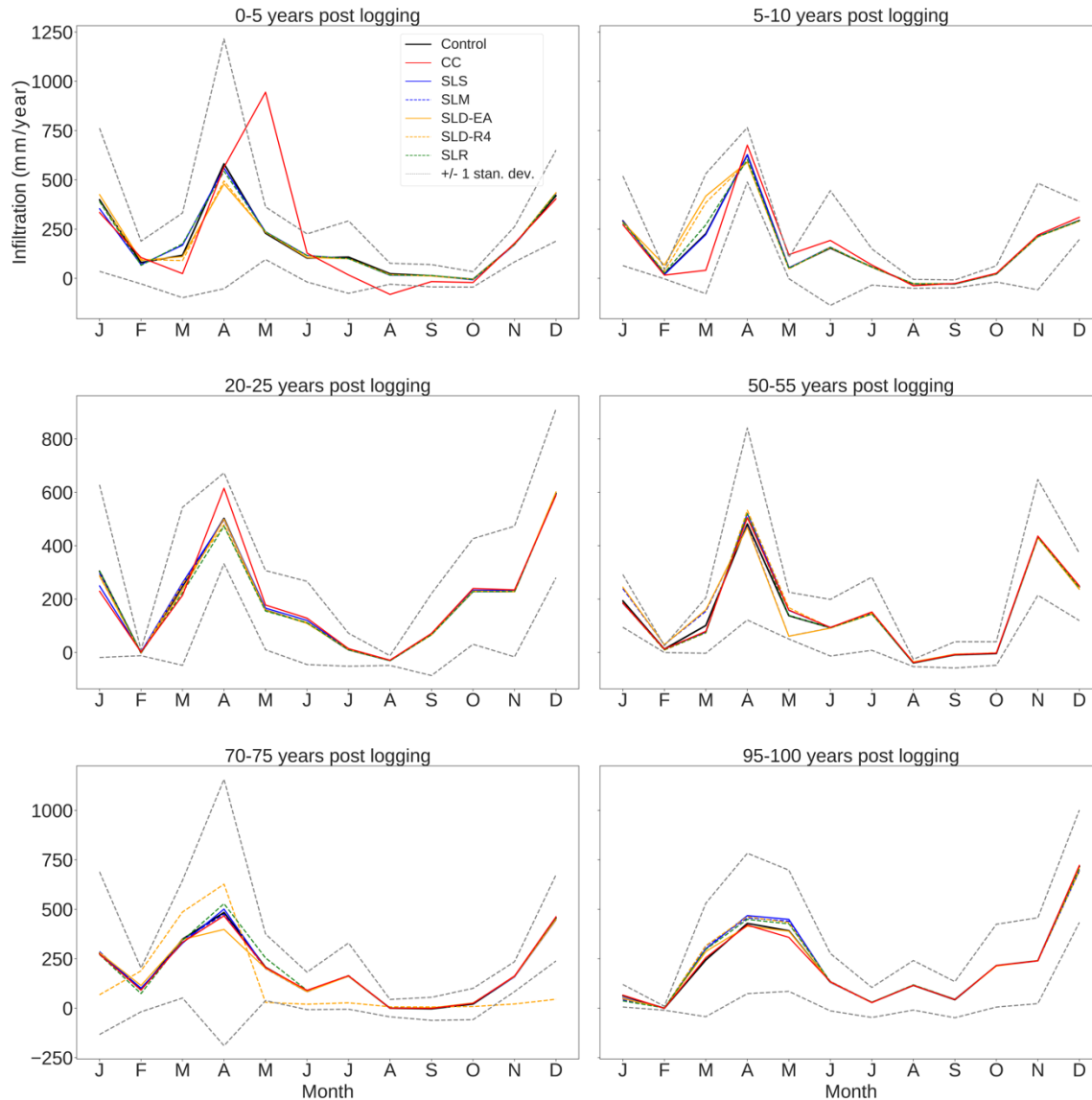


**Figure 3.10** Seasonal mean QIN with +/- 1 std. from the control scenario at different 5-year increments post-logging. Please note the different scale on the y-axes.

#### Changes in the Seasonal Trends Compared to the Single Date Logging Scenario

The seasonal infiltration (QIN) was the only variable in which the modeled results occurred outside of the one standard deviation envelope of SLS. The resulting seasonal infiltration of SLD-R4 was near 0 from November to December which was below the one standard deviation (B4.7). All the other seasonal values of functional variables were within the one standard deviation envelope of SLS (B4).

## Discussion

For this study we sought to determine if delays to timber harvest activities impacted the structure and ecohydrologic function of the forest. We also aimed to determine the necessity of including more temporally detailed management practices within vegetation demography models. The selective logging scenarios had a larger and longer lasting influence on the resulting structure of the modeled forest than the function (e.g. GPP). Small changes in the timing of the logging impacted the stem density and BA up to 100 years post-logging. The clearcut scenario (the most intensive logging scenario) had the largest initial impact (up to ten years post-logging) on the functional variables. However, we found no long-term changes to productivity (GPP and NPP) or the hydrologic fluxes (ET, QR, and QIN) regardless of the type or timing of the logging scenarios.

The selective logging scenarios resulted in structural variables (LAI, area of trees, BA, and stem density) that deviated from the control scenario long term (>50 years post-logging). The clearcut scenario resulted in an initially large response of the structural variables relative to an intact forest (i.e. the control scenario). However, once these recovered, the resulting forest from the clearcut scenario was similar to the modeled control forest. For all logging scenarios, the modeled forests recovered AGB values within approximately 12 to 13 years which is close to the recovery times found by Clyatt et al. (2016) following thinning and fuels treatments in ponderosa pine forests. With the clearcut scenario, all vegetation was removed, and the modeled forest was regrown from bare ground. Minor differences in modeled results between the clearcut and control scenario were likely the result of slight differences in the climate forcing at the time the

logging treatment occurred. However, for the selective logging scenarios, only a select fraction of trees was removed, therefore the forests from the selective logging scenarios recovered under very different light environments and initial stem density than in the clearcut scenario. Within FATES, smaller trees can take advantage of the gaps left by the removal of large trees and are promoted to the canopy level. Minor variation in the timing of treatments in the selective logging scenarios led to long term changes in stem densities between the selective logging scenarios by interrupting the normal promotion scheme. Promotion of the remaining trees played an important role in the resulting structure of the selective logging scenarios while the germination, seed density, and recruitment played a more important role in the resulting forest structure for the clearcut scenario since the trees there grew back from bare ground. This shows that the germination and recruitment processes determine the resulting modeled forest structure of FATES. However, initial seedling density, the initial recruitment height of seedlings or saplings, and the seed germination rate are hard coded parameters within the model.

In this study FATES produced the same forest function, even with different forest structure. Despite the long-term changes to stem density and forest structure, there was no corresponding long-term change to the hydrologic variables (ET, QR, and QIN) or the productivity variables (GPP and NPP). However, short term (up to 10 years post-logging) these variables were greatly impacted by the clearcut scenario showing that only the most intense logging treatments produced changes to these processes. Empirical studies show that removing vegetation impacts surface hydrology by increasing surface runoff and water yield and decreasing ET (Bosch and Hewlett, 1982; Moore and Wondzell, 2005; Zhang et al., 2017). With less trees to take up water, more water can infiltrate the soil or

reach streams. However, once vegetation begins to grow back, the increases in runoff (QR) and infiltration (QIN) and the decrease in ET will recover or reverse (Bosch and Hewlett, 1982). The clearcut scenario removed the most vegetation compared to the selective logging scenarios and resulted in the largest changes to hydrologic variables. The selective logging scenarios only removed a fraction of medium to large trees, leading to a very small response of the modeled QR, QIN, and ET to the selective treatments.

The lack of long-term response to the GPP and NPP corresponding to different modeled forest structures may be due to a relatively quick recovery of plants and their canopy. After a disturbance, the understory cohorts are promoted to the canopy layer. Additionally, many of our selective logging scenarios resulted in nearly 100% area of trees per grid cell and increased LAI relative to the control and clearcut scenarios. This may mean that the GPP or NPP will be similar regardless of the details of the structure if the area of trees on the grid cell or LAI are large or if the canopy layer is full. There may be a limit to the GPP that can occur, for example all the modeled forests may be as productive as they can be given the PFT, climate conditions, and the resulting LAI and area of trees. The disconnect between the relative changes in forest structure and function may also be a result of the communication between FATES and the host land model (CLM in this study). Some of the detail of the cohort structure may be lost in CLM, since CLM is a “big leaf box model” and treats the vegetation photosynthesis as one large leaf. The resulting GPP, NPP, ET and surface processes (QR, QIN) might get smoothed, so to speak, when calculated by CLM.

These results point to potential changes or to updates to FATES. The recruitment schemes could be updated within FATES to better capture the plant regrowth post-

disturbance. Currently in FATES seeds are assumed to be evenly distributed across the site with a set germination rate and a minimum height for newly recruited plants (Fisher et al., 2015). When a patch is disturbed, at the next time step the given fraction of seeds available on the patch will germinate. One way to improve this could be to enforce a delay or stagger the germination and recruitment of plants following different disturbance types. The germination rate could be dependent on current conditions instead of being hardcoded into the specific model simulation. Assuming evenly spaced seeds and an even germination rate may remove some of the landscape heterogeneity FATES seeks to capture.

#### Necessity of More Temporally Detailed Logging Practices in Land Surface Models

One of the main objectives of this work was to determine if LSMs should include a more detailed representation of management timing, specifically for treatments involving vegetation removals. Based on the results of this modeling study and the results of Huang et al. (2020), we think further research is needed to determine whether temporal details of management activities need to be considered when the goal of model simulations is to examine the energy, water, and productivity for forests after harvest treatments. Given that these variables all recover relatively quickly and maintain that recovery regardless of the resulting forest structure, the inter-project activities do not need to be specified. However, representing continuous activities or realistic harvest intensities are useful. If research questions focus on the impact of logging on forest structure and composition, then we recommend including the detailed timing of the activities within the logging scenario. From this study we demonstrated that representing the multiple activities within a project and delays in the implementation of those

activities can have long term impacts on stem density, BA, and LAI relative to a more simplistic harvest activity.

## Limitations

### Model Challenges

There were several limitations and assumptions in the model set up and scenarios. First, we only included one plant functional type (PFT) in the model setup. We did not calibrate the model for coexistence with other common conifer species such as Douglas fir or other PFTs such as grasses or shrubs. In reality, there are several other conifer species that could be included as a separate functional type within model simulations. Coexistence of PFTs within the model may be important for producing realistic forest structure. For the selective logging simulation in the Amazon, Huang et al. (2020) represented a forest with two competing tree PFTs, an early and late successional tree. In their simulations, they had a low stem density relative to observations and a bias towards larger trees. In this study, the simulations produced a dense forest biased towards smaller trees even with changes to the initial seedling density made in the parameter file (Table 3.1). Additionally, we did not include any grass or shrub PFTs within the model. Grass and shrub growth and changes in herbivory patterns following thinning has been shown to influence forest productivity and carbon cycle in ponderosa pine forests (Doughty et al., 2021).

Although fire is an important part of the forest ecology in this area, for these model simulations we did not include fire. We kept fire off to isolate the impact of logging events on modeled outputs of forest productivity and to avoid potential errors from overlapping logging dates within the vegetation management driver with fire events.

If multiple PFTs were used in this study, then fire may be essential for the simulations to produce realistic proportions of the tree PFTs (Buotte et al., 2021).

Using a “brute force” approach to parameterize the PFT for ponderosa pine was inefficient, and we may not be able to transfer these parameters to a larger scale (Haung et al., 2016). Additionally, the model was not perfectly calibrated in terms of AGB, LAI, or GPP. We used a site with no Fluxtowers, which made it difficult to calibrate model outputs to carbon fluxes, and we did not consider energy fluxes. We assumed that inventory or census data from USFS FIA and from BBEF would be more useful for calibration. Here we only used FIA data to estimate the stem density of different size classes for southern Idaho. FIA data can be difficult to work with even with a package available in R (Stanke et al., 2020). Several western states do not track data in a way to determine growth rates, and the spatial locations of plots are not available to the public. Pre- and post-logging data from BBEF are available from studies conducted in the 1950s and 1960s, but funding is not available to continue data collection at these locations. Therefore, we could not compare the model results from 50 to 100 years post-logging to post-logging observations at BBEF.

#### Timber Harvest Assumptions

For the scenarios themselves, we did not consider the fact that the USFS has time constraints to when they can carry out timber harvest activities. Therefore, the timing of some of our treatments may not be representative of how the USFS would carry out timber harvests. For example, in the multi-date logging scenario (SLM), logging two harvests occurred in December which would most likely not happen in an actual project. Harvesting trees in the winter could inhibit the growth and recruitment of young trees due

to colder weather and less daylight. Conversely, harvesting trees in drought conditions could also inhibit the growth of trees as younger pines may be more prone to cavitation. Additionally, we tested projects with only selective logging activities. While selective logging and group selection cuts are common for ponderosa pine forests there would likely be an intermediate activity performed before a harvest, such as a thin. The USFS may also choose to remove trees for different objectives, for example to remove only trees of a certain age or remove trees with a specific final BA as an objective. However, this work still serves as a good baseline for the relative importance of the timing of forest management and the role of delays in management on the resulting structure and functioning of a temperate forest.

#### Future Work

This research accomplished the goal of determining that more realistic timing of management projects should be included in land surface models. There are many opportunities to test this hypothesis better and to determine impacts to forest structure, functioning, and larger scale impacts. To better address the role of the timing of forest management activities, one could simulate some of the more realistic management options from the vegetation management driver at different times throughout the year. For example, simulating the same activity but for each month of the year. Other future work could include scaling these scenarios and any future simulations up to a larger area or region. To scale up one needs to consider the coexistence of multiple coniferous functional types, especially if the scenarios were to include more diverse climatic conditions. Including fire in the simulations may also be useful, however the vegetation driver may not work properly if a patch burns on the same day as a simulated harvest. To

mitigate this technical issue, one could use the final timestep of a simulation with fire on as the starting point for the new simulations with management activities but with fire turned off. Initialization of the model from inventory data should be used to assess if this helps with producing the correct forest structure in which to run the logging scenarios.

### **Conclusion**

From this study we found that small changes in the timing of logging treatments resulted in long term changes to modeled BA and stem densities relative to an intact forest and relative to each of the logging scenarios. Functional variables such as GPP, NPP, ET, QR and QIN were all initially the most impacted by the clearcut scenario and hardly impacted by the selective logging scenarios. The resulting modeled forest function was similar across scenarios regardless of the resulting modeled forest structures. We encourage researchers interested in the structure of a forest following logging to consider the temporal details of timber harvest projects if simulating logging scenarios using LSMs. Researchers interested in the impact of logging practices on the long-term carbon flux and productivity of a forest may not need to include a more detailed temporal representation of logging practices within vegetation demographic models such as FATES, however, we encourage more research into the role of management timing on resulting forest function. Forest managers may find these results useful as there are many implications to forest health based on forest structure and density (Bottero et al., 2017; Sohn et al., 2016).

## CHAPTER FOUR: A METHOD TO IMPROVE PARAMETERIZATION OF TEMPERATE CONIFER FORESTS

### **Introduction**

Forest managers are seeking to apply management techniques that will increase a forest's resistance and resilience in the face of a changing climate and the threat of megadisturbances (Graham et al., 2007; Millar and Stephenson, 2015; North et al., 2022). Land surface models (LSMs) are potentially useful tools within a management context as they capture biogeophysical and biogeochemical processes that are lacking in the individual based models commonly used in the US Forest Service (Bonan, 2008; Bonan and Doney, 2018; Dixon et al., 2018). Until recently, forest management has been coarsely represented in LSMs. However, there have been many improvements to representing forest management LSMs, such as including the indirect mortality from logging (Huang et al., 2020) and including rotation ages and "assisted expansion" or planting of trees (Littleton et al., 2020). The new vegetation management driver within the Functionally Assembled Terrestrial Ecosystem Simulator hosted in the Community Land Model (FATES-CLM) may prove beneficial for understanding long term changes to forest structure and productivity following management activities (Rady et al., 2022). This driver allows the type of management activity, the timing of the activity, and the intensity of the activity to vary by plant functional type (PFT). We recently used this driver to simulate multiple timber harvest scenarios at a single point in Idaho, however,

we found that too few trees within a large size class (30-50cm diameter at breastheight (DBH)) were simulated relative to observations (see Chapter 3).

A challenge of working with FATES-CLM is model calibration. Given the complexity and scope of models such as FATES-CLM, there are many uncertain parameters that need to be adjusted in order to produce realistic modeled outputs of forest productivity and carbon cycling. Hand tuning parameters at a single point is common but inefficient, computationally expensive, and potentially not scalable (Dagon et al., 2020; Huang et al., 2016). Others in the CLM and FATES-CLM community have suggested various ways to sample parameter space more efficiently and objectively, such as through machine learning (Dagon et al., 2020), through a methodology in which parameter ensembles are filtered based on constraints to competing PFTs and ecological conditions before scaling up to a region (Buotte et al., 2021), or through sampling observed and unobserved plant trait data in a covariance matrix to create random tropical PFTs (Koven et al., 2020).

Our objective in this study was to parameterize FATES-CLM in a way that allows trees to grow large enough for harvest using the novel vegetation management driver. To parameterize the model for a semiarid, temperate conifer forest we developed a technique to generate parameter ensembles based on previous work by Buotte et al. (2019) and Koven et al. (2020). We focused on generating ranges of plant trait data and allometric parameters for 10 common conifer species in Idaho. From this we generated two 100-member parameter ensembles, a single-PFT parameterization based on 10 conifer species in Idaho, and a two-PFT parameterization with one PFT based on pine species and a second PFT based on Douglas fir and western hemlock. We ran each 100-member

parameter ensemble with two different climate forcing datasets for a single point in southern Idaho.

For this study we wanted to answer several very specific questions. Can we successfully grow large trees (>50 cm DBH) for a general PFT representing conifers in Idaho? Can we successfully grow competing trees representing two different groups of conifer species in Idaho? Can we grow them to at least 50 cm DBH? When growing large trees, can we maintain reasonable values for outputs of GPP, AGB, and LAI?

### **Methods**

To answer these questions, we tested a range of parameter values in a series of single point simulations using the Functionally Assembled Terrestrial Ecosystem Simulator within the Community Land Model (FATES-CLM, here just FATES). Vegetation dynamics within FATES are sensitive to the climate data used to force the model. Coexistence and plant distribution in FATES are emergent properties in the model driven by the competition of plant strategies or advantages of the different PFTs that are included (Fisher et al., 2015). For these simulations we tested ensembles with different climate and coexistence conditions. We used two different climate forcings, the CRUNCEP dataset (0.5degree-by-0.5degree resolution) and the higher resolution WRF dataset (1km-by-1km), which was developed specifically within the Pacific Northwest and Intermountain West. We also ran simulations with either a single conifer PFT or with two PFTs. We then compared the modeled results to observations of aboveground biomass (AGB), leaf area index (LAI), gross primary productivity (GPP), and the stem density of large trees. We examined those ensembles that could grow large trees (>50 cm

diameter at breast height, DBH) to determine any patterns in parameter distributions for coexistence or for the different climate forcing conditions.

### FATES Model Description

Here we worked to parameterize FATES because of its potential utility within a management or forestry context, i.e. we wanted to parameterize FATES to model large trees. FATES is a version of an ecosystem demography model which bridges the gap between individual based models and the “big leaf” representation of vegetation within the Community Land Model (CLM). Each grid cell within the FATES model is composed of a single column that shares water and soil. On this column multiple patches are classified based on their time since disturbance. The time since disturbance is meant to represent heterogeneity in the ecosystem, for example as canopy gaps or mature forests. The plant population is grouped into plant functional types (PFTs) based on trait similarity. Within FATES, PFTs are defined through functional traits which drive competition for light, water, and nutrients. Each PFT is further divided into size cohorts based on height. Cohorts all compete for water and nutrients and, within the same patch, compete for light based on their height classification and position in the canopy or understory.

Since our study is focused on growing large trees, here we describe in more detail the process of carbon assimilation and allocation within FATES which determine tree growth. The parameters in the equations describing photosynthesis, respiration, carbon allocation and tree growth and the parameterized functional plant traits associated with these processes are important for our study. For more thorough descriptions of the FATES model please see Fisher et al., 2015, Koven et al., 2020, and the FATES technical

documentation online at 10.5281/zenodo.3517271. (For more detailed descriptions of the CLM see Lawrence et al., 2019 and the CLM technical documentation online at [https://escomp.github.io/ctsm-docs/versions/release-clm5.0/html/tech\\_note/index.html](https://escomp.github.io/ctsm-docs/versions/release-clm5.0/html/tech_note/index.html).)

### Carbon Assimilation and Allocation in FATES

As cohorts grow, they are partitioned into the canopy or understory, with different photosynthetic implications for each level. Photosynthesis for all C<sub>3</sub> plants is based on the models of Farquhar et al. (1989) and Collatz et al. (1991). The leaf level photosynthesis is determined by the minimum of three limiting factors: a light or energy limiting rate, a rubisco limiting rate, and a triose-phosphate limiting rate. The leaf layer photosynthetic capacity,  $V_{\text{cmax}}$ , or the maximum rate of carboxylation through the Rubisco enzyme, is a component of both the rubisco limiting and triose-phosphate limiting rates. Leaf level photosynthesis is integrated through the canopy, and cohort level photosynthesis is a function of the plant's crown area and exposed leaf area index. The complement to leaf photosynthesis is leaf respiration when the carbohydrates created through photosynthesis are consumed and carbon dioxide is released back through the leaf. In FATES, leaf respiration is a function of a base level of leaf respiration and the amount of nitrogen relative to carbon in the leaf. As with photosynthesis, respiration is integrated through the canopy such that cohort level respiration is a function of crown area and exposed leaf area.  $V_{\text{cmax}}$  from the photosynthesis equation and nitrogen stoichiometry for different plant tissues, including leaves, are PFT specific traits that are parameterized within FATES.

The net carbon assimilated during photosynthesis and respiration is determined at a daily time step. If the carbon per cohort is net negative, then the carbon from the

storage pool is depleted at a decreasing rate through time. If the carbon per cohort is net positive, FATES prioritizes the allocation of that carbon to first replenish carbon storage, then compensate for tissue turnover, then replenish the target level of carbon in plant organs, and finally grow the plant's stem diameter. The target levels of carbon storage in plant organs are allometric targets specific to each PFT and a function of the stem diameter. In FATES there are six target biomass pools: leaf, stem, seed, coarse root, fine root, and non-structural storage. In general, the below ground biomass pools are proportional to above ground biomass pools.

### Plant Allometry in FATES

Allometric functional forms and parameters are PFT specific. Within FATES allometric functions are modularized which allows for PFTs with different allometric parameters to coexist (Koven et al., 2020). Allometric functions and their parameters can help to designate PFT specific plant strategies, tolerances, or growth rates to reflect successional processes in the forest or following disturbance and generate heterogeneity in PFT distributions through space and time. There are four different types of allometric models for each PFT: height, crown area, sapwood cross-sectional area, and target biomass pools. Allometric equations relate the diameter of a plant to other morphological characteristics of the plant. For this study we updated parameters from the equations for diameter to height, diameter to leaf biomass, and diameter to crown area. For the diameter to height allometry we used the equation from O'Brien et al. (1995). The diameter to leaf biomass was modeled using the equation from Saldarriaga et al. (1988). While those studies and equations came from tropical forests, we determined they were appropriate here after fitting curves from each equation to plant data compiled from the

study region. For the crown area allometry we used a two-parameter power function with a capped allometry based on a maximum diameter at breast height (Koven et al., 2020).

#### Updating FATES PFTs to Represent Conifers in Idaho

Plant dynamics within FATES-CLM are controlled by approximately 200 parameters. Previous sensitivity analyses of CLM (Massoud et al., 2019) and FATES-CLM (Buotte et al., 2021; Koven et al., 2020) show a common list of traits that are highly sensitive and thus impactful for parameterization optimization. These parameters include: the specific leaf area (SLAMAX and SLATOP), the Rubisco limiting component of photosynthesis (VCMAX), the allometric parameters relating diameter at breast height to height (D2H1 and D2H2), above ground biomass, and leaf biomass and crown area (D2BL1, D2BL2 and D2CAMIN, D2CAMAX), wood density (WOOD\_DENS), leaf longevity (LEAF\_LONG), and rates of mortality (background and carbon starvation (CSTARV)). For this study we chose to generate distributions for these parameters, with the exception of the diameter to above ground biomass and background mortality parameters (Table 4.1). We also generated distributions of parameter values for leaf carbon-to-nitrogen ratios (LEAFN). For this study we assumed distributions and correlations between traits based on compiled data.

**Table 4.1 List of parameters investigated in this study**

<b>Parameter name</b>	<b>Description</b>	<b>Abbreviation</b>
fates_leaf_slamax fates_leaf_slatop	Maximum specific leaf area (SLA) (m <sup>2</sup> /gC) SLA at top of canopy (m <sup>2</sup> /gC)	SLATOP, SLAMAX
fates_leaf_vcmaxtop25	Maximum carboxylation rate of Rubisco at 25°C, canopy top	VCMAX
fates_prt_nitr_stoich_p1	Nitrogen stoichiometry, parameters 1 for leaf tissue (gN/gC)	LEAFN
fates_leaf_long	Leaf longevity (i.e., turnover timescale) (year)	LEAF_LONG
fates_wood_density	Mean density of woody tissue in plant (g/cm <sup>3</sup> )	WOOD_DENS
fates_allom_d2h1 fates_allom_d2h2	Parameters 1 and 2 for the O'Brien et al. 1995 diameter to height allometry (intercept, or c)	D2H1, D2H2
fates_allom_d2bl1 fates_allom_d2bl2	Parameters 1 and 2 of the diameter to leaf biomass allometry	D2BL1, D2BL2
fates_mort_scalar_cstarvation	Maximum mortality rate from carbon starvation (1/year)	CTARV

For this study we considered the ten most common conifer species in Idaho which would all be generalized under the evergreen needleleaf tree PFT within FATES (Table 4.2). We compiled trait data from several sources including the Plant Trait Database (TRY, Kattge et al., 2019) and the Biomass and Allometry Database (BAAD, Falster et al., 2015). Previous work by Buotte et al. (2021) compiled a large dataset of plant traits focused on trees located in the western USA with over 70% of data from California

specifically. We modified and built upon this dataset to include several more conifer species common within Idaho and removing species not relevant to the study. With the exception of ponderosa pines and Douglas fir, most traits and species data are lacking for Idaho specifically. Therefore, we used information from the western USA, focusing on more interior and arid locations, and avoiding data from the coastal ranges. Based on the distributions of the compiled plant trait data, we used normal distributions for the  $V_{\text{cmax}}$ , wood density, and leaf longevity, and we used lognormal distributions for the specific leaf area, and nitrogen per leaf area. For carbon starvation we assumed lognormal distributions following Koven et al. (2020). We added these six parameter values to a trait covariance matrix.

**Table 4.2 List of 10 Common Conifer Species in Idaho**

<b>Species</b>	<b>Common Name</b>	<b>Traits</b>
<i>Pinus ponderosa</i>	Ponderosa pine	Low density, shade intolerant (PFT 1)
<i>Pinus monticola</i>	Western white pine	Low density, shade intolerant (PFT 1)
<i>Pinus contorta</i>	Lodgepole pine	Low density, shade intolerant (PFT 1)
<i>Pseudotsuga menziesii</i>	Douglas fir	High density, shade tolerant (PFT 2)
<i>Tsuga heterophylla</i>	Western hemlock	High density, shade tolerant (PFT 2)
<i>Picea endelmanni</i>	Engelman spruce	Low density, shade tolerant
<i>Abies grandis</i>	Grand fir	Low density, shade tolerant
<i>Abies lasiocarpa</i>	Subalpine fir	Low density, shade tolerant
<i>Thuja plicata</i>	Western red cedar	Low density, shade tolerant
<i>Larix occidentalis</i>	Western larch	High density, shade intolerant

For the allometric parameters, we sampled the available data to generate parameter distribution for the two diameter-to-height allometric parameters (D2H1, D2H2), the diameter to crown area parameters (D2CAMIN, D2CAMAX), and the diameter to leaf biomass parameters (D2BL1, D2BL2) (Table 4.1). Allometric observations were obtained from Falster et al. (2015), Idaho specific US Forest Service Forest Inventory and Analysis (FIA) census data, and projects within the Boise Basin Experimental Forest (BBEF). We had significantly more data for the diameter and height of Idaho conifers. We randomly sampled 1000 height and diameter pairs, and using the allometric equation, calculated the optimal parameter values 100 times to create a

distribution of parameter values. We had less data for crown area and leaf biomass so we used a different sampling approach. First, we determined the optimal parameters by fitting the respective allometric equations to the available crown area and leaf biomass data from Falster et al. (2015). For these parameter values, we assumed a normal distribution with the optimal parameter as the mean and the standard deviation as the mean divided by ten. We then synthesized 100 parameters based on the distribution. Using this ensemble of synthetic “optimal” parameter values in the allometry equations, we estimated and plotted the modeled crown area or leaf biomass for each parameter with the observed data. From a qualitative visual inspection of the crown area or leaf biomass scatter plots, the parameters that created outlier values were removed from the synthesized parameters. The resulting parameters were then included in the trait matrix.

The above processes resulted in a 12x12 trait covariance matrix from which we could generate parameter values for use in FATES simulations (Figure 4.1). We followed the general methods as described by Koven et al. (2020) to generate these parameter ensembles. This resulted in a 100-member ensemble of parameterizations for a single-PFT representing conifer species in Idaho. We repeated the processes described above in order to generate a 100-member parameter ensemble with two PFTs (PFT1-pine and PFT2-fir). To do so, we subset the compiled plant trait data and allometric data from the ten Idaho conifer species for three pine species (ponderosa pine, lodgepole pine, and western white pine) to parameterize PFT1-pine. PFT1-pine is assumed to be shade intolerant and has a lower wood density ( $<0.4 \text{ gC/m}^3$ ). We also subset the larger ten-species data for Douglas fir and Western hemlock to parameterize PFT2-fir. We assumed the same distributions for the plant trait data and followed the same methodology for

generating the allometric parameters. PFT2-fir is assumed to be shade tolerant and has a higher wood density compared to PFT1-pine ( $>0.4 \text{ gC/m}^3$ ).

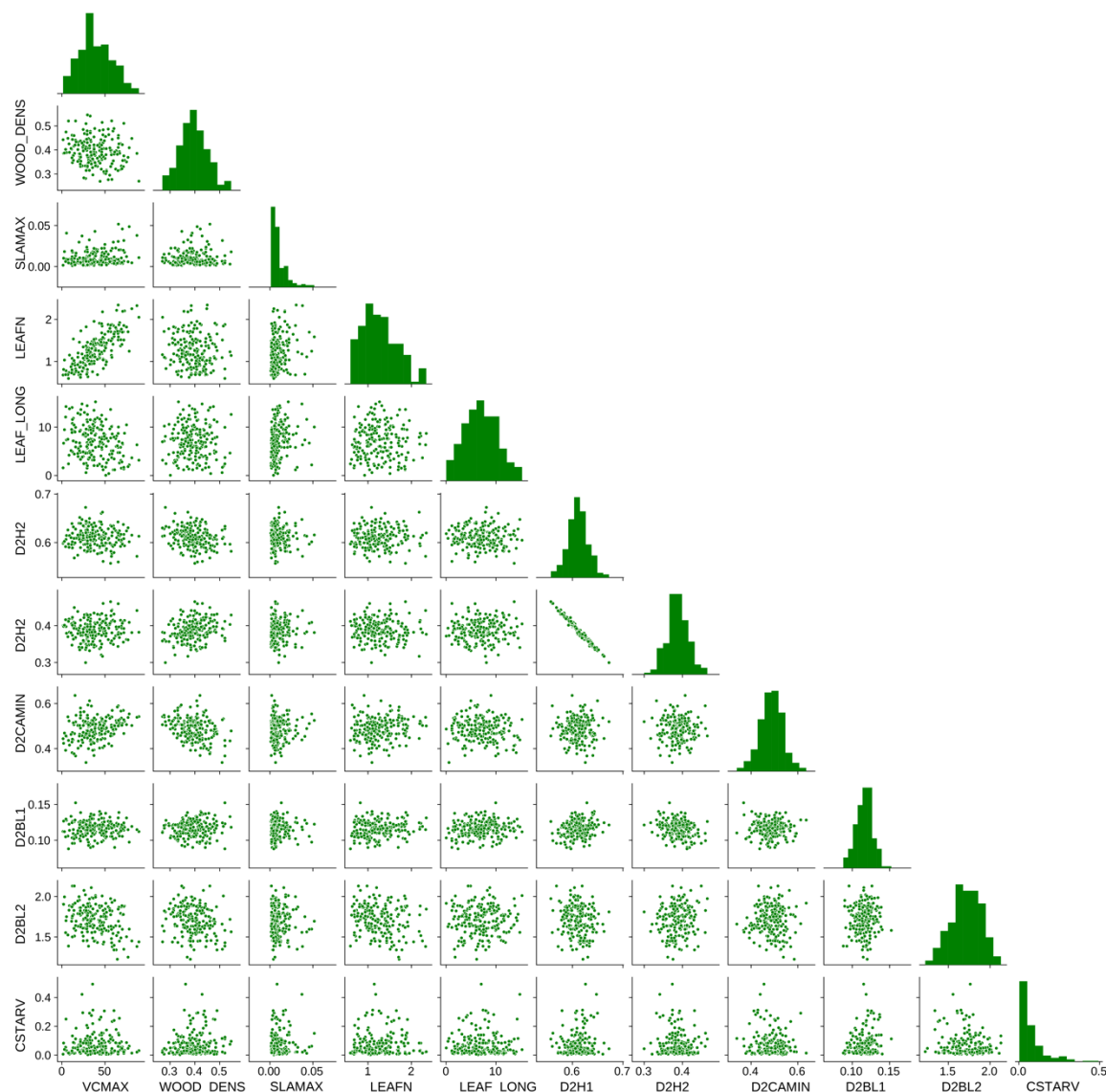


**Figure 4.1** Trait matrix of the synthetic trait values for the 10 common conifer species in Idaho.

### Model Simulation Setup

We ran each of the resulting parameterizations for a single grid cell in southern Idaho at the Boise Basin Experimental Forest (BBEF, Figure 4.2). This specific grid cell was approximately  $15.5 \text{ km}^2$  and at approximately 1300 m elevation. Many locations in

the BBEF are dominated by ponderosa pine with lodgepole pine and Douglas fir (Graham and Jain, 2004). Historically, frequent, low severity fires in the area would have left open, ponderosa dominant forest, however with fire management practices a lack of fire has increased the number of competing trees, specifically Douglas fir (Graham and Jain, 2004). The climate in the area could be considered semi-arid or Mediterranean with warm, dry summers and cool, wet winters. Temperature here ranges from  $-4^{\circ}\text{C}$  in the winter to  $19^{\circ}\text{C}$  in the summer and has average annual precipitation of 635 mm which mostly falls from October through June (Graham and Jain, 2004), with about large fraction falling as snow in the winter. Soils in the area are granitic and have a pH ranging from 5.5 to 7.0 (Graham and Jain, 2004).

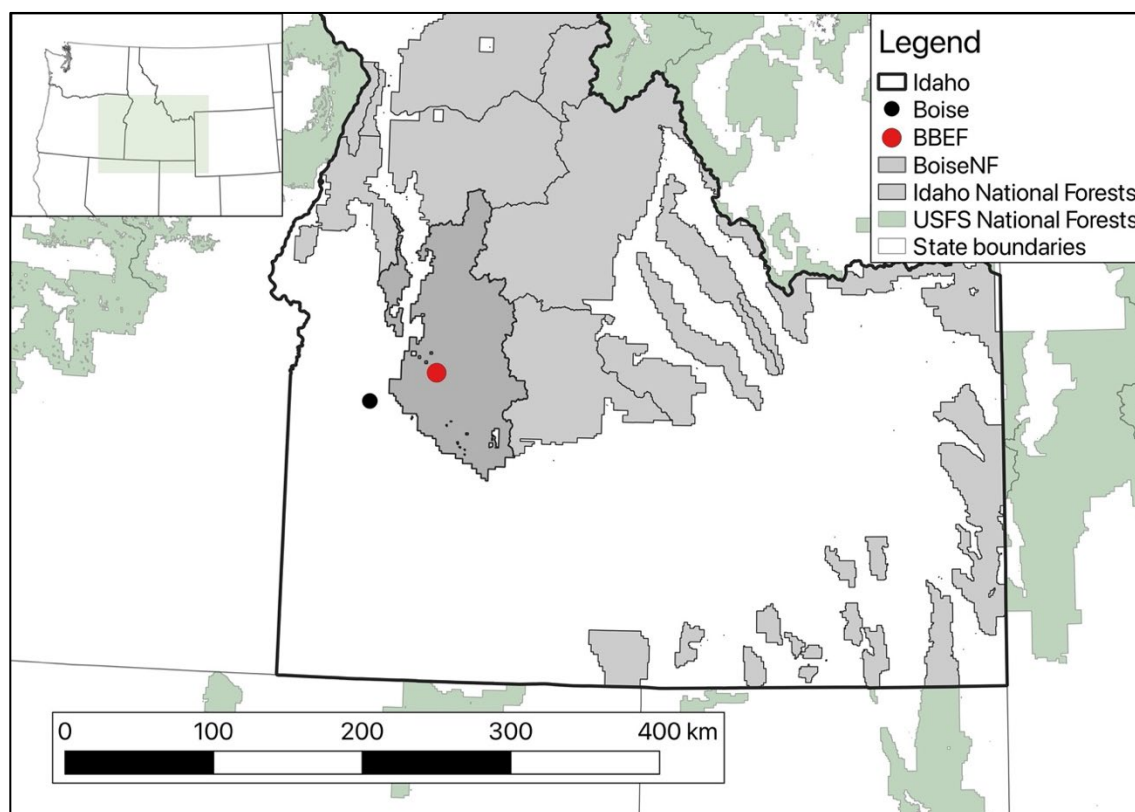


**Figure 4.2** Location map for the single point scale at the Boise Basin Experimental Forest (BBEF, red circle).

For these simulations we used the 0.5degree-by-0.5degree Climate Research Unit and National Centers for Environmental Prediction (CRUNCEP, CRU in this study, Viovy, 2018) climate data as well as a 1km-by-1km resolution Weather Research Forecasting (WRF, Flores et al., 2016). The CRU forcing was recycled from 1979-2014 for this study. The WRF forcing was cycled from 1988-2015. Each simulation was initiated from bare ground and ran for 150 years. In total we ran 400 simulations, one simulation for each of the 100 single-PFT ensembles and the 100 multi-PFT ensembles using both CRU and WRF as a forcing.

### Model Analysis

We compared the modeled ensemble mean gross primary productivity (GPP), leaf area index (LAI), and aboveground biomass (AGB) from the last 50 years of the simulation to target data. We compared the modeled GPP to MODIS data for the BBEF area as well as the average GPP from two of the Metolius Fluxtower sites in Oregon. The Metolius sites represent an old and young ponderosa pine forest on basaltic soils in a climate similar to BBEF (Law, 2016 and 2022). We compared the modeled LAI to remotely sensed LAI from MODIS for the area of BBEF (Myneni and Park, 2015). We compared the modeled AGB to the biomass maps from Wilson et al. (2013) which were calculated based on FIA data from the US Forest Service. We also compared modeled stem densities of large trees to FIA census data for ponderosa pines in southern Idaho for the 1991 inventory.

From the modeled outputs we classified ensembles as “successful” or “unsuccessful” depending on whether they grew plants into the 50 to 60 cm at DBH size class. Using this simple classification, we compared the parameter distributions for

successful and unsuccessful ensembles for both the parameter ensembles. We used a two-sample Kolmogorov–Smirnov (KS) test to determine the difference in parameter distributions between the successful and unsuccessful single-PFT ensembles and the successful and unsuccessful two PFT ensembles.

Model simulations were completed using the National Center for Atmospheric Research (NCAR) Cheyenne high performance computer system (CISL, 2019). All analyses were completed using Python in Jupyter Notebooks on the NCAR Casper data analysis and visualization cluster (CISL, 2019). Notebooks will be made available in the main author's GitHub repository.

## **Results**

### Differences Between the Climate Forcings

There were differences between the two climate forcing datasets used in this study. The WRF dataset is a 1km-by-1km resolution forcing (Flores et al., 2016) while the CRU dataset is a 0.5degree-x-0.5degree resolution forcing (Viovy, 2018). The WRF forcing was wetter than the CRU forcing in December and January, while the CRU forcing was wetter than the WRF forcing in June and July (Figure 4.3). In general, the WRF forcing had more precipitation as snow in the winter and early spring compared to the CRU forcing data (Figure 4.3). The WRF forcing data was warmer than the CRU forcing data from January through September (Figure 4.4). The CRU forcing data was slightly warmer than the WRF forcing data in November and December.

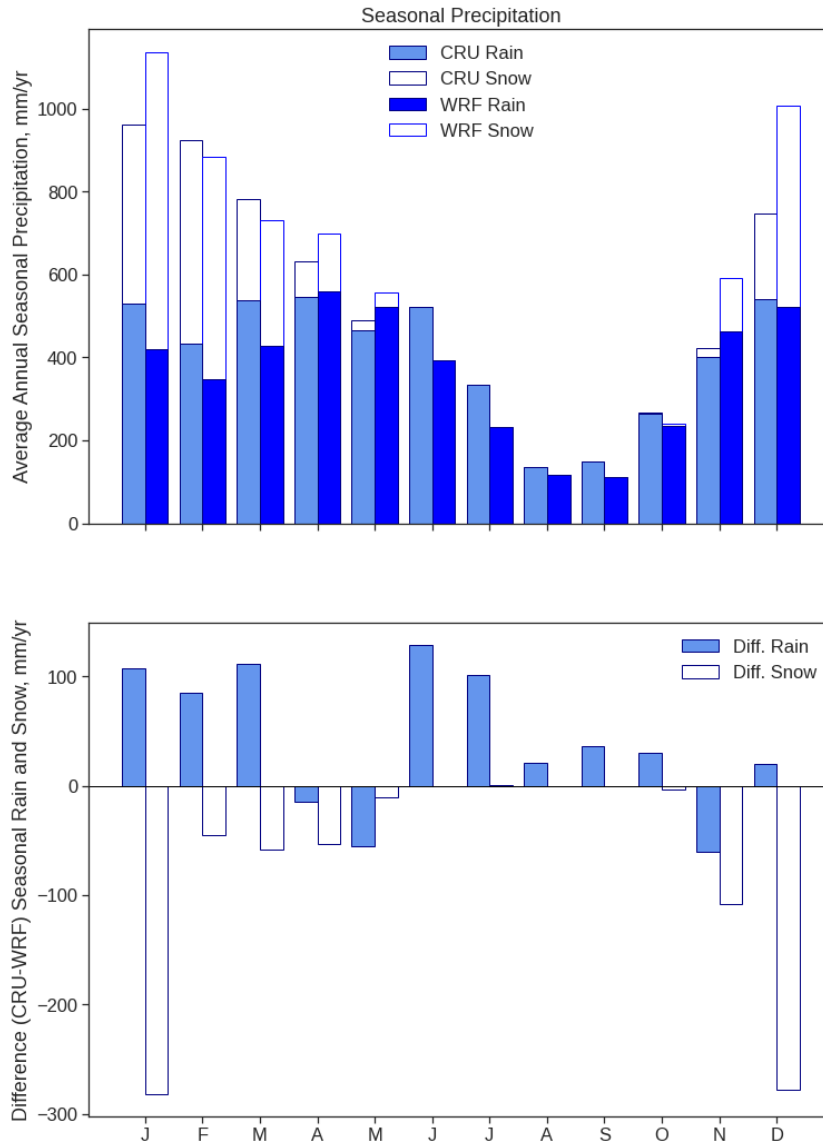


**Figure 4.3 Differences between the CRUNCEP and WRF seasonal precipitation. Negative values occur where the WRF data is greater (i.e. wetter) than the CRUNCEP data.**

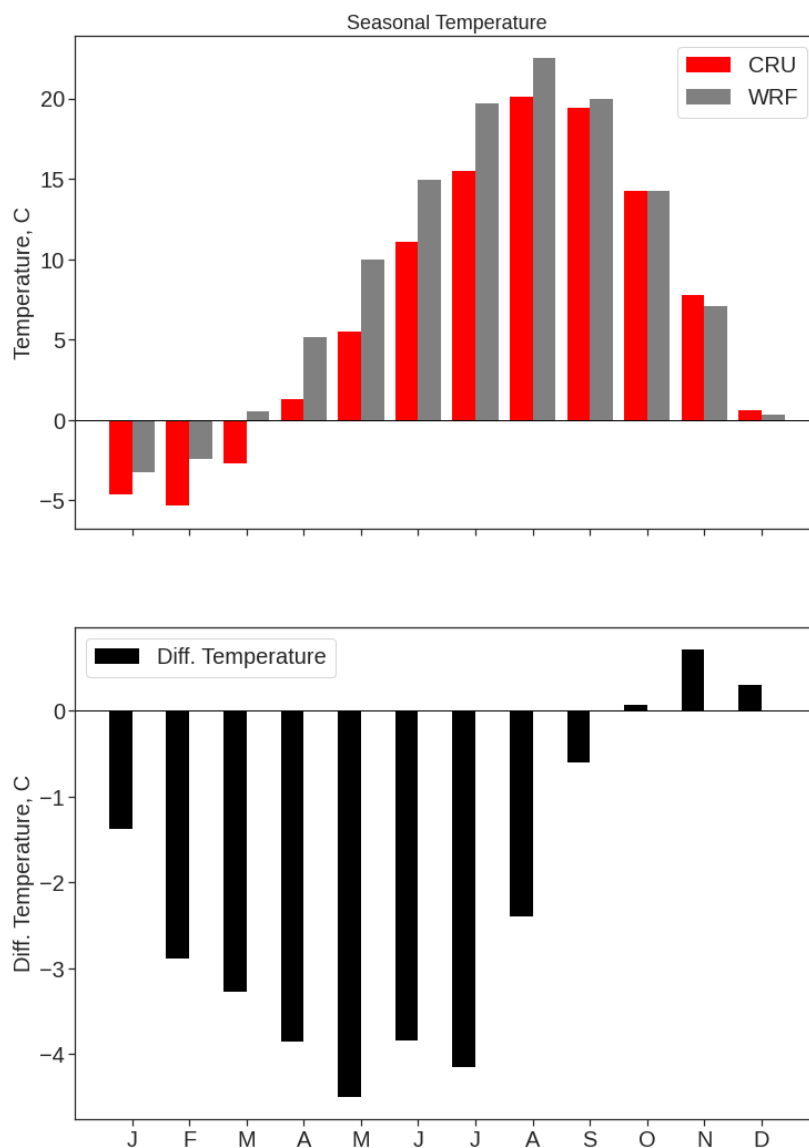


**Figure 4.4** Differences between the CRUNCEP and WRF seasonal temperature. Negative values occur where the WRF data is greater (i.e. warmer) than the CRUNCEP data.

#### Comparison to Observed AGB, LAI, and GPP

The single-PFT WRF and CRU ensembles both resulted in a bimodal distribution of mean ensembles GPP values. For both single-PFT climate ensembles there was a large peak near zero GPP and a smaller peak near 750 gC/m<sup>2</sup>/yr and 1000 gC/m<sup>2</sup>/yr for the CRU and WRF forcings, respectively (Figure 4.5). The single-PFT WRF ensembles could produce a larger ensemble mean GPP relative to the CRU ensembles. However, 18% of

the WRF ensembles failed, meaning that vegetation did not grow and resulted in no GPP. Even when the non-producing GPP ensembles were removed, the large peak in near-zero values for GPP remained for the WRF ensembles. All of the single-PFT CRU ensembles could produce GPP, but again, there was a large number of near-zero ensembles. The second peak of GPP values fell between the GPP values for the young and mature Metolius Ameriflux sites.

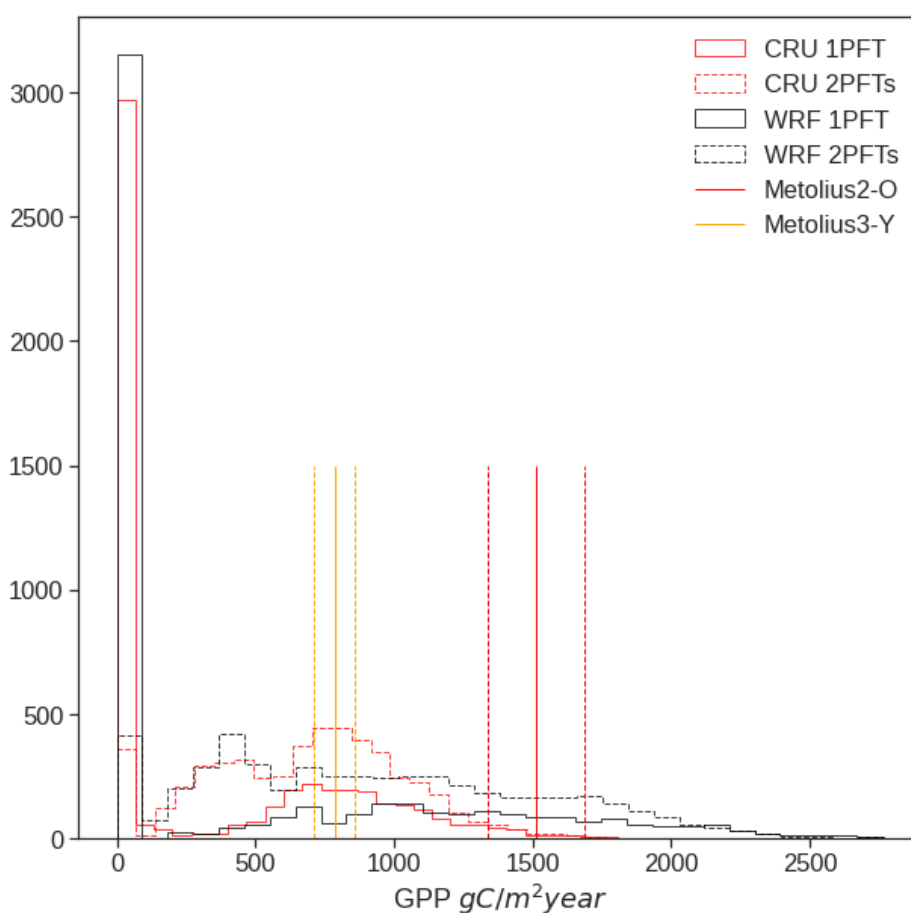


**Figure 4.5** Histogram of ensemble mean GPP for the last 50 years of the simulation. Vertical lines are the mean and standard deviation observed GPP from two Metolius Ameriflux tower site.

The multi-PFT WRF and CRU ensembles both resulted in a sharp decrease in the number of ensembles that produced near zero GPP compared to the single-PFT ensembles (Figure 4.5). The multi-PFT CRU ensembles became multi-modal with peaks of GPP near zero, 500 gC/m<sup>2</sup>yr, and 750 gC/m<sup>2</sup>yr. The multi-PFT WRF ensembles maintained a bimodal distribution, but the second peak shifted to approximately 400 gC/m<sup>2</sup>yr. However, the tail of the multi-modal GPP WRF values extended to over 2000 gC/m<sup>2</sup>yr.

The single and multi-PFT ensembles all resulted in a lognormal distribution of mean ensemble LAI values (Figure 4.6). For both single-PFT climate ensembles there was a large peak near zero LAI. For both multi-PFT climate ensembles the distribution of mean ensemble LAI remains lognormal, but there was a reduction to the near-zero peak. As with GPP, the WRF ensembles were able to produce much larger LAI values compared to the CRU ensembles. The tail of the distribution decreased with the multi-PFT ensembles compared to the single-PFT ensembles.

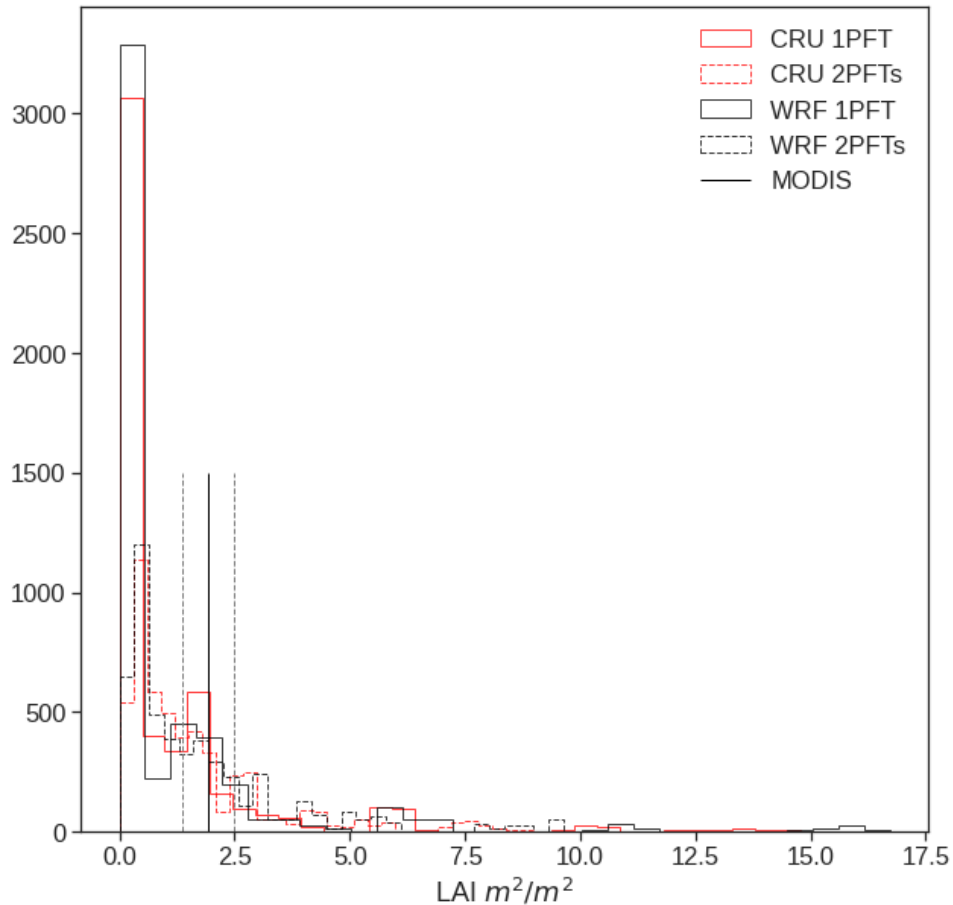


**Figure 4.6** Histogram of ensemble mean LAI for the last 50 years of the simulation. Vertical lines are the mean and standard deviation from MODIS derived LAI.

The single and multi-PFT WRF ensembles could produce much larger mean annual ABG values compared to the single and multi-PFT CRU ensembles (Figure 4.7). The single-PFT WRF ensembles were generally smoother than the single-PFT CRU ensembles, however both seemed to maintain a positive trajectory through time. The multi-PFT ensembles led to lower overall ABG for both climate scenarios. Additionally, the multi-PFT ensembles seemed to have more annual variability in ABG compared to the single-PFT ensembles. The histogram of ABG from the Boise National Forest, where the single point for the simulations is located, is shown in Figure 4.8, and has a mean near  $2650 \text{ gC}/m^2$  (the thick black line in Figure 4.7) (Wilson et al., 2013). Assuming a normal

distribution for AGB, values above two standard deviations ( $\sim 5900 \text{ gC/m}^2$ ) may not be reasonable, however the maximum observed AGB for Boise National Forest is 18910  $\text{gC/m}^2$  (Wilson et al., 2013).

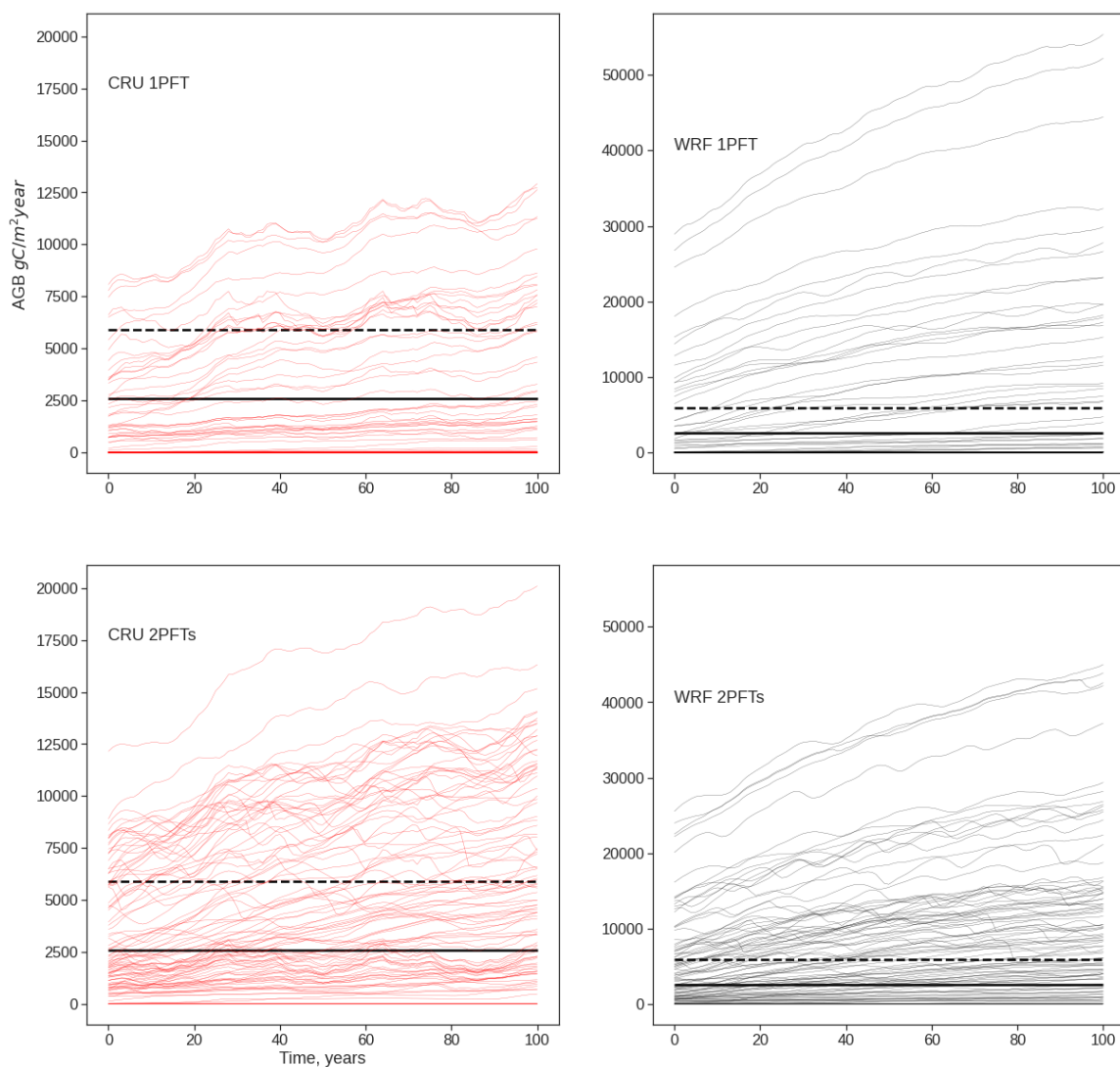


**Figure 4.7 Spider plots of annual mean AGB from each ensemble. The solid horizontal line is the mean observed AGB ( $2560 \text{ gC/m}^2$ ) and the dashed horizontal line is  $+2$  standard deviations of AGB ( $5900 \text{ gC/m}^2$ ) from Wilson et a. (2013) for the Boise National Forest, where the Boise Basin Experimental Forest is located.**

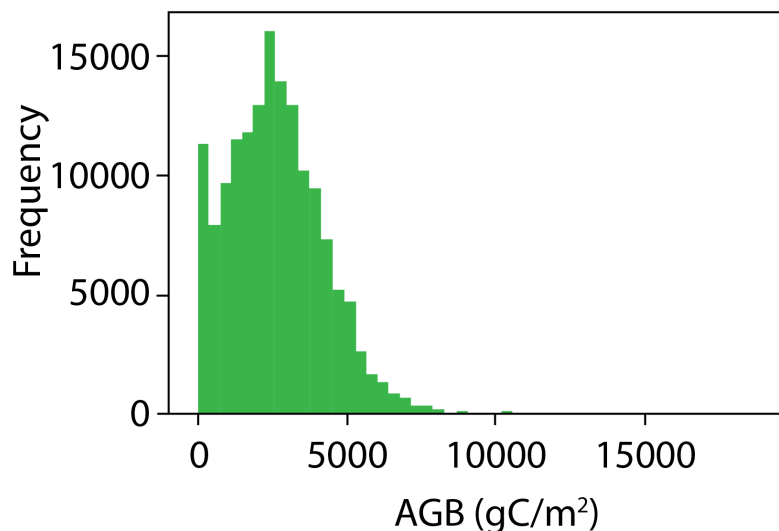


**Figure 4.8** Histogram of observed AGB at Boise National Forest from Wilson et al., 2013.

#### Success at Growing Large Trees: Single-PFT Ensembles

One of the main goals of this study was to successfully grow trees to at least 50 cm DBH at this single point scale. The single-PFT ensembles were able to produce trees within the 50-60 cm size class. Of the WRF single-PFT ensembles, 30% of the parameter ensembles grew large trees (Table 4.3). Of the CRU single-PFT ensembles, 31% of the parameter ensembles grew large trees.

**Table 4.3** “Successful” ensembles and list of ensembles outside of reasonable AGB values.

Scenario	Ensembles >0.0 GPP (%)	“Successful” Ensembles (grew trees >50 cm DBH) (%)	Ensembles > +2 std AGB (%)	Ensembles > max. AGB (%)
CRU-1PFT	100	31	13	0
WRF-1PFT	82	30	5	11
CRU-2PFTs	100	87	15	1
WRF-2PFTs	100	88	15	15

In general, the single-PFT WRF ensembles that grew large trees produced mean ensemble GPP between the values from the young and mature Metolius sites (Figure 4.9). However, some of the single-PFT WRF ensembles still produced GPP that was greater than 2500 gC/m<sup>2</sup>yr. The single-PFT CRU ensembles that grew large trees had a mean ensemble GPP between the values for the young and mature Metolius sites. The single-PFT ensembles produced mean ensemble LAI values that were very similar to the LAI values from MODIS (Figure 4.10). Again, the single-PFT WRF ensembles were able to produce much larger LAI values than the single-PFT CRU ensembles. The single-PFT WRF ensembles resulted in some of the largest AGB values (Figure 4.7). Eleven of the single-PFT WRF ensembles resulted in AGB greater than the maximum observed at Boise National Forest (Table 4.3). None of the single-PFT CRU ensembles that grew large trees resulted in AGB greater than the maximum observed at Boise National Forest. While some of the successful parameterizations produced reasonable GPP, AGB, or LAI individually, none of the single-PFT ensembles resulted in a parameterization that grew larger trees and produced reasonable ranges of GPP, LAI, or AGB. In this study, the reasonable range for LAI was plus or minus two standard deviations from the MODIS derived mean. The reasonable range for GPP was the minus two standard deviations from the mean for the young Metolius site and plus two standard deviations of the mean for the mature Metolius site. We considered any AGB value between the minimum and maximum for Boise National Forest to be reasonable.

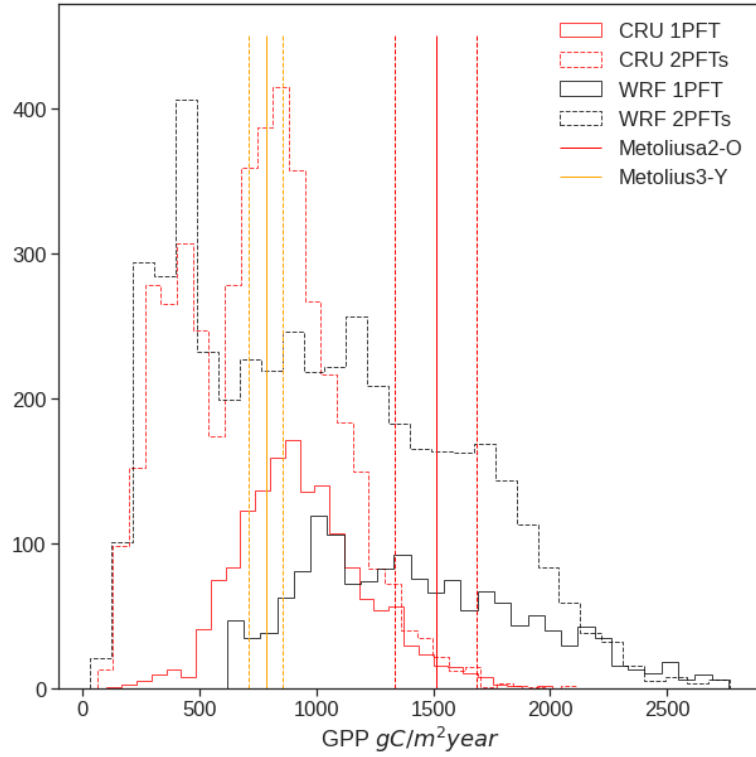


**Figure 4.9** Histogram of “successful” ensemble mean GPP for the last 50 years of the simulation. Vertical lines are the mean and standard deviation observed GPP from two Metolius Ameriflux tower site.

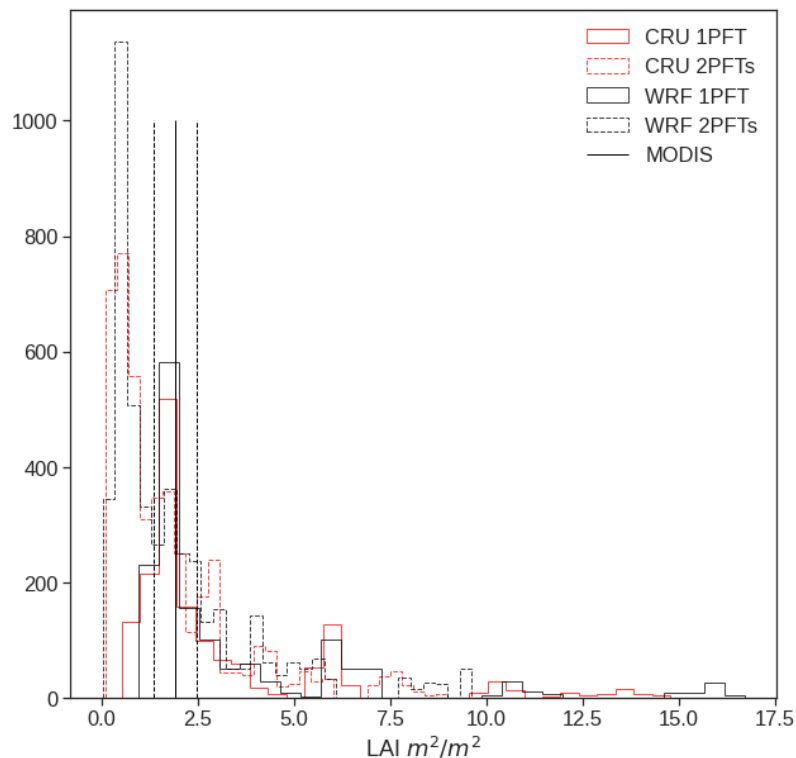


**Figure 4.10** Histogram of “successful” ensemble mean LAI for the last 50 years of the simulation. Vertical lines are the mean and standard deviation from MODIS derived LAI.

The trait matrix in Figure 4.11 shows the parameter values color coded for successful or unsuccessful single-PFT ensembles. A visual inspection of the trait matrix showed that `VCMAX`, `WOOD_DENS`, `D2CAMIN(MAX)`, `LEAFN`, and `SLAMAX(TOP)` all had different kernel density estimates (KDE) for the successful ensembles compared to the unsuccessful ensembles. We calculated the p-values for the distribution using the two-sample KS test from the Python `scipy stats` package (Virtanen et al., 2020). The results from this test are shown in Table 4.4. From the KS tests we found that `VCMAX`, `WOOD_DENS`, `LEAF_LONG`, `D2CAMIN(MAX)`, `LEAFN`, and `SLAMAX(TOP)` all had significantly different ( $p\text{-value} < 0.05$ ) distributions of parameter values for the successful single-PFT ensembles compared to the unsuccessful ensembles.

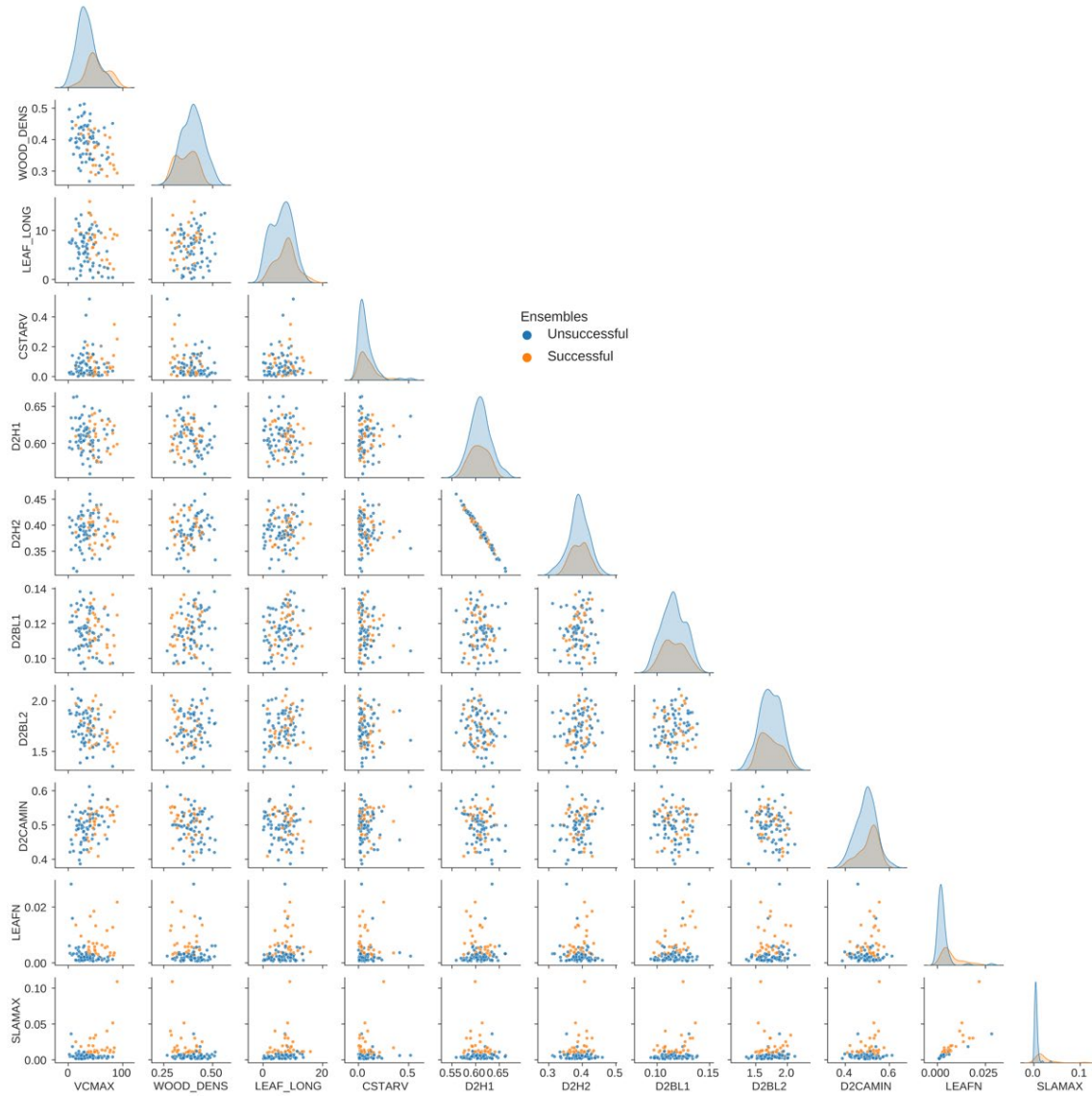


**Figure 4.11** Trait matrix of single-PFT ensembles color coded for successful (orange) and unsuccessful (blue) parameterizations.

**Table 4.4 Results from the KS test for the multi-PFT ensembles. Each parameter value corresponds to the success of growing its corresponding PFT. \* p-values < 0.05**

Parameter	KS value	p-value
VCMAX	0.524	3.081E-11*
WOOD_DENS	0.287	0.001*
CSTARV	0.211	0.038*
D2H1	0.172	0.143
D2H2	0.148	0.279
D2BL1	0.162	0.189
D2BL2	0.114	0.594
D2CAMIN(MAX)	0.091	0.836
LEAFN	0.280	0.002*
SLAMAX(TOP)	0.661	1.414E-18*

#### Success at Growing Large Trees: Multi-PFT Ensembles

The multi-PFT ensembles were able to produce trees within the 50-60 cm size class. Of the WRF multi-PFT ensembles, 87% of the parameter ensembles grew large trees (Table 4.3). Of the CRU multi-PFT ensembles, 88% of the parameter ensembles successfully grew large trees.

We assumed the same reasonable values for GPP, AGB, and LAI. From the successful multi-PFT ensembles both the WRF and CRU scenarios resulted in 71 ensembles within a reasonable range of GPP, AGB, and LAI (Figures 4.9 and 4.10). The multi-PFT ensembles all produced lower mean ensemble values for GPP, AGB, and LAI relative to the single-PFT ensembles.

The trait matrix (Figure 4.12) shows the parameter values color coded for successful or unsuccessful multi-PFT ensembles. Figure 4.13 only shows the parameter values from PFT1-pine, a similar trait matrix for PFT2-fir values can be found in the appendix C. A visual comparison of the trait matrix and KDE did not reveal any obvious difference in the parameter values for successful or unsuccessful multi-PFT ensembles. We performed a KS test for the distributions of parameter values for PFT1-pine and PFT2-fir and their success at growing PFT1-pine, PFT2-fir or both. From this test we found that none of the parameter distributions were significantly different (p-value < 0.05) from each other (Table 4.5). The lowest p-values were found for WOOD\_DENS (0.058) and LEAF\_LONG (0.076) for PFT1-pine and successfully growing PFT1-pine and for LEAFN (0.074) of PFT2-fir for growing PFT2-fir.

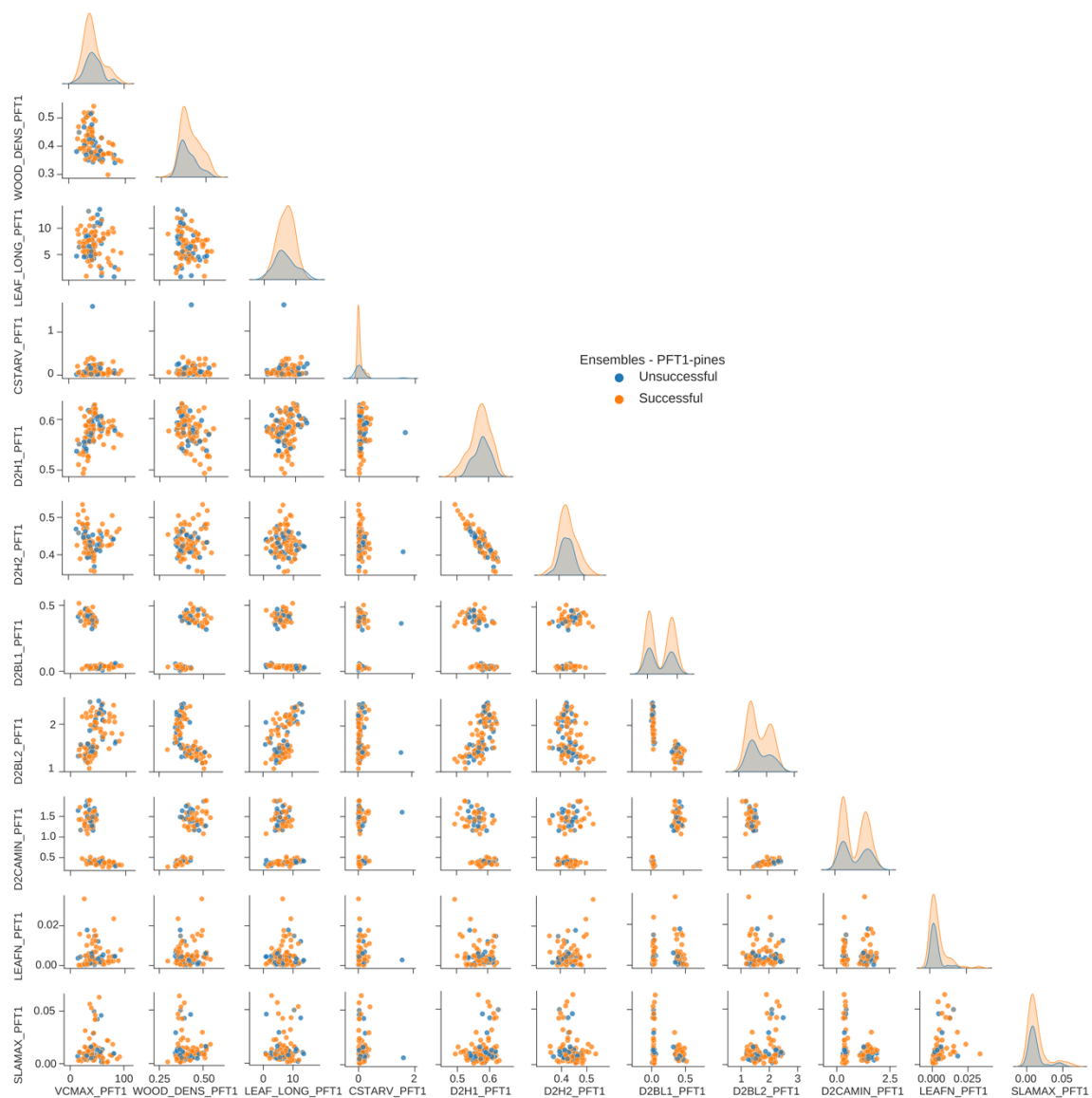


**Figure 4.12 Trait matrix of PFT1-pine parameter values for multi-PFT ensembles color coded for parameterization that successfully (orange) and unsuccessfully (blue) grew PFT1-pines >50cm DBH.**

**Table 4.5 Results from the KS test for the multi-PFT ensembles. Each parameter values corresponds to the success of growing its corresponding PFT.**

Parameter	KS value	p-value
VCMAX_PFT1	0.169	0.150
VCMAX_PFT2	0.153	0.384
WOOD_DENS_PFT1	0.199	0.058
WOOD_DENS_PFT2	0.198	0.135
LEAF_LONG_PFT1	0.191	0.076
LEAF_LONG_PFT2	0.118	0.704
CSTARV_PFT1	0.170	0.148
CSTARV_PFT2	0.144	0.458
D2H1_PFT1	0.145	0.294
D2H1_PFT2	0.163	0.310
D2H2_PFT1	0.171	0.144
D2H2_PFT2	0.127	0.616
D2BL1_PFT1	0.103	0.708
D2BL1_PFT2	0.137	0.520
D2BL2_PFT1	0.103	0.708
D2BL_PFT2	0.107	0.806
D2CAMIN(MAX)_PFT1	0.108	0.657
D2CAMIN(MAX)_PFT2	0.183	0.194
LEAFN_PFT1	0.163	0.180
LEAF_PFT2	0.218	0.074
SLAMAX(TOP)_PFT1	0.181	0.105

Parameter	KS value	p-value
SLAMAX(TOP)_PFT1	0.205	0.111

## Discussion

### Impacts of Different Climate Forcing Data on Plant Functional Response

Ecosystem functioning in LSMs are sensitive to the climate forcing data used (Bonan, 2019; Medvigy et al., 2010). In this study we used two different climate forcing datasets to drive the ensemble simulations, WRF (1km-by-1km resolution) and CRU (0.5degree-by-0.5degree resolution). The WRF climate dataset is generally warmer but also snowier than the CRU dataset. Duarte et al. (2022) showed that within mountainous conifer forests in the western US, wetter and warmer climates may lead to a positive bias in modeled AGB values using CLM. Our results agreed with Duarte et al. (2022), all the modeled mean ensemble values of AGB (as well as GPP and LAI) were higher for the WRF ensembles than the modeled values from the CRU ensembles and also higher than observations. Duarte et al (2022) also found that the resolution of the climate data did not make a significant difference in the modeled AGB. In our study, not only were the climate forcings at different resolutions, but the difference in temperature and precipitation provided by the two models were also quite different. Here, the higher resolution WRF dataset may capture more detailed topographic impacts on snow distribution and therefore represent more snow than the coarser scale CRU dataset captured for the same area. This has important implications on plant growth. A relatively snowier climate forcing may provide water to plants at different times compared to a rainier climate forcing dataset even if the amount of precipitation is roughly the same.

Water is stored in the snowpack until melt or evaporation releases it to the soil interface where it may leave as runoff or enter the soil column for plant use. This snowmelt may occur at more beneficial times for plant use and could lead to higher soil water contents for the WRF data driven simulations at a time where the less snowy CRU climate driven simulations may already have drier soils.

### Single-PFT Ensembles and Parameter Distributions

The single-PFT parameter ensembles in this study could not produce a model output that grew trees into the 50-60cm size class and had reasonable values of GPP ( $\pm$  two standard deviations of the young and mature Metolius Ameriflux sites), LAI ( $\pm$  two standard deviations of the MODIS derived values), and AGB (the range of values from Wilson et al., 2013). While none of the single-PFT parameterizations were successful and “reasonable”, there was a distinct difference between the parameter distributions that could grow large trees in the single-PFT parameterizations which was lost once we added competition of two species specific PFTs (Tables 4.3 and 4.4). Of the parameters that had two distinct distributions of values, SLAMAX, LEAFN, VCMAX, WOOD\_DENS, D2CAMIN, and LEAF\_LONG had the lowest p-values from the KS tests meaning the distributions of parameter values for successful and unsuccessful ensembles were significantly different from each other. Within FATES, these parameters directly and indirectly impact plant growth and carbon assimilation (photosynthetic capacity, i.e. shade tolerance).

The parameters WOOD\_DENS, LEAF\_LONG and D2CAMIN are all important for determining a PFTs growth strategy which have important implications for the composition of the forest post-disturbance (e.g. fast growing plants outcompeting slow

growing plants following a disturbance). For example, the allometric equation used in this study calculated AGB and leaf biomass as a function of wood density. As wood density decreases, the cost to grow biomass also decreases, meaning that PFTs with relatively lower wood density may have a growth advantage over PFTs with a higher wood density. A plant with a relatively higher value for LEAF\_LONG will allocate less resources to leaf growth, which allows PFTs with longer life turnover to allocate carbon elsewhere instead of to new leaf growth. The diameter to crown area coefficients (D2CAMIN) control the rate of canopy spread with implications for the total LAI which in turn can impact the integration of photosynthesis to the cohort level and the resulting carbon assimilation and allocation.

The parameters SLAMAX, LEAFN, and VCMAX all impact the leaf level photosynthesis within a tree and the modeled GPP, and a PFT's relative value of these parameters are associated with different shade tolerances. In FATES, this trio of parameters can be configured to influence a plant's response to the light environment (i.e. shade tolerance) (e.g. Buotte et al., 2019). For example, PFTs with a relatively lower VCMAX values would have a photosynthetic advantage over those PFTs with a higher VCMAX in the shade. These values would be coordinated within a real plant (Wright et al., 2004), but within FATES they are allowed to vary to define trait specific PFTs (Koven et al., 2020). Since we sampled a larger distribution of values for the single-PFT ensembles, we may have had ensembles that did not reflect a realistic proportion of these parameter values. This lack of coordination may have led to model failures (e.g., where GPP was 0), as well as impacted the assimilation and allocation of photosynthetic carbon to the point that trees could not grow large.

These results highlight the importance of representing plant strategies for growth and shade tolerance. The classification of the PFT1-pine and PFT2-fir were selected explicitly to evaluate the parameter values that would differentiate shade tolerances. Although we did modify the parameters that influence plant growth, we did not alter these parameters to differentiate growth strategies between the two PFTs.

#### Species Specific PFTs and Modeled Outputs

Our simulations that used the multi-PFT ensembles resulted in a narrower range of reasonable values of GPP, LAI, and AGB compared to the single-PFT ensembles. These findings are the opposite of those observed by Koven et al. (2020) using this method for benchmarking experiments within Panama. However, like Koven et al. (2020) the multi-PFT ensembles were able to produce large trees. One important difference between our study and Koven et al. (2020) was that we created multiple PFTs based on specific species with different plant strategies while they made no prior assumptions about the plant strategies. Their PFTs were determined by randomly creating a vector of parameter values from a large trait matrix based on observations. Conversely, the parameter matrices for PFT1-pines and PFT2-fir were generated from smaller datasets subset by species. There was less of a range of parameter values to sample from for each of the PFTs. By sampling from smaller datasets for the more specific PFTs compared to the single-PFT ensembles, we were reducing the differences between the adjusted parameters values in the ensemble members which accounted for the narrowing of the range in modeled GPP, LAI, and AGB (also seen in Koven et al., 2020).

From the K-S tests, we found no significant differences in the parameter distributions of successful multi-PFT ensembles compared to unsuccessful multi-PFT

ensembles. This was true for ensembles that successfully grew PFT1-pines or PFT2-fir. The differences between the successful and unsuccessful multi-PFT parameter ensembles essentially disappeared when we constrained the parameter values for the two PFTs because the trait matrix for each of the PFTs came from a smaller subset of plant trait data. There was less of a range and variance of certain parameters (e.g. LEAF\_LONG, D2H1, D2H2, and SLAMAX) which meant that unsuccessful ensembles could have very similar parameter values to those from successful ensembles. This result highlights the importance of parameter selection and parameter coordination within FATES, especially when working to represent more species specific PFT coexistence. For example, unsuccessful and successful parameter ensembles could have very similar values for some parameters but small differences in another parameter could be the difference between success or failure. This also emphasizes the sensitivity of FATES to allometry and the allometric parameters which could be the reason that small changes to one parameter (i.e. an allometric parameter) can strongly impact tree growth and the resulting distribution of competing PFTs.

### Limitations

There were several limitations to this study due to factors we did not include in the simulations. First, the simulations could have been run for a longer amount of time. Often, a spinup period is required to produce reliable modeled outcomes, and these spinup times can last from 100 to over 1000 years (Buotte et al., 2019; Huang et al., 2020; see also Chapter 3). Based on previous logging simulation studies using FATES in which AGB, GPP, and LAI compared reasonably well to observations and a few large trees could grow, we assumed that 150 years would be ample time for these ensemble

simulations (see Chapter 3). We ran these simulations from bare ground for 150 years which was long enough to equilibrate AGB for many of the single and multi-PFT ensembles but not all. Future work could include running these ensembles for a longer period. Additionally, we only used tree PFTs and did not include any shrub or grass PFTs. Grass and shrub growth have been shown to influence forest productivity and carbon cycle in ponderosa pine forests (Doughty et al., 2021). We did not include fire in this study even though our location historically had frequent, low severity fires (Graham and Jain, 2004). Representing the fire regime in semiarid temperate conifer forests is important for forest composition (Nemani et al., 2003). Including fire within the FATES simulations may be necessary to produce the proper proportion of coexisting PFTs within a semi-arid forest (Buotte et al., 2021). However, adding fire to FATES simulations adds another layer of complexity to the model. The fire module used within FATES (SPITFIRE, adapted from Thonicke et al., 2010) would require the user to determine additional plant trait parameters, such as bark thickness and crown height, as well as fire condition parameters such as fuel drying ratios. This additional parameterization of the fire module was outside the scope of this study but can be considered in future work.

We did not constrain parameter values between the two PFTs to make sure that the values were in the correct proportion for the assumed plant strategy. For example, we did not check that the  $V_{\text{cmax}}$  values for PFT2-fir were always lower than the  $V_{\text{cmax}}$  values for PFT1-pine to represent PFT2-fir's shade tolerance. Recently, Buotte et al. (2021) successfully applied constraints to PFT values in a similar experiment simulation using FATES in the Sierra Nevada of California. Buotte et al. (2021) also applied ecological

constraints after performing single point scale runs to further reduce the set of parameterizations that met their criteria for reasonable forest function and composition.

We did not alter the plant hydraulic trait parameters in this study partly due to a lack of data to inform a range of parameter values. Here we were able to model reasonable AGB, GPP and LAI without adjusting hydraulic trait parameters. However, this is an important parameter to consider. Moustakis et al. (2022) found that the productivity of dry ecosystems may be sensitive to future changes in rainfall, and recent studies suggest that the soil water potential at which stomata close is an important parameter to consider for modeled outputs (Buotte et al., 2019; Duarte et al., 2022).

### Future Work

In the future we would like to use the successful multi-PFT ensembles in simulations covering the northern Intermountain West of the United States (100,000s km<sup>2</sup> scale). To do so we will need to confirm the correct parameter values between the two PFTs as well as define ecological constraints (i.e., shade tolerant pine has lower  $V_{\text{max}}$  than fir) on the expected proportion of PFTs in the simulated forest. Given the fire history of Idaho forests, as these simulations are scaled up, we will also need to include fire.

The results of this study have brought up interesting questions: What could be some of the implications of growing larger trees in vegetation management scenarios? Would having larger trees mean having more trees to cut? Would changes to growth rates result in changes to the number of trees cut at the specified harvest date? What would be the long-term impact of those changes on forest structure and function? While we could only speculate about the answers to these questions, they provide a guide for experimentation moving forward.

## Conclusion

In this study we sought to parameterize the FATES model for a single point in southern Idaho in such a way that the model could grow large conifer trees and simulate observed ranges of GPP, LAI, and AGB. We found that adding coexistence allowed for more successful (i.e., trees could reach at least 50 cm DBH) and reasonable (i.e., within the range of observed GPP, LAI, and AGB) parameter ensembles relative to single-PFT parameter ensembles. Our results showed that multiple parameter ensembles generated from a distribution of parameter values could produce successful and reasonable results in this specific area. Additionally, parameter ensembles produced these results under two different climate forcings: a coarse (0.5degree-x-0.5degree) resolution, relatively cooler and drier climate; and a fine (1km-by-1km) resolution, relatively warmer and snowier climate.

Complex ecosystem models may benefit from parameter values that are described by sample distributions instead of hard coded into the model. This is particularly true for those parameters that may be spatially variable or are coefficients from equations, such as the allometry equations used here. Overconfidence in parameter values that come from observational data or are coefficients from equations and hard coded parameters may reduce the agility of complex models and the reliance on such parameters in hydrologic models has been questioned (Mendoza et al., 2015). At the risk of computational cost, we should not aim to pick exact parameter values but instead use a range of values in simulation ensembles (Mendoza et al., 2015; Prihodko et al., 2008; Saltelli, 2019). This study also highlights the risk of calibrating or optimizing a model such as FATES-CLM for one PFT. While there are very specific cases in which one would desire to optimize

one PFT at a time (e.g., timber plantations or forests clearly dominated by one species), leaving out coexisting species may, paradoxically, introduce a hidden axis of complexity that would place constraints on the range of suitable parameter values.

## CHAPTER FIVE: CONCLUSIONS

The overarching goal of this research was to better understand the dynamics of forest management, a human - environment system, and better represent that system within a LSM. Human systems contain a degree of randomness and stochasticity, in this research, the randomness comes from regulatory processes and requirements and how constituencies may respond. We can quantify, to some extent, what factors will influence the likelihood of a forest management project being delayed. We can also quantify some temporal metrics of management that we can use to generate realistic time series of management activities in forests. When used as input to LSMs such as FATES-CLM, alternative scenarios of management led to long-term differences in forest structure but minor differences in ecohydrologic function. However, these ecohydrologic functions may not be accurately captured by the current model structure due to the germination and recruitment processes following a disturbance or due to the relationship between FATES and its host land model. While the modeling community often focuses on the functional results, forest managers may be more interested in the modeled changes to forest structure. The size of trees and the density of forests not only impact forest health, but also influences what activities a forest manager may choose to pursue within a given location (Bottero et al., 2017; Graham et al., 2007; North et al., 2022). Therefore, parameterizing LSMs to simulate more realistic forest structures, in this case large trees, is important *if* there is a desire within the LSM community for the models to be used or considered by forest managers. Here we discuss a few options for future work to build on

the research here and to further investigate the human aspects of forest management and the modeling aspects of forest management.

### Future Directions

Forest management exists within a complex social-environmental system. For future work, there is an opportunity to incorporate social data such as forest visitation rates, rates of public comment, and population data (e.g., proximity of forest to large urban centers) within our survival analysis (Chapter 2) to better understand the temporal aspects of management. Additionally, there are a variety of political science frameworks that could be used to qualitatively investigate the timing of management practices. The advocacy coalition framework could highlight important advocate groups working to influence management within a location or identify the types of activities that inspire advocate group involvement (Sabatier and Weible, 2007). Using information about a given coalition that is working to influence forest management in different locations and their success rates will provide information on the likelihood of project delay. However, converting the results from such qualitative studies to quantities useful within a LSM still pose a challenge.

Novel and creative ways to incorporate social data or drivers into LSMs should be explored because our results from Chapter 3 highlight a need to include more detailed temporal aspects of human activities within LSMs. We used a simple Markov chain (MC) to predict the days an activity would occur within an average timber harvest. This MC model could be further developed to include more types of activities. Additionally, an agent-based modeling approach could be developed to drive management activity within LSMs. In this case forest managers could be categorized into different Agent Functional

Types (AFT) based on their objectives or risk tolerance (similar to Kaiser et al., 2020). The AFTs could then react to different simulated forest conditions from FATES-CLM which could trigger the logging, thinning, or replanting activities of the vegetation management driver.

There have been many promising developments in representing forest management in LSMs (Huang et al., 2020; Littleton et al., 2020; Rady et al., 2022). With the capability of the new vegetation management driver in FATES-CLM to select activity types and rates based on PFTs, parameterization and calibration of the model at a larger scale would be beneficial. Scaling up, particularly within the mountainous forests of the western US, requires several considerations. In many western forests, fire is a significant consideration. Within FATES-CLM fire may be necessary to produce the correct PFT ratios and abundance (Buotte et al., 2021). In addition to fire, climate is another important consideration in western US forests. Parameters calibrated at a single point with a specific micro-climate are not always transferable to a larger scale (Huang et al., 2016). Scaling these simulations up in mountainous areas has its own complications because of the interaction between climate, topography, and vegetation. The elevation of an area impacts the partitioning of precipitation into either rain or snow, while the slope and aspect of mountainous areas can impact the amount of solar radiation available for photosynthesis and plant growth. Finer resolution climate datasets may better capture the impact of elevation on precipitation and precipitation partitioning. For example, within Chapter 4 the higher resolution WRF climate forcing data captured more precipitation as snow compared to the lower resolution CRU data. A higher resolution climate forcing which better captures precipitation as snow combined with the hillslope hydrology option

for CLM and FATES may be beneficial for scaling up in mountainous regions. The hillslope hydrology model (Swenson et al., 2019) uses a representative hillslope to connect land columns and capture lateral flow between the columns. The hillslope model would better predict the distribution of soil moisture within the area which could have large impacts on the water available for plant growth and the resulting modeled PFT's composition and distribution on the land surface. However, previous research by Duarte et al. (2022) found that the resolution of the climate forcing did not produce significant differences in modeled AGB for simulations conducted using CLM in the intermountain west of the United States.

As a last note about parameterization, using FATES-CLM to simulate forest management may require new ways to parameterize and represent competing PFTs. From a forestry perspective, even different types of pines that would normally be grouped into a single-PFT have different material uses. Exploring the relationship between the uses of plants and their plant traits may provide novel ways to classify PFTs, especially if agent-based model drivers were to be included in LSMs. Building on this, we envision coproduction strategies in which forest managers from the USFS or private industry could work with the LSM community to provide insight and ideas for how to parameterize and operationalize management decisions and strategies for use within the models.

### **Use of Land Surface Models for Forest Management**

Novel forms of forest management such as an anticipatory approach (Field et al., 2020) or a triage approach (Millar et al., 2007) may be necessary to manage forests for resilience in response to a changing climate and disturbance regimes, resistance to

disturbances, or adaptation (Bradford et al., 2018). Additionally, as more governments set goals for carbon neutrality, LSMs will be useful to a variety of managers, policy makers, and other stakeholders to determine to use of forests for carbon offsets. These management goals and challenges and a desire to make informed decisions would benefit from coproduction, where climate scientists and land surface modelers meet with forest managers, policy makers, and stakeholders to identify key modeling questions. These participants would identify decisions that could be informed by these model outputs, and together they would define the research scope, questions, methodologies, results, and the strategies for using the results of the determined scientific endeavors (Beier et al., 2016).

While forest managers are unlikely to learn how to use earth system models, LSMs, and dynamic vegetation models, these models are important and valuable tools for coproduction, if done correctly. These models aid in identifying forested ecosystems which are vulnerable to disturbances, and the models also aid in determining the potential impacts of tree die offs due to those disturbances or through management derived disturbances as used in this research (Buotte et al., 2018; Swann et al., 2018). Part of an adaptive or anticipatory management approach and coproduction includes prioritizing management treatments quickly and effectively (Millar et al., 2007). This prioritization would be greatly aided by using LSMs to test forest response to alternative management scenarios, including testing the timing of those treatments. LSMs, when coupled with atmospheric models, can be used to determine when favorable conditions exist for treatments. As we tested in Chapter 3, LSMs can also be used to show potential outcomes if those treatments do not occur during those favorable conditions due to delays in management implementation.

### **Model Complexity and Model Fidelity**

There is an inherent tension found in the desire to increase model fidelity without necessarily increasing model complexity, uncertainty, or error. While including more detailed forest management makes a model more realistic, it also makes a model more complex. Increased realism in a model may not necessarily mean that model results better reflect reality (Figure 5.1). Given the stochasticity of human systems, incorporating human related actions and potential decision making would add more potential for model uncertainty and therefore model error (Figure 5.2, from Saltelli, 2019). Additionally, we found that many different parameterizations of multiple PFTs, albeit constrained by specific species data, could produce reasonable results (Chapter 4). The necessity of inflexible and hard coded parameters in complex hydrologic models was addressed by Mendoza et al. (2015). Many of the parameters hard coded within CLM and FATES may have spatial variability, measurement uncertainty, may be functions of other conditions, or are entirely made up. These results raise important questions of application (i.e. which parameterization to use) and whether one should be looking for a single, optimal parameterization for use in complex land surface models.

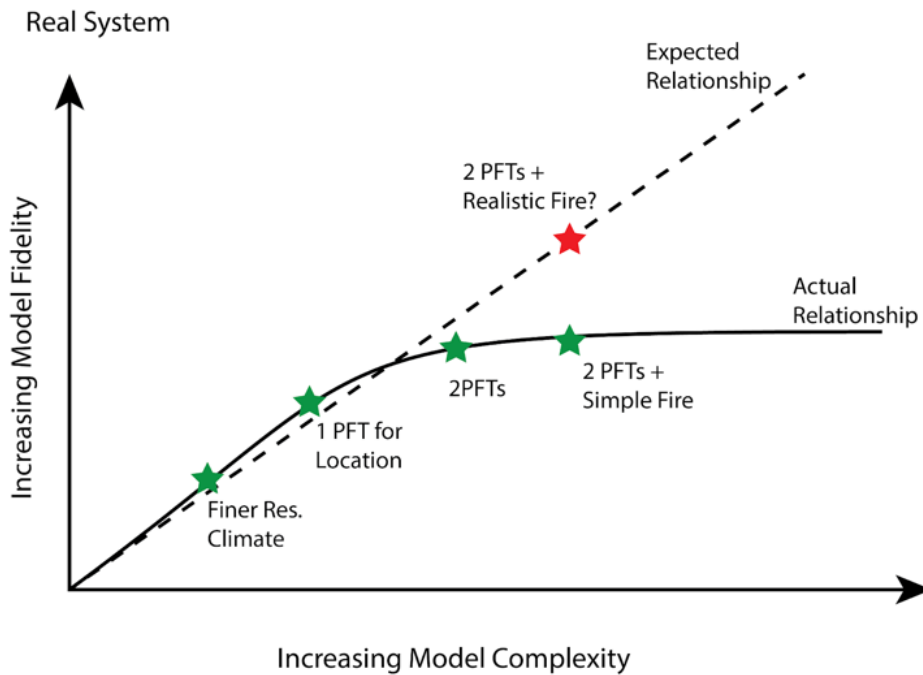


**Figure 5.1** The expected relationship between the realism of results from LSMs and increasing model complexity with the actual relationship. Here we show that continually adding realistic aspects (e.g. fire, multiple PFTs) may not improve model results to the extent anticipated.

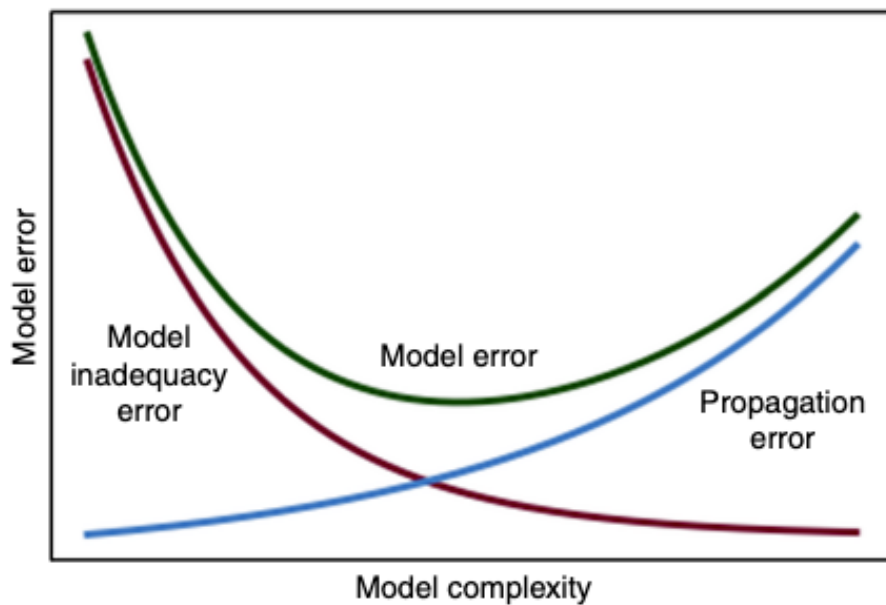


**Figure 5.2** A conceptual model of changes to model error with increasing model complexity. Figure 1 from Saltelli, 2019.

## REFERENCES

- Abatzoglou, J. T. (2013). Development of gridded surface meteorological data for ecological applications and modelling. *International Journal of Climatology*, 33(1), 121–131. <https://doi.org/10.1002/joc.3413>
- Anderson, S. E., Hodges, H. E., & Anderson, T. L. (2013). Technical Management in an Age of Openness: The Political, Public, and Environmental Forest Ranger: Technical Management in an Age of Openness. *Journal of Policy Analysis and Management*, 32(3), 554–573. <https://doi.org/10.1002/pam.21697>
- Beier, P., Hansen, L. J., Helbrecht, L., & Behar, D. (2017). A how-to guide for coproduction of actionable science. *Conservation Letters*, 10(3), 288-296.
- Bewick, V., Cheek, L., & Ball, J. (2004). Statistics review 12: survival analysis. *Critical care*, 8(5), 1-6.
- Bixler, A., Bixler, R. P., Ellison, A., & Moseley, C. (2016). Administrative and judicial review of NEPA decisions: Risk factors and risk minimizing strategies for the Forest Service.
- Bonan, G. (2019). *Climate Change and Terrestrial Ecosystem Modeling*. Cambridge University Press.
- Bonan, G. B. (2008). Forests and Climate Change: Forcings, Feedbacks, and the Climate Benefits of Forests. *Science*, 320(5882), 1444–1449. <https://doi.org/10.1126/science.1155121>
- Bonan, G. B. (2016). Forests, Climate, and Public Policy: A 500-Year Interdisciplinary Odyssey. *Annual Review of Ecology, Evolution, and Systematics*, 47(1), 97–121. <https://doi.org/10.1146/annurev-ecolsys-121415-032359>

- Bonan, G. B., & Doney, S. C. (2018). Climate, ecosystems, and planetary futures: The challenge to predict life in Earth system models. *Science*, 359(6375), eaam8328. <https://doi.org/10.1126/science.aam8328>
- Bosch, J. M., & Hewlett, J. D. (1982). A review of catchment experiments to determine the effect of vegetation changes on water yield and evapotranspiration. *Journal of Hydrology*, 55(1), 3–23. [https://doi.org/10.1016/0022-1694\(82\)90117-2](https://doi.org/10.1016/0022-1694(82)90117-2)
- Bottero, A., D'Amato, A. W., Palik, B. J., Bradford, J. B., Fraver, S., Battaglia, M. A., & Asherin, L. A. (2017). Density-dependent vulnerability of forest ecosystems to drought. *Journal of Applied Ecology*, 54(6), 1605–1614. <https://doi.org/10.1111/1365-2664.12847>
- Box-Steffensmeier, J. M., & Jones, B. S. (1997). Time is of the Essence: Event History Models in Political Science. *American Journal of Political Science*, 41(4), 1414–1461. <https://doi.org/10.2307/2960496>
- Bradford, J. B., Betancourt, J. L., Butterfield, B. J., Munson, S. M., & Wood, T. E. (2018). Anticipatory natural resource science and management for a changing future. *Frontiers in Ecology and the Environment*, 16(5), 295–303. <https://doi.org/10.1002/fee.1806>
- Broussard, S. R., & Whitaker, B. D. (2009). The Magna Charta of Environmental Legislation: A historical look at 30 years of NEPA-Forest Service Litigation. *Forest Policy and Economics*, 11(2), 134–140. <https://doi.org/10.1016/j.forpol.2008.12.001>
- Buotte, P. C., Koven, C. D., Xu, C., Shuman, J. K., Goulden, M. L., Levis, S., Katz, J., Ding, J., Ma, W., Robbins, Z., & Kueppers, L. M. (2021). Capturing functional strategies and compositional dynamics in vegetation demographic models. *Biogeosciences*, 18(14), 4473–4490. <https://doi.org/10.5194/bg-18-4473-2021>
- Buotte, P. C., Levis, S., Law, B. E., Hudiburg, T. W., Rupp, D. E., & Kent, J. J. (2019). Near-future forest vulnerability to drought and fire varies across the western United States. *Global Change Biology*, 25(1), 290–303. <https://doi.org/10.1111/gcb.14490>

- Clyatt, K. A., Keyes, C. R., & Hood, S. M. (2017). Long-term effects of fuel treatments on aboveground biomass accumulation in ponderosa pine forests of the northern Rocky Mountains. *Forest Ecology and Management*, 400, 587–599.  
<https://doi.org/10.1016/j.foreco.2017.06.021>
- Cobb, R. C., Ruthrof, K. X., Breshears, D. D., Lloret, F., Aakala, T., Adams, H. D., Anderegg, W. R. L., Ewers, B. E., Galiano, L., Grünzweig, J. M., Hartmann, H., Huang, C., Klein, T., Kunert, N., Kitzberger, T., Landhäusser, S. M., Levick, S., Preisler, Y., Suarez, M. L., ... Zeppel, M. J. B. (2017). Ecosystem dynamics and management after forest die-off: A global synthesis with conceptual state-and-transition models. *Ecosphere*, 8(12), e02034. <https://doi.org/10.1002/ecs2.2034>
- Collatz, G. J., Ball, J. T., Grivet, C., & Berry, J. A. (1991). Physiological and environmental regulation of stomatal conductance, photosynthesis and transpiration: A model that includes a laminar boundary layer. *Agricultural and Forest Meteorology*, 54(2), 107–136. [https://doi.org/10.1016/0168-1923\(91\)90002-8](https://doi.org/10.1016/0168-1923(91)90002-8)
- Computational and Information Systems Laboratory. 2019. Cheyenne: HPE/SGI ICE XA System (University Community Computing). Boulder, CO: National Center for Atmospheric Research. doi:10.5065/D6RX99HX.
- Congressional Western Caucus. 2020. Letter to Congress: September 22, 2020. Available online at [https://westerncaucus.house.gov/uploadedfiles/congressional\\_western\\_caucus\\_-\\_forestry.pdf](https://westerncaucus.house.gov/uploadedfiles/congressional_western_caucus_-_forestry.pdf); last accessed Mar. 24, 2021.
- Consolidated Appropriations Act of 2012, H. R. 2055, 112th Cong. § 428 (2011). <https://www.govinfo.gov/content/pkg/BILLS-112hr2055enr/pdf/BILLS-112hr2055enr.pdf>
- Costanza, R., de Groot, R., Braat, L., Kubiszewski, I., Fioramonti, L., Sutton, P., Farber, S., & Grasso, M. (2017). Twenty years of ecosystem services: How far have we come and how far do we still need to go? *Ecosystem Services*, 28, 1–16.  
<https://doi.org/10.1016/j.ecoser.2017.09.008>

- Cox, D. R. (1972). Regression Models and Life-Tables. *Journal of the Royal Statistical Society: Series B (Methodological)*, 34(2), 187–202. <https://doi.org/10.1111/j.2517-6161.1972.tb00899.x>
- Craig, R. K., Ruhl, J. B., Brown, E. D., & Williams, B. K. (2017). A proposal for amending administrative law to facilitate adaptive management. *Environmental Research Letters*, 12(7), 074018. <https://doi.org/10.1088/1748-9326/aa7037>
- Dagon, K., Sanderson, B. M., Fisher, R. A., & Lawrence, D. M. (2020). A machine learning approach to emulation and biophysical parameter estimation with the Community Land Model, version 5. *Advances in Statistical Climatology, Meteorology and Oceanography*, 6(2), 223–244. <https://doi.org/10.5194/ascmo-6-223-2020>
- Daily, G. C., Alexander, S., Ehrlich, P., Goulder, L., Lubchenko, J., Matson, P. A., Mooney, H. A., Postel, S., Schneider, S. H., Tilman, D., Woodwell, G. M. (1997) *Ecosystem services: benefits supplied to human societies by natural ecosystems. Issues in Ecology 2.* Ecological Society of America, Washington DC
- Deardorff, J. W. (1978). Efficient prediction of ground surface temperature and moisture, with inclusion of a layer of vegetation. *Journal of Geophysical Research: Oceans*, 83(C4), 1889–1903. <https://doi.org/10.1029/JC083iC04p01889>
- Dixon, G. E. (2018). *Essential FVS: A user's guide to the Forest Vegetation Simulator* (p. 226). Fort Collins, CO, USA: US Department of Agriculture, Forest Service, Forest Management Service Center.
- Doughty, C. E., O. Prýs-Jones, T., Abraham, A. J., & Kolb, T. E. (2021). Forest Thinning in Ponderosa Pines Increases Carbon Use Efficiency and Energy Flow From Primary Producers to Primary Consumers. *Journal of Geophysical Research: Biogeosciences*, 126(3), e2020JG005947. <https://doi.org/10.1029/2020JG005947>

- Duarte, H. F., Raczka, B. M., Bowling, D. R., Wang, A., Buotte, P. C., & Lin, J. C. (2022). How can biosphere models simulate enough vegetation biomass in the mountains of the western United States? Implications of meteorological forcing. *Environmental Modelling & Software*, 148, 105288. <https://doi.org/10.1016/j.envsoft.2021.105288>
- Falster, D. S., Duursma, R. A., Ishihara, M. I., Barneche, D. R., FitzJohn, R. G., Vårhammar, A., Aiba, M., Ando, M., Anten, N., Aspinwall, M. J., Baltzer, J. L., Baraloto, C., Battaglia, M., Battles, J. J., Bond-Lamberty, B., van Breugel, M., Camac, J., Claveau, Y., Coll, L., ... York, R. A. (2015). BAAD: A Biomass And Allometry Database for woody plants: Ecological Archives E096-128. *Ecology*, 96(5), 1445–1445. <https://doi.org/10.1890/14-1889.1>
- FAO. 2018. The State of the World's Forests 2018 - Forest pathways to sustainable development. Rome. Licence: CC BY-NC-SA 3.0 IGO. Retrieved from <http://www.fao.org/3/I9535EN/i9535en.pdf>
- Farquhar, G. D. (1989). Models of Integrated Photosynthesis of Cells and Leaves. *Philosophical Transactions of the Royal Society of London. Series B, Biological Sciences*, 323(1216), 357–367.
- Field, J. P., Breshears, D. D., Bradford, J. B., Law, D. J., Feng, X., & Allen, C. D. (2020). Forest Management Under Megadrought: Urgent Needs at Finer Scale and Higher Intensity. *Frontiers in Forests and Global Change*, 3. <https://www.frontiersin.org/article/10.3389/ffgc.2020.502669>
- Fisher, R. A., & Koven, C. D. (2020). Perspectives on the Future of Land Surface Models and the Challenges of Representing Complex Terrestrial Systems. *Journal of Advances in Modeling Earth Systems*, 12(4), e2018MS001453. <https://doi.org/10.1029/2018MS001453>

- Fisher, R. A., Koven, C. D., Anderegg, W. R. L., Christoffersen, B. O., Dietze, M. C., Farrior, C. E., Holm, J. A., Hurtt, G. C., Knox, R. G., Lawrence, P. J., Lichstein, J. W., Longo, M., Matheny, A. M., Medvigy, D., Muller-Landau, H. C., Powell, T. L., Serbin, S. P., Sato, H., Shuman, J. K., ... Moorcroft, P. R. (2018). Vegetation demographics in Earth System Models: A review of progress and priorities. *Global Change Biology*, 24(1), 35–54.  
<https://doi.org/10.1111/gcb.13910>
- Fisher, R. A., Muszala, S., Versteinstein, M., Lawrence, P., Xu, C., McDowell, N. G., ... & Bonan, G. (2015). Taking off the training wheels: the properties of a dynamic vegetation model without climate envelopes, CLM4. 5 (ED). *Geoscientific Model Development*, 8(11), 3593-3619. doi:10.5194/gmd-8-3593-2015
- Fleischman, F., Struthers, C., Arnold, G., Dockry, M., & Scott, T. (2020). US Forest Service Implementation of the National Environmental Policy Act: Fast, Variable, Rarely Litigated, and Declining. *Journal of Forestry*, 118(4), 403–418.  
<https://doi.org/10.1093/jofore/fvaa016>
- Flores, A. N., Masarik, M., & Watson, K. (n.d.). *A 30-Year, Multi-Domain High-Resolution Climate Simulation Dataset for the Interior Pacific Northwest and Southern Idaho* [Data set]. Boise State University.  
<https://doi.org/10.18122/B2LEAFD001>
- Graham, R. T. (1999). The effects of thinning and similar stand treatments on fire behavior in western forests (Vol. 463). US Department of Agriculture, Forest Service, Pacific Northwest Research Station.
- Graham, R. T., & Jain, T. B. (2004). Boise Basin Experimental Forest (Idaho). In: Adams, Mary Beth; Loughry, Linda H.; Plaughner, Linda, L., comps. *Experimental forests and ranges of the USDA Forest Service*. Gen. Tech. Rep. NE-321. Newtown Square, PA: US Department of Agriculture, Forest Service, Northeastern Research Station. p. 111-112., 321, 111-112.

- Graham, R. T., Jain, T. B., & Sandquist, J. (2007). Free selection: a silvicultural option. In In: Powers, Robert F., tech. editor. Restoring fire-adapted ecosystems: proceedings of the 2005 national silviculture workshop. Gen. Tech. Rep. PSW-GTR-203, Albany, CA: Pacific Southwest Research Station, Forest Service, US Department of Agriculture: p. 121-156 (Vol. 203, pp. 121-156).
- Grumbine, R. E. (1994). What Is Ecosystem Management? *Conservation Biology*, 8(1), 27–38. <https://doi.org/10.1046/j.1523-1739.1994.08010027.x>
- Huang, M., Ray, J., Hou, Z., Ren, H., Liu, Y., & Swiler, L. (2016). On the applicability of surrogate-based Markov chain Monte Carlo-Bayesian inversion to the Community Land Model: Case studies at flux tower sites. *Journal of Geophysical Research: Atmospheres*, 121(13), 7548-7563.
- Huang, M., Xu, Y., Longo, M., Keller, M., Knox, R. G., Koven, C. D., & Fisher, R. A. (2020). Assessing impacts of selective logging on water, energy, and carbon budgets and ecosystem dynamics in Amazon forests using the Functionally Assembled Terrestrial Ecosystem Simulator. *Biogeosciences*, 17(20), 4999–5023. <https://doi.org/10.5194/bg-17-4999-2020>
- Kaiser, K. E., Flores, A. N., & Hillis, V. (2020). Identifying emergent agent types and effective practices for portability, scalability, and intercomparison in water resource agent-based models. *Environmental Modelling & Software*, 127, 104671.
- Kaplan, E. L., & Meier, P. (1958). Nonparametric Estimation from Incomplete Observations. *Journal of the American Statistical Association*, 53(282), 457–481. <https://doi.org/10.2307/2281868>
- Kattge, J., Bönisch, G., Díaz, S., Lavorel, S., Prentice, I. C., Leadley, P., Tautenhahn, S., Werner, G. D. A., Aakala, T., Abedi, M., Acosta, A. T. R., Adamidis, G. C., Adamson, K., Aiba, M., Albert, C. H., Alcántara, J. M., Alcázar C, C., Aleixo, I., Ali, H., ... Wirth, C. (2020). TRY plant trait database – enhanced coverage and open access. *Global Change Biology*, 26(1), 119–188. <https://doi.org/10.1111/gcb.14904>

- Keele, D. M., Malmshemer, R. W., Floyd, D. W., & Perez, J. E. (2006). Forest Service land management litigation 1989–2002. *Journal of Forestry*, *104*(4), 196–202.
- Keele, D. M., & Malmshemer, R. W. (2018). Time Spent in Federal Court: U.S. Forest Service Land Management Litigation 1989–2008. *Forest Science*, *64*(2), 170–190. <https://doi.org/10.1093/forsci/fxx005>
- Koven, C. D., Knox, R. G., Fisher, R. A., Chambers, J. Q., Christoffersen, B. O., Davies, S. J., Detto, M., Dietze, M. C., Faybishenko, B., Holm, J., Huang, M., Kovenock, M., Kueppers, L. M., Lemieux, G., Massoud, E., McDowell, N. G., Muller-Landau, H. C., Needham, J. F., Norby, R. J., ... Xu, C. (2020). Benchmarking and parameter sensitivity of physiological and vegetation dynamics using the Functionally Assembled Terrestrial Ecosystem Simulator (FATES) at Barro Colorado Island, Panama. *Biogeosciences*, *17*(11), 3017–3044. <https://doi.org/10.5194/bg-17-3017-2020>
- Krieger, D. J. (2001). Economic Value of Forest Ecosystem Services: A Review. 40.
- Laband, D. N., González-Cabán, A., & Hussain, A. (2006). Factors that Influence Administrative Appeals of Proposed USDA Forest Service Fuels Reduction Actions. *Forest Science*, *52*(5), 477–488. <https://doi.org/10.1093/forestscience/52.5.477>
- Law, B. (2016). AmeriFlux AmeriFlux US-Me3 Metolius-second young aged pine [Data set]. AmeriFlux; Oregon State University. <https://doi.org/10.17190/AMF/1246077>
- Law, B. (2022). AmeriFlux FLUXNET-1F US-Me2 Metolius mature ponderosa pine [Data set]. AmeriFlux; Oregon State University. <https://doi.org/10.17190/AMF/1854368>

- Lawrence, D. M., Fisher, R. A., Koven, C. D., Oleson, K. W., Swenson, S. C., Bonan, G., Collier, N., Ghimire, B., van Kampenhou, L., Kennedy, D., Kluzek, E., Lawrence, P. J., Li, F., Li, H., Lombardozzi, D., Riley, W. J., Sacks, W. J., Shi, M., Vertenstein, M., ... Zeng, X. (2019). The Community Land Model Version 5: Description of New Features, Benchmarking, and Impact of Forcing Uncertainty. *Journal of Advances in Modeling Earth Systems*, *11*(12), 4245–4287. <https://doi.org/10.1029/2018MS001583>
- Littleton, E. W., Harper, A. B., Vaughan, N. E., Oliver, R. J., Duran-Rojas, M. C., & Lenton, T. M. (2020). JULES-BE: Representation of bioenergy crops and harvesting in the Joint UK Land Environment Simulator vn5.1. *Geoscientific Model Development*, *13*(3), 1123–1136. <https://doi.org/10.5194/gmd-13-1123-2020>
- Malmsheimer, R. W., Keele, D., & Floyd, D. W. (2004). National Forest Litigation in the US Courts of Appeals. *Journal of Forestry*, *102*(2), 20–25. <https://doi.org/10.1093/jof/102.2.20>
- Manabe, S. (1969). CLIMATE AND THE OCEAN CIRCULATION: I. THE ATMOSPHERIC CIRCULATION AND THE HYDROLOGY OF THE EARTH'S SURFACE. *Monthly Weather Review*, *97*(11), 739–774. [https://doi.org/10.1175/1520-0493\(1969\)097<0739:CATOC>2.3.CO;2](https://doi.org/10.1175/1520-0493(1969)097<0739:CATOC>2.3.CO;2)
- Massoud, E. C., Xu, C., Fisher, R. A., Knox, R. G., Walker, A. P., Serbin, S. P., Christoffersen, B. O., Holm, J. A., Kueppers, L. M., Ricciuto, D. M., Wei, L., Johnson, D. J., Chambers, J. Q., Koven, C. D., McDowell, N. G., & Vrugt, J. A. (2019). Identification of key parameters controlling demographically structured vegetation dynamics in a land surface model: CLM4.5(FATES). *Geoscientific Model Development*, *12*(9), 4133–4164. <https://doi.org/10.5194/gmd-12-4133-2019>
- Medvigy, D., Wofsy, S. C., Munger, J. W., Hollinger, D. Y., & Moorcroft, P. R. (2009). Mechanistic scaling of ecosystem function and dynamics in space and time: Ecosystem Demography model version 2. *Journal of Geophysical Research: Biogeosciences*, *114*(G1). <https://doi.org/10.1029/2008JG000812>

- Medvigy, D., Wofsy, S. C., Munger, J. W., & Moorcroft, P. R. (2010). Responses of terrestrial ecosystems and carbon budgets to current and future environmental variability. *Proceedings of the National Academy of Sciences*, 107(18), 8275–8280. <https://doi.org/10.1073/pnas.0912032107>
- Mendoza, P. A., Clark, M. P., Barlage, M., Rajagopalan, B., Samaniego, L., Abramowitz, G., & Gupta, H. (2015). Are we unnecessarily constraining the agility of complex process-based models? *Water Resources Research*, 51(1), 716–728. <https://doi.org/10.1002/2014WR015820>
- Millar, C. I., & Stephenson, N. L. (2015). Temperate forest health in an era of emerging megadisturbance. *Science*, 349(6250), 823–826. <https://doi.org/10.1126/science.aaa9933>
- Miller Jr, R. G. (2011). *Survival Analysis*. John Wiley & Sons.
- Miner, A. M. A., Malmshemer, R. W., & Keele, D. M. (2014). Twenty Years of Forest Service Land Management Litigation. *Journal of Forestry*, 112(1), 32–40. <https://doi.org/10.5849/jof.12-094>
- Miner, A. M. A., Malmshemer, R. W., Keele, D. M., & Mortimer, M. J. (2010). RESEARCH ARTICLE: Twenty Years of Forest Service National Environmental Policy Act Litigation. *Environmental Practice*, 12(2), 116–126. <https://doi.org/10.1017/S1466046610000116>
- Mitchell, T. D., & Jones, P. D. (2005). An improved method of constructing a database of monthly climate observations and associated high-resolution grids. *International Journal of Climatology: A Journal of the Royal Meteorological Society*, 25(6), 693–712.
- Moorcroft, P. R., Hurtt, G. C., & Pacala, S. W. (2001). A Method for Scaling Vegetation Dynamics: The Ecosystem Demography Model (ed). *Ecological Monographs*, 71(4), 557–586. [https://doi.org/10.1890/0012-9615\(2001\)071\[0557:AMFSVD\]2.0.CO;2](https://doi.org/10.1890/0012-9615(2001)071[0557:AMFSVD]2.0.CO;2)

- Moore, R. D., & Wondzell, S. M. (2005). Physical hydrology and the effects of forest harvesting in the Pacific Northwest: a review. *Journal of the American Water Resources Association*. 41 (4): 763-784.
- Morgan, T. A., & Baldrige, J. (2015). Understanding costs and other impacts of litigation of Forest Service projects: A Region One case study. Missoula, MT: Bureau of Business and Economic Research.
- Mortimer, M. J., Stern, M. J., Malmshemer, R. W., Blahna, D. J., Cerveny, L. K., & Seesholtz, D. N. (2011). Environmental and Social Risks: Defensive National Environmental Policy Act in the US Forest Service. *Journal of Forestry*, 109(1), 27–33. <https://doi.org/10.1093/jof/109.1.27>
- Moustakis, Y., Fatichi, S., Onof, C., & Paschalis, A. (2022). Insensitivity of Ecosystem Productivity to Predicted Changes in Fine-Scale Rainfall Variability. *Journal of Geophysical Research: Biogeosciences*, 127(2), e2021JG006735. <https://doi.org/10.1029/2021JG006735>
- Myneni, Ranga, Knyazikhin, Yuri, & Park, Taejin. (2015). MCD15A2H MODIS/Terra+Aqua Leaf Area Index/FPAR 8-day L4 Global 500m SIN Grid V006 [Data set]. NASA EOSDIS Land Processes DAAC. <https://doi.org/10.5067/MODIS/MCD15A2H.006>
- National Research Council. 2008. Hydrologic Effects of a Changing Forest Landscape. Washington, DC: The National Academies Press. <https://doi.org/10.17226/12223>.
- Neary, D. G., Ice, G. G., & Jackson, C. R. (2009). Linkages between forest soils and water quality and quantity. *Forest Ecology and Management*, 258(10), 2269–2281. <https://doi.org/10.1016/j.foreco.2009.05.027>
- Nemani, R. R., Keeling, C. D., Hashimoto, H., Jolly, W. M., Piper, S. C., Tucker, C. J., Myneni, R. B., & Running, S. W. (2003). Climate-Driven Increases in Global Terrestrial Net Primary Production from 1982 to 1999. *Science*, 300(5625), 1560–1563. <https://doi.org/10.1126/science.1082750>

- Nie, M. (2008). The underappreciated role of regulatory enforcement in natural resource conservation. *Policy Sciences*, 41(2), 139–164. <https://doi.org/10.1007/s11077-008-9060-4>
- Nie, M., & Metcalf, P. (2016). National Forest Management: The Contested Use of Collaboration and Litigation. *Environmental Law Reporter News & Analysis*, 46, 10208.
- North, M. P., Tompkins, R. E., Bernal, A. A., Collins, B. M., Stephens, S. L., & York, R. A. (2022). Operational resilience in western US frequent-fire forests. *Forest Ecology and Management*, 507, 120004. <https://doi.org/10.1016/j.foreco.2021.120004>
- O'Brien, S. T., Hubbell, S. P., Spiro, P., Condit, R., & Foster, R. B. (1995). Diameter, Height, Crown, and Age Relationship in Eight Neotropical Tree Species. *Ecology*, 76(6), 1926–1939. <https://doi.org/10.2307/1940724>
- Oswalt, S. N., Smith, W. B., Miles, P. D., & Pugh, S. A. (2019). *Forest Resources of the United States, 2017: A Technical Document Supporting the Forest Service 2020 RPA Assessment* (WO-GTR-97; p. WO-GTR-97). U.S. Department of Agriculture, Forest Service. <https://doi.org/10.2737/WO-GTR-97>
- Pan, Y., Birdsey, R. A., Fang, J., Houghton, R., Kauppi, P. E., Kurz, W. A., Phillips, O. L., Shvidenko, A., Lewis, S. L., Canadell, J. G., Ciais, P., Jackson, R. B., Pacala, S. W., McGuire, A. D., Piao, S., Rautiainen, A., Sitch, S., & Hayes, D. (2011). A Large and Persistent Carbon Sink in the World's Forests. *Science*, 333(6045), 988–993. <https://doi.org/10.1126/science.1201609>
- Pielke, R. A., Sr., Avissar, RonI., Raupach, M., Dolman, A. J., Zeng, X., & Denning, A. S. (1998). Interactions between the atmosphere and terrestrial ecosystems: Influence on weather and climate. *Global Change Biology*, 4(5), 461–475. <https://doi.org/10.1046/j.1365-2486.1998.t01-1-00176.x>
- Pitman, A. J. (2003). The evolution of, and revolution in, land surface schemes designed for climate models. *International Journal of Climatology*, 23(5), 479–510. <https://doi.org/10.1002/joc.893>

- Predmore, S. A., Stern, M. J., Mortimer, M. J., & Seesholtz, D. N. (2011). Perceptions of Legally Mandated Public Involvement Processes in the U.S. Forest Service. *Society & Natural Resources*, 24(12), 1286–1303.  
<https://doi.org/10.1080/08941920.2011.559617>
- Prihodko, L., Denning, A. S., Hanan, N. P., Baker, I., & Davis, K. (2008). Sensitivity, uncertainty and time dependence of parameters in a complex land surface model. *Agricultural and Forest Meteorology*, 148(2), 268–287.  
<https://doi.org/10.1016/j.agrformet.2007.08.006>
- Purves, D. W., Lichstein, J. W., Strigul, N., & Pacala, S. W. (2008). Predicting and understanding forest dynamics using a simple tractable model. *Proceedings of the National Academy of Sciences*, 105(44), 17018–17022.  
<https://doi.org/10.1073/pnas.0807754105>
- Rady, Joshua, & FATES Development Team. (2022). The Functionally Assembled Terrestrial Ecosystem Simulator (FATES) with the Vegetation Management Module (VM) (VM.1.0.0). Zenodo. <https://doi.org/10.5281/zenodo.6536487>
- Rady, J. M., Shuman, J. K., & Thomas, R. Q. (2022) Simulating Comprehensive Forest Management in FATES with the Vegetation Management Module [Manuscript in preparation]. Forest Resources and Environmental Conservation, Virginia Tech.
- Rönnqvist, M., D'Amours, S., Weintraub, A., Jofre, A., Gunn, E., Haight, R. G., Martell, D., Murray, A. T., & Romero, C. (2015). Operations Research challenges in forestry: 33 open problems. *Annals of Operations Research*, 232(1), 11–40.  
<https://doi.org/10.1007/s10479-015-1907-4>
- Running, Steve, Mu, Qiaozhen, & Zhao, Maosheng. (2015). *MOD17A2H MODIS/Terra Gross Primary Productivity 8-Day L4 Global 500m SIN Grid V006* [Data set]. NASA EOSDIS Land Processes DAAC.  
<https://doi.org/10.5067/MODIS/MOD17A2H.006>
- Ruple, J., & Tanana, H. (2020). Debunking the Myths Behind the NEPA Review Process.
- Ruple, J. C., & Race, K. M. (2020). Measuring the NEPA Litigation Burden: A Review of 1,499 Federal Court Cases. *Environmental Law*, 50(2), 479–522.

- Ruple, J., & Tanana, H. (2020). Debunking the Myths Behind the NEPA Review Process. *SSRN Electronic Journal*. <https://doi.org/10.2139/ssrn.3520212>
- Sabatier, P. A., & Weible, C. M. (2007). The advocacy coalition framework. *Theories of the policy process*, 2, (pp. 189-220). <http://dx.doi.org/10.4324/9780367274689-7>
- Saldarriaga, J. G., West, D. C., Tharp, M. L., & Uhl, C. (1988). Long-term chronosequence of forest succession in the upper Rio Negro of Colombia and Venezuela. *The Journal of Ecology*, 938-958.
- Saltelli, A. (2019). A short comment on statistical versus mathematical modelling. *Nature communications*, 10(1), 1-3.
- Sato, H., Itoh, A., & Kohyama, T. (2007). SEIB–DGVM: A new Dynamic Global Vegetation Model using a spatially explicit individual-based approach. *Ecological Modelling*, 200(3–4), 279–307. <https://doi.org/10.1016/j.ecolmodel.2006.09.006>
- Simmons, E. A., Morgan, T. A., Berg, E. C., Zarnoch, S. J., Hayes, S. W., & Thompson, M. T. (2014). Logging utilization in Idaho: current and past trends. Gen. Tech. Rep. RMRS-GTR-318. Fort Collins, CO: US Department of Agriculture, Forest Service, Rocky Mountain Research Station. 15 p., 318.
- Smith, B., Prentice, I. C., & Sykes, M. T. (2001). Representation of Vegetation Dynamics in the Modelling of Terrestrial Ecosystems: Comparing Two Contrasting Approaches within European Climate Space. *Global Ecology and Biogeography*, 10(6), 621–637.
- Sohn, J. A., Saha, S., & Bauhus, J. (2016). Potential of forest thinning to mitigate drought stress: A meta-analysis. *Forest Ecology and Management*, 380, 261–273. <https://doi.org/10.1016/j.foreco.2016.07.046>
- Spedicato, G. (2017). Discrete Time Markov Chains with R. *The R Journal*, 9, 84–104. <https://doi.org/10.32614/RJ-2017-036>
- Stanke, H., Finley, A. O., Weed, A. S., Walters, B. F., & Domke, G. M. (2020). rFIA: An R package for estimation of forest attributes with the US Forest Inventory and Analysis database. *Environmental Modelling & Software*, 127, 104664. <https://doi.org/10.1016/j.envsoft.2020.104664>

- Stern, M. J., Predmore, S. A., Morse, W. C., & Seesholtz, D. N. (2013). Project risk and appeals in U.S. Forest Service planning. *Environmental Impact Assessment Review*, 42, 95–104. <https://doi.org/10.1016/j.eiar.2012.11.001>
- Stern, M. J., Predmore, S. A., Mortimer, M. J., & Seesholtz, D. N. (2010). From the office to the field: Areas of tension and consensus in the implementation of the National Environmental Policy Act within the US Forest Service. *Journal of Environmental Management*, 91(6), 1350–1356. <https://doi.org/10.1016/j.jenvman.2010.02.016>
- Swann, A. L. S., Laguë, M. M., Garcia, E. S., Field, J. P., Breshears, D. D., Moore, D. J. P., Saleska, S. R., Stark, S. C., Villegas, J. C., Law, D. J., & Minor, D. M. (2018). Continental-scale consequences of tree die-offs in North America: Identifying where forest loss matters most. *Environmental Research Letters*, 13(5), 055014. <https://doi.org/10.1088/1748-9326/aaba0f>
- Swenson, S. C., Clark, M., Fan, Y., Lawrence, D. M., & Perket, J. (2019). Representing intrahillslope lateral subsurface flow in the community land model. *Journal of Advances in Modeling Earth Systems*, 11(12), 4044-4065.
- Team, R. Core. (2020). R: A Language and Environment for Statistical Computing. R Foundation for Statistical Computing, Vienna, Austria: Available at: <https://www.R-project.org/>.
- Teich, G. M. R., Vaughn, J., & Cortner, H. J. (2004). National Trends in the Use of Forest Service Administrative Appeals. *Journal of Forestry*, 102(2), 14–19. <https://doi.org/10.1093/jof/102.2.14>
- Therneau, T. M., & Lumley, T. (2015). Package ‘survival’. *R Top Doc*, 128(10), 28-33.
- Thonicke, K., Spessa, A., Prentice, I. C., Harrison, S. P., Dong, L., & Carmona-Moreno, C. (2010). The influence of vegetation, fire spread and fire behaviour on biomass burning and trace gas emissions: Results from a process-based model. *Biogeosciences*, 7(6), 1991–2011. <https://doi.org/10.5194/bg-7-1991-2010>

- USFS (2021) The Forest Inventory Analysis Database: Database Description and User Guide for Phase 2(version 9.0.1) Available at:  
[https://www.fia.fs.fed.us/library/database-documentation/current/ver90/FIADB%20User%20Guide%20P2\\_9-0-1\\_final.pdf](https://www.fia.fs.fed.us/library/database-documentation/current/ver90/FIADB%20User%20Guide%20P2_9-0-1_final.pdf)  
(Accessed 15 May 2021).
- Viovy, N. (2018). *CRUNCEP Version 7—Atmospheric Forcing Data for the Community Land Model* (p. 1.238 Tbytes) [NetCDF]. UCAR/NCAR - Research Data Archive.  
<https://doi.org/10.5065/PZ8F-F017>
- Virtanen, P., Gommers, R., Oliphant, T. E., Haberland, M., Reddy, T., Cournapeau, D., Burovski, E., Peterson, P., Weckesser, W., Bright, J., van der Walt, S. J., Brett, M., Wilson, J., Millman, K. J., Mayorov, N., Nelson, A. R. J., Jones, E., Kern, R., Larson, E., ... van Mulbregt, P. (2020). SciPy 1.0: Fundamental algorithms for scientific computing in Python. *Nature Methods*, 17(3), 261–272.  
<https://doi.org/10.1038/s41592-019-0686-2>
- Westerling, A. L., Hidalgo, H. G., Cayan, D. R., & Swetnam, T. W. (2006). Warming and Earlier Spring Increase Western U.S. Forest Wildfire Activity. *Science*, 313(5789), 940–943. <https://doi.org/10.1126/science.1128834>
- Wickham, H. (2016). *ggplot2: elegant graphics for data analysis*. springer.
- Wilkinson, C. F. (1992). *Crossing the Next Meridian: Land, Water, and the Future of the West*. Island Press.
- Wilson, B. T., Woodall, C. W., & Griffith, D. M. (2013). Imputing forest carbon stock estimates from inventory plots to a nationally continuous coverage. *Carbon Balance and Management*, 8(1), 1. <https://doi.org/10.1186/1750-0680-8-1>
- Wilson, R. K. (2014). *America's Public Lands: From Yellowstone to Smokey Bear and Beyond*. Rowman & Littlefield.

- Wright, I. J., Reich, P. B., Westoby, M., Ackerly, D. D., Baruch, Z., Bongers, F., Cavender-Bares, J., Chapin, T., Cornelissen, J. H. C., Diemer, M., Flexas, J., Garnier, E., Groom, P. K., Gullas, J., Hikosaka, K., Lamont, B. B., Lee, T., Lee, W., Lusk, C., ... Villar, R. (2004). The worldwide leaf economics spectrum. *Nature*, 428(6985), 821–827. <https://doi.org/10.1038/nature02403>
- Zhang, M., Liu, N., Harper, R., Li, Q., Liu, K., Wei, X., Ning, D., Hou, Y., & Liu, S. (2017). A global review on hydrological responses to forest change across multiple spatial scales: Importance of scale, climate, forest type and hydrological regime. *Journal of Hydrology*, 546, 44–59. <https://doi.org/10.1016/j.jhydrol.2016.12.040>

APPENDIX A

## Appendices for Chapter 2

**Table A1 Table of Variables in the Full FS-PALS Dataset**

<b>Variable Name</b>	<b>Description</b>	<b>Original Dataset</b>
Project Number	The unique number associated with the NEPA project.	UMN-PALS, FS_ACT
NEPA Name	The name of the NEPA project.	UMN-PALS, FS_ACT
Region	The USFS administrative region where the project took place.	UMN-PALS, FS_ACT
Region_01	Binary variable. 1 = project is within the region and 0 = project not within the region.	Created for FS-PALS
Region_02	Binary variable. 1 = project is within the region and 0 = project not within the region.	Created for FS-PALS
Region_03	Binary variable. 1 = project is within the region and 0 = project not within the region.	Created for FS-PALS
Region_04	Binary variable. 1 = project is within the region and 0 = project not within the region.	Created for FS-PALS
Region_05	Binary variable. 1 = project is within the region and 0 = project not within the region.	Created for FS-PALS
Region_06	Binary variable. 1 = project is within the region and 0 = project not within the region.	Created for FS-PALS
NEPA Status	The status of the NEPA analysis, either Completed, Canceled, On Hold, or In Progress	UMN-PALS
Init Date	The date the NEPA analysis was initiated.	UMN-PALS

<b>Variable Name</b>	<b>Description</b>	<b>Original Dataset</b>
Decision Date	The date the decision for the NEPA analysis was signed.	UMN-PALS
NEPA type	The type of NEPA documentation require, either Environmental Impact Statement (EIS), Environmental Assessment (EA), or Categorical Exclusion (CE).	UMN-PALS
NEPA_CE	Binary variable. 1 = NEPA analysis type completed for the project and 0 = NEPA analysis type not completed for the project	Created for FS-PALS
NEPA_EA	Binary variable. 1 = NEPA analysis type completed for the project and 0 = NEPA analysis type not completed for the project	Created for FS-PALS
NEPA_EIS	Binary variable. 1 = NEPA analysis type completed for the project and 0 = NEPA analysis type not completed for the project	Created for FS-PALS
Litigated	Whether the NEPA project was litigated agaisnt. 0 = no litigation, 1 = litigation	UMN-PALS
Elapsed Days	The number of days from the NEPA analysis initiation date and the date the decision was signed.	UMN-PALS
Decision Level	The level at which the decision was signed. Either Ranger District, National Forest/Grassland, or NRA/NSA/NM.	UMN-PALS
Plan Date Min	The date planned for the earlier(iest) treatments in a project.	FS-ACT
Plan Date Max	The date planned for the last treatments in a project.	FS-ACT

<b>Variable Name</b>	<b>Description</b>	<b>Original Dataset</b>
Comp Date Min	The date the earlier(iest) treatments in a project were actually completed.	FS-ACT
Comp Date Max	The date the last treatments in a project were actually completed.	FS-ACT
Units Planned	The planned area treated in acres.	FS-ACT
Units Completed	The actual area treated in acres.	FS-ACT
Median Time Lag	The median time lag of activities or treatments within a project. Calculated as the difference between the Plan and Comp Date for each activity from the FS-ACTS dataset.	Calculated from FS-ACT
th	Proportion of project that involved timber harvest treatments	Determined from FS-ACT, the number of activities for each project that came from the respective th, hf, rf, or tsi USFS datasets.
hf	Proportion of project that involved hazardous fuel treatments	Determined from FS-ACT, the number of activities for each project that came from the respective th, hf, rf, or tsi USFS datasets.
rf	Proportion of project that involved reforestation treatments	Determined from FS-ACT, the number of activities for each project that came from the respective th, hf, rf, or tsi USFS datasets.
tsi	Proportion of project that involved timber stand improvement treatments	Determined from FS-ACT, the number of activities for each project that came from the

Variable Name	Description	Original Dataset
		respective th, hf, rf, or tsi USFS datasets.
Completed	Whether the project is fully completed. 0 = incomplete (censored) 1 = fully completed	FS-ACT
Percent Completed	Proportion of completed to incomplete activities within a project.	Determined from FS-ACT
Plan Proj. Duration	The duration of the project as planned. The difference between the Plan Date Max and Plan Date Min	Determined from FS-ACT
Comp Proj. Duration	The duration of the project as completed. The difference between the Comp Date Max and the Comp Date Min	Determined from FS-ACT
Project Delay	The delay is the start of the project. The difference between the Plan Date Min and the Comp Date Min	Determined from FS-ACT
Initiated	Whether the project is has been started. Determined by whether a Comp Date Min value exists showing that at least one activity in the project has been completed. 1 = the project has been started and 0 = project has not been started (censored)	Determined from FS-ACT
size	Cumulative size of a project. The sum of the planned units for each activity of a project.	Determined from FS-ACT
overlap	The number of days from the day the NEPA decision was signed to the completion of the earliest planned activity (Comp Date Min).	Determined from UMN-PALS and FS-ACT.

<b>Variable Name</b>	<b>Description</b>	<b>Original Dataset</b>
OVERLAP_DAYS	Binary variable. 1 = overlap occurred (overlap <0) and 0 = overlap did not occur (overlap >= 0).	Created for FS-PALS

**Table A.2 Correlation matrix of covariates and project delay**

	Project delay duration (days)	Project planned size (acres)	Relative size	Project planned size (acres)	Elapsed days	Overlap (days)	Overlap (binary)	Region 1	Region 2	Region 3	Region 4	Region 5	Region 6	% th	% rf	% hf	% tsi						
Project delay (days)	1.000	0.065	-0.080	0.052	0.061	0.059	-0.001	-0.005	0.026	0.070	0.136	0.133	0.020	0.032	0.046	0.017	0.033	0.002	0.172	0.12	0.03	0.02	
Project planned duration (days)	0.065	1.000	0.288	0.233	0.131	0.011	0.530	0.200	0.381	0.089	0.299	0.222	0.013	0.026	0.050	0.039	0.022	0.033	-	0.071	0.02	0.02	0.06
NEPA, CE	-0.288	1.000	0.871	-0.871	-0.148	-0.406	-0.406	-0.210	-0.336	-0.490	-0.034	-0.047	0.011	0.072	0.028	0.047	0.030	0.030	0.025	0.209	0.10	0.03	0.10
NEPA, EA	0.052	0.233	1.000	1.000	0.088	0.320	0.095	0.173	0.173	0.329	0.011	0.024	0.011	0.053	0.017	0.017	0.040	0.036	0.182	0.09	0.02	0.08	0.07
NEPA, EIS	0.061	0.131	0.339	1.000	0.128	0.202	0.239	0.341	0.341	0.354	0.046	0.048	0.043	0.043	0.023	0.062	0.016	0.019	0.071	0.02	0.01	0.03	0.05
Litigated	0.059	0.011	0.148	0.088	1.000	0.080	0.029	0.096	0.096	0.135	0.020	0.028	0.149	0.055	0.026	0.045	0.025	0.054	0.051	0.00	0.00	0.03	0.01
Relative size	-0.001	0.530	0.406	0.320	0.202	1.000	1.000	0.314	0.427	0.245	0.207	0.140	0.066	0.008	0.066	0.048	0.031	0.003	0.084	0.08	0.08	0.04	0.02
Project planned size (acres)	-0.005	0.065	0.288	0.233	0.131	0.011	0.530	1.000	0.449	0.186	0.086	0.089	0.066	0.029	0.128	0.008	0.045	0.003	0.025	0.03	0.03	0.09	0.00
Project activities (count)	0.026	0.381	0.089	0.299	0.222	0.020	0.026	0.050	1.000	0.170	0.169	0.161	0.022	0.043	0.083	0.080	0.023	0.084	0.036	0.05	0.05	0.02	0.01

Elapsed days	0.070	0.089	-	0.490	0.329	0.354	0.135	0.245	0.186	0.170	1.000	0.062	0.025	0.053	-	0.009	-	0.027	0.027	0.006	0.068	-	0.06	-	0.04	0.04
Overlap (days)	0.136	0.299	-	0.034	0.011	0.046	0.020	0.207	0.086	0.169	0.062	1.000	0.482	-	0.046	0.066	0.043	0.012	0.089	0.039	0.049	0.01	-	0.04	0.07	0.02
Overlap (binary)	0.133	0.222	-	0.047	0.024	0.048	0.028	0.140	0.089	0.161	0.025	0.482	1.000	-	0.068	0.064	0.011	-	0.120	0.025	-	0.04	-	0.05	0.01	0.01
Region 1	-	0.020	-	0.011	0.011	0.043	0.149	-0.066	-0.066	-0.022	0.053	-0.046	-0.068	1.000	0.162	0.128	0.179	0.251	-	0.226	0.067	0.02	-	-	0.03	0.05
Region 2	0.032	0.026	-	0.072	0.053	0.043	-0.055	0.008	0.029	0.043	-0.007	-0.066	-0.064	-	1.000	-	-	-	-	0.205	0.076	-	-	-	0.01	0.06
Region 3	-	0.046	-	0.028	0.017	-	-0.026	0.066	0.128	-0.083	0.009	-0.043	0.011	-	0.128	0.116	0.129	0.181	-	0.163	0.104	-	0.01	0.07	-	0.00
Region 4	-	0.017	-	0.047	0.017	-	-0.045	0.048	-0.008	-0.080	-0.027	-0.012	-0.058	-	0.179	0.162	0.129	1.000	-	0.227	0.082	-	0.11	-	0.05	0.01
Region 5	0.033	0.022	0.030	-	0.040	0.016	0.025	-0.031	-0.045	0.023	-0.027	0.089	0.120	-	0.251	0.228	0.181	0.251	-	0.319	0.066	-	0.00	0.08	0.00	0.00
Region 6	0.002	0.033	-	0.025	0.036	-	-0.054	-0.003	0.003	0.084	0.006	0.039	0.025	-	0.226	0.205	0.163	0.227	-	1.000	0.090	0.00	-	0.05	0.11	0.09
% th	0.172	-0.071	-	0.209	0.182	0.071	0.051	-0.084	-0.025	0.036	0.068	0.049	-0.062	0.067	0.076	0.104	0.082	0.066	-	0.090	1.000	-	-	-	0.54	0.24
% rf	-	0.122	-	0.100	-	0.091	0.026	-0.085	-0.035	-0.050	-0.134	0.010	0.040	0.024	0.008	0.014	0.030	0.007	-	0.009	0.110	-	1.00	-	0.53	0.10

% hf	-	0.028	0.031	-	0.024	0.015	-	-0.034	0.098	0.039	-0.024	0.066	-0.070	-0.011	-	0.037	0.012	-	0.072	0.115	0.006	-	0.112	0.545	-	1.0	-	0.3	0.3	43
	0.033																													
% tsi	-	0.069	0.101	-	0.087	0.035	-	-0.013	0.042	0.007	0.051	-0.043	0.042	0.051	-	0.052	0.067	0.001	-	0.080	0.059	-	0.248	0.1	-	1.0	-	0.3	0.0	
	0.027																													

\* th = timber harvest, rf = reforestation, hf = hazardous fules, tsi = timber stand improvement

### A3. Survival Analysis Methods

#### Data Combination

The UMN-PALS and FS-ACT datasets were combined for the years 2005 through 2018 to create the PALS-ACT dataset. To combine the datasets, FS-ACT data were grouped by NEPA project number keeping the minimum planned and completed dates and summing the area treated for all activities and counting the number of all activities within a project. The two datasets were then joined by the NEPA project number. If the project names from the two datasets did not match, then those projects and related activities were removed. Several temporal variables were created for the combined dataset including the planned and completed project duration, the project delay, a binary variable for project initiation, and overlap. We also created “dummy”, binary variables for each of the regions, the types of NEPA analysis, and the overlap. We created these dummy variables for use in the Cox proportional hazards model, which does not work well with categorical data. This resulted in a combined dataset with 3557 unique NEPA projects and 39 variables (S1). All the code for downloading and aggregating the data is included in the GitHub repository.

#### Survival Analysis

Survival analysis is a statistical technique that determines the probability of an event occurring within a duration of time and the effect size of different variables on the probability of that event occurring (Box-Steffensmeier and Jones, 1997; Miller, R. G., 2011). This technique is common in the medical field to analyze clinical trials. Within the context of forest management, it has been used in a variety of ways, from examining legal proceedings (Keele and Malmsheimer, 2018), sustainable development (Kitikidou

and Apostolopoulou, 2011), and tree mortality (Uzoh and Mori, 2012) to predicting timber harvests (Melo et al., 2017) and forest fire containment (Morin et al., 2015; Tremblay et al., 2018).

There are three main outcomes of interest from survival analyses for our purposes: i) the survival function, ii) the hazard function, and iii) the hazard ratio. The survival function,  $S(t)$ , is the probability of 'survival' past point  $t$ , time (eq 1).

$$S(t) = P(T > t)$$

Where  $t$  is a point in time, and  $T$  is the duration. Here, the survival function defines the probability that past time  $t$ , a project will "survive", or continue to be delayed.  $T$  refers to the duration of a project delay.

The hazard function, or rate, is the probability of the event occurring immediately after time  $t$  given that it has not occurred up to time  $t$  (eq 2). In this case the hazard rate describes the probability at time  $t$  of a project being initiated at the next time step given that it has not yet been started at time  $t$ .

$$h(t) = P(T < t + \Delta t | T > t)$$

The hazard ratio describes the relationship between the hazard rates for the participants (in this case projects) with different treatments (i.e. litigated or not litigated) (eq 3).

$$HazardRatio = \frac{h(t)_{litigated}}{h(t)_{not\ litigated}}$$

In this study, the event of interest is whether or not the earliest activity of a project has been completed. At that point we consider the project initiated. The duration is the project delay in days. In other words, a project *survives* with continued delay, and a project *dies* once initiated. Within survival analyses, an event is right-censored if the

participant did not experience the event by the end of the observation period. In this study, censored events are kept in the study with a project delay that was calculated based on the end of the period of observation.

#### Kaplan Meier Estimation

We determined a project's survival probability,  $S(t)$  as a function of a project's delay using the non-parametric Kaplan-Meier survival analysis (Kaplan and Meier, 1958). Here a project's survival is estimated using the product limit method (eq 4).

$$\hat{S}(t) = \prod_{t_i < t} \left(1 - \frac{d_i}{n_i}\right)$$

Where  $d_i$  is the number of projects initiated up to point  $i$ , and  $n_i$  is the number of projects at risk of initiation at time  $t$ .

#### Cox Proportional Hazards Model

The Cox proportional hazards model is a semiparametric regression model that determines the effect a covariate has on the “risk” of project initiation at any point in time (Cox, 1972). We used this method to determine the impact of project characteristics on project survival (eq. 5).

$$\ln(HAZ) = \ln(h_0(t)) + b_1x_1 + \dots + b_kx_k$$

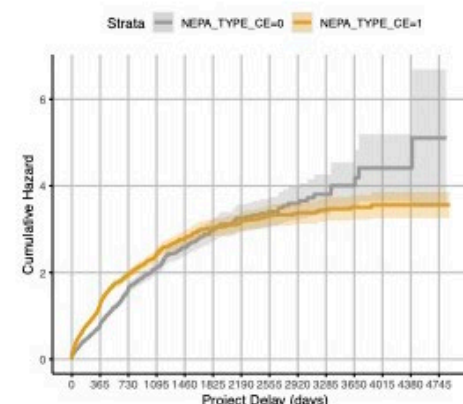
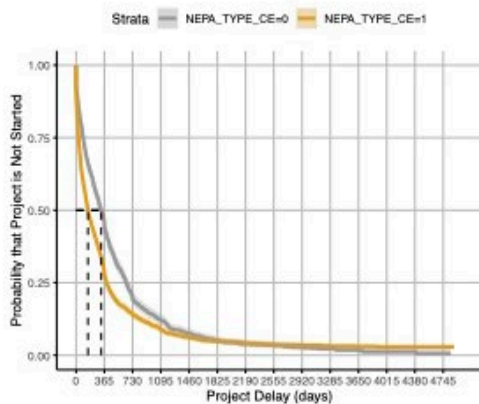
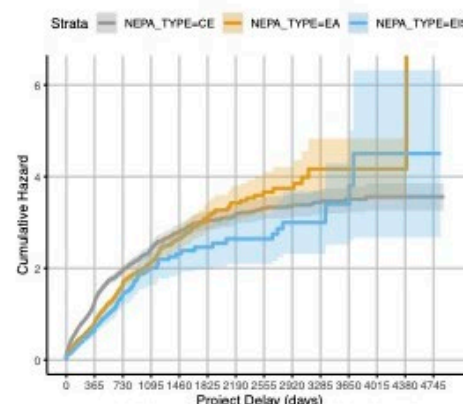
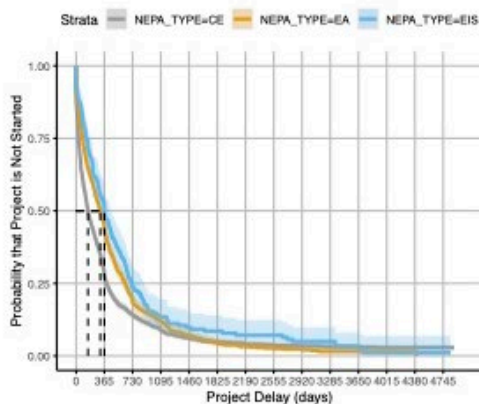
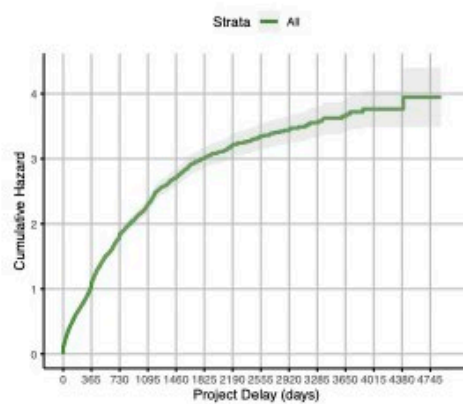
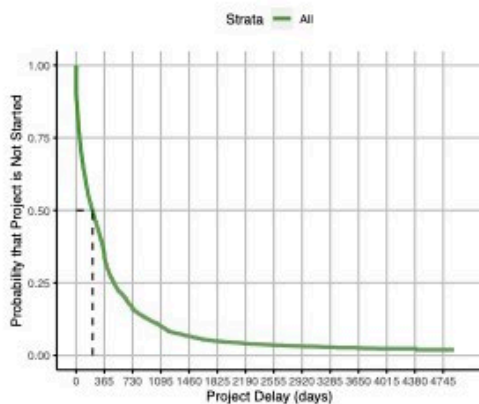
Where HAZ is the is hazard function  $h(t)$  (eq. 2),  $\ln(h_0(t))$  is equal to  $b_0$  which is the intercept term of the regression, and  $b_1x_1, \dots, b_kx_k$  are the covariates  $b_k$  and their respective effects  $x_k$ .

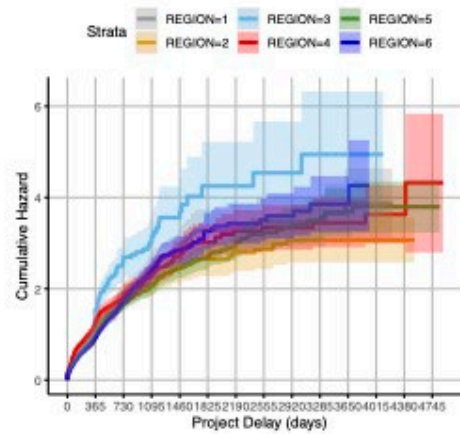
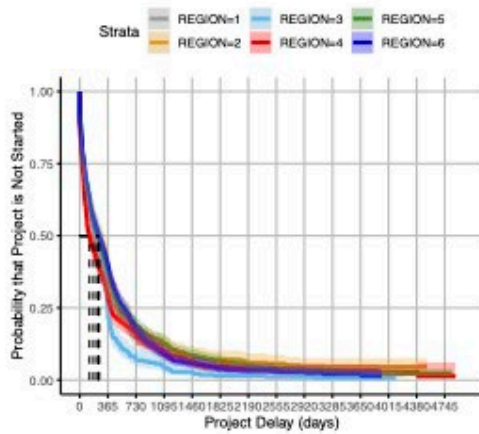
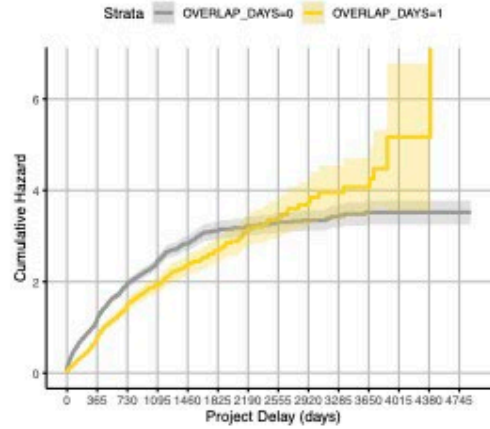
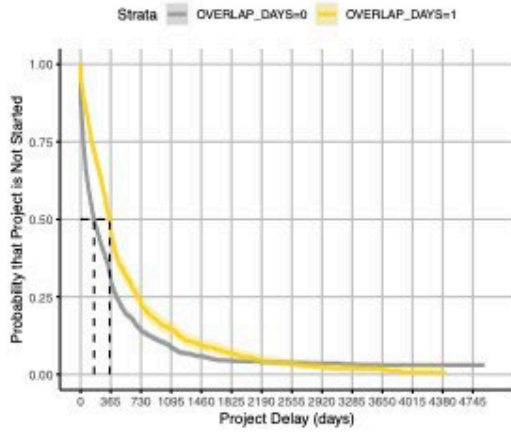
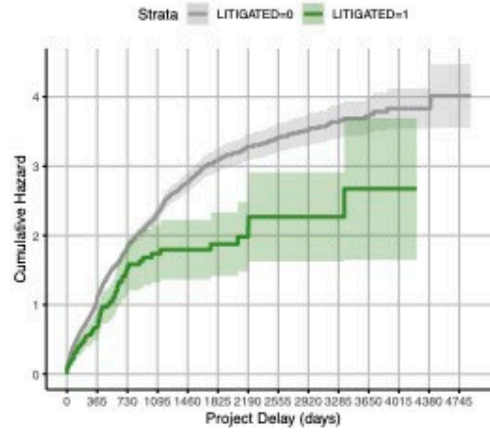
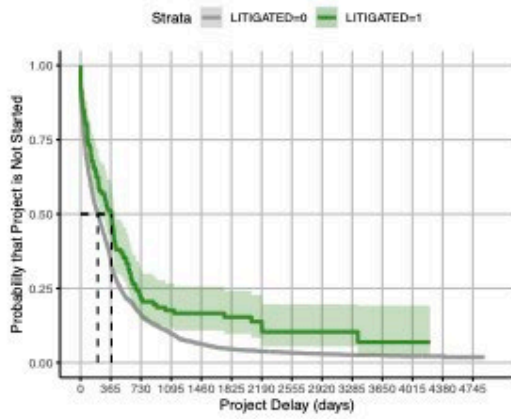
All the R code for the analyses is included in the GitHub repository.

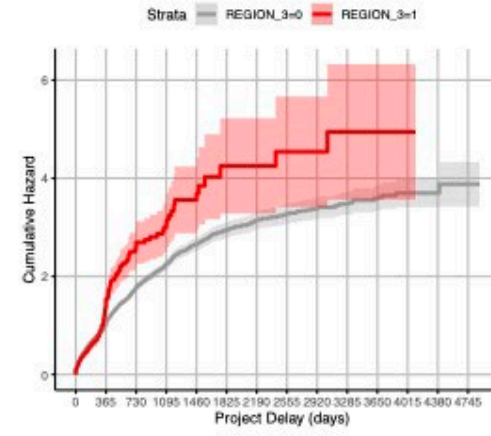
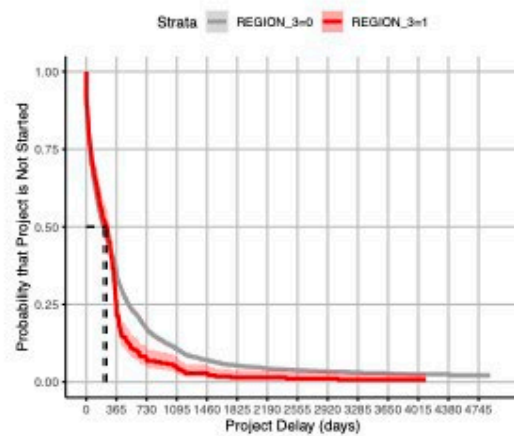
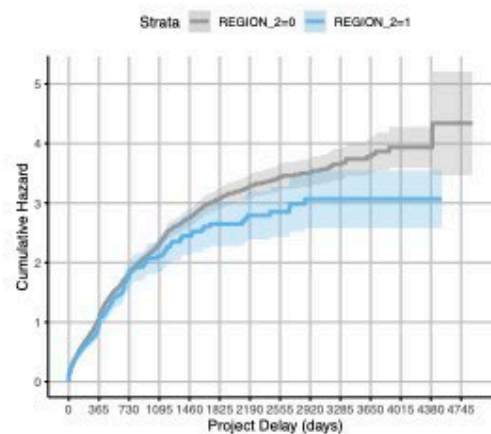
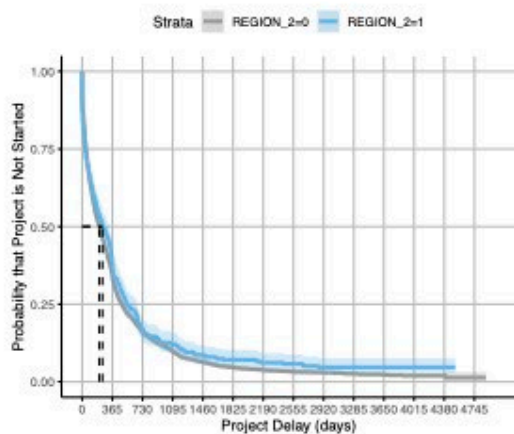
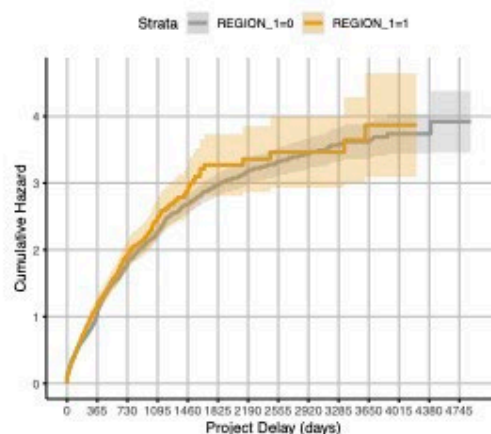
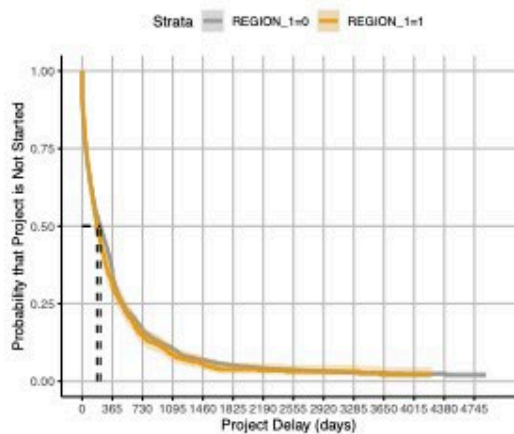
References

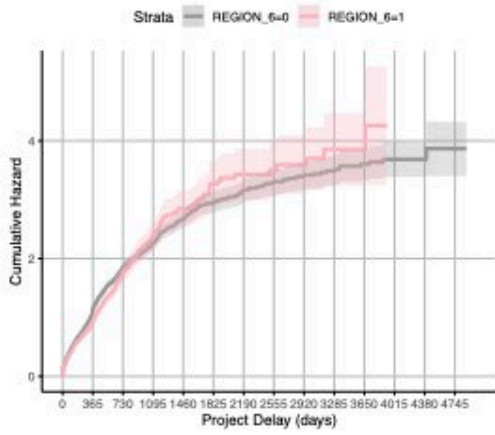
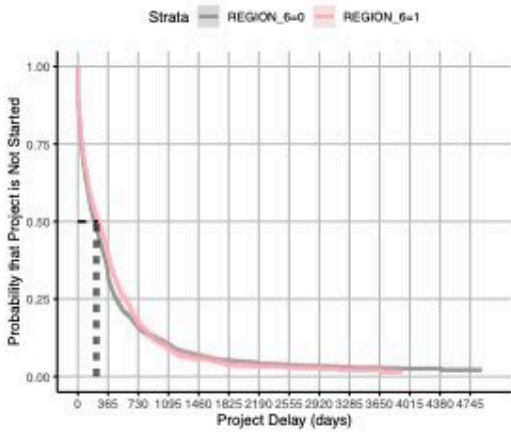
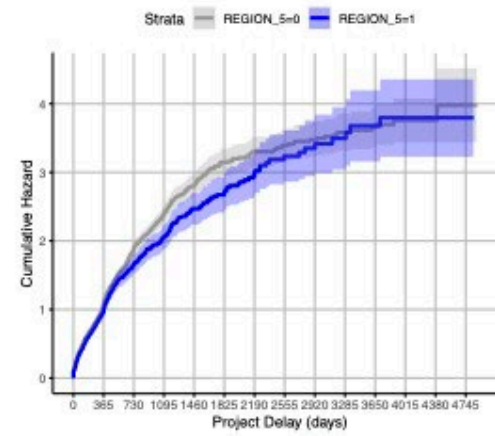
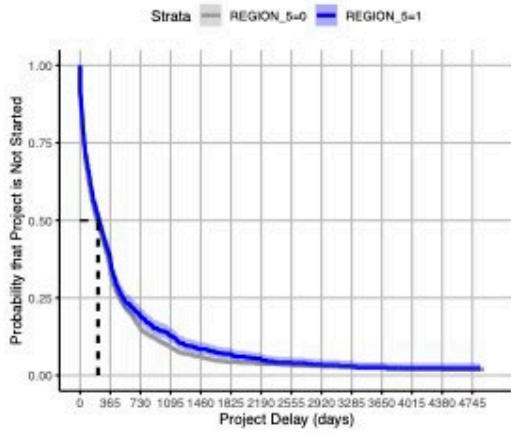
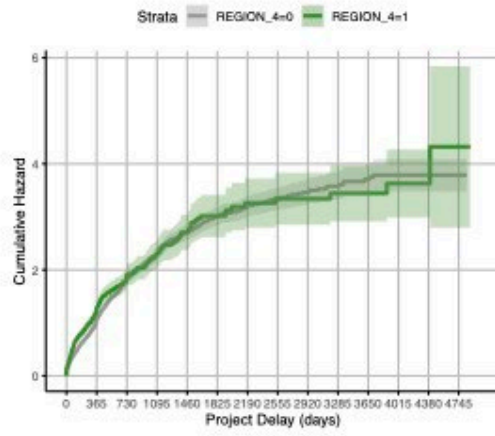
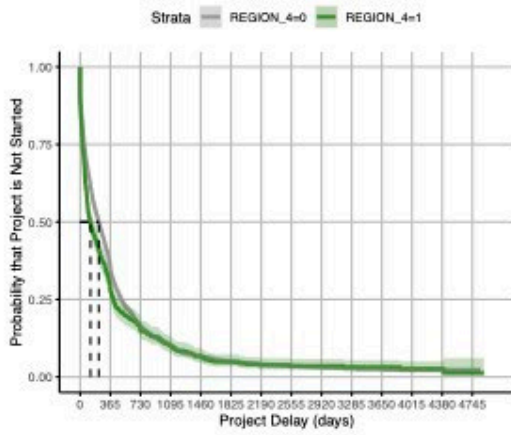
- Box-Steffensmeier, J. M., and B. S. Jones. 1997. Time is of the essence: Event history models in political science. *American Journal of Political Science* 41(4):1414-1461.
- Cox, D. R. 1972. Regression Models and Life-Tables. *Journal of the Royal Statistical Society. Series B (Methodological)* 34(2), 187-220.
- Kaplan, E. L. and P. Meier. 1958. Nonparametric Estimation from Incomplete Observations. *Journal of the American Statistical Association* 53(282):457-481.
- Keele, D. M., R. W. Malmshemer. 2018. Time Spent in Federal Court: U.S. Forest Service Land Management Litigation 1989-2008. *Forest Science* 64(2):170-190.
- Kitikidou, K. and E. Apostolopoulou. 2011. Applying survival analysis for assessment of forests sustainable development. *Renewable and Sustainable Energy Reviews* 15(1):851-855.
- Melo, L., R., Schneider, R. Manso, J. P. Saucier, and M. Fortin. 2017. Using survival analysis to predict the harvesting of forest stands in Quebec, Canada. *Canadian Journal of Forest Research* 47(8):1066-1074.
- Miller Jr, R. G. 2011. *Survival Analysis*, Volume 66. John Wiley & Sons.
- Morin, A. A., A. Albert-Green, D. G. Woolford, and D. L. Martell. 2015. The use of survival analysis methods to model the control time of forest fires in Ontario, Canada. *International Journal of Wildland Fire* 24(7):964-973.
- Tremblay, P. O., T. Duchesne, and S. G. Cumming. 2018. Survival analysis and classification methods for forest fire size. *PLOS ONE* 13(1): e0189860.
- Uzoh, F. C. and S. R. Mori. 2012. Applying survival analysis to managed even-aged stands of ponderosa pine for assessment of tree mortality in the western United States. *Forest Ecology and Management* 285:101-122.

A4 Kaplan-Meier survival curves and cumulative hazard plots for all binary and categorical data

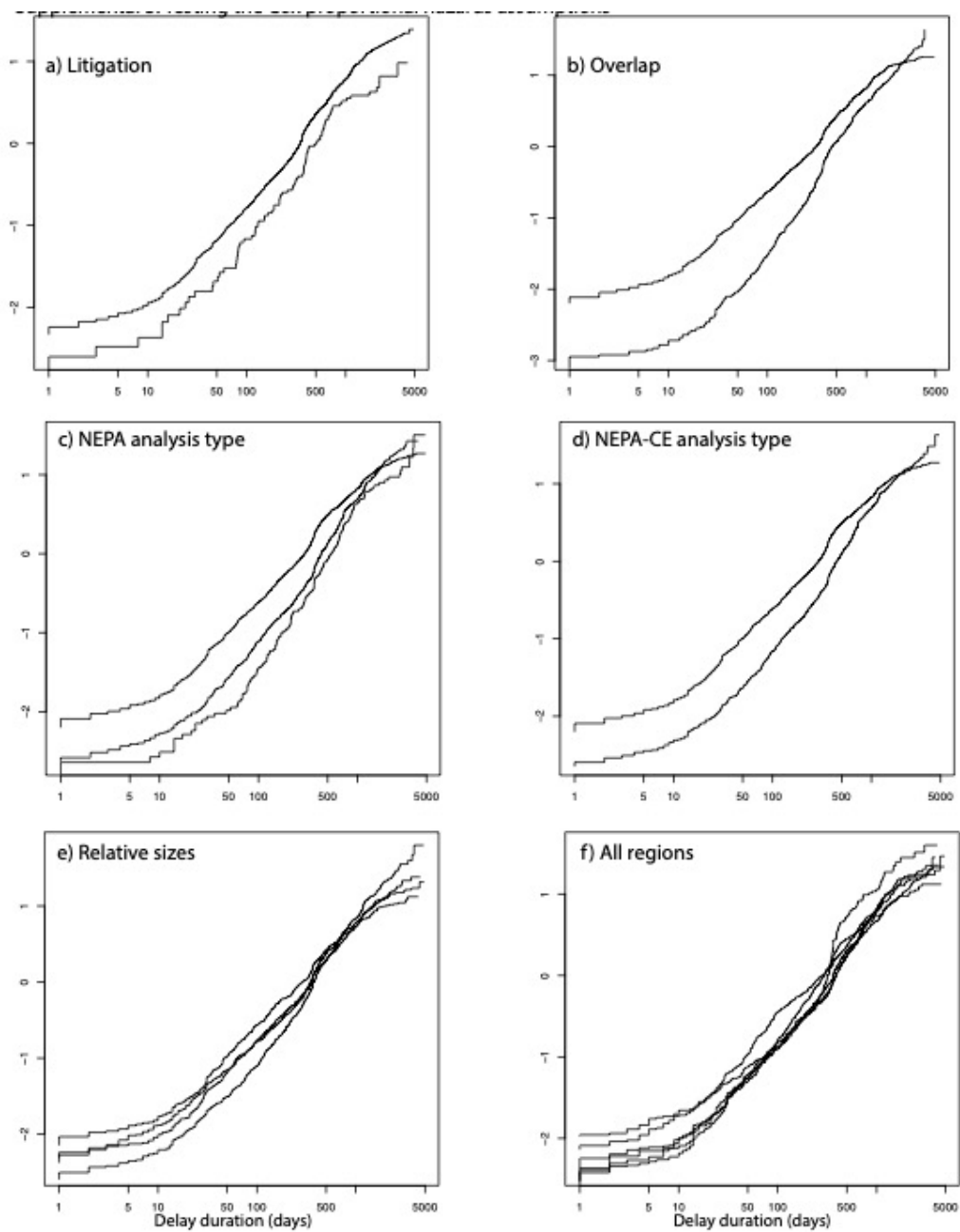




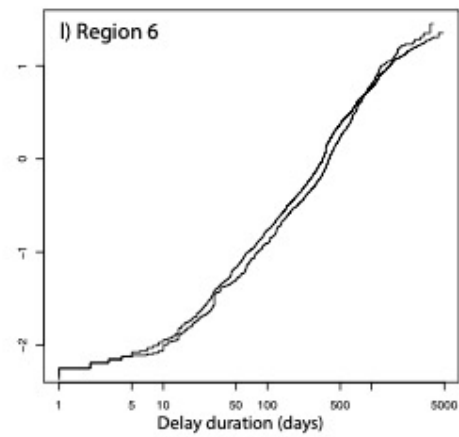
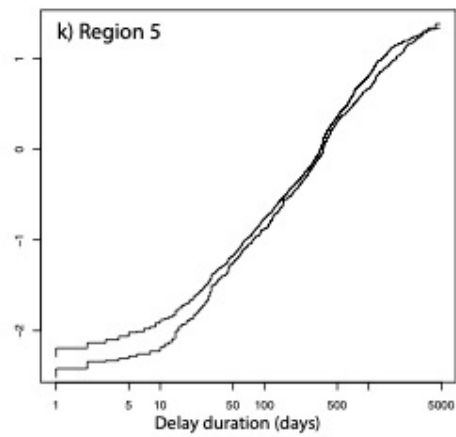
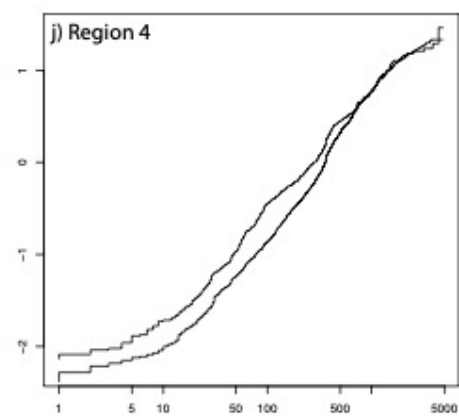
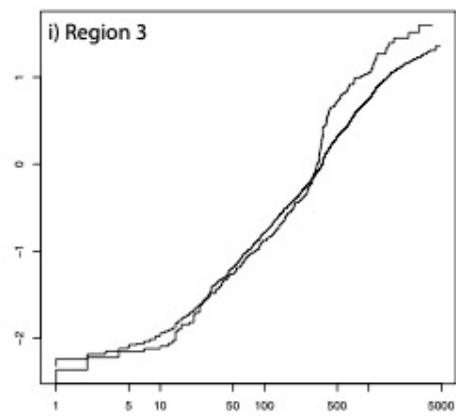
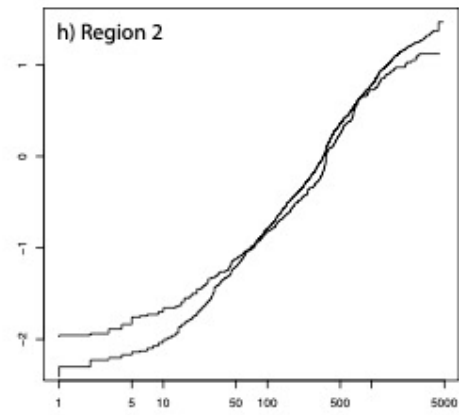
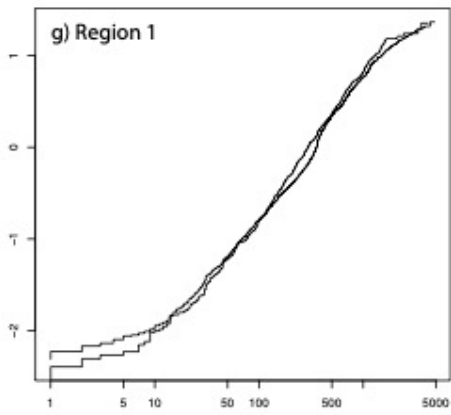




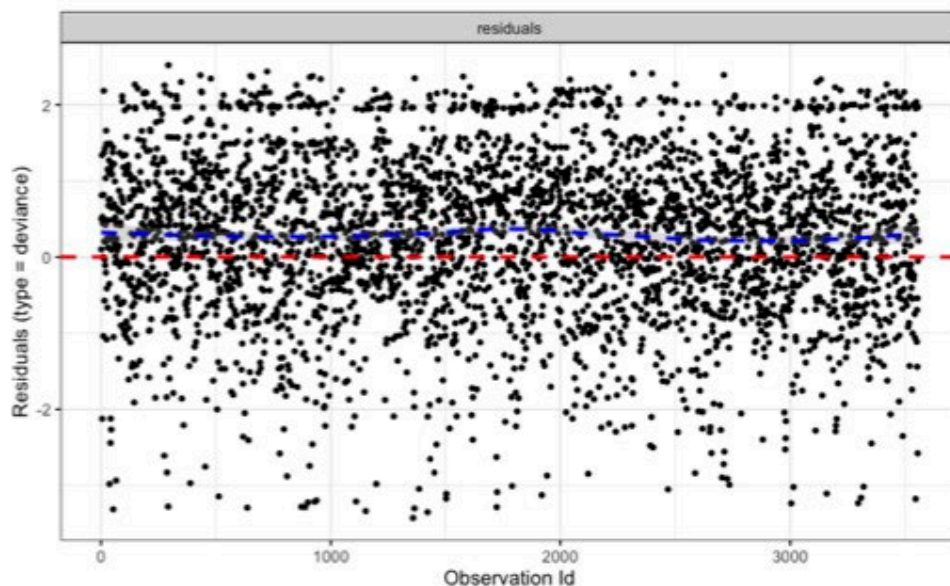
## A5 Testing the Cox proportional hazards assumptions



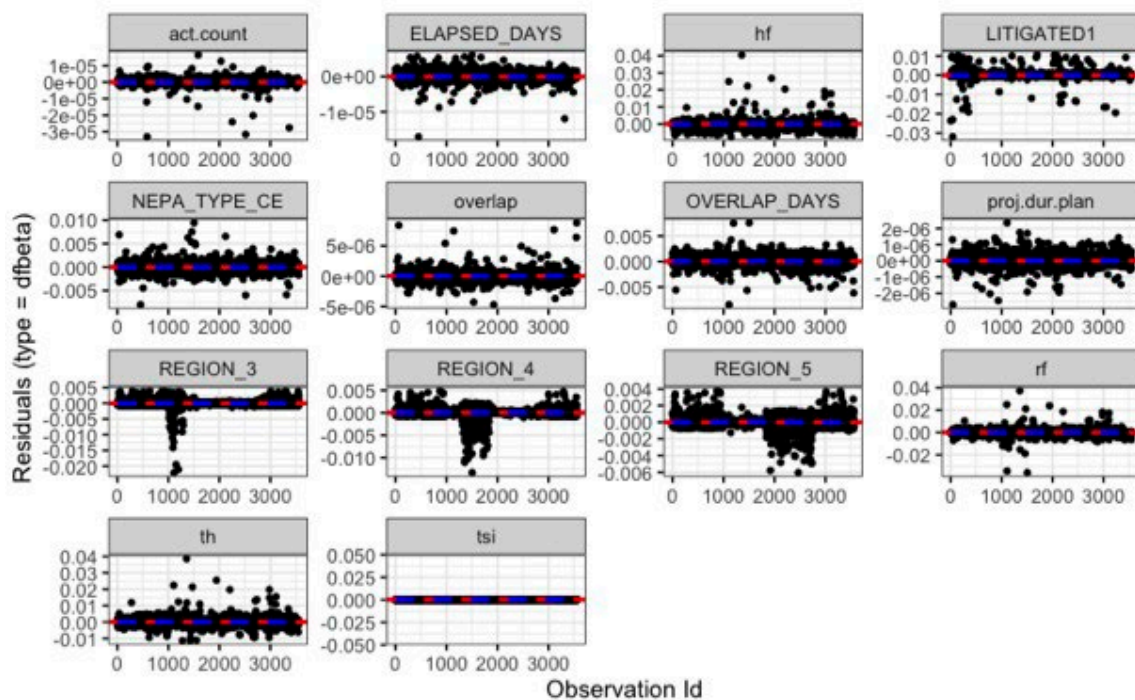
55. (a-l) Results from the c-log-log test for proportionality. Within the Cox proportional hazards model, the hazard ratios are assumed to be proportional. The curves for each covariate tend to remain parallel and do not overlap or cross until the higher ranges of delay duration where there are less projects.



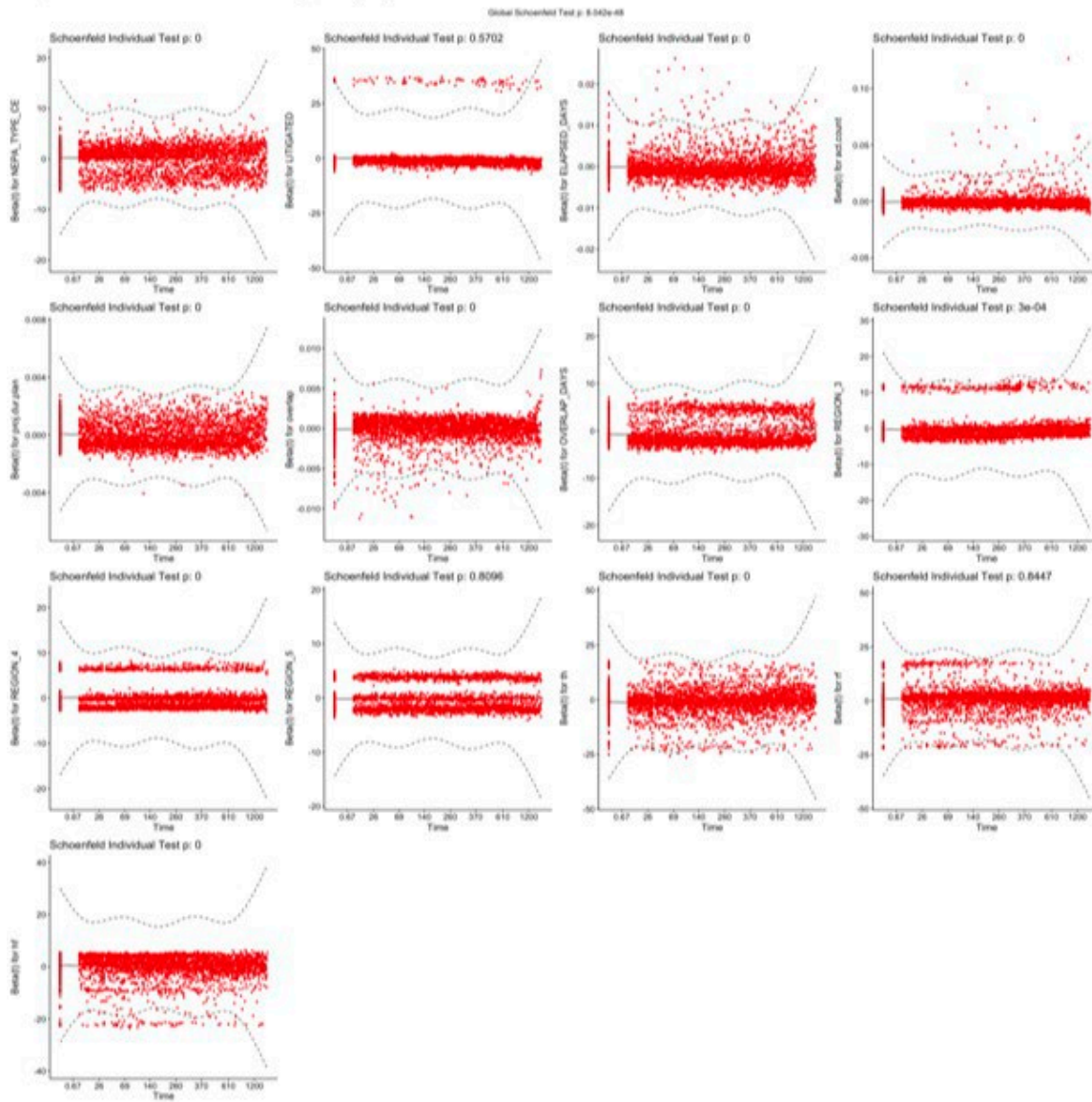
m) Deviance residuals for the larger Cox proportional hazards multivariate model.



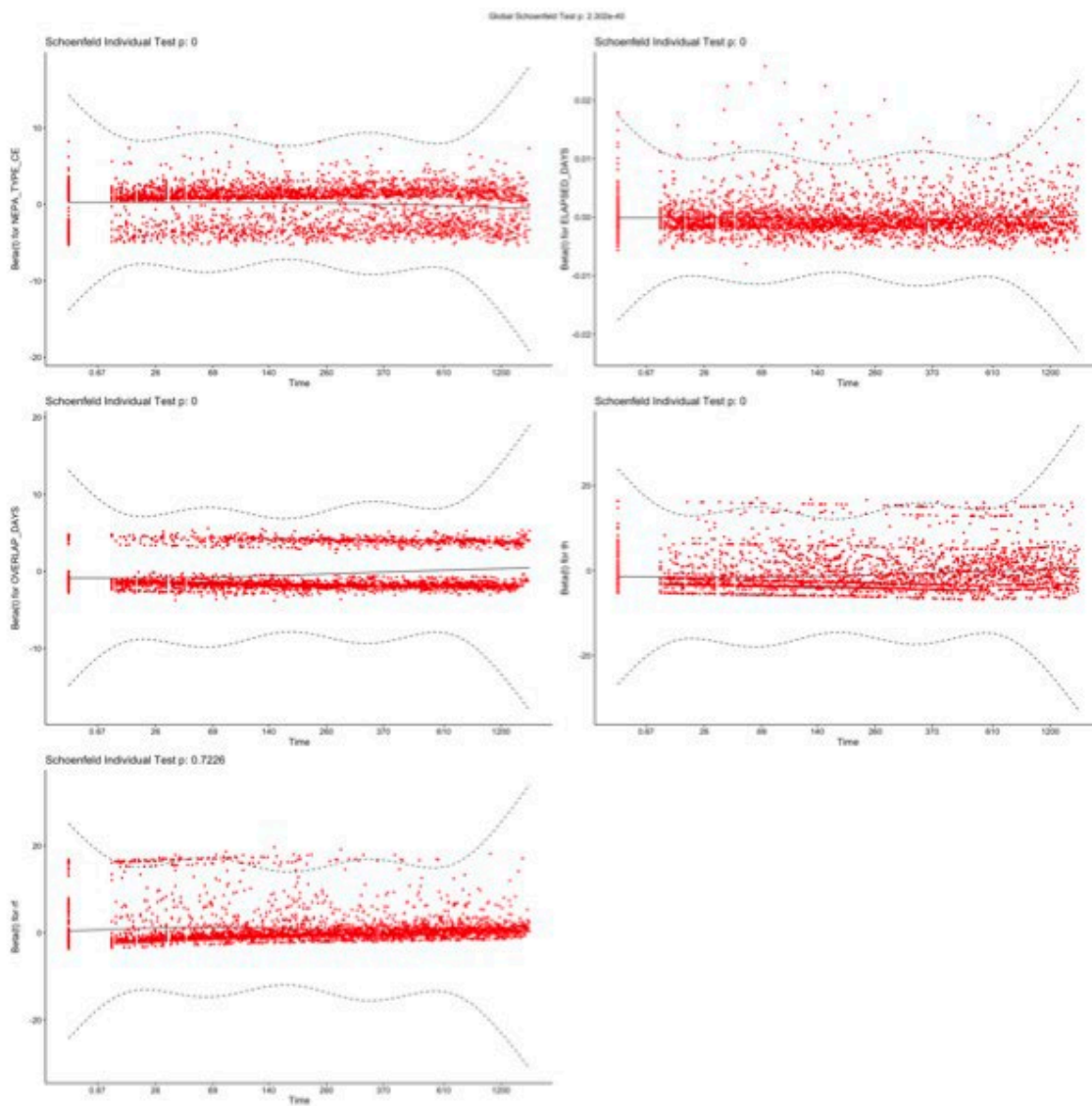
n) Residuals for each beta (covariate) of the larger Cox proportional hazards multivariate model.



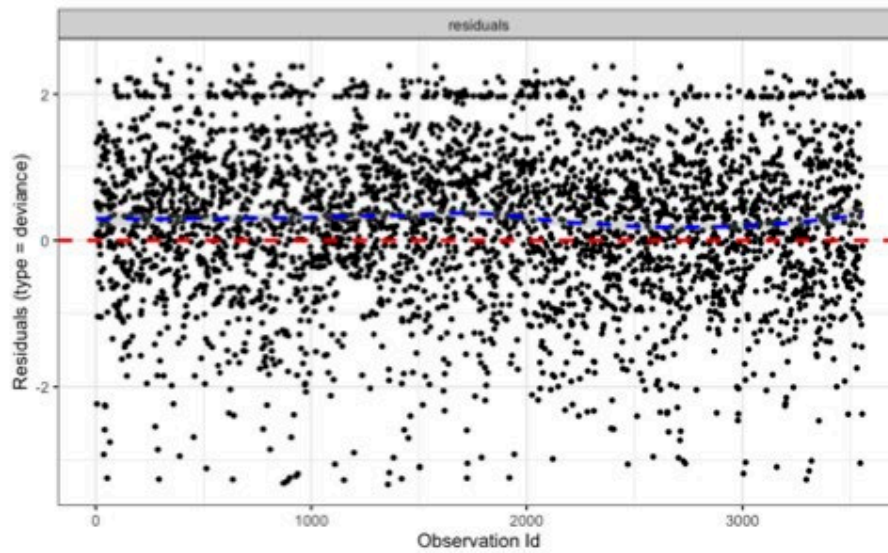
o) Schoenfeld test results for the larger Cox proportional hazards multivariate model.



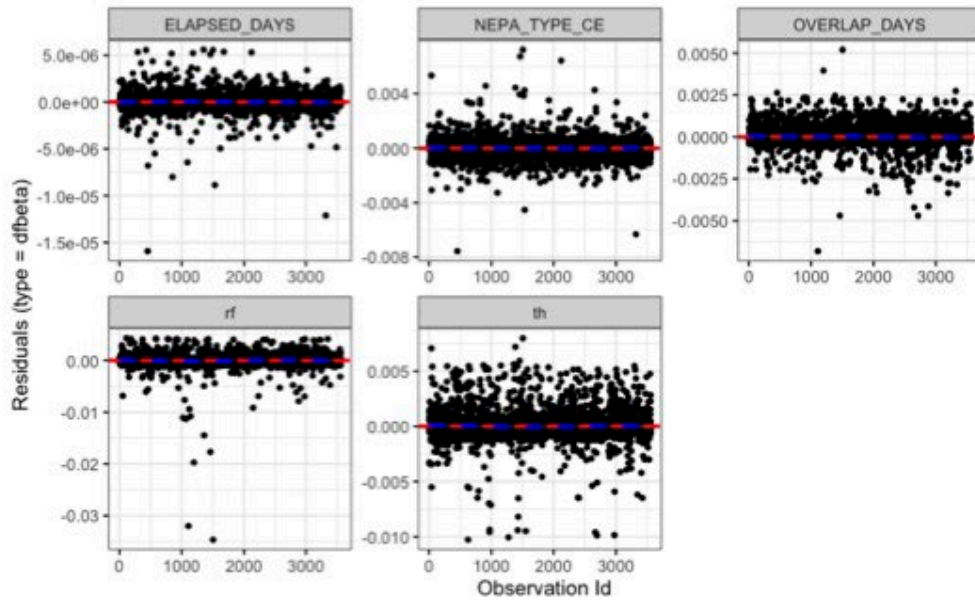
r) Schoenfeld test results for the final Cox proportional hazards multivariate model.



p) Deviance residuals for the final Cox proportional hazards multivariate model.



q) Residuals for each beta (covariate) of the final Cox proportional hazards multivariate model.

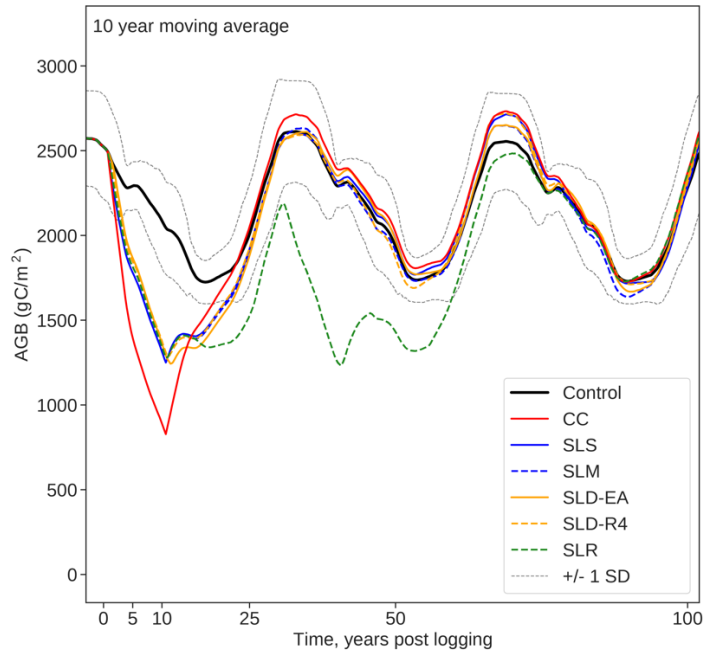


APPENDIX B

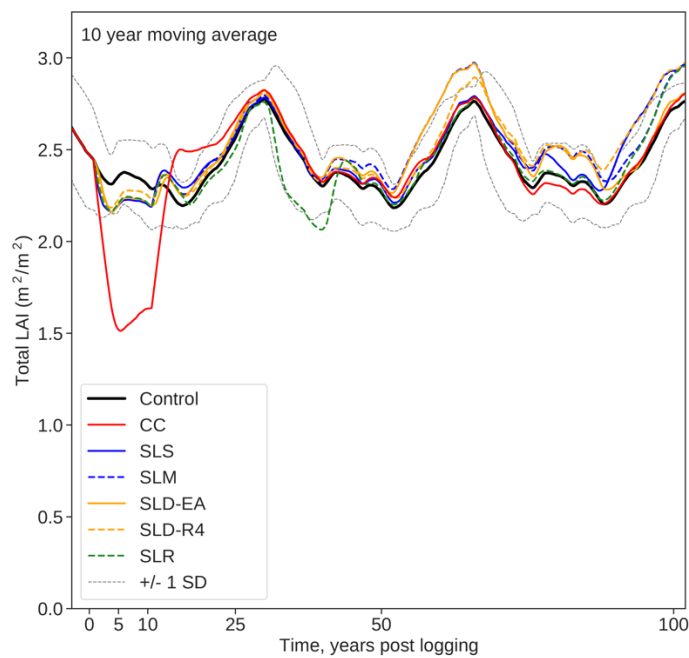
### Appendices for Chapter 3

#### B1 Ten Year Moving averages of the structural variables compared to the control

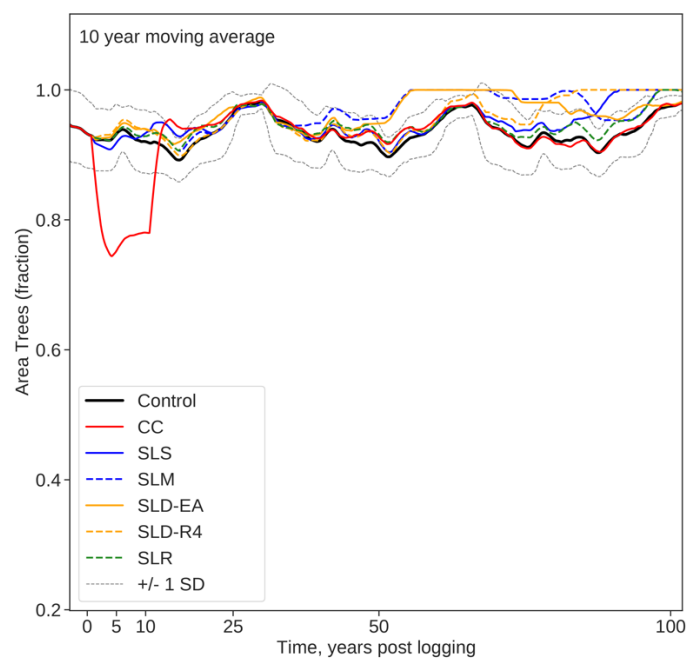
##### scenario



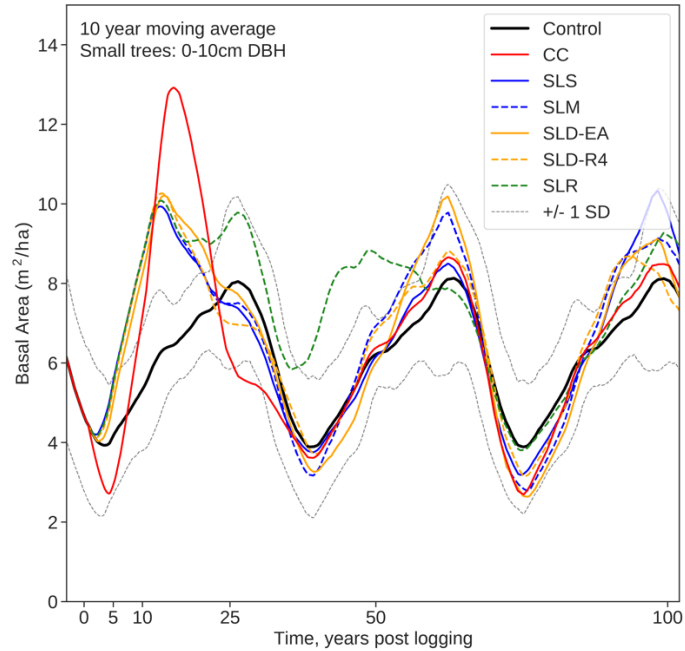
**Figure B1.1** Ten year moving average of AGB.



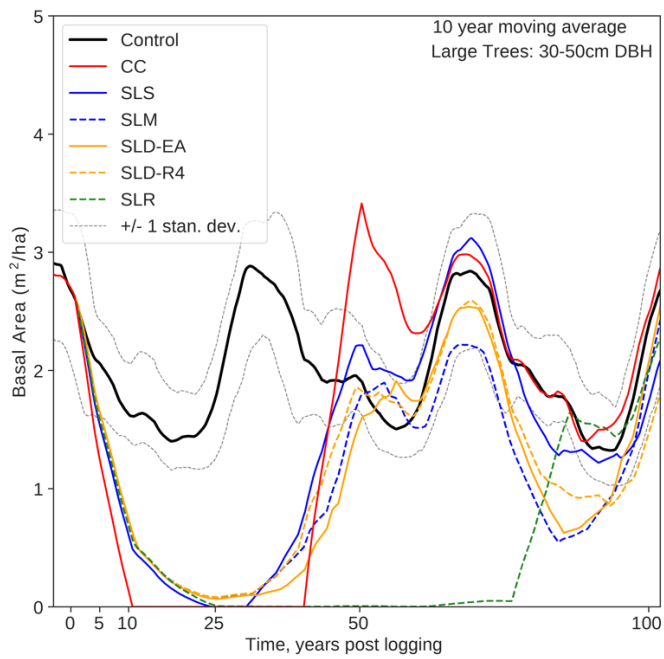
**Figure B1.2** Ten year moving average of LAI.



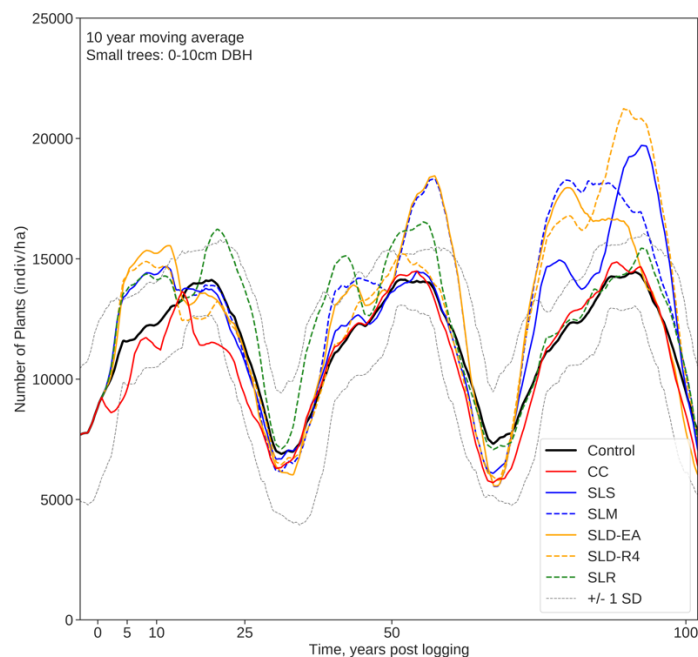
**Figure B1.3** Ten year moving average of the area of trees per grid cell.



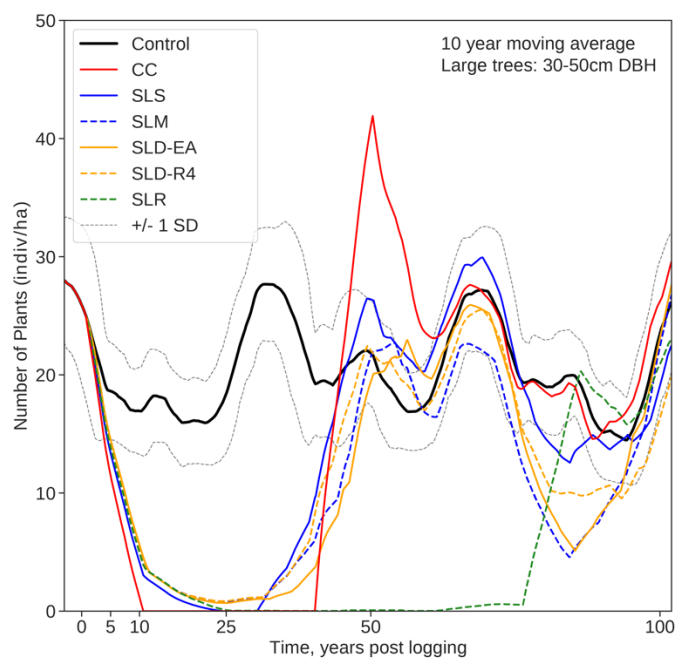
**Figure B1.4** Ten year moving average of the BA of small trees (0-10cm diameter at breast height, DBH).



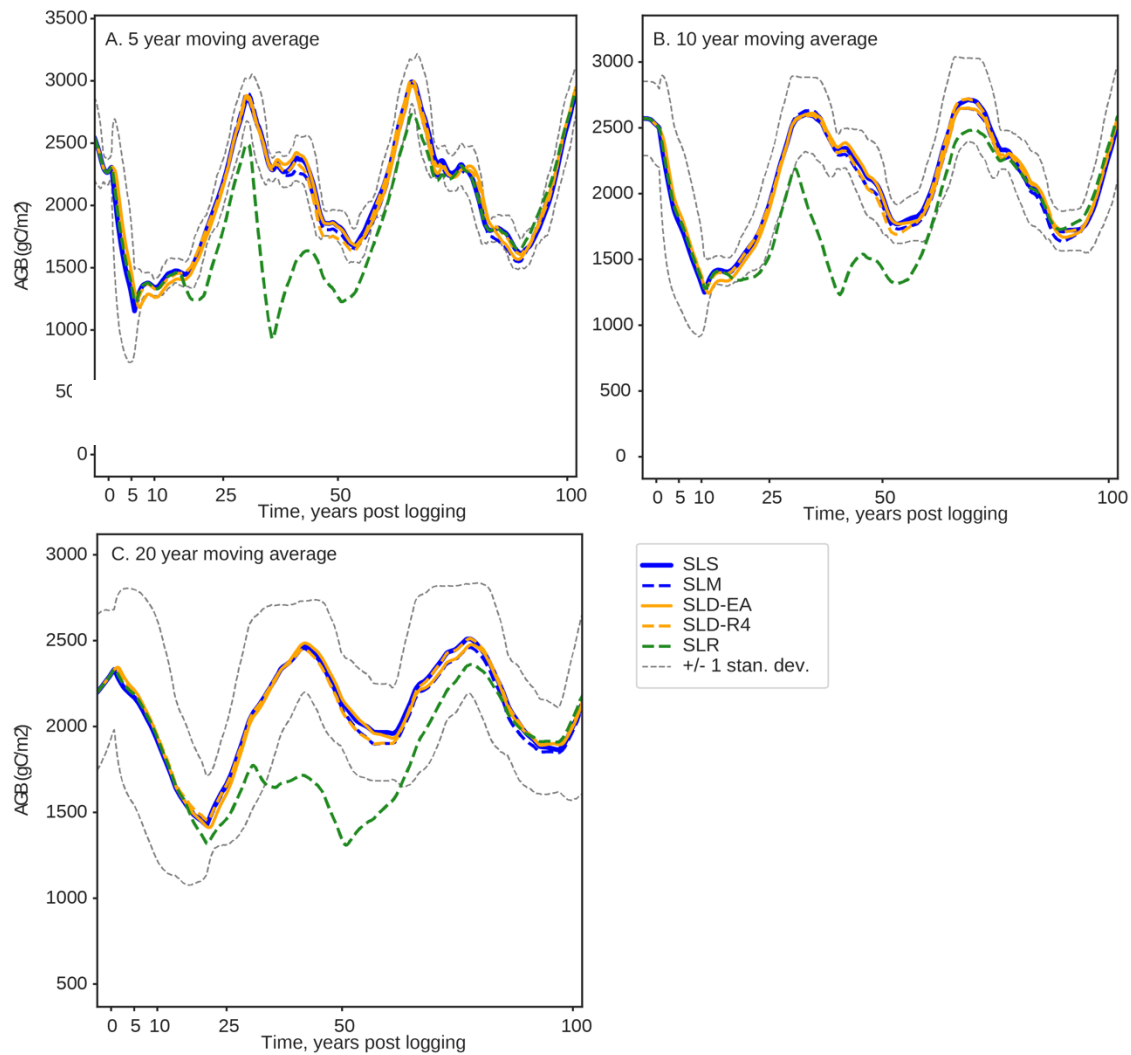
**Figure B1.5** Ten year moving average of the BA of large trees (30-50cm DBH).



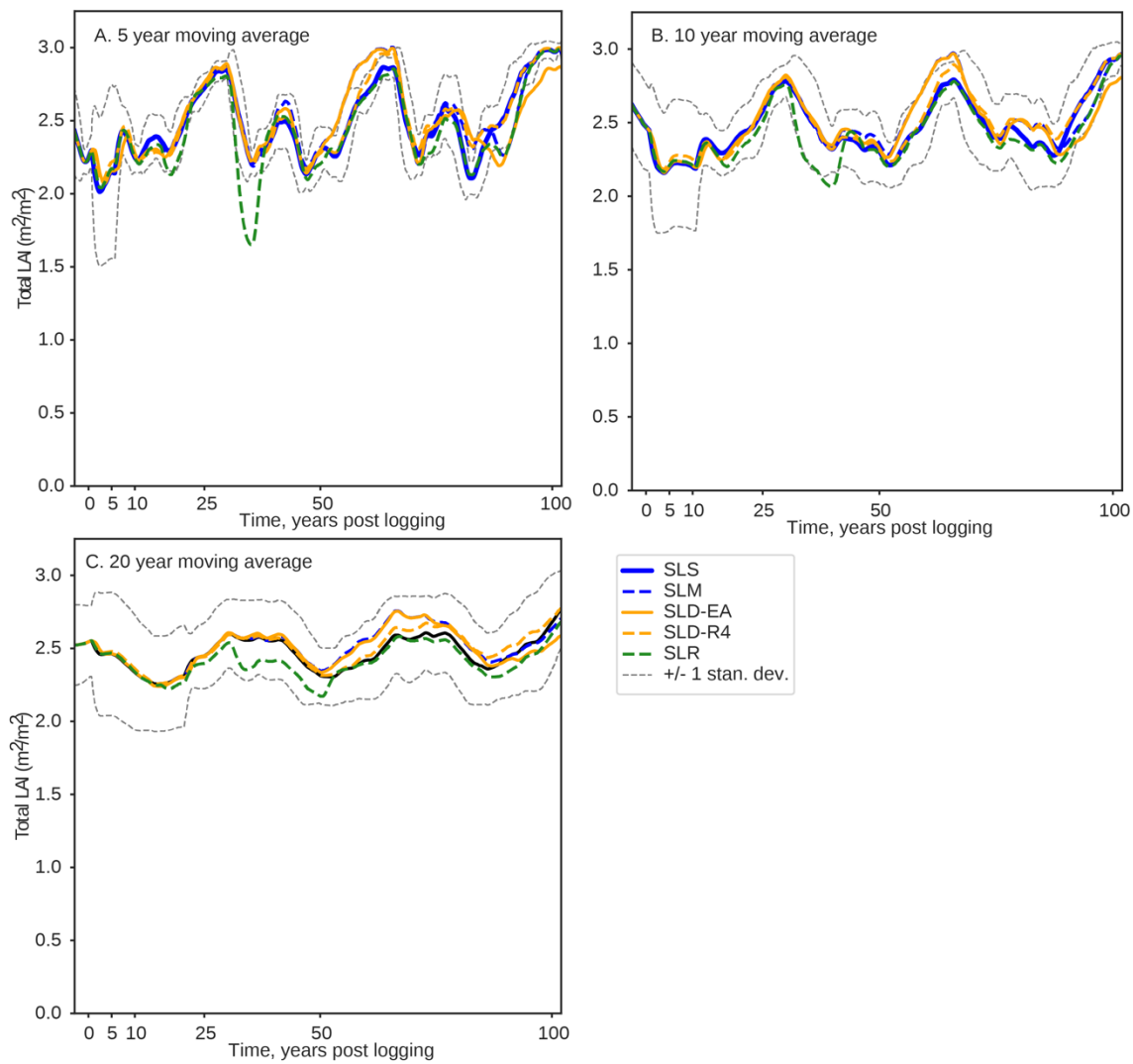
**Figure B1.6** Ten year moving average of the number of plants per hectare of small trees (0-10cm DBH).



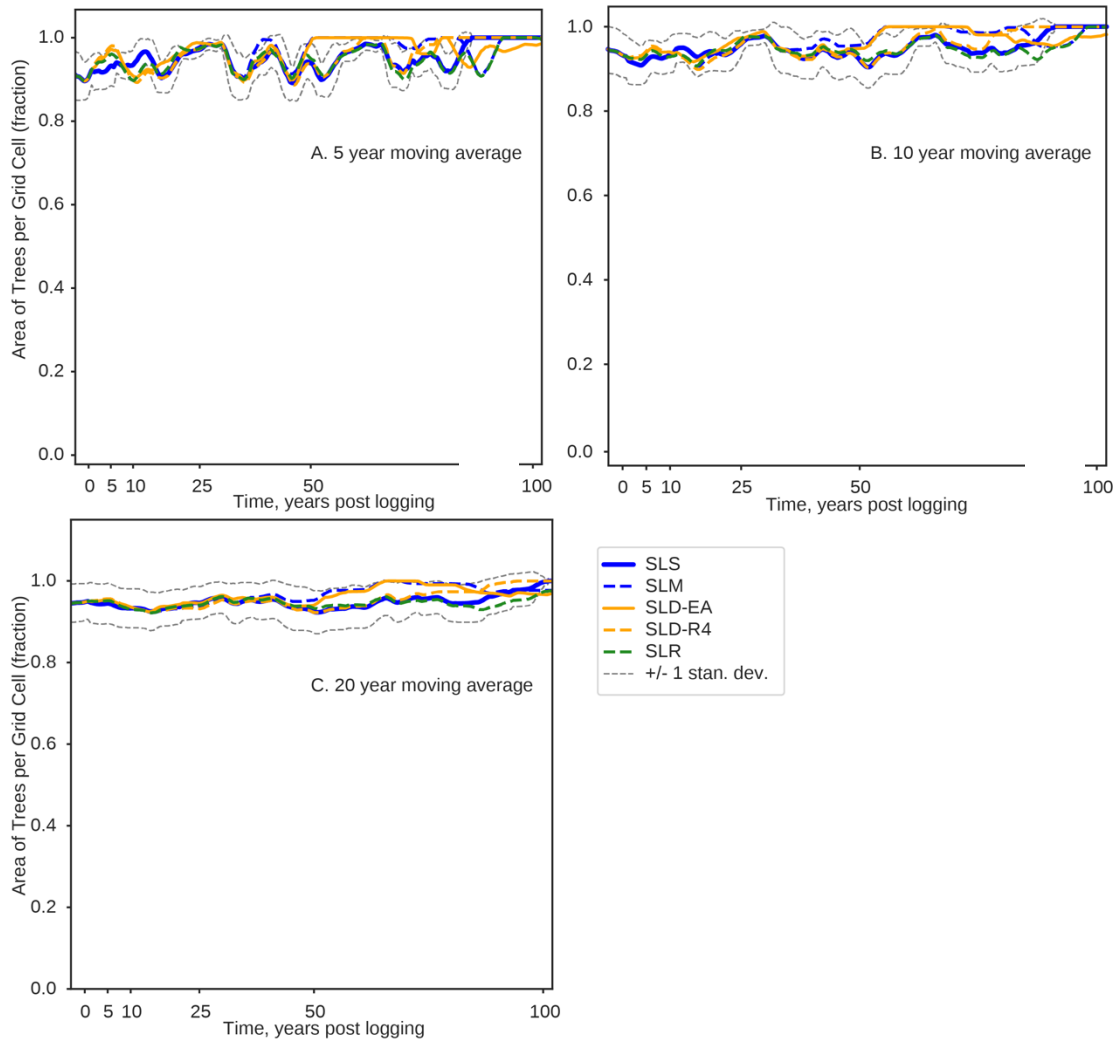
**Figure B1.7** Ten year moving average of the number of plants per hectare of large trees (30-50cm DBH).

B2 Moving averages of the structural variables compared to scenario SLS

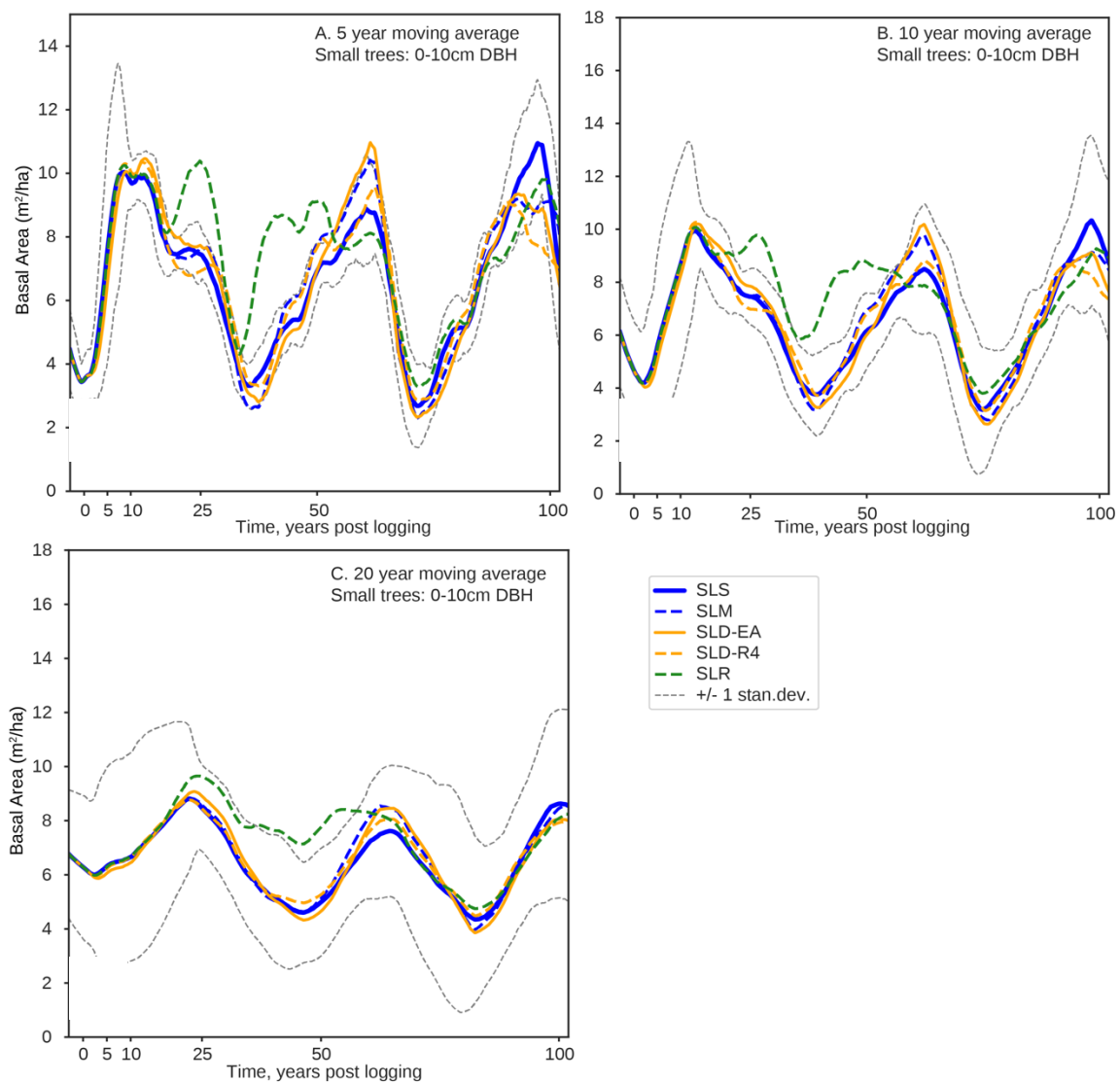
**Figure B2.1** Five (A), 10-(B), and 20-year (C) moving average of AGB compared to the selective logging at a single date scenario (SLS).



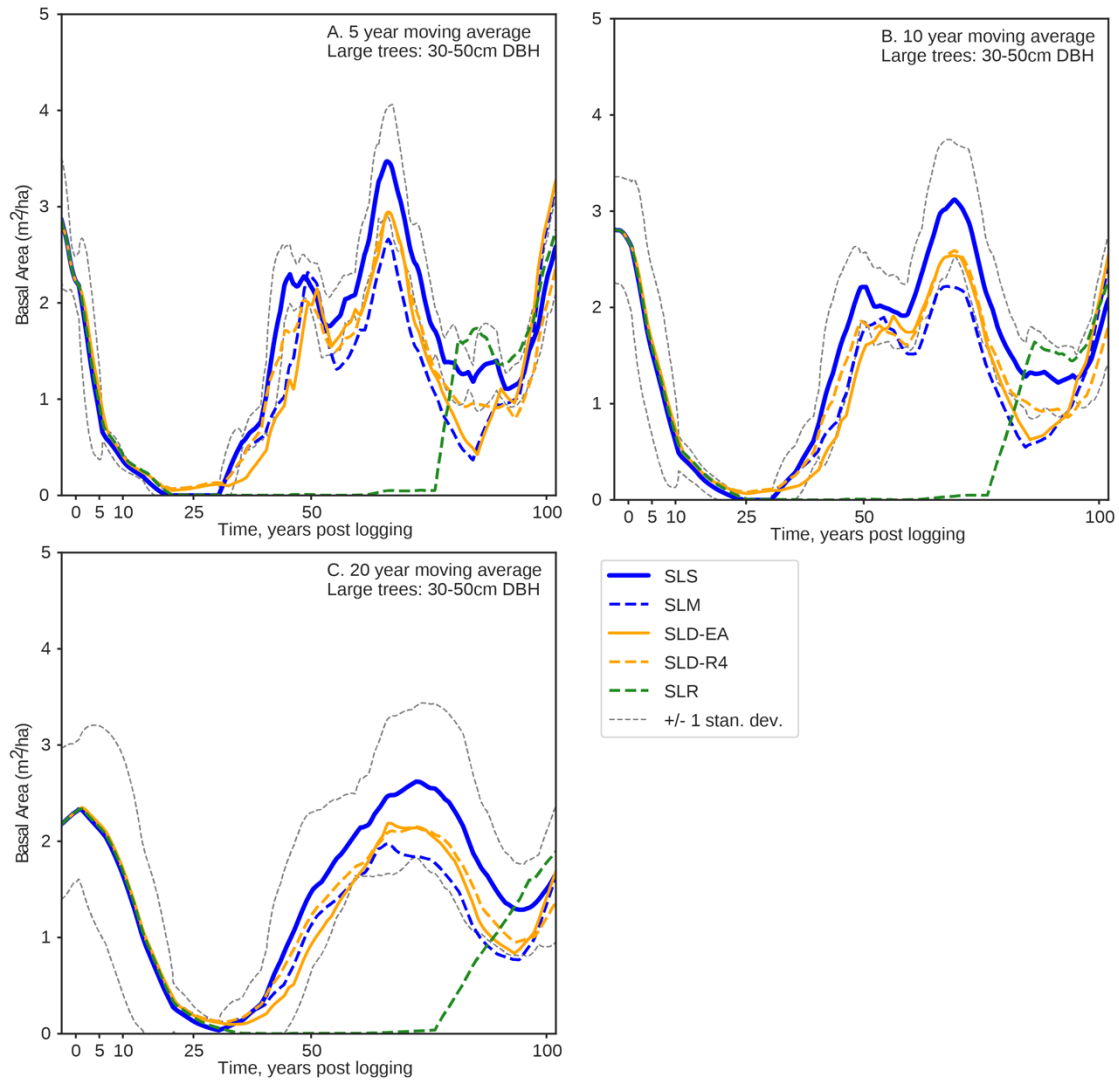
**Figure B2.2** Five (A), 10-(B), and 20-year (C) moving average of LAI compared to the selective logging at a single date scenario (SLS).



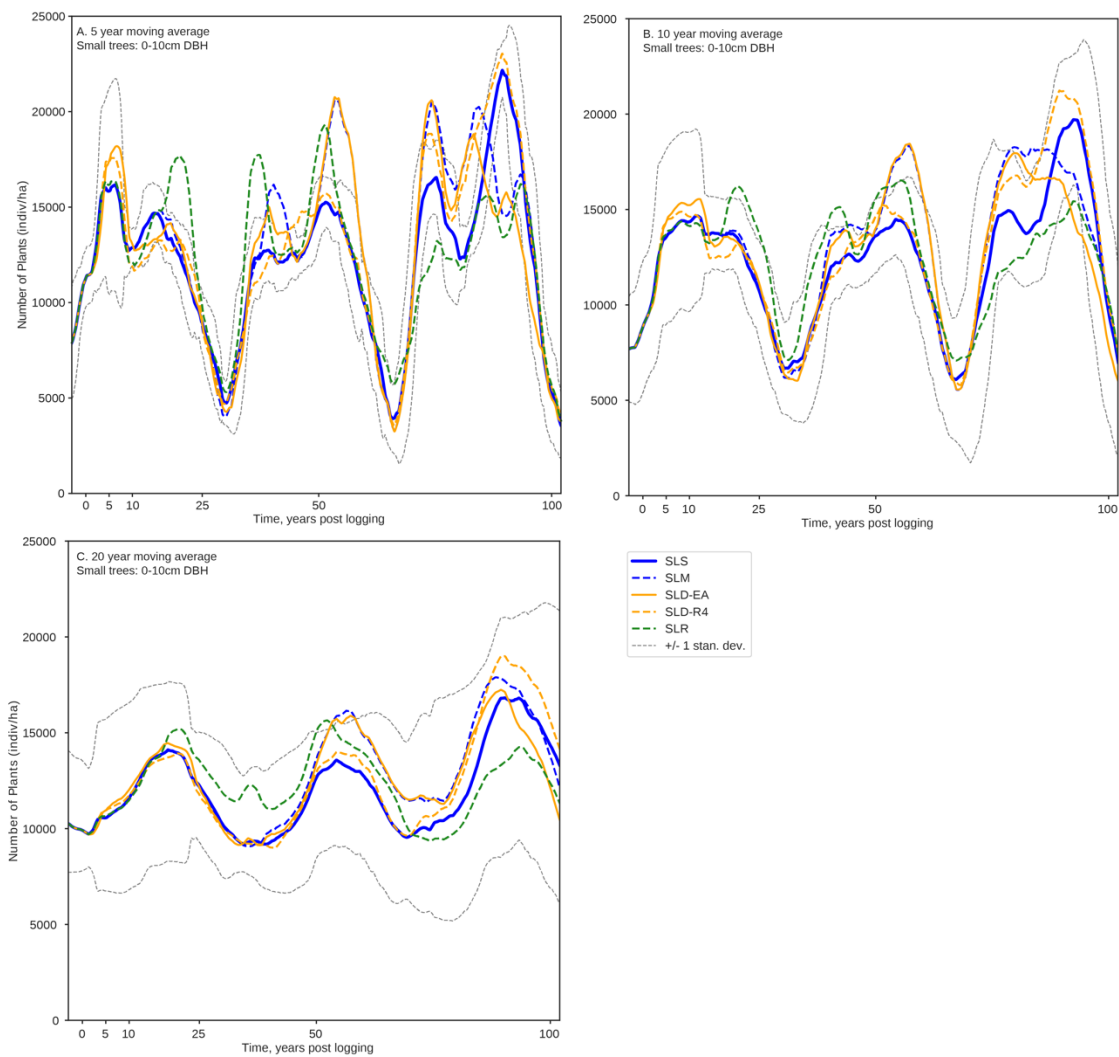
**Figure B2.3** Five (A), 10-(B), and 20-year (C) moving average of area of trees per grid cell compared to the selective logging at a single date scenario (SLS).



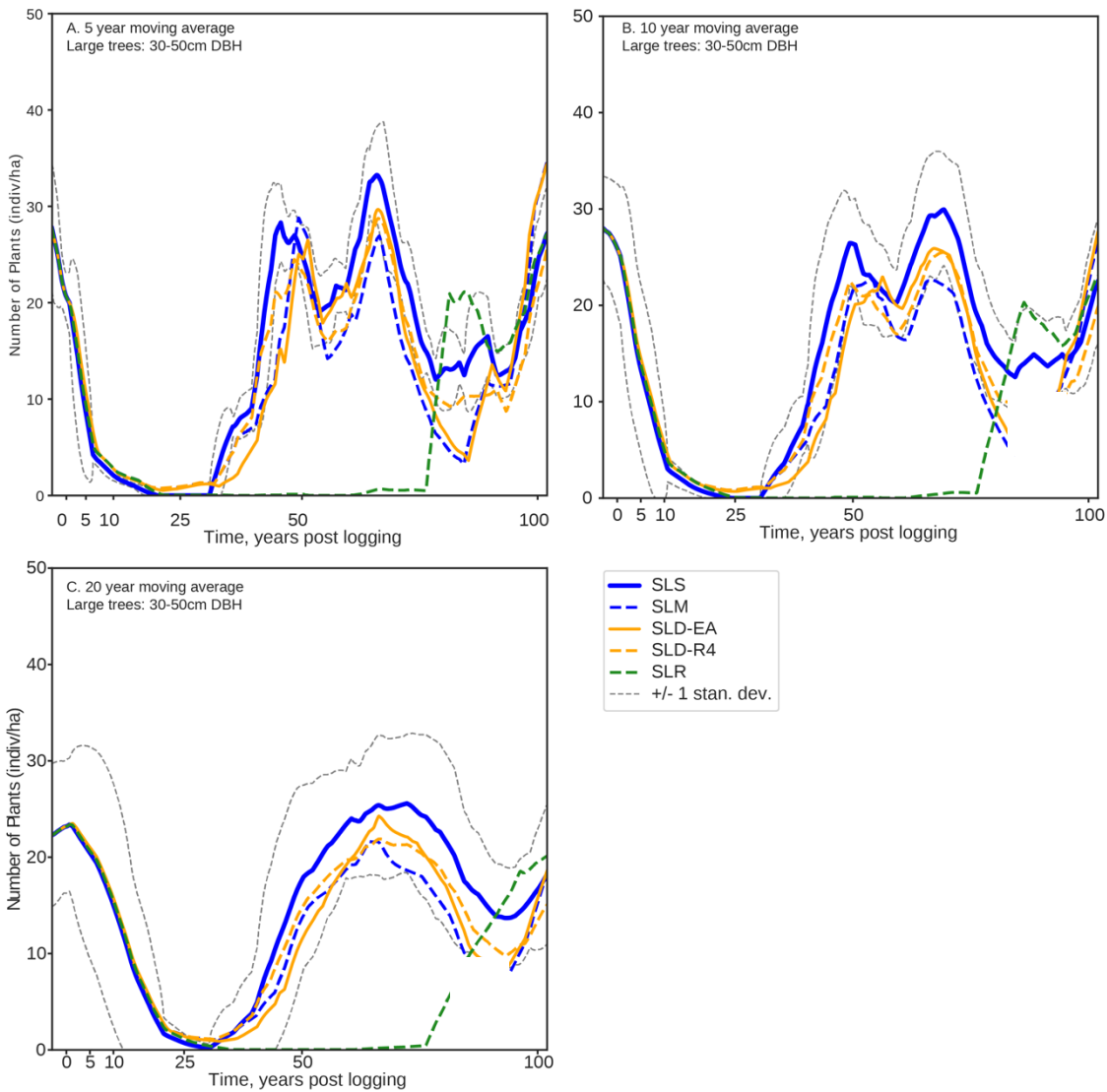
**Figure B2.4** Five (A), 10-(B), and 20-year (C) moving average of BA of small trees compared to the selective logging at a single date scenario (SLS).



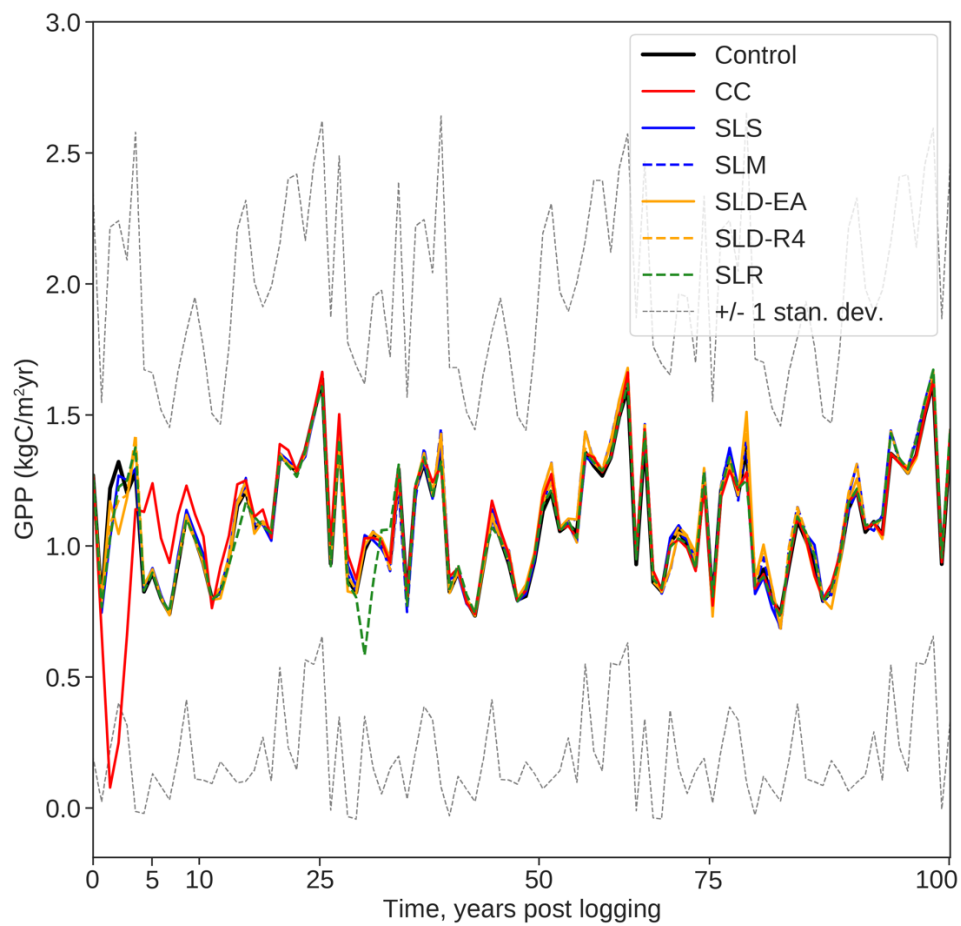
**Figure B2.5** Five (A), 10-(B), and 20-year (C) moving average of BA of large trees compared to the selective logging at a single date scenario (SLS).



**Figure B2.6** Five (A), 10-(B), and 20-year (C) moving average of number of plants of small trees compared to the selective logging at a single date scenario (SLS).



**Figure B2.7** Five (A), 10-(B), and 20-year (C) moving average of number of plants of large trees compared to the selective logging at a single date scenario (SLS).

B3 Annual means of the functional values

**Figure B3.1 Annual mean GPP with +/- one standard deviation of the control scenario.**

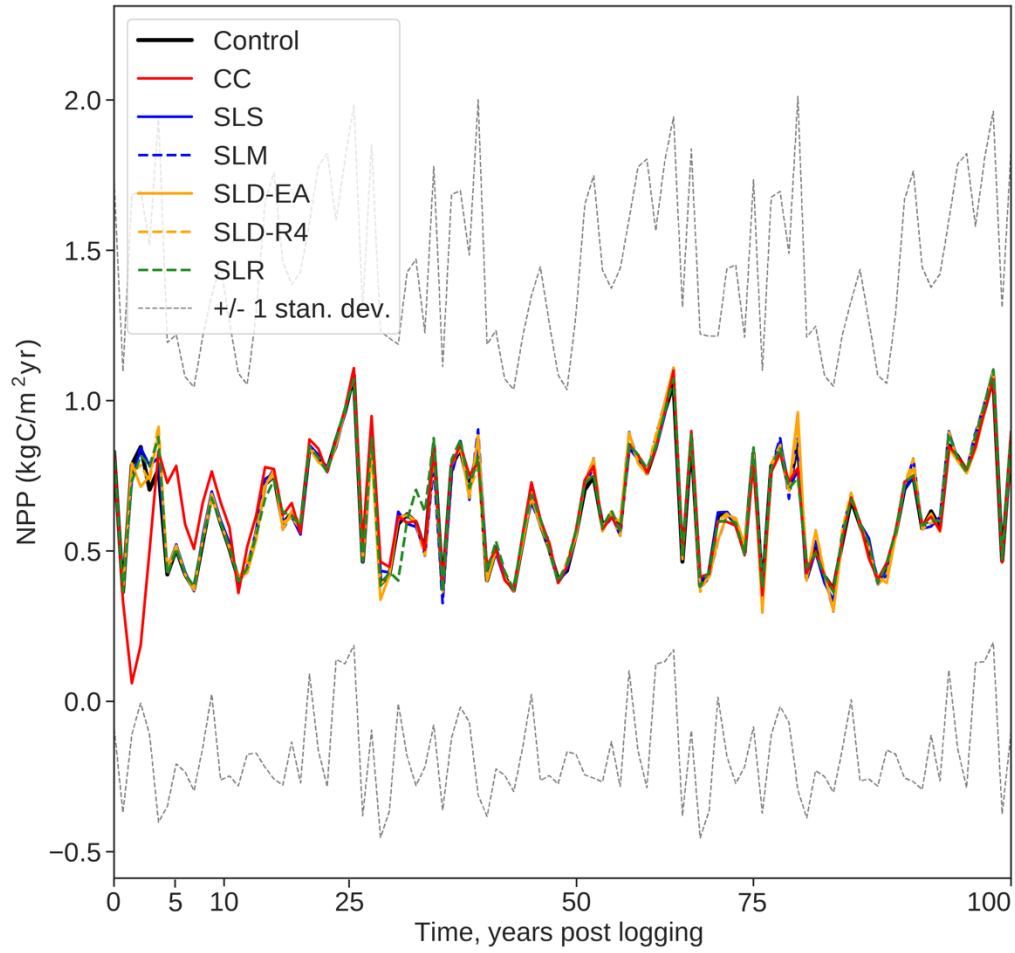


**Figure B3.2 Annual mean NPP with +/- one standard deviation of the control scenario.**

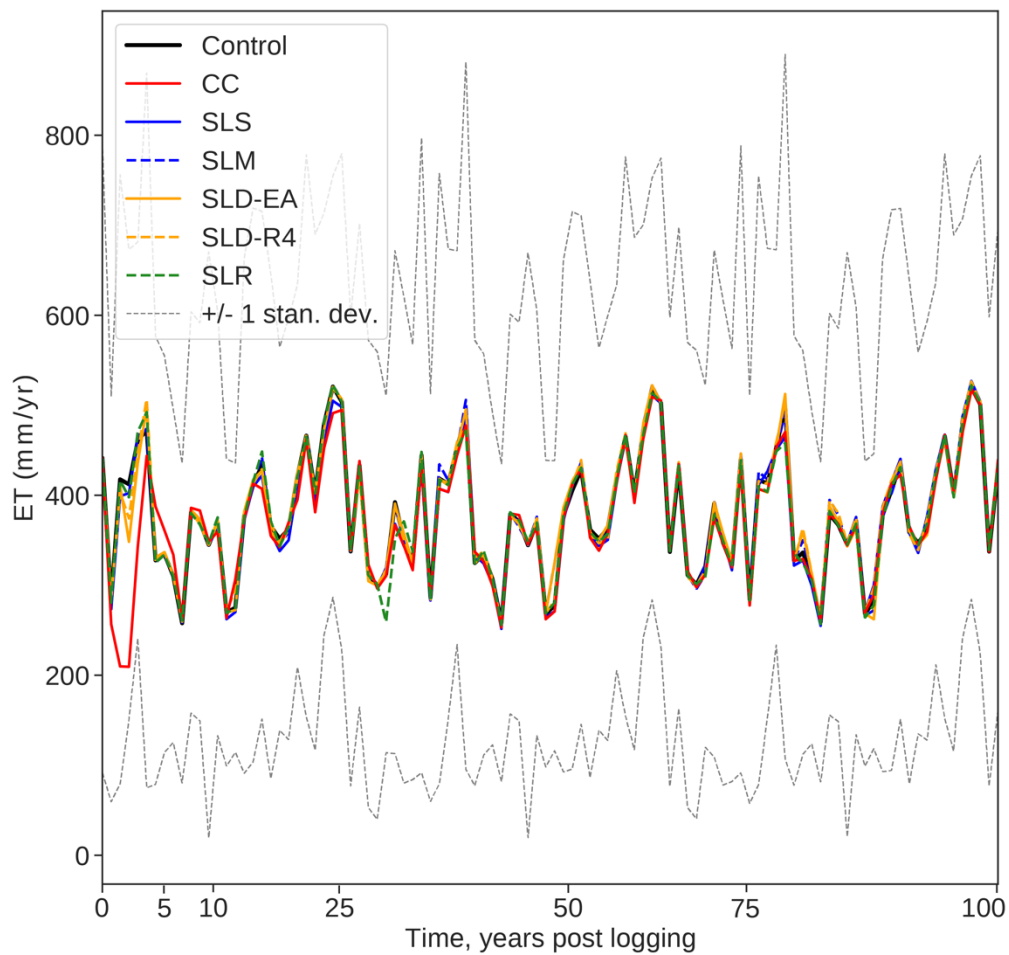


**Figure B3.3 Annual mean ET with +/- one standard deviation of the control scenario.**

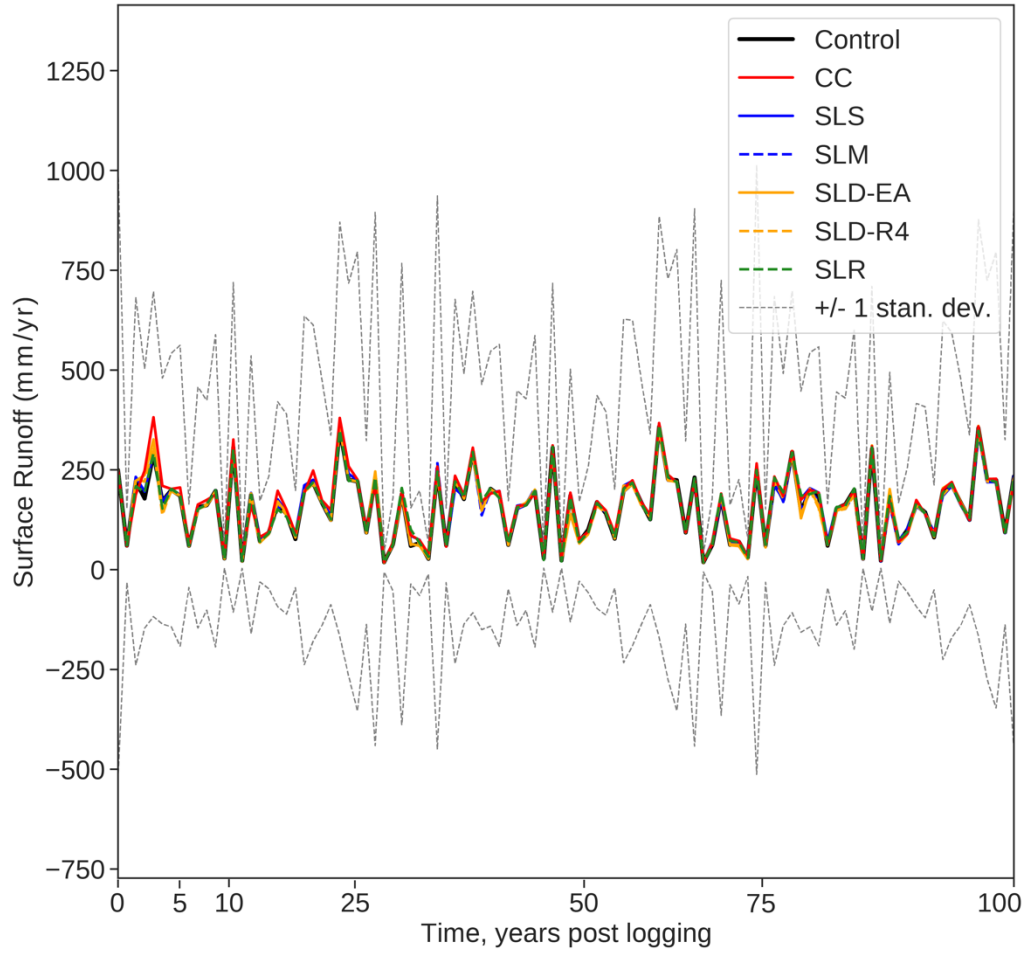


**Figure B3.4 Annual mean QR with +/- one standard deviation of the control scenario.**

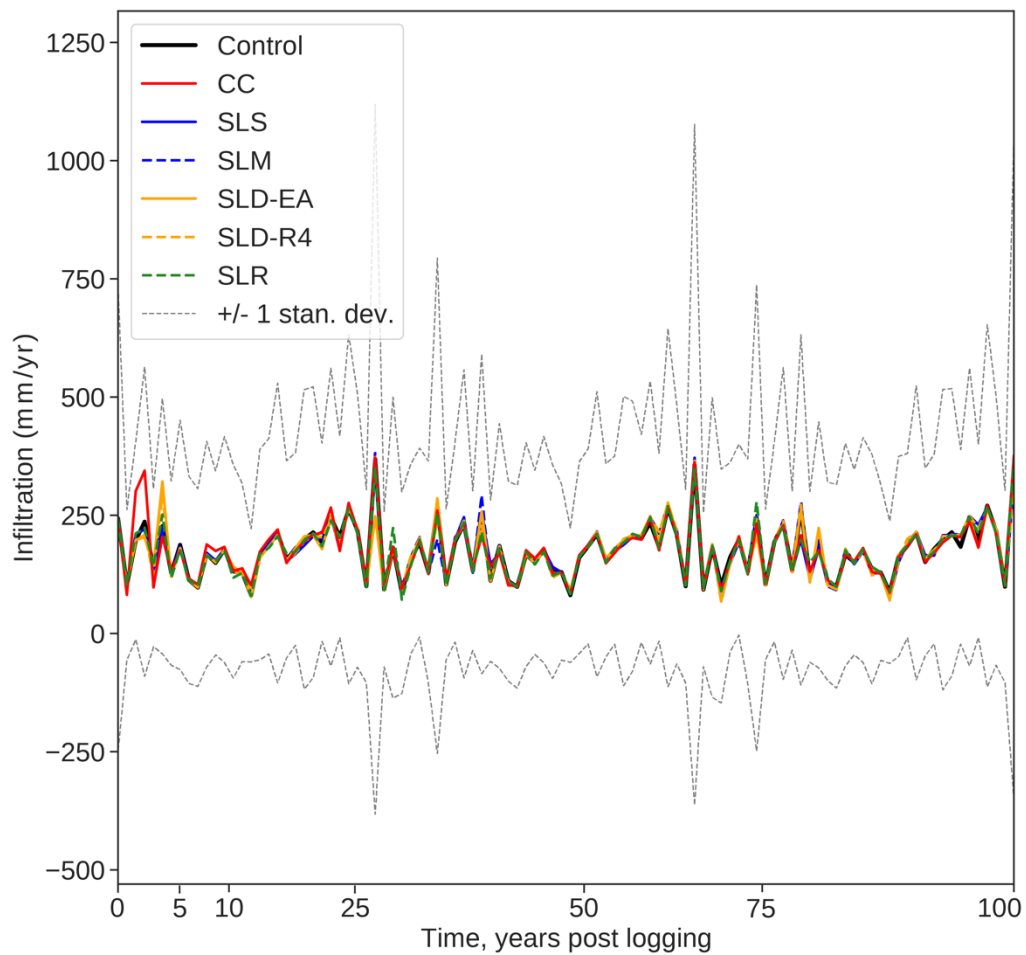


**Figure B3.5 Annual mean QIN with +/- one standard deviation of the control scenario.**

## B4 Seasonal averages of functional variables compared to control or scenario 1-SL

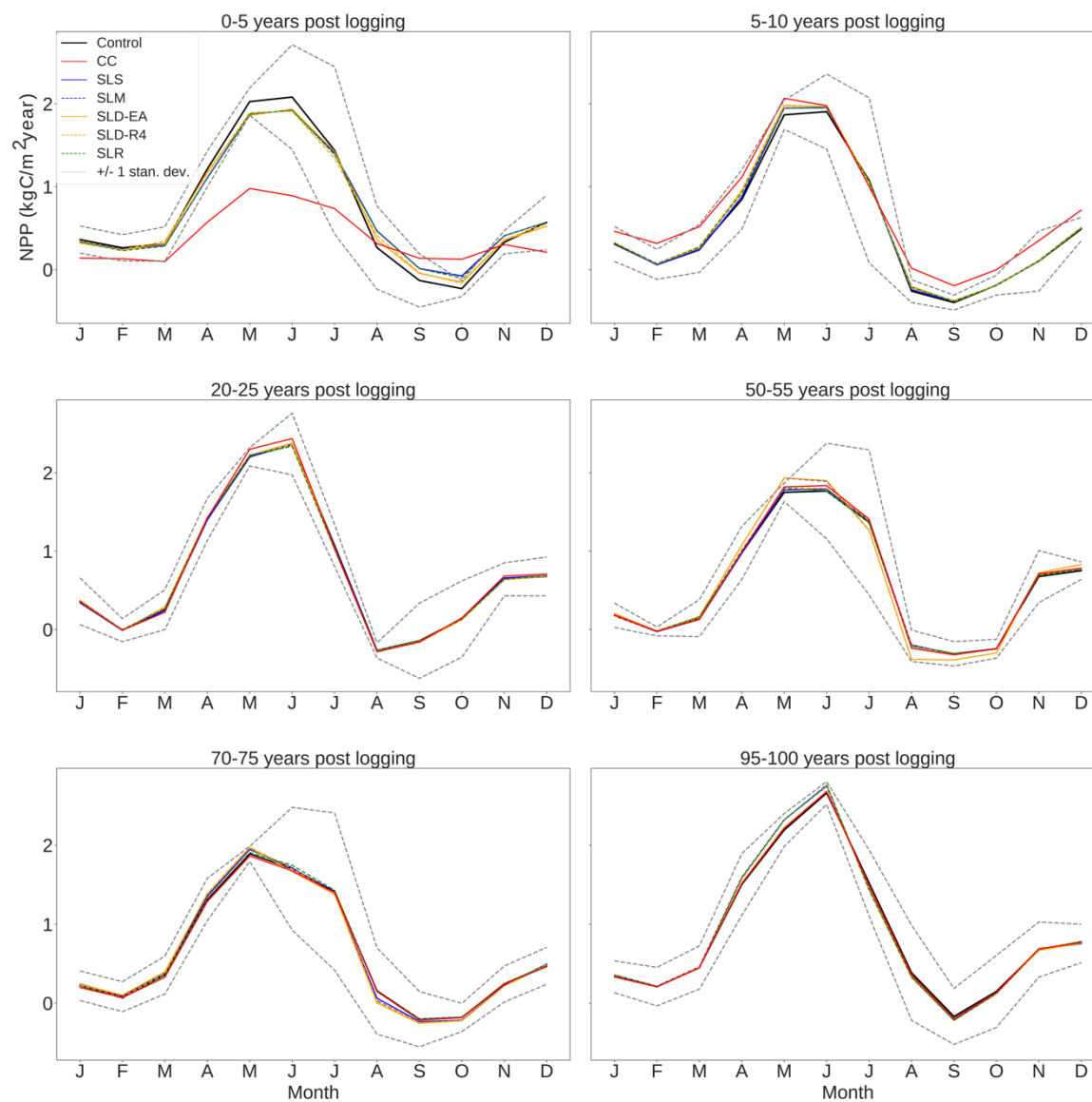


**Figure B4.1** Seasonal mean NPP with  $\pm$  one standard deviation from the control scenario at different 5-year increments post-logging.

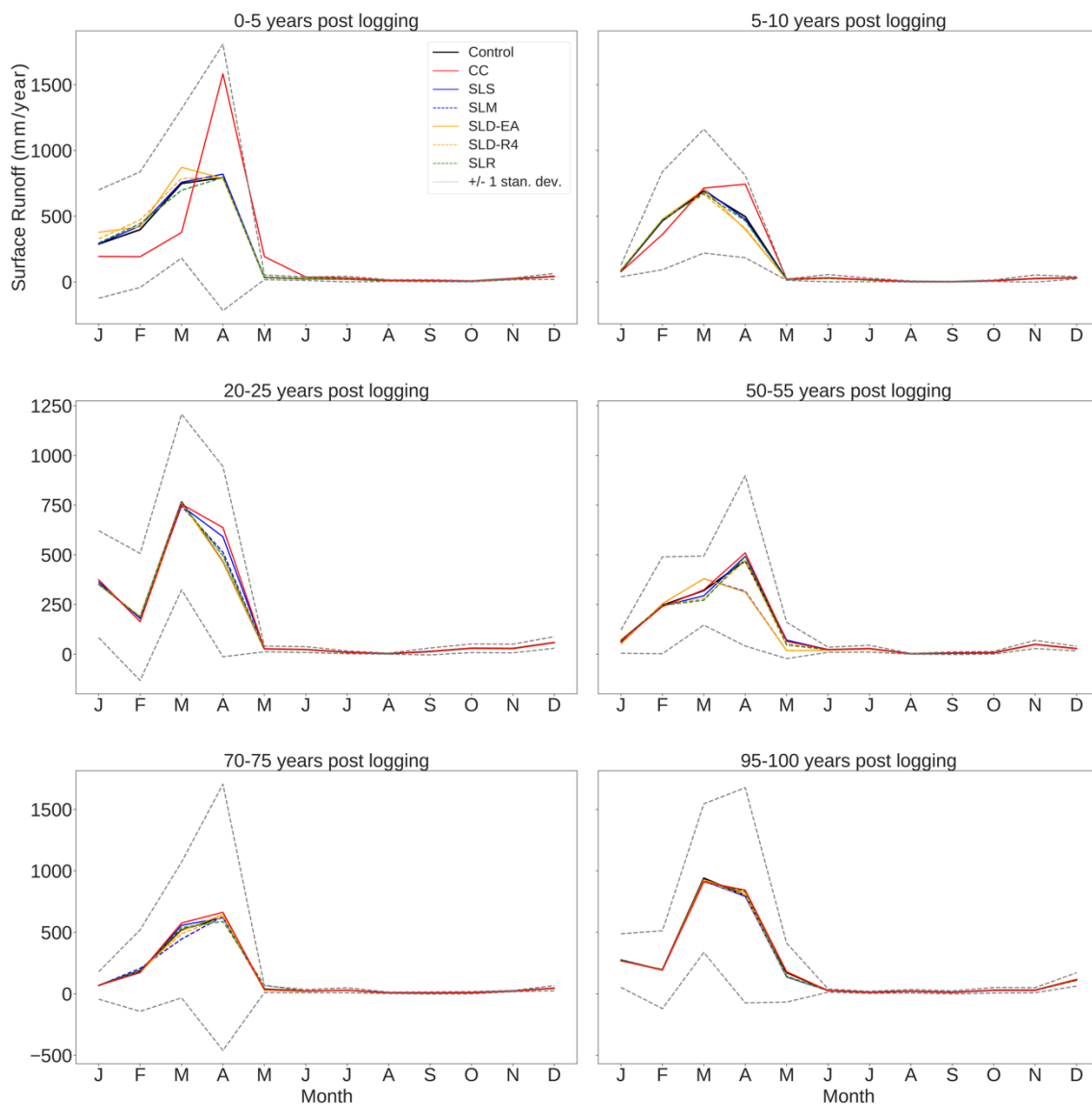


**Figure B4.2** Seasonal mean surface runoff (QR) with +/- one standard deviation from the control scenario at different 5-year increments post-logging. Please note the different scale on the y-axes.

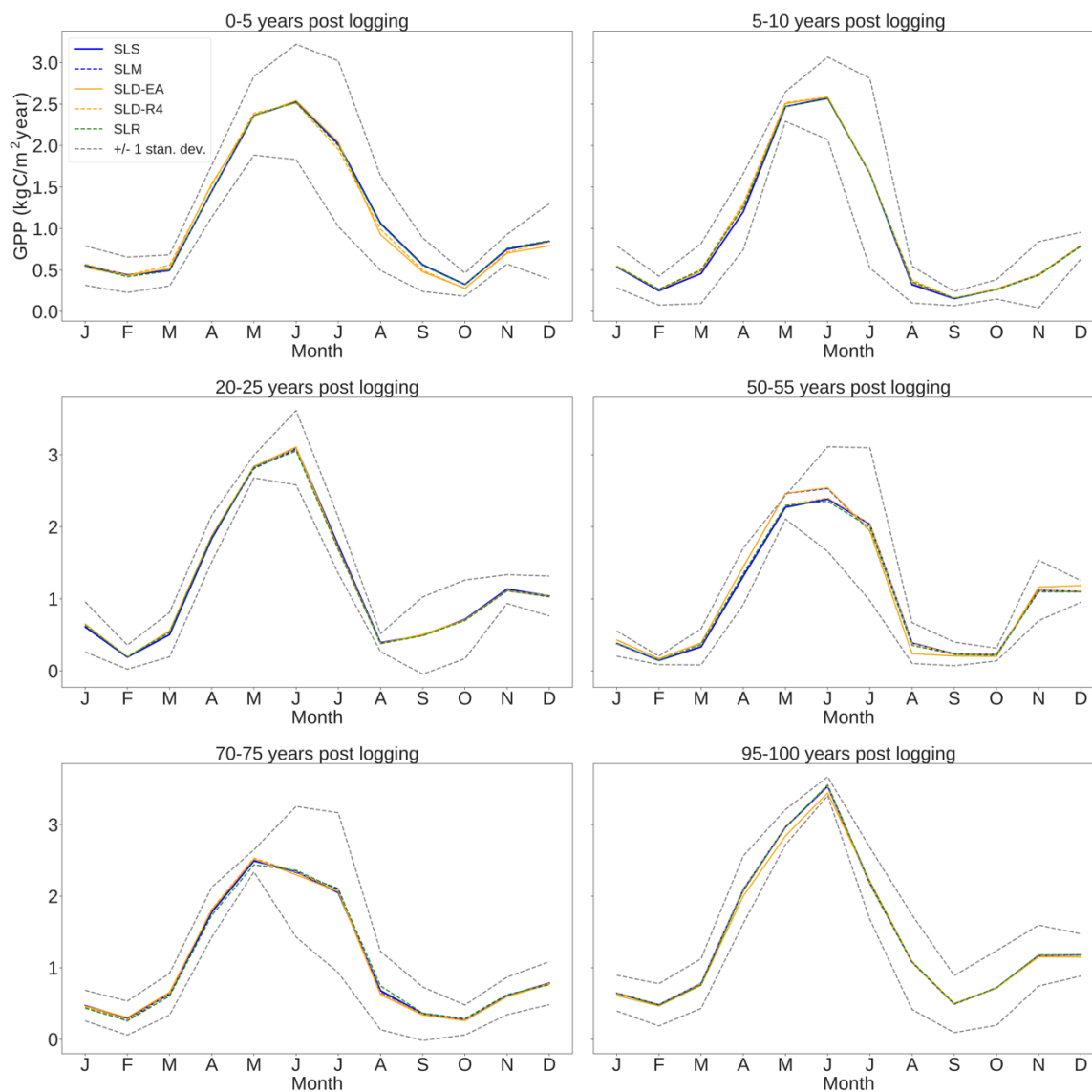


**Figure B4.3** Seasonal average GPP with +/- one standard deviation of scenario SLS at different 5-year increments post-logging. Please note the different y-axes on the top row of figures.

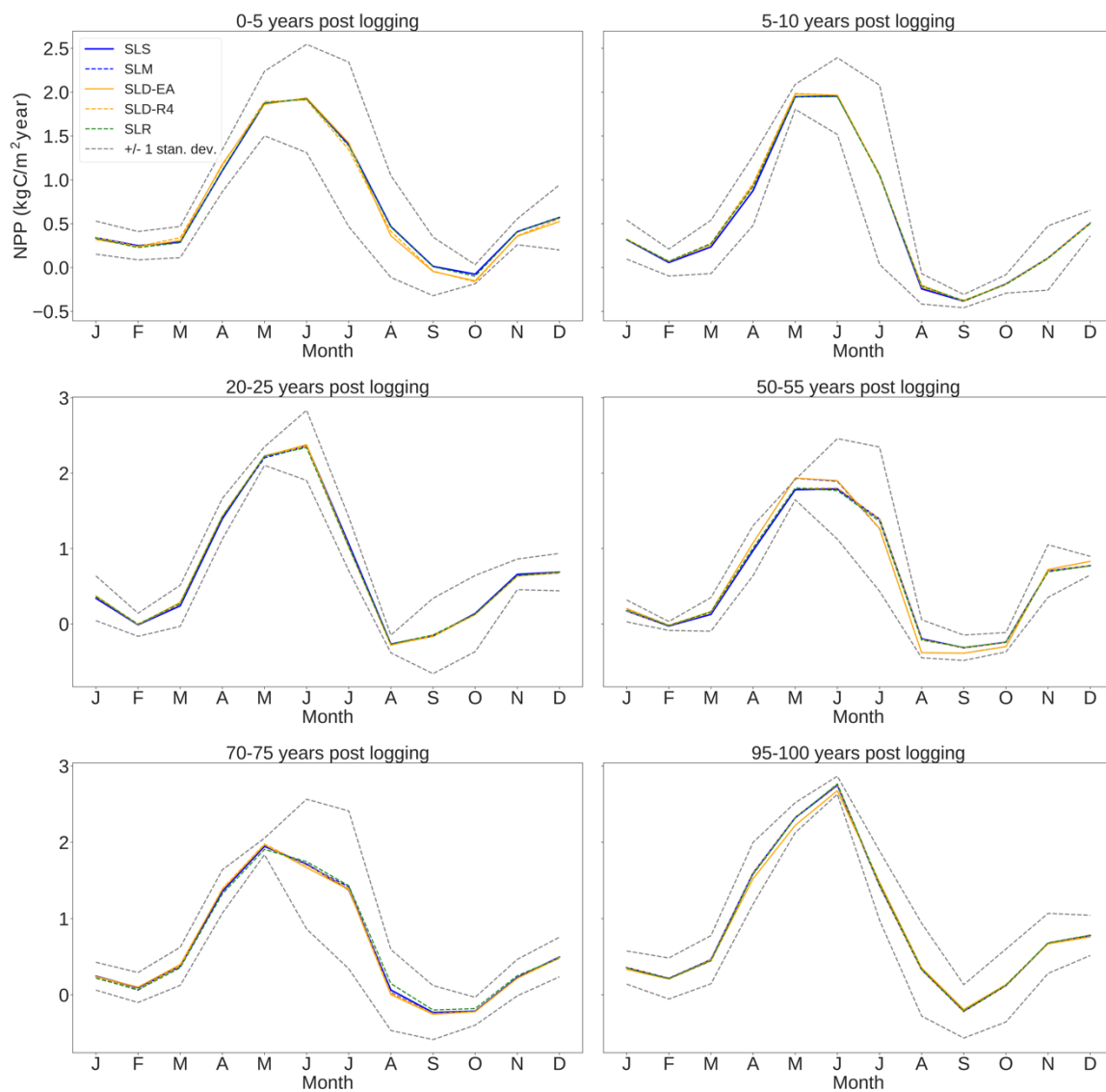


**Figure B4.4 Seasonal average NPP with  $\pm$  one standard deviation of scenario SLS at different 5-year increments post-logging. Please note the different y-axes on the top row of figures.**

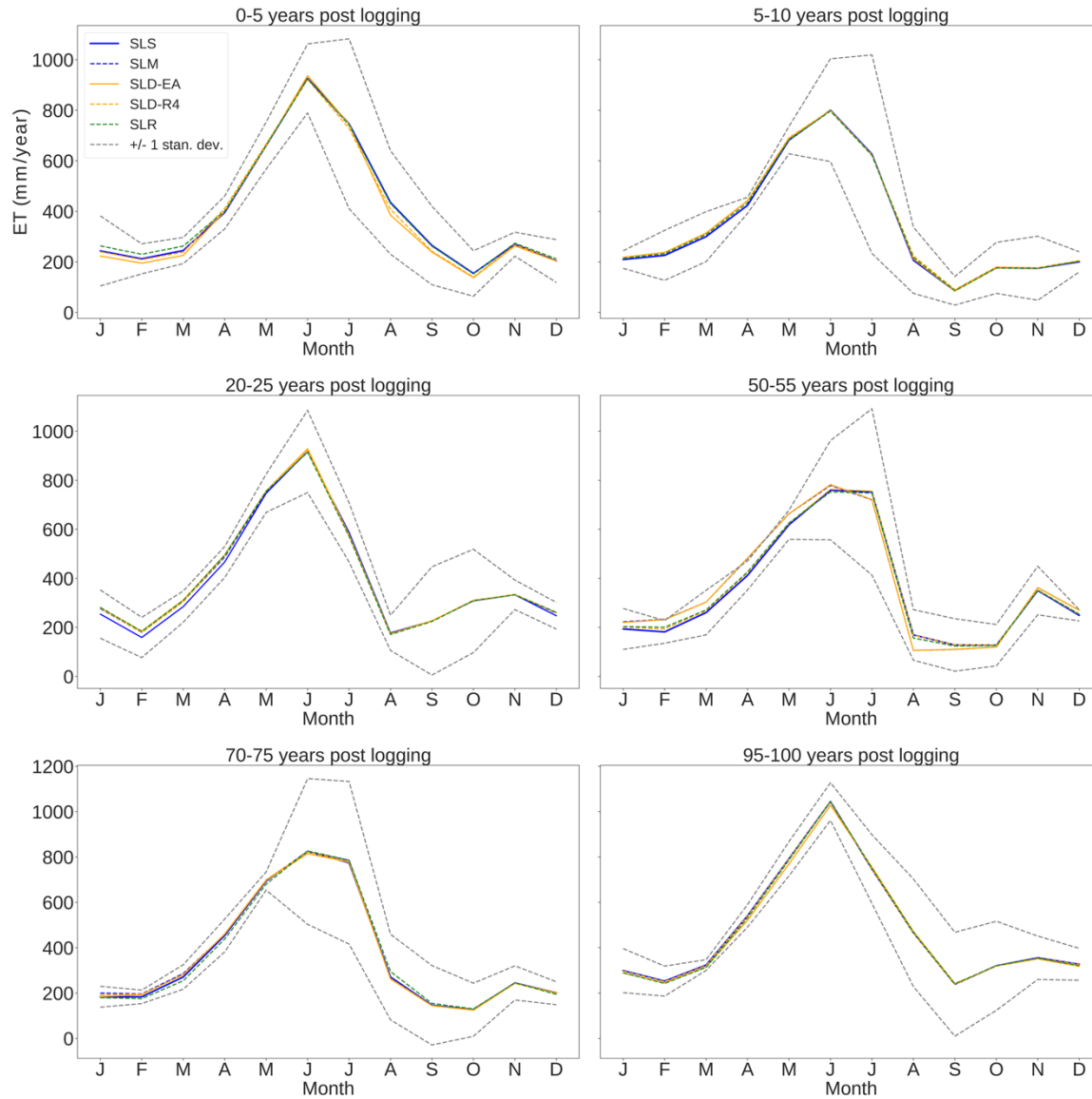


**Figure B4.5 Seasonal average ET with +/- one standard deviation of scenario SLS at different 5-year increments post-logging. Please note the different y-axes on the bottom row of figures.**

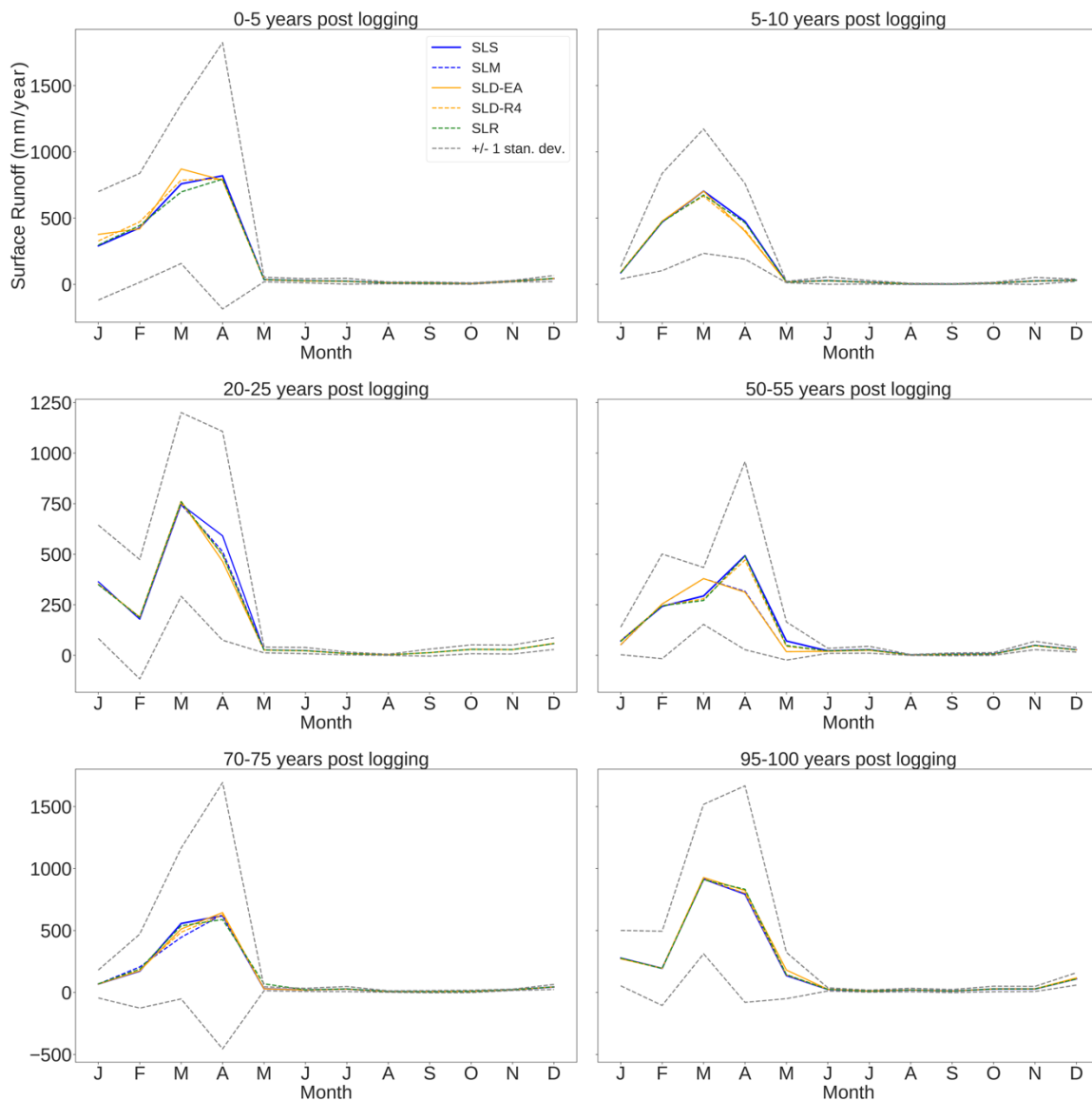


**Figure B4.6** Seasonal average surface runoff (QR) with +/- one standard deviation of scenario SLS at different 5-year increments post-logging. Please note the different y-axes in the middle row of figures.

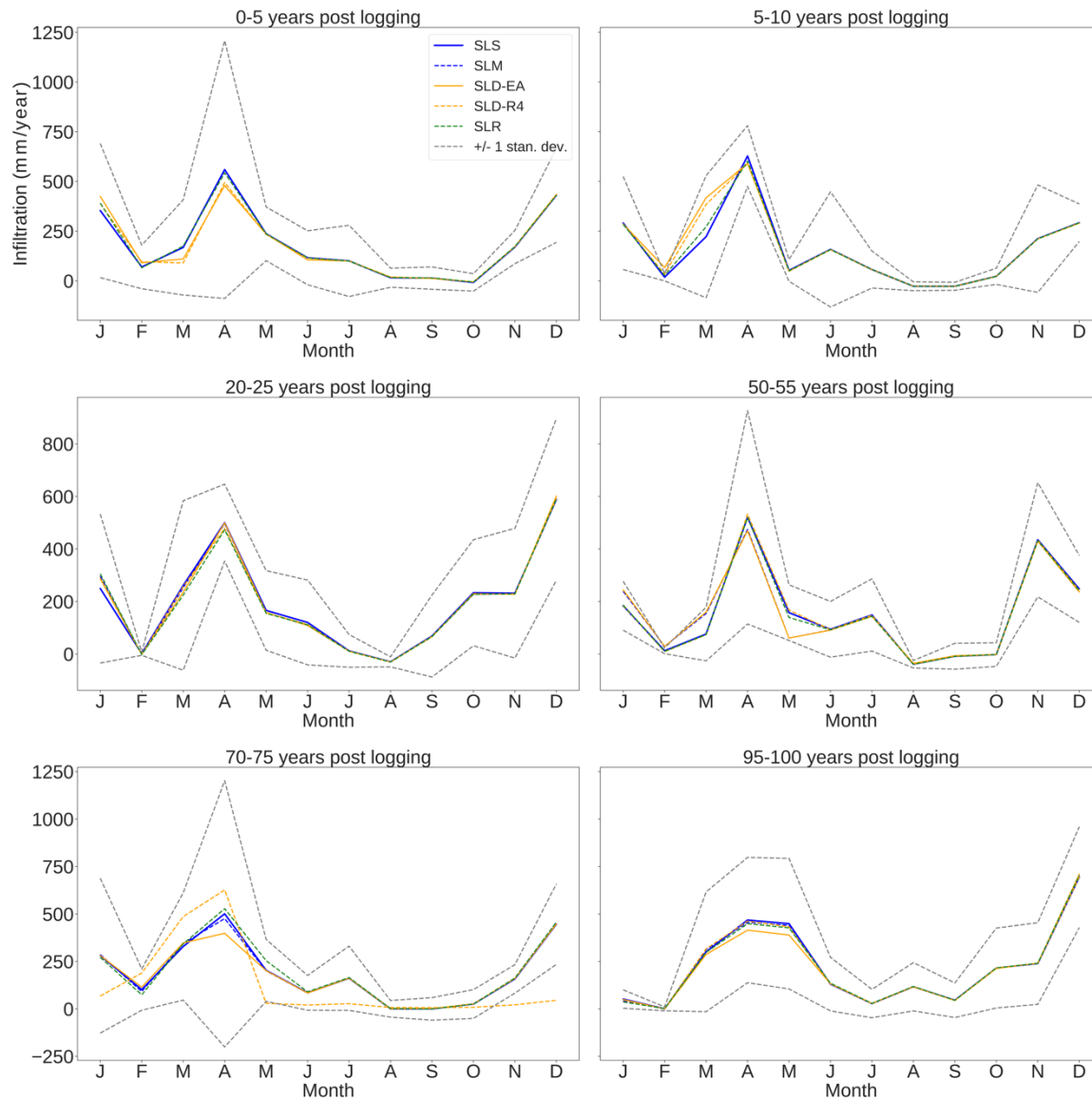


**Figure B4.7 Seasonal average Infiltration (QIN) with +/- one standard deviation of scenario SLS at different 5-year increments post-logging. Please note the different y-axes on all the rows of figures.**

APPENDIX C

Appendix for Chapter 4

C.1 Trait Matrix of Parameter values from PFT1-pines and from PFT2-fir for the multi-

PFT ensembles

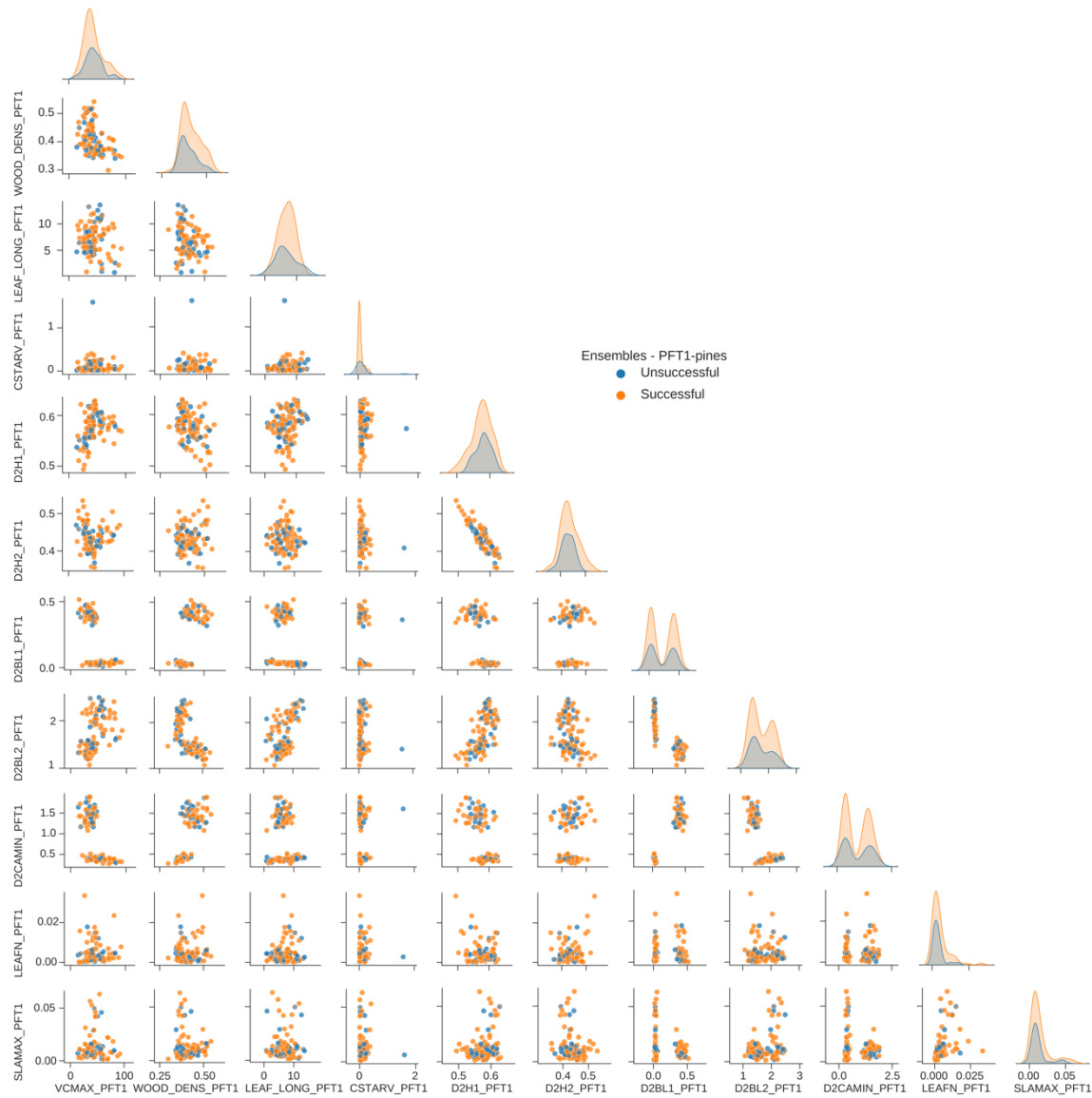


**Figure C.1** Trait matrix of PFT1-pines parameter values for multi-PFT ensembles color coded for parameterization that successfully (orange) and unsuccessfully (blue) grew PFT1-pines >50cm DBH.

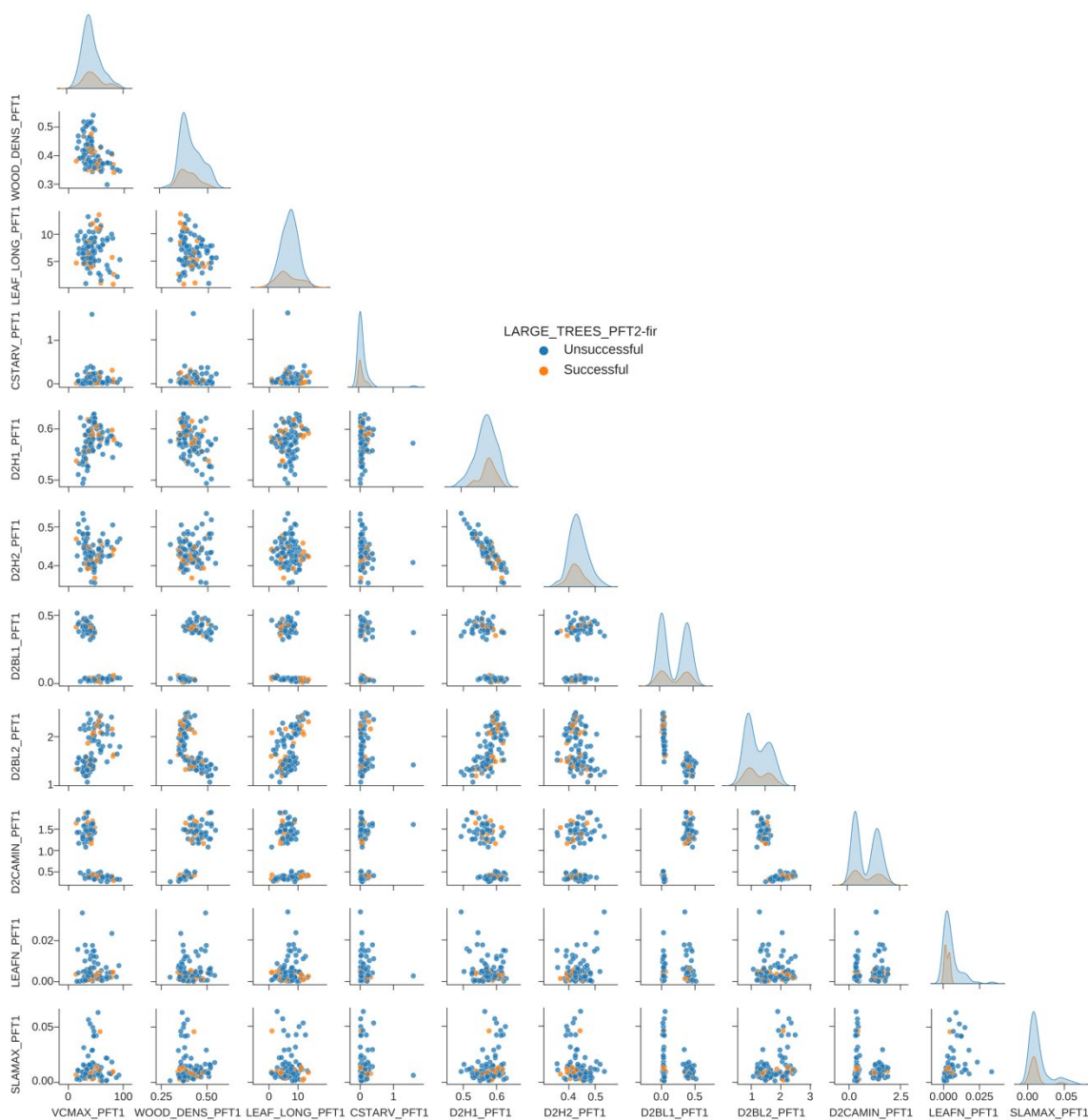


**Figure C.2 Trait matrix of PFT2-fir parameter values for multi-PFT ensembles color coded for parameterization that successfully (orange) and unsuccessfully (blue) grew PFT2-pines >50cm DBH.**